CLIMATIC CHANGE AND ITS IMPACTS

ADVANCES IN GLOBAL CHANGE RESEARCH

VOLUME 19

The titles published in this series are listed at the end of this volume.

CLIMATIC CHANGE AND ITS IMPACTS

An Overview Focusing on Switzerland

by

Martin Beniston

Department of Geosciences,
University of Fribourg, Switzerland

KLUWER ACADEMIC PUBLISHERS
NEW YORK, BOSTON, DORDRECHT, LONDON, MOSCOW

eBook ISBN: 1-4020-2346-4
Print ISBN: 1-4020-2345-6

Created in the United States of America

Visit Springer's eBookstore at: http://ebooks.kluweronline.com
and the Springer Global Website Online at: http://www.springeronline.com

Table of contents

Foreword

Climatic change is a rapidly evolving domain that has prompted the publication of numerous scientific works in recent years. These publications reflect both the public and scientific interest in the topic, as well as the progress in science that observation and modeling has allowed since concerns were raised about the human influence on climate in the last quarter of the 20th century.

This book provides an overview of climate processes, variability and change and applies the general principles related to these issues to the particular case of Switzerland. Although a small country, Switzerland is located in a region of complex topography where climate processes can often be of a very dynamic nature due to the presence of the Alps. Indeed, monitoring of climate in mountains may enable the early detection of the anthropogenic climate signal more readily than other regions, particularly those where urbanization or low-level boundary-layer processes can contaminate data and thereby lead to difficulties in disaggregating different signals in the record. In addition, there is a remarkable density of observational data in Switzerland, ranging from climate, ecology, and land-use, to socio-economic statistics. Access to high quality data enables a comprehensive assessment of climate processes and their long-term trends, comparisons of modeling techniques with real-world data, and environmental and socio-economic investigations of the impacts of climatic change on the natural, social, and economic environments.

This book principally draws upon recent scientific work by the author, based on research conducted within scientific networks both in Switzerland and Europe. It contains in a single volume an overview of the fundamentals of climate, methods of observation and modeling of the climate system, and applications of these basic concepts and paradigms to the particular case of Switzerland. The focus on the alpine region serves to highlight regional climatic change at low, medium, and high-elevation sites as observed over the past 100 years, and the latest climate model data enables a look into coming decades as climate responds to increasing concentrations of greenhouse gases in the atmosphere. Consideration is given to shifts in mean climate and extremes in the 20th century and the latter part of the 21st

century, and to the impacts of expected change on the alpine cryosphere, hydrology, and vegetation as well as on certain managed systems such as agriculture, energy supply and tourism.

The book is aimed primarily at an academic audience from the graduate level and beyond, but may attract the interest of the general public as it strives to strike a balance between descriptive and technical aspects related to the diverse topics that are addressed. The monograph is a contribution to international efforts aimed at furthering the understanding of the intricacies of climate at local and regional scales, and the consequences of regional climatic change on the alpine domain.

Chapter 1

Climate, the environment, and humankind: lessons from the past

1.1. INTRODUCTION

Climatic change and in particular the notion of "global warming" is a theme of scientific concern that has come into the realm of public awareness since the early 1990s. The severity of the potential impacts of climatic change, in particular in the developing world, has prompted international action at the level of governments to address the problem. The United Nations Framework Convention on Climate Change (UN-FCCC) was negotiated at the 1992 United Nations Conference on Environment and Development (UNCED, Rio de Janeiro, Brazil) despite the large range of uncertainties that are inherent to current understanding of the intricacies of mechanisms within the system that lead to its complex behavior. Although subsequent international meetings aimed at implementing the governing articles of the UN-FCCC have made very slow progress, as for example the 1997 Kyoto Protocol that set a calendar for reducing greenhouse-gas emissions, there is nevertheless an unprecedented level of concern among the community of nations that climatic change is a genuine problem with potentially far-reaching consequences for environmental and socio-economic systems.

The realization that human beings need to be concerned by the only "life-support system" that the Earth and its environment provides stems perhaps in part from the fact that until fairly recently, the evolution of humankind was largely dependent on the quality of the environment and the resources it provides in terms of water, food, and favorable health conditions. This is still the case today, despite current levels of technology and apparent resilience in the face of often hostile environments in many parts of the world.

It thus seems appropriate to begin this book by providing a short historical overview of the relationship between humankind and its environment, in order to place it within the bounds of current and future environmental and climatic conditions. A particular emphasis in this chapter will be placed on population migrations as a possible indicator of critical environmental thresholds that reduce the capacity of communities to remain within the lands that they were accustomed to.

Human activities in most parts of the world are transforming the global environment. Ecosystems subjected to the stress factors of global environmental change become more susceptible to the emergence, invasion, and spread of opportunistic species. When subject to multiple stresses, natural environments may exhibit reductions in resilience and regenerative capabilities. It is sometimes assumed that the time scales associated with environmental change are long and that, in many situations, the environment may find a new equilibrium, if not its original state. Environmental upheavals have occurred in the past, along with species extinctions, and yet the planet has "survived" and evolution has continued. However, it is possible that anthropogenic pressure is accelerating change and that many systems may not adapt to rapid rates of change, even if they could adapt to the amplitude of change over longer time periods. According to Myers and Tickel (2001), there have been more changes in the environment in the last 200 years than in the last 2,000, and more changes in the last 20 years than in the last 200. The rate of species extinction is now well beyond the natural rate, in what is sometimes referred to today as the "biotic holocaust".

A number of factors that contribute to global environmental change include the following, many of which are primarily human-induced:

- Land use change
- Land degradation
- Desertification
- Deforestation
- Loss of biodiversity
- Hazardous wastes (toxic, chemical and nuclear)
- War
- Air pollution
- Ozone depletion
- Climatic change

Many of these elements can act in a synergistic manner, thereby compounding the stress situation for the environment and the adverse effects this may have on human activities and the carrying capacity of a particular region. Of all the factors listed above, and with the exception of hazardous wastes, climatic change is the slowest and longest-lived element of global

environmental change. Many of the historical links between humans and their environment are therefore closely related to climatic conditions.

Humans are not only the receptors of environmental change both directly or indirectly, but they are also in numerous instances the drivers of change. Demography can in addition play a significant role in shaping the course of environmental degradation (Jolly and May, 1993; Davis and Bernstram, 1993). High population growth in many parts of the world is linked to environmental damage because local inhabitants attempt to maintain or improve their resource base and economic level through the over-exploitation of their environment (Commoner, 1991; Pebley, 1998). This is carried out in general without any long-term environmental management strategy; resources can thus become rapidly depleted or ineffective.

Through technological advances and seemingly adequate resources, the industrialized world in particular lives under the impression that basic life-supporting resources are abundant and quasi-unlimited. However, one is acutely reminded that famine and disease are still widespread in many parts of the world at the beginning of the 21st century, and that over 350 million persons do not have access to potable water (UNCWR, 1998). Even in technologically-advanced societies, however, water, food and health all constitute basic, interrelated needs for human survival. These elements are all highly dependent on environmental factors such as climate, and are sensitive to even slight shifts in existing environmental conditions. Such changes may upset the delicate balance that, in some countries, favors a high degree of food security, water quality and quantity, and sanitary conditions. Under adverse conditions, it can be surmised that the severe depletion of an essential resource could lead to out-migration, with persons moving from a region affected by resource loss to regions where the resource is still sufficient to sustain both the local and the migrant populations. Because environmental change is recognized to be a possible cause for population migration, the term "environmental refugees" has emerged in recent years (Jacobson, 1988). Although there is no official or legal recognition of this term in the United Nations nomenclature, the High Commission for Refugees (UNHCR, 1993), in the early 1990s, already identified four root causes of refugee flows, which include political instability, economic tensions, ethnic conflict, and environmental degradation. For the first time, a possible link between environmental degradation and refugee flows has been acknowledged by an official, international body. Furthermore, the UNHCR recognized that the numbers of displaced persons internationally was much larger than indicated by the statistics on refugee flows; in other words, the accepted causes of migration (e.g., political and ethnic strife, economic hardship) could not entirely explain the numbers of refugees identified by

the UNHCR. The question remains, therefore, whether these differences could be explained by *environmental refugees.*

This introductory chapter will make the case that, in one form or another, environmental change and its impacts on the basic resources for human sustenance have in the past been a dominant driving force behind population migrations. It will then be suggested that accelerating global change in the 21st century may lead to situations where it once again becomes the major cause for out-migration from particular regions. Migrations recorded during the 19th and 20th centuries, on the other hand, are embedded within complex political, social, and economic contexts and are not solely driven by adverse environmental factors. Some of the 20th century migrations may well have underlying environmental causes as well, but these causes are difficult to disaggregate from the other factors. The subtle links between economic, political, and environmental causes of migration will certainly be present in coming decades, but in some instances the environmental factor may dominate once again in the future as it did in the past.

1.2. POPULATION MIGRATIONS IN THE PAST

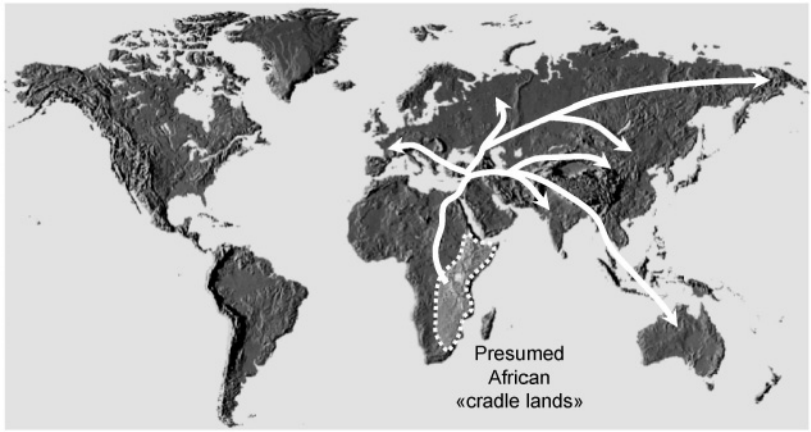

Figure 1.1. Possible migration routes of early humankind (Adapted from Cavalli-Sforza et al., 1995).

It is generally accepted, on the basis of extensive international of archaeological and anthropological research that *Homo sapiens* emerged from the so-called African "cradle-lands", within the region of the East African Rift Valley. At some stage in the past 2-3 million years,

environmental conditions in the Rift Valley favored the evolution of a new species of primate. Migrations of primitive populations began several hundred thousand years ago, perhaps due to epidemics (one of the three basic factors for human sustenance) in a changing climate, or as a result of insufficient food for the increasing populations (Gibson, 1996). The routes followed by early man over several centuries reveal trails that lead to Europe, Central Asia, and perhaps also Australia, as shown in Figure 1.1. Genetic information provides evidence that any given population retains clues to its ancient roots, and common ancestries can be confirmed and human migrations traced by comparing the DNA frequencies of present-day populations (Cavalli-Sforza et al., 1995). Early migrations of modern humans out of Africa have been traced by analysis of DNA sequences; more recent human migrations have been followed through genetic trails as well.

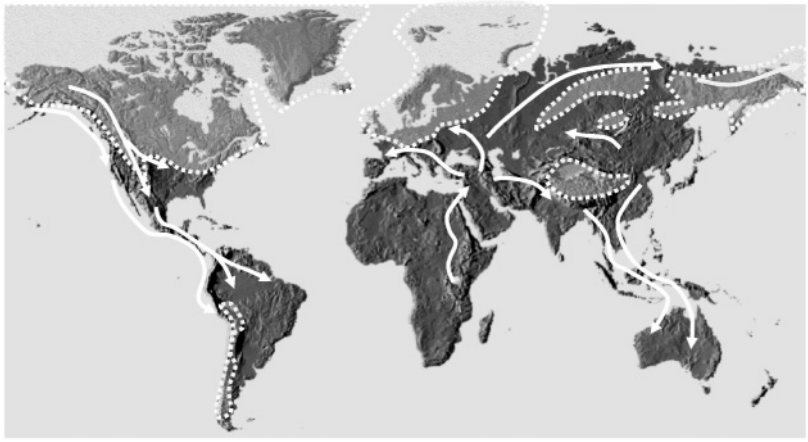

Figure 1.2. Migration routes during the last glacial maximum (Adapted from Elias, 1997). Semi-transparent shading indicates extent of continental ice caps. Shaded regions delimited by dots represent the extent of continental glaciers at that time.

About 120 thousand years ago, a more advanced species of primitive man (the Neanderthal) appeared during the last interglacial period, and spread throughout Europe, Africa and Asia, probably in search of sufficient resources to sustain the growing members of these tribes (Harris, 1991). These were replaced progressively by modern people originating in Africa (Pavolov et al., 2001), about 40 thousand years before present (BP). At the height of the last major ice age, about 25 thousand years BP, a new wave of migrations began, as populations searched for regions with less extreme climates than those affecting many parts of the Northern Hemisphere.

Archaeological evidence indicates that land routes across Central Asia, and coastal routes into Australia and along the shores of the Americas circumvented the extensive ice-caps during the last glacial maximum, as illustrated schematically in Figure 1.2 (Elias, 1997). These population movements led to the settlement of populations with enhanced technological capabilities (more efficient tools; clothing to resist the cold; more efficient hunting weapons; boats capable of navigating in coastal waters) in different parts of the world (Monastersky, 2000).

During this same period, certain areas of the Northern Hemisphere mid-latitudes were less affected by the extreme conditions of the last glacial maximum than others. One such region is the Dordogne and Aquitaine of south-western France, which has undergone continuous human colonization for over 400 thousand years – a record for Europe. Climatic conditions in the Dordogne Valley appear to have been reasonably clement, thereby allowing settlement rather than out-migration, and the progressive development of primitive skills and hunting techniques. Archaeological findings suggest that around 50 thousand years BP (before present), the first ritual burials of the dead took place in the caves near Padirac in the Dordogne Valley. Such rites mark the cultural transition to modern man, and this took place in a region where environmental conditions remained favorable to human development over a sufficient time span to allow cultural development to take place above and beyond day-to-day survival (Bordes, 1973).

During the last glacial maximum, the Dordogne and Aquitaine regions of France were probably isolated from the rest of the world. To the south, the snow-covered Pyrenees were certainly a daunting physical obstacle to migration; to the east, the Massif Central was probably an inhospitable highland area swept by high winds and extreme cold for most of the year; to the north, extending towards the ice fields which reached as far as London, the vegetation cover was essentially reminiscent of today's northern tundra, i.e., yielding little in terms of food; and to the west, the Atlantic was a hostile and stormy ocean (see Figure 1.3, adapted from Clottes, 2001). With little options open to them, the inhabitants of the Dordogne made the best of their environment; indeed, all the "ingredients" for the survival of early civilizations were to be found here: abundant water and food, a relatively mild climate in the middle of very cold conditions, sufficient protection from enemies in the cliff-and-cave landscape of the Dordogne, and yet sufficient open spaces to enable hunting and thereby to ensure sustenance (Bordes, 1973).

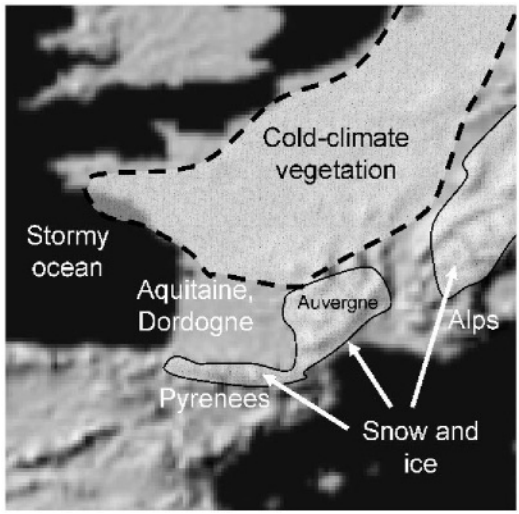

Figure 1.3. The Dordogne and Aquitaine regions of southwest France at the height of the last ice age (Adapted from Clottes, 2001).

Figure 1.4. 25,000-year old cave paintings in Pech Merle, in the Lot Valley of southwestern France (Courtesy: Centre de Préhistoire de Pech Merle, F-46330 Cabrerets, France).

It is during this period, from about 30 thousand years BP onwards, that pictoral evidence of a radical change in human culture emerges through the use of art to record and, perhaps, to convey to later generations elements of the living environment to which the Dordogne inhabitants were accustomed.

The techniques, style and colors used by these painters in caves such as Lascaux or Pech Merle (Figure 1.4) bear witness to the fact that the "climatic oasis" of the Dordogne during the last ice age was a key region for human cultural and technological development. However, it is also a sign that if the carrying capacity of the environment is sufficiently high, then there is no necessity for major migrations to occur.

About 11 thousand years BP, the present interglacial period, also known as the Holocene, began. Many of the large continental glaciers melted, and as a consequence, the ocean levels rose by 100 m, and new species of animals and plants replaced others which were becoming rapidly extinct, such as the mammoth and the saber-toothed tiger. In parts of the Middle East, in what is today Syria and Iraq, people took up two different ways of life, namely nomadic and sedentary (Teitelbaum and Winter, 1993).

Nomads herded sheep, cattle and other animals. They also gathered plants, but meat and milk were their staple diet. Many of the nomads lived on the steppes stretching from Europe across Asia to northern China. As climates changed, nomads were sufficiently mobile to move on to more hospitable and productive regions. Simultaneously, other populations began sedentary agriculture by planting seeds such as barley, wheat, rice and maize, which not only allowed an improvement in their diets, but could also be stored and eaten throughout the year (McCorriston and Hole, 1991). As a result, migrating in search of food became less of a necessity, and sedentary agriculture led to the building of the first permanent settlements. In some areas, however, soils would tend to lose their fertility after a few years and the farmers moved on, burning down forests and shrub-lands to make new fertile ground for a few more years (Armelagos, 1991). This was the start of the destruction of the world's forest which began in the Mediterranean area (Greece, for example) and which, for the tropical rain forest, is still continuing today. The early destructions of certain biomes are also the first sign that human activities are not only influenced by the environment, but that humankind is also capable of significantly disturbing its environment (Cohen, 1977).

During the Holocene optimum, which lasted from about 6,000 to 5,000 years BP, temperatures were between 2 and 4°C warmer than currently; precipitation patterns were also different from those of today, with geographical zones such as the Sahara experiencing far more rainfall than today (Crowley and North, 1991). Indeed, rock paintings in the Tassili N'Ajjer of southern Algeria depict hunting scenes, bearing witness to the fact that grasslands and game such as deer were present in what is currently one of the more arid regions of the planet. In Iraq, Egypt, India and China, river valleys flooded every spring and replaced the minerals of the soil,

thereby allowing soils to remain fertile for many years and enabling villages to grow into cities. The settled way of life led to an increase in food production and population. Technologies developed rapidly, from farming tools, clay pottery and bricks, wheels, cast bronze tools and weapons, to reading and writing. As in the earlier times of the Dordogne, the carrying capacity of the environment in the Middle East and southern Asia allowed populations to evolve culturally and technologically without moving on to other regions by necessity (Clottes, 2001).

The relative stability of environmental conditions, allowing rapid progress in human technology and culture, was not the only influencing factor for reducing or limiting out-migration. As food supplies became sufficient for larger numbers of people due to farming practices and the storage of food to avert famine during more difficult times, and because technology and shelter were available to a much larger extent, the size of populations grew far more rapidly than in the past (Cohen, 1977). As a result the carrying capacity of the environment became insufficient once a critical threshold of population was exceeded in some communities. If demographic growth began to outpace food supply, then a time inevitably came when there was insufficient food supply to sustain an entire, growing population, and out-migration would become once again an option. Strife or epidemics, which could sometimes curtail increasing populations and allow the survivors to remain in their usual environment, could in some instances avert the necessity for out-migration (Armelagos, 1991).

It is believed that the sudden disappearance of the Anasasi Indians, in the American Southwest, may be an early example of the combined environmental and social upheavals leading to population out-migration. The Anasasi were known for their advanced community structures (Jones and Cordell, 1985), exemplified by the superb architectural remains in Mesa Verde (Colorado; see Figure 1.5) or Bandelier (Arizona), for example. The large threshing surfaces and communal ovens found in Mesa Verde bear witness to the fact that the Anasasi were essentially farmers. Over the several hundred years of Anasasi presence in the Southwest United States, paleo-climate reconstructions suggest that a number of severe droughts intervened, each one capable of severely depleting food stocks. However, until the sudden disappearance of the Anasasi, food stockpiled to survive periods of drought were generally sufficient to sustain the indigenous populations. According to one hypothesis (e.g., Cordell, 1984), it is only when the Anasasi population exceeded a certain critical level that food stocks were no longer capable of nourishing the entire population during the droughts that ensued. This could explain their rapid disappearance, perhaps through migrations to various destinations which were perceived as less inhospitable.

Figure 1.5. Ruins of Anasasi cave-village in Mesa Verde National Park, Colorado, USA (Courtesy: National Park Service, Washington, D.C., USA).

The examples that have been succinctly presented here show that populations have responded to environmental stresses, particularly climatic change and its impacts on food and water resources, and health, by migrating to areas with more abundant food and water, and improved health conditions. Following the last major ice age, a more clement climate and the discovery of agriculture reduced the need to migrate, until the capacity of sedentary agricultural practices to sustain rapidly-growing populations was no longer possible.

1.3. POPULATION MIGRATIONS IN THE 20TH CENTURY

The 20th century has seen unprecedented social and economic changes, many of which have been the primary drivers of migration. Two world wars and many regional conflicts, highlighting opposing ideologies and shifting alliances, have also been major actors in population displacements. Throughout the 20th century, the interactions between economics, politics and environmental stress have become increasingly complex, thereby rendering more difficult than previously any single cause-to-effect relationship. Earlier deterministic cause and effect models where a set of environmental stresses resulted in a particular response (e.g., migration) from individuals and communities are no longer the norm where out-

migration is the result of numerous concurrent causes. Some 20th century population displacements may have occurred with certain forms of environmental catastrophe, where there is no option but to move, but the most visible migrations have definitely been linked to conflict and economic hardship. In addition, simple cause-to-effect models break down in more complex social structures since, in general, levels of sensitivity and perception by communities to a major stress are typically high, and thus there exist different levels of ability to cope with environmental stresses. The tolerance thresholds of populations are highly variable, being surpassed very readily in some, and being almost insurmountable in others. A proper appreciation and understanding of the complexity and diversity of human responses to environmental degradation is essential in order identify the complexities of migration in past decades.

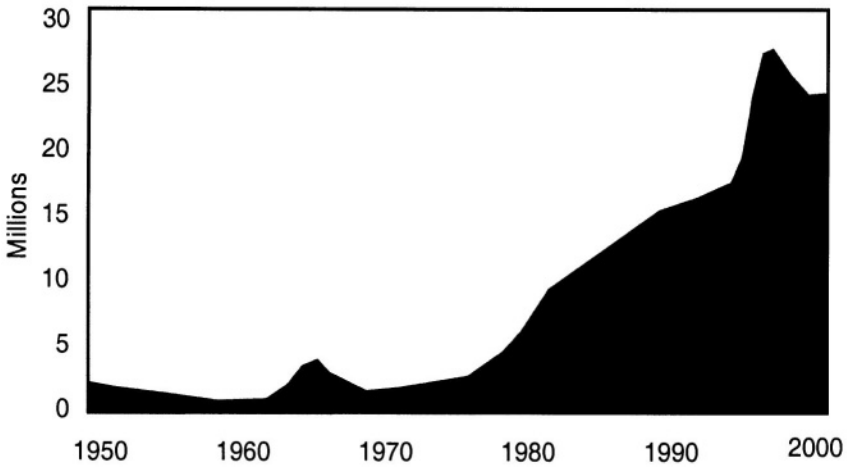

Figure 1.6. Refugees under the protection of the United Nations High Commission for Refugees (UNHCR, 2000).

Figure 1.6 shows the trends in the numbers of persons currently under the protection of the UN High Commission for Refugees (UNHCR, 2000), and in particular the spectacular rise from less than 5 million in the late 1970s to over 25 million in 2000. This is only part of the overall picture, however, because the mandate of the UNHCR is basically to offer aid and protection to victims of political persecution and conflicts. Furthermore, it is necessary to differentiate between internally-displaced persons (IDPs, who migrate within national boundaries in order to escape the consequences of civil war, for example), and forced migration of persons who flee across international boundaries. In terms of the actual numbers of migrants worldwide, in

addition to those officially registered by the UNHCR, figures vary widely and range in the early 1990s from about 80 million according to the International Office of Migrations to over 100 million in 1993 (Castles and Miller, 1993). The UNHCR (1995) acknowledges that collecting accurate statistical data on refugees and asylum-seekers is *"one of the most problematic issues"* confronting the agency. Using 1990 data from UN sources, Westing (1992) for example notes that in addition to officially recognized refugees (roughly 40% of total displaced persons), there were cross-border refugees (10%), and internal refugees (51%). In total, the 1990 figures amount to 41.5 million persons, which represents a 60% increase on the numbers of displaced persons estimated in 1986. On the basis of these figures, Westing (1992) further speculates that the growth is due to the addition of "environmental refugees." Jacobson (1988) noted already that *"environmental refugees have become the single largest class of displaced persons in the world",* a statement that is partially upheld by the UNHCR (1993) which admits that there are *"clear links between environmental degradation and refugee flows"*. Other drivers for migration in the 20th century are linked to demography, economic restructuring and increasing economic disparities. In the latter part of the 20th century, these disparities have been the root cause of many displacements of people, from the developing countries to the industrialized world because of perceived economic attactivity of North America and Europe, for example, and "South-to-South" migration as persons move within countries or groups of countries within the developing world.

It is perhaps symptomatic of the large number of social and economic upheavals witnessed in the 20th century that the focus of migration studies has been these more obvious driving forces. This should not overshadow the fact that, however, there have been environmental factors that have led to forced migrations in the 20th century also. These include natural disasters such as earthquakes, hurricanes, droughts and floods; industrial accidents, leading, for example, to the evacuation of a 30-km radius around the Tchernobyl nuclear power station in the Ukraine, following the 1996 disaster; development projects such as dams and irrigation projects which have displaced over the last 25 years more than 20 million persons in India alone (Fornos, 1991), etc.

1.4. POSSIBLE ENVIRONMENTAL CHANGE AND POPULATION MIGRATIONS IN THE 21ST CENTURY

1.4.1. Preamble

In coming decades, population growth, increasing pressure on resources, and persistent inequalities in resource access imply that scarcities will affect many environmentally sensitive regions with a severity, speed, and scale unprecedented in history. Many countries lack the social institutions that are essential prerequisites to ensure social and technical solutions to face up to problems of scarcity. In the face of significant external stress, population displacement often indicates the breakdown of social resilience. For example, in the context of food security, displacement and coping strategies reflect an extreme manifestation of vulnerability. Coping strategies generally represent short-term adaptations to extreme events; they are usually involuntary, and rarely prepare the way to reducing a population's vulnerability to future famine situations.

Dwindling resources in an uncertain political, economic and social context are capable of generating conflict and instability, but the causal mechanisms are often indirect. Scarcities of cropland, fresh water, and forests constrain agricultural and economic productivity. Such situations are capable of generating population movements (Myers, 1993). In the extreme, such a situation can contribute to local or regional conflicts, which may increase over time as environmental scarcities worsen; while such conflicts may not be as conspicuous as wars at an international level, there is nevertheless a potential for significant repercussions for the security interests in both the developing and the industrialized countries. Such internal, resource-based conflicts can affect international trade relations, produce humanitarian disasters, and lead to growing numbers of refugee flows (Parnwell, 1993).

In the complex issues that can result in migration of populations in the 21st century, it will be increasingly necessary to distinguish between voluntary migration and forced migration. Voluntary migration can occur for a number of reasons, particularly economic and political or ideological. Forced migration, on the other hand, has a number of root causes, also to be found in political and economic domains, in particular war and ethnic strife, etc. In this context, environmental factors for migration can be considered to be an indirect consequence of decisions taken in the political and/or economic arenas. While sea-level rise is an obvious environmental driver that may significantly impact many low-lying coastal regions around the

world, sea-level rise is a consequence of a warming global climate, itself in part the result of economic and industrial policies leading to enhanced greenhouse-gas emissions.

Environmental issues are thus seen to be an expression of underlying economic and political factors. Similarly, population migrations may be triggered by conflicts resulting from resource depletion. In this sense, migration does not occur because of the direct consequence of environmental change but rather as a result of a complex series of inter-linked factors in which single, clear-cut cause-to-effect relations may not be identifiable. Causes of migration are thus seen to be embedded deep within a confluence of processes and patterns.

1.4.2. Water resources

If present consumption patterns are sustained, the global annual water demand is likely to increase from 4,130 km^3 in 1990 to 5,190 km^3 in 2020 (Shiklomanov, 2001). Because of increasing population, the additional demand will be accompanied by a sharp decline in water availability per capita. While a consumption of 1,000 m^3 of water per year and per capita is considered a standard for "well-being", currently less than 50% of the world's population reaches this level (UNCWR, 1998).

Against this backdrop of social and ecological problems, water resources will most likely come under increasing pressure. Significant changes in climatic conditions will affect demand, supply and water quality. In regions which are currently sensitive to water stress (arid and semi-arid mountain regions), any shortfalls in water supply will enhance competition for water use for a wide range of economic, social, and environmental applications. In the future, such competition will be sharpened as a result of larger populations, which will lead to heightened demand for irrigation and perhaps also industrialization, at the expense of drinking water (Noble and Gitay, 1998).

Projections of annual water availability per capita by the 2020s point to a declining trend in all parts of the world, including those that are considered to have ample water resources (IPCC, 2001). Figure 1.7 illustrates the possible changes in water availability per capita for a number of countries around the world. It is seen that in most cases, water amount will dwindle in large part due to population growth; the superimposed reductions resulting from climatic change will exacerbate the situation stressed by demography but will certainly not be the dominant factor leading to reduced water availability. The World Bank (1995) estimates that about 600 million people

in Africa will suffer from water shortage and dwindling water quality. Shifting precipitation belts account for only a fraction of this reduction; rapid population growth, urbanization and economic expansion place additional burdens on water supply.

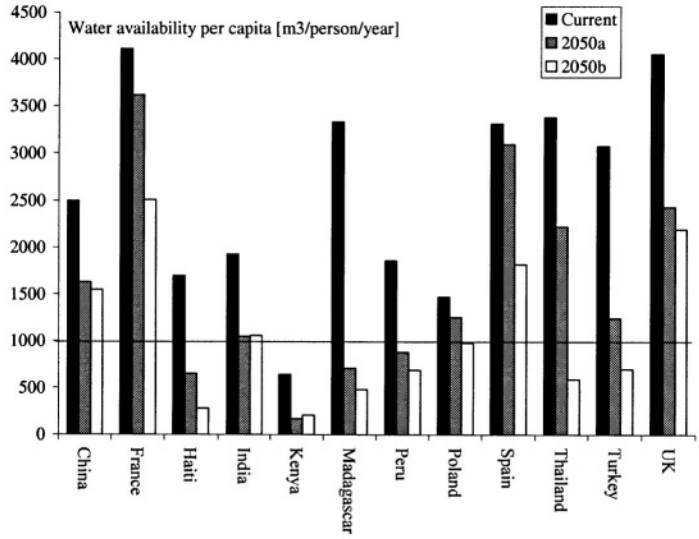

Figure 1.7. Water availability per capita by 2050 for selected countries in the industrialized and the developing world, for scenarios with constant climate (2050a) and with changing climate (2050b), following IPCC (1998).

In Latin America, which accounts for 35% of global freshwater, the impacts of climate change are expected to occur in the more arid regions of the continent, which are often associated with the rain-shadow influences of the Andes ranges. Shifts in water demands will depend on population growth, industrial expansion, and agricultural potential. In many countries of the region, water availability is expected to decline, which is likely to generate potential for international conflicts. The IPCC (1998) estimates that water availability per capita and per annum will decrease from 4,750 m^3 in 1990 to 2,100 m^3 in Mexico by 2025, without any change in climate, i.e., due to population and economic growth. Based on several GCM simulations, projected shifts in precipitation in a warmer climate yield a range of 1,740 - 2,010 m^3. For Peru, the respective set of figures are 1,860 m^3, 880 m^3 resulting from demography alone, and 690 - 1,020 m^3 with climatic change, i.e., close to or below the minimum requirements for « well-being ».

Water resources in tropical Asia are very sensitive to tropical cyclones and fluctuations in their trajectories and intensity. The dominant effect of the Monsoon may be perturbed in a changing climate. Runoff in the Ganges, for example, is more than 6 times that of the dry season. As elsewhere in the world, water resources will become increasingly vulnerable to increasing population growth, urbanization, industrial development and agriculture, as shown by Schreir and Shah (1996). An impacts assessment study by Mirza (1997) for a number of Himalayan basins contributing to the Ganges has shown that changes in the mean runoff in different sub-basins ranged from 27 to 116% in a climate forced by a doubling of CO_2 concentrations relative to their pre-industrial levels. The sensitivity of basins to climate change is seen to be greater in the drier catchments than in the wetter ones. However, water demand is greatest in the dry season in India, and demand cannot be met by supply in this season. Shifts in the timing and intensity of the Monsoon, and the manner in which the Himalayan range intercepts the available precipitable water content of the atmosphere, will have major impacts on the timing and amount of runoff in river basins such as the Ganges, the Brahmaputra or the Irrawaddy. Amplification or weakening of the Monsoon circulations would indirectly impact upon agriculture and fisheries, freshwater supply, storage capacity, and salinity control.

In Africa, where over 60% of the continent's rural population and 25% of its urban population does not have access to safe drinking water (IPCC, 1998), climatic change will exacerbate the current situation. The expected degradation will in part be due to increasing population pressures and insufficient financial resources to ameliorate the existing problems of water supply and quality.

Furthermore, Africa has a large number of rivers that cross or form international boundaries, so that the sharing of a dwindling resource could ultimately lead to regional conflicts. Armed disputes over water resources may well be a significant social consequence in an environment degraded by pollution and stressed by climatic change, as in the Middle East (Lonergan and Brooks, 1994). The potential for forced migration, either directly because of insufficient water to sustain growing populations, or indirectly because of armed conflicts, is clearly present.

A more rational approach to the conservation and use of what is probably the most vital single resource for humankind is thus crucial. New initiatives are aimed at conservation and distribution of water within the developing world so that their inhabitants, in particular women, can avoid spending a large part of their working lives merely carrying drinking water for their families (Engelman and Leroy, 1993).

1.4.3. Food security

Food security is also threatened by climatic change, both directly by changing temperature and precipitation patterns, and indirectly through the losses of agricultural land by sea-level rise, enhanced wind and water erosion. In addition, human-induced land-use change linked to deforestation and desertification, have already reduced the agricultural potential of many regions in the world (IPCC, 2001).

The world food system involves a complex dynamic interaction of producers and consumers, inter-linked through global markets. World agriculture generates over US$1,300 billion in annual revenue. Related activities include input production and acquisition, transportation, storage and processing, and these generate additional revenue estimated at US$ 4,000 billion on an annual basis (IPCC, 1998). Although agricultural productivity has increased to keep pace with growing world population over the last century, there are still close to 1 billion people who are under-nourished. Furthermore, agriculture is probably the most vulnerable of all human activities to weather and climate variability; the chief controls on agricultural yields include temperature, precipitation, soil moisture, carbon dioxide levels, and disease and pests (themselves largely climate-dependent). Any changes in one or more of these controlling factors may have profound, non-linear effects on productivity. The Food and Agricultural Organization (FAO, 2000) has warned that by 2020, agricultural yields should almost double in order to keep up with demographic trends and the diversification of consumption patterns. It is unlikely that the "green revolution" of the 20th century will be reiterated, even when taking into account new technologies such as genetic engineering, because competition for land and climatic change may negate all or part of the progress made in agricultural productivity.

The impacts of climatic change on agriculture can be assessed at different scales including crop yield, farm or sector profitability, regional economic activity or hunger vulnerability. Impacts depend on biophysical and socio-economic response. The effects of climate on agriculture in individual countries cannot be considered in isolation, because in addition to the close links between agriculture and climate, it is necessary to take into account the international nature of food trade and food security, and the need to consider the impacts of climate change in a global context.

Agricultural production will be affected by the severity and pace of climate change. If change is gradual, there will be time for political and social institutions to adjust. Slow change may also enable natural biota to adapt. Many untested assumptions lie behind efforts to project the potential

influence of climatic change on crops. In addition to the magnitude and rate of change, the stage of growth during which a crop is exposed to drought or heat is important. Moreover, temperature and seasonal rainfall patterns vary from year to year and region to region, regardless of long-term trends in climate. Temperature and rainfall changes induced by climate change will likely interact with carbon dioxide levels, fertilizers, insects, plant pathogens, weeds, and the soil's organic matter to produce unanticipated responses. In many parts of the world, generally warmer temperatures and longer hot periods will put additional stress on certain crops. Corn, for example, has a stress limit at about 35 °C which, when exceeded for any length of time, can exert irreversible physiological damage to the plant. The United States Midwest, one of the world's principal cereal-producing regions, could be particularly vulnerable to prolonged heat, heightening the potential for crisis in the global food supply. The 1988 drought in the Midwest resulted in severe shortfalls in corn yields, and for the first time since the Second World War, the United States was a net importer of cereals rather than an exporter. A warmer and drier climate at critical times of the year could increase the frequency of crop failures.

Rainfall, however, remains the major limiting factor in the growth and production of crops worldwide. Adequate moisture is critical for plants, especially during germination and fruit development. Any changes to rainfall patterns will also reduce soil water contents. In certain semi-arid and arid zones, the soil moisture often allows plants to survive a short drought period; a warmer climate, accompanied by more evaporation, less precipitation and associated reductions in soil moisture recharge, would spell disaster for regions where agriculture is only just viable today.

Based on projections of economic, technological, and climatic trends, maps of yield changes for corn have been compiled by Parry et al. (1999) for various periods in the future. Figure 1.8 illustrates the changes in wheat yields in 2050 compared to the 1990 baseline; with the exception of western Europe, Canada, and the Russian Federation, almost all countries are projected to suffer yield reductions. Shortfalls range from 10% in Argentina or Australia, to over 25% in India and Mexico (Parry et al., 1999). The collateral effects of severe shortfalls include financial fragilization, as the less wealthy countries import food at the expense of vital hard-currency reserves.

A large range of extreme weather events, which may increase in frequency and severity in certain parts of the world, may compound the stress effects of a warming *average* climate. Drought, fire and heat waves are one category of extremes which need to be considered, while heavy precipitation and hail are another category that can adversely affect

agricultural production. These events may be offset to some extent in colder regions by a lower frequency of spring frosts, which are often damaging to plants at the beginning of their growth cycle.

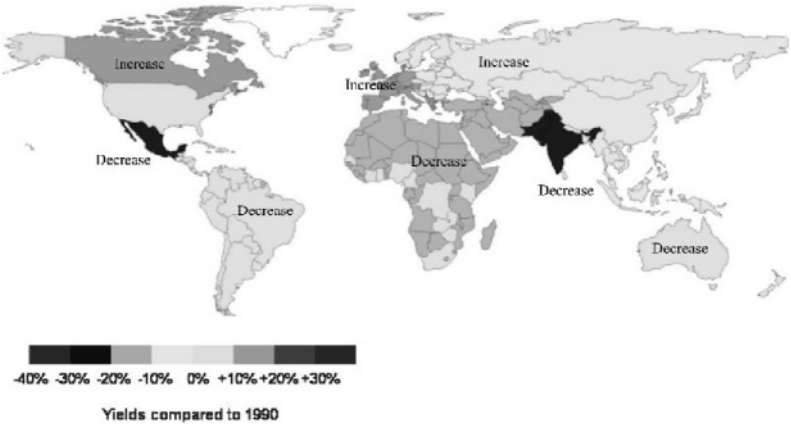

Figure 1.8. Projections of changes in corn yields in 2050 (Parry et al., 1999).

While these issues related to changes in agricultural yields do not necessarily imply that shortfalls in basic foodstuffs would lead to out-migrations, they do convey the delicate situation in which countries with growing populations are likely to find themselves in the future. Internal migrations are likely, as populations move out of the agricultural zones which are affected the most into other rural areas where conditions are less acute or, possibly, into urban areas in search of work, shelter, food and water.

Vulnerability is low in regions where agriculture is well adapted to current climate variability, or where market and institutional factors allow a redistribution of agricultural surpluses to make up for shortfalls. In order to plan ahead and reduce the impacts of climatic change on agriculture, long-term agricultural policy options should be carried out in parallel to other concerns, such as erosion, loss of topsoil, salinization, soil and water pollution. Furthermore, improved water management and irrigation practices should be implemented to help reduce the adverse effects of droughts and heat-waves that are likely to be on the increase in a warmer global climate.

1.4.4. Health: the particular case of malaria

In terms of human health, there are many determinants that can all interact with one another (McMichaels et al., 1996). Human biological and psychological factors are primary determinants, but ecological and global systems are also involved, as are economics and access to health care, which shape vulnerability of societies to disease. Shifts in environmental conditions, interacting with the biology of disease agents, can exert profound effects. Changes in how land is used affect the distribution of disease carriers, such as rodents or insects, while climate influences their range, and affects the timing and intensity of outbreaks. Changing social conditions, such as the growth of multimillion-inhabitant cities in the developing world and widespread ecological change, are today contributing to the spread of infectious diseases. This will be exemplified here by looking into one of the best-known vector-borne diseases, malaria.

The occurrence of vector-borne diseases such as malaria is determined by the abundance of vectors and intermediate and reservoir hosts, the prevalence of disease-causing parasites and pathogens suitably adapted to the vectors, and the human or animal hosts and their resilience in the face of the disease (McMichaels and Haines, 1997). Local climatic conditions, especially temperature and moisture, are also determinant factors for the establishment and reproduction of the *Anopheles* mosquito (Epstein et al., 1998). The possible development of the disease in mountain regions thus has relevance, because populations in uplands where the disease is currently not endemic may face a new threat to their health and well-being as malaria progressively invades new regions under climatic conditions favorable to its development. (Martens et al., 1999).

The occurrence of vector-borne diseases is widespread, ranging from the tropics and subtropics to the temperate climate zones. With few exceptions, they do not occur in the cold climates of the world, and are absent above certain altitudes even in mountain regions of the tropical and equatorial belt (WHO, 1999). At elevations above 1,300 – 1,500 m in Africa and tropical Asia, the *Anopheles* mosquito can currently neither breed nor survive; as a result, malaria is almost totally absent from many highlands of the tropical zone (Craig et al., 1999).

Vectors require specific ecosystems for survival and reproduction. These ecosystems are influenced by numerous factors, many of which are climatically-controlled. Changes in any of these factors will affect the survival and hence the distribution of vectors (Kay et al., 1989). Global climatic change projected by the IPCC (2001) may have a considerable impact on the distribution of vector-borne diseases. A permanent change in

one of the abiotic factors may lead to an alteration in the equilibrium of the ecosystem, resulting in the creation of either more or less favorable vector habitats. At the present limits of vector distribution, the projected increase in average temperature is likely to create more favorable conditions, both in terms of latitude and altitude for the vectors, which may then breed in larger numbers and invade formerly inhospitable areas.

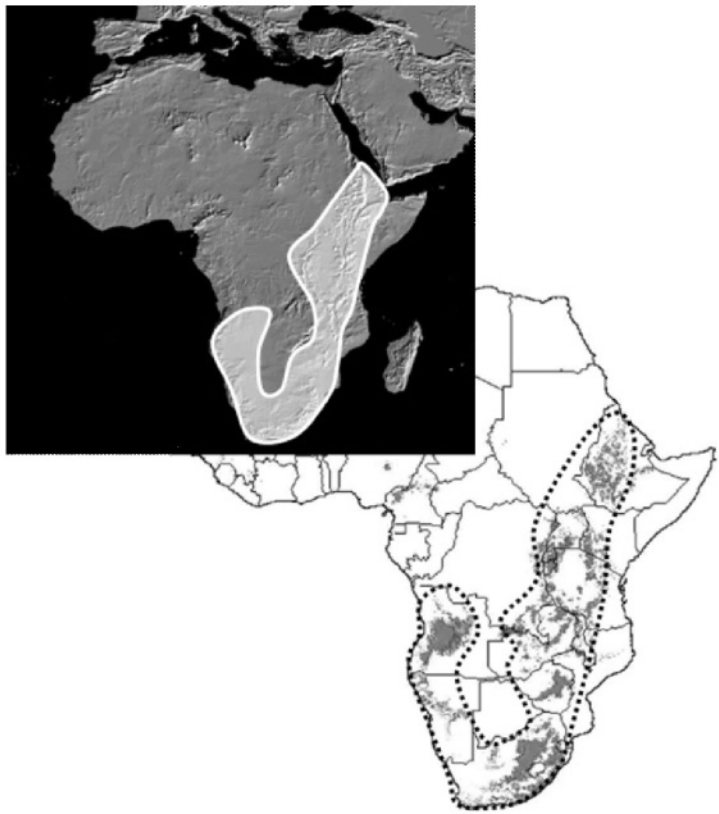

Figure 1.9. Possible incidence of malaria in Africa with a 1°C increase in mean annual temperatures. The intensity of the grey color is proportional to the rate of infection. Inset map shows regions of eastern and southern Africa above the 1,000 m altitude level.

The infection rate for malaria is an exponential function of temperature (WHO, 1990); small increases in temperature can lead to a sharp reduction in the number of days of incubation. Regions at higher altitudes or latitudes may thus become hospitable to the vectors; disease-free highlands that are today found in parts of Ethiopia and Kenya, for example, may be invaded by

vectors as a result of an increase in the annual temperature. If this were to occur, then the number of persons infected by malaria would increase sharply.

Lindsay and Martens (1998) and Martens et al. (1999) have investigated the possible changes in the distribution of malaria. Increases in temperature and rainfall would most probably allow malaria vectors to survive in areas immediately surrounding their current distribution limits. How far these areas will extend both in terms of altitude and latitude depends upon the extent of warming. The IPCC (1998) has published maps of increases in the incidence of malaria in Africa, as given in Figure 1.9 for a modest warming scenario of +1°C with respect to current climate. It is seen that the regions with the sharpest rise in the rate of infection are those which lie above 1,000 m (as given in the inset map). In these highland regions, even a modest rise in temperature may lead to a spread of the disease into hitherto disease-free regions. Figure 1.10 illustrates that the trend may already be discernible in a number of highland regions of Africa, such as Zambia and Rwanda (Loevinsohn, 1994). It is seen here that there is a quasi-exponential increase in the incidence of malaria, which is, at least in part, consecutive to changing climatic conditions for the period 1975-1990.

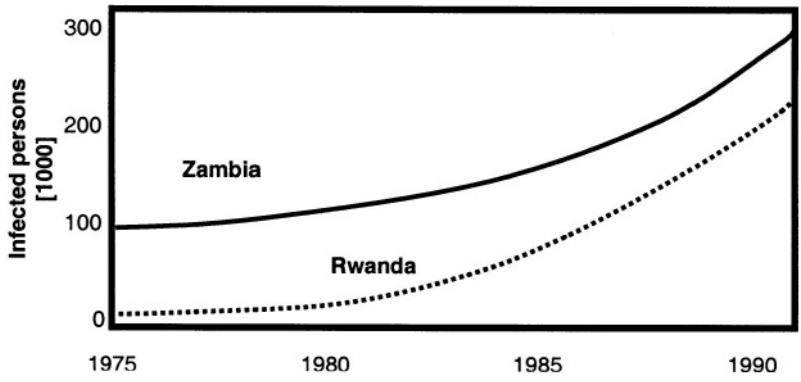

Figure 1.10. Recent increases in the infection by malaria in two upland countries of Africa, Rwanda (dotted line) and Zambia (solid line).

This conclusion is in apparent contradiction to a number of studies that attempt to play down any clearly discernible link between observed climatic change and increases in malaria in the East African highlands. One recent study by Hay et al. (2002) concludes that, at least for Kenyan uplands, there have been no climatic trends of sufficient importance for transmission of the disease during the 20th century. The authors furthermore state that because of

the high spatial and temporal variability of East African climate, *"claimed associations between local malaria resurgences and regional changes in climate are overly simplistic"*. While this may indeed be a logical conclusion for the relatively modest changes in climate observed in the region, it may not hold when changes are of greater amplitude. A particular example is the intensification of malaria in Colombia during episodes of El Niño, whereby mean temperatures increase and mean precipitation decreases with respect to normal conditions (Poveda et al., 2001). Such links between abrupt but significant changes in climate and the annual cycle of malaria development and transmission may help further our understanding of the links between environmental and epidemiological factors, both on the short term (ENSO cycles) and the longer term (climatic change).

Africa is not the only continent to be affected by the increase in vector-borne diseases; in certain countries where the disease has been eradicated in the second half of the 20th Century, particular strains of malaria are resurging. There are reports from various low to medium elevation upland sites in Turkey, Tajikistan, Uzbekistan, Turkmenistan and the Urals that malaria is being transmitted in rural populations, with close to epidemic proportions in south-eastern Anatolia (Wilson et al., 2001).

It is often difficult to associate any particular change in the incidence of a particular disease with a given change in a single environmental factor. It is necessary to place the environment-related health hazards in a population context, such as age, level of hygiene, socio-economic level, and health status (McMichaels and Kovats, 2000). These phenomena could contribute to migration from one rural region to another and from rural to urban areas (Myers, 1993). In addition, if climatic change were to be accompanied by an increase in the intensity of certain forms of natural hazards, such as cyclones, floods, or drought, these would compound the effects on human health. Moreover, such catastrophes can generate large refugee and population movements, with a need for resettlement in what are often already densely populated areas (Pebley, 1998).

Forecasting the climate change impacts on health is complex, because populations have different vulnerabilities to change and susceptibility to disease. These depend on the general levels of hygiene practices, clothing, housing, medical and agricultural traditions. Adaptation of populations to the spread of malaria and other vector-borne diseases is determined by the economic level of a given population, the quality and coverage of medical services, and the integrity of the environment. There are numerous side-effects of environmental change that can impact upon health and well-being, including hygrothermal stress and enhanced levels of air pollution. While these aspects are not in themselves exclusive to mountain regions, however,

many of the changes will have indirect effects by modifying natural ecosystems, affecting such aspects as food production, vector-borne diseases, and the equilibrium between a number of other infectious and non-infectious diseases (McMichaels and Kovats, 2000).

In conclusion, there will be numerous interacting root causes, from politics and economics, to profound changes in the environment (sea-level rise, deforestation, soil degradation, and climatic change) that are likely to impact heavily upon water resources and food security, as well as on human health. The extent to which the reductions in water supply and shortfalls in agricultural yields, or changing patterns of disease, may actually force extensive out-migration, is a matter of debate. The IPCC (2001) notes that one of the greatest effects of climate change may be on human migration, as millions of people will be displaced due to shoreline erosion, coastal flooding, agricultural disruption, and dwindling water resources. Following the first assessment report of the IPCC (1990) which had already raised this issue, Myers (1993) projected that about 150 million "environmental refugees" may represent one of the direct consequences in the "greenhouse world" of the 21st century. There is no certainty associated with this particularly figure, and it may be an overstatement. But it helps to raise the awareness to these issues and to stimulate thought and action in order to institutionally and legally prepare for refugees in larger numbers than hitherto experienced.

1.5. CONCLUSIONS TO CHAPTER 1

As societies have become more complex in cultural and technological terms in recent decades, the interactions between environmental and economic issues have become more subtle, and as a consequence, it has become increasingly difficult to separate different drivers of migration, i.e., political, environmental, economic, ethnic, from one another. Population movements themselves have environmental effects and there will thus be a number of economic, political and environmental impacts resulting from the displacement of persons forced from their homelands (Westing, 1992; Tickell, 1990). Issues such as the sharing of resources between increasing numbers of persons in a region of immigration, land tenure, ethnic rivalry and regional conflicts are likely to emerge as issues that will need urgent attention in the near future.

While a number of adaptive measures can be taken to reduce the adverse effects of environmental change and the potential for out-migration that such change may induce, there is a need to address some of the root issues in an

internationally-coordinated manner. Immigration policies in the industrialized world need to be reviewed in order to allow some form of open, well-regulated migrations rather than solutions aimed at keeping migrants out of the prospective host countries. These will require a change of attitude within segments of the population of the host countries in terms of the acceptance of immigrants and their integration within their host society. In the developing world also, policies will need to be altered, in particular in order to remove the "push" factors of migration. A review of current resource-use practices, that are often very poorly managed and thereby generate considerable environmental degradation, will be needed. There is also a crucial necessity to improve land policies, valuation and property rights, in order to reduce the wish or the tendency for out-migration. Because the problem is one of balancing peoples' needs and wants with available resources, solutions will likely involve flexible policies not only related to population movement but also to movements of goods and capital to achieve efficient and equitable distributions.

In view of the current barriers to migration in most parts of the world, the social, economic and political consequences of migration at these scales are far from trivial. Most governments are today ill-equipped in legislative terms to deal with this type of situation, and it is at this level that urgent attention is already needed *today* to prepare for the future.

Chapter 2

THE CLIMATE SYSTEM

2.1. ENERGY FOR THE SYSTEM

The Sun provides the overwhelming share of energy available for the Earth and its various physical, chemical, and biological components; close to 99.7% of the energy supplied to the Earth is of solar origin, while the remaining 0.3% is related to tectonic and geothermal processes.

The electromagnetic spectrum consists of numerous wave bands, ranging from microwave radiation to X-rays, and includes visible light and infrared radiation, for example. These different forms of radiation are emitted and transmitted in the form of waves that are described by their wave-length and their frequency. In principle, the higher the frequency, the smaller the wavelength and the higher the energy emitted. Two laws of radiation physics describe the energy and wave-lengths of a given segment of the electromagnetic spectrum. The first law is described by the Stefan-Boltzmann equation that quantifies the flux of energy radiated as a function of the temperature of the emitting body in terms of the following relationship:

$$F=\sigma T^4 \qquad (2.1)$$

where F is the energy flux in W/m^2, σ the Stefan-Boltzmann constant (5.67×10^{-8} $W/m^2/K^4$), and T is the surface temperature of the emitter in degrees Kelvin.

The second law is Wien's Law, that relates the wave-length corresponding to the maximum intensity of radiation for a particular temperature, and reads:

$$\lambda max = \alpha/T \qquad (2.2)$$

where λ is measured in μm, α is Wien's constant (2,897 K^{-1}), and T is the temperature of the emitter in degrees Kelvin. The surface temperature of the Sun is 6,000 K, and hence the wave-length corresponding to peak energy is close to 0.5 μm, which corresponds to the visible part of the electromagnetic spectrum.

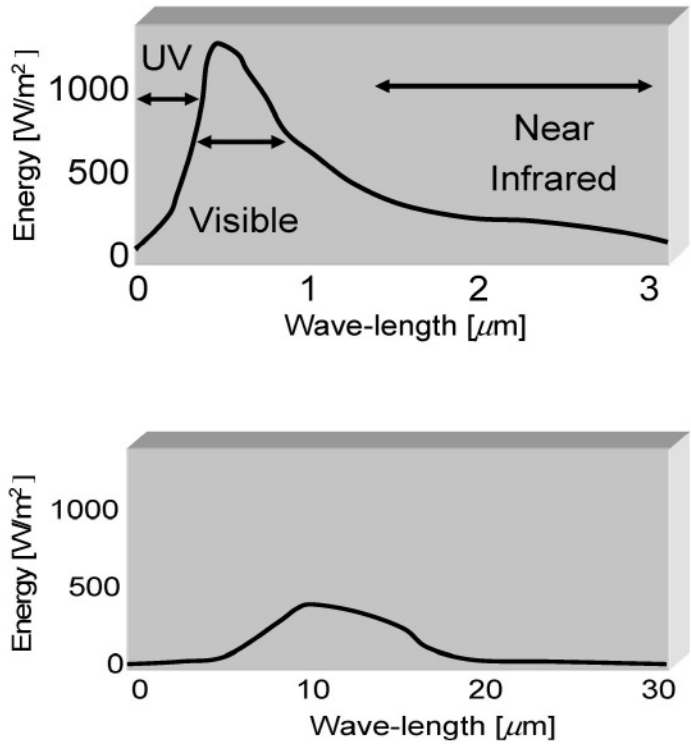

Figure 2.1. Solar energy spectrum (upper) and terrestrial infrared spectrum (lower).

However, the presence of a number of trace constituents within the Earth's atmosphere, collectively known as *greenhouse gases* complicates the overall energy balance to a large degree. The molecules of the various gases such as water vapor, carbon dioxide and methane are sensitive to the wave-lengths typical of outgoing terrestrial radiation. They enter into excitation modes that change their rotation and vibration characteristics as they absorb and re-emit infrared radiation in all directions. The action of greenhouse gases is thus to partially trap outgoing terrestrial radiation and to redistribute

this radiation as heat in the atmosphere. Indeed, without the heat-trapping effect of greenhouse gases, it is estimated that the average surface temperature of the Earth would be about -18°C, or 33°C colder than its current global value. Figure 2.2 highlights the absorption spectra of ozone, water vapor, and carbon dioxide. Ozone is seen to absorb energy within the solar and terrestrial wavelengths, while water vapor and carbon dioxide absorb well within the infrared segments of the electromagnetic spectrum.

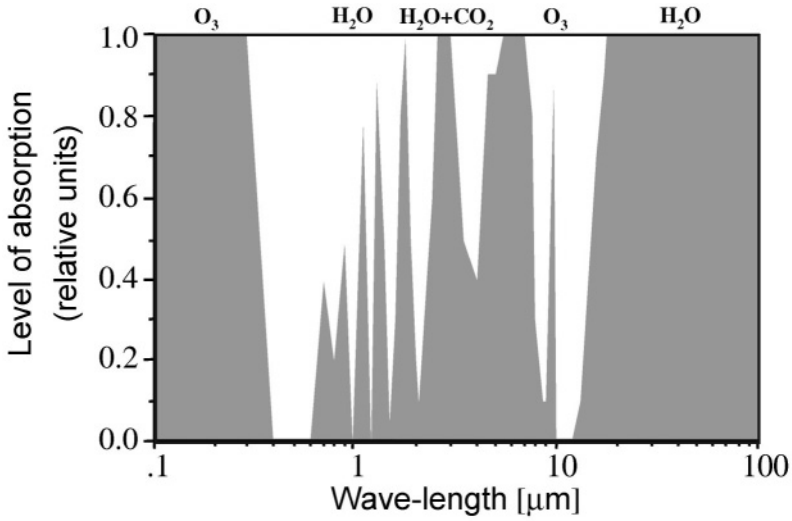

Figure 2.2. Absorption bands in the solar and infrared parts of the electromagnetic spectrum. 1 represents total absorption of a particular wave-length or wave band.

According to Kirchoff's Law, a molecule that absorbs radiation at a particular wave-length re-emits radiation at that same wave-length, whereas wave-lengths that are not absorbed are not emitted. The infrared energy emitted from the Earth's surface is thus fragmented into two parts, as seen in equation 2.3:

$$I\uparrow = I\uparrow(a) + I\uparrow(s) \qquad (2.3)$$

where $I\uparrow$ is the net emission of infrared radiation, $I\uparrow(a)$ is the infrared energy absorption by the atmosphere, and $I\uparrow(s)$ is the infrared energy lost to space.

The energy absorbed by the atmosphere can itself be fractioned into several components, as seen in the following equation:

$$I\uparrow(a) = I\downarrow + I\uparrow_a(s) \qquad (2.4)$$

with $I\downarrow$ the infrared energy re-emitted by the atmosphere back to the Earth's surface and $I\uparrow_a(s)$ the atmospheric infrared energy lost to space.

The effective infrared energy emitted from the surface is thus:

$$I = I\uparrow - I\downarrow = I\uparrow(s) + I\uparrow_a(s) \qquad (2.5)$$

The various components of the infrared emission by the Earth and the absorption and re-emission by the atmosphere are schematically illustrated in Figure 2.3.

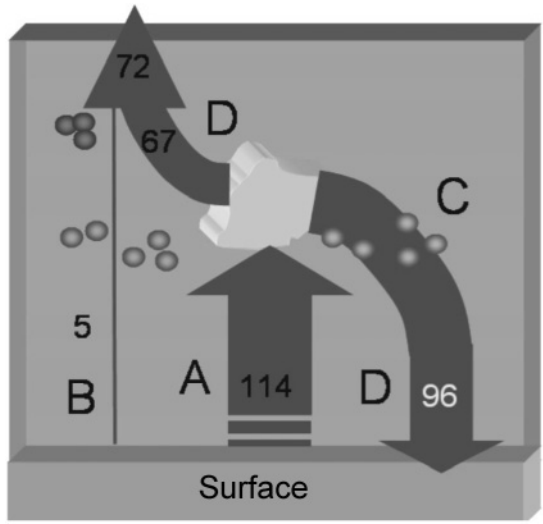

Figure 2.3. Infrared emissions by the Earth, and absorption and re-emission by the atmosphere, as a percentage of incoming solar radiation. A: Emission from the Earth; B: Direct loss to space; C: Absorption by gas and water molecules; D: Re-emission by atmospheric greenhouse gases.

A latitudinal profile of infrared radiation is shown in Figure 2.4; the inverse scale on the ordinate highlights the fact that the Earth loses energy at all latitudes, and slightly more so in the equatorial zone, where the highest emission rates are related to the maximum surface temperatures, as stipulated by the Stefan-Boltzmann equation 2.1.

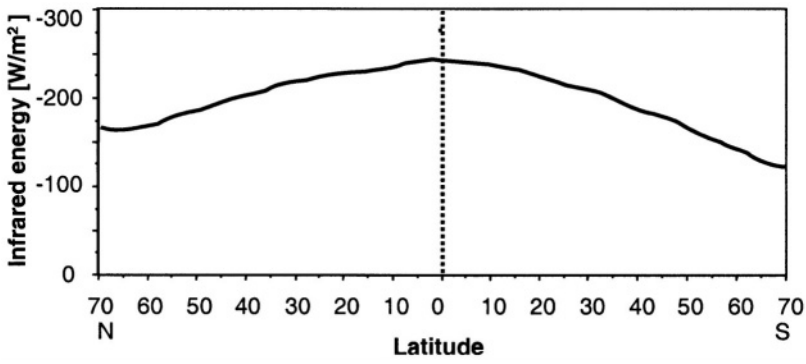

Figure 2.4. Latitudinal distribution of infrared energy. The inverse scale on the ordinate highlights the fact that the Earth loses heat at all latitudes (long-term annual average).

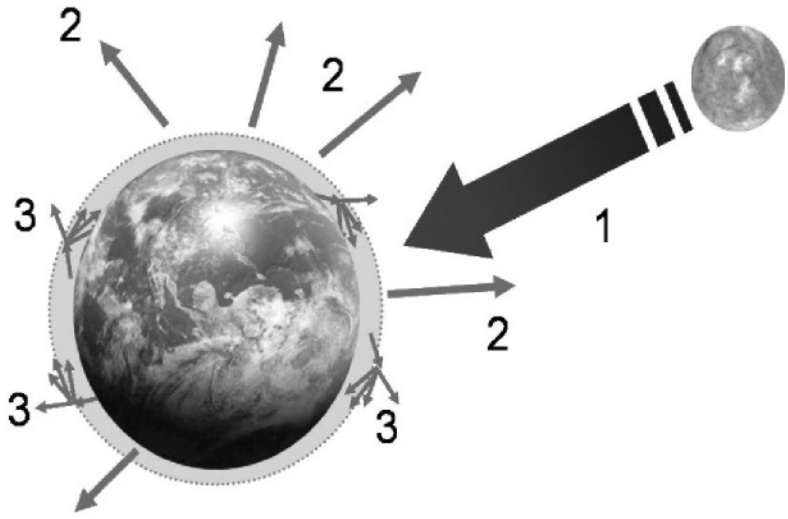

Figure 2.5. A schematic illustration of the energy balance of the Earth and the greenhouse effect. Solar radiation (1) streams towards the Earth that in turn releases energy to space (2) in the form of infrared radiation. Part of this energy is absorbed and re-emitted in the form of heat into the atmosphere (3), by a number of trace gases that are sensitive to the wave-lengths typical of the infrared spectrum (the so-called greenhouse gases).

Figure 2.5 provides a schematic representation of the radiation balance in the Earth's atmosphere. The solar energy that is intercepted at the top of the atmosphere corresponds to an average 1,468 W/m^2, known as the *"Solar constant"*. Its value is a function of the energy emitted from the outer layer

of the Sun and the distance that separates the Earth from the Sun, and can actually vary by a few tenths of percent due to the eccentricity of the Earth's orbit around the sun, sunspot cycles, etc. On a global average, only about 50% of the energy available at the top of the atmosphere actually reaches the Earth's surface, as illustrated in Figure 2.6, because of the interaction between solar radiation and the matter that lies in its path through the atmosphere.

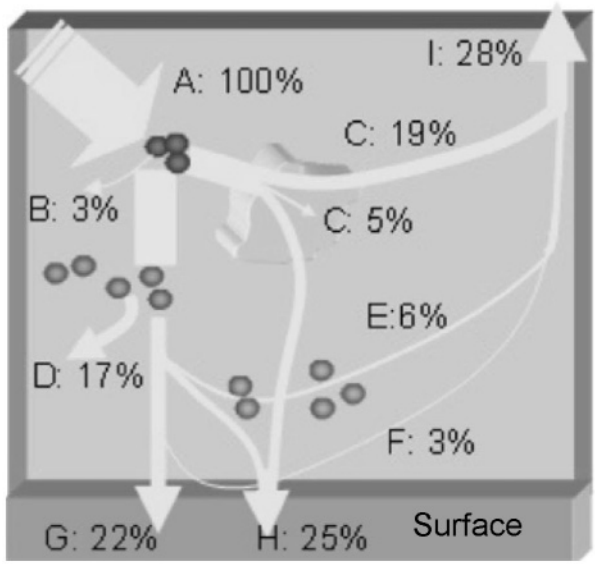

Figure 2.6. Absorption and reflection of solar radiation within the atmosphere, as a percentage of incoming solar energy (A). B: absorption by stratospheric ozone; C: absorption and reflection by air molecules; D: absorption and reflection by aerosols; E: dispersion by air molecules; F: surface dispersion; G: Direct solar radiation intercepted at the surface; H: Diffuse solar radiation received by the surface; I: Solar energy directly lost to space.

Part of the energy is absorbed by ozone molecules in the middle and upper stratosphere, while another part is absorbed, reflected or dispersed by air molecules. Solid particulate matter and clouds also reflect solar energy; clouds can in particular reflect considerable amounts of solar radiation according to the surface area that they cover. The radiation absorbed by the surface is a combination of direct solar energy that has not been reflected or absorbed in its path through the atmosphere, and diffuse solar radiation that has been diffracted and dispersed by air molecules. It can be quantified through the following equation:

$$Q_s = C_r + A_r + C_a + A_a + (Q + q)(1 - \alpha) + (Q + q)\alpha \qquad (2.6)$$

where Q_s is the incident solar radiation, C_r the fraction of radiation reflected by clouds, A_r is the reflection by air molecules and aerosols, C_a is the absorption by clouds, A_a is the absorption by air molecules and aerosols, Q is the direct component of solar radiation and q its diffuse (indirect) counterpart, and α is the reflectivity of the surface. More precisely, α is the fraction of reflected radiation at a particular wavelength.

Surface	Albedo
New snow	90
Old snow	50
Light soils	30
Vegetation	20
Dark soils	10
Clouds	50 – 90
Water surfaces*	10 – 70
Planetary albedo	36

Table 2.1. Albedos of characteristic surfaces in %. (*: Range of albedos for water surfaces depends on the solar zenith angle).

The heating efficiency of the radiation that actually reaches the ground depends on the energy per unit surface area. Because of the sphericity of the Earth, energy intercepted in the equatorial zone is concentrated over a much smaller surface area than the same quantity of energy reaching the mid or the high latitudes. As a result, there is an imbalance in the distribution of heat between the Equator and the Poles. In addition, the albedo of the surface defined in equation 2.6 determines the amount of incident solar energy that can be effectively used to heat a particular surface. Only the fraction of radiation that is not reflected by a surface can be employed to heat that surface; white surfaces, by reflecting a large quantity of radiation, do not warm as much as dark surfaces that are subject to the same amount of radiation. The heterogeneity in space and time of the reflectivity of the Earth's surface adds an additional degree of complexity to the radiative energy balance of the Earth. Table 2.1 provides an estimate of the albedos of typical surfaces. Water is seen to be the substance with the greatest range of reflectivity, from almost black to almost white, according to the zenith angle of the sun,.

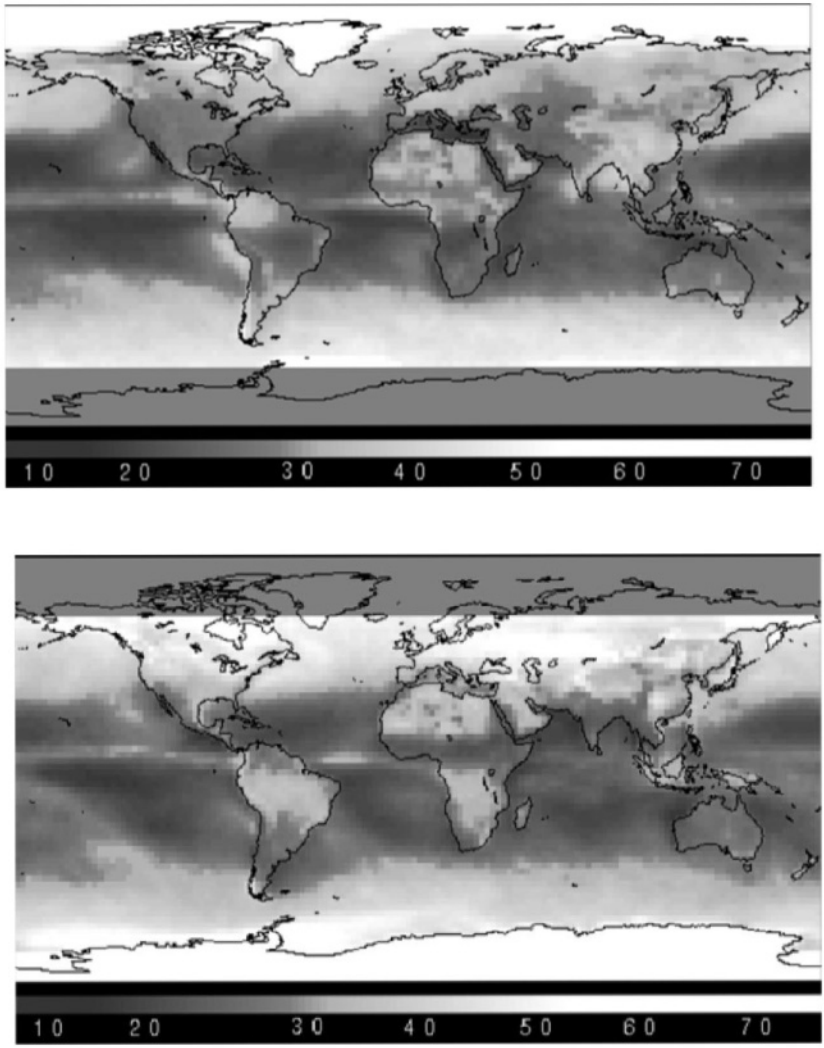

Figure 2.7. Average surface albedo in June (upper) and December (lower), based on satellite information. The scale given at the bottom ranges from less than 10% albedo (dark) to over 70% (white).

Figure 2.7 shows the seasonal difference of surface albedo as retrieved from satellite imagery, based on the ERBE (Earth Radiation Budget Experiment; e.g., Lee et al., 1987; Harrison et al., 1990) data set. Albedo exhibits a clear seasonal cycle over both the continents and in the oceans; these differences are related to the biological activity of terrestrial vegetation

and marine organisms, that respond to seasonal temperature cycles through enhanced or reduced photosynthesis and a resulting change in the pigmentation and thus the reflectivity of the organisms. Other changes in albedo are related to the distribution of seasonal snow, as seen in the high reflectivity over Northern Hemisphere continents in winter. The grey cutoff region in the polar zones is related to the arctic night conditions over Antarctica in June and over the boreal zone in December.

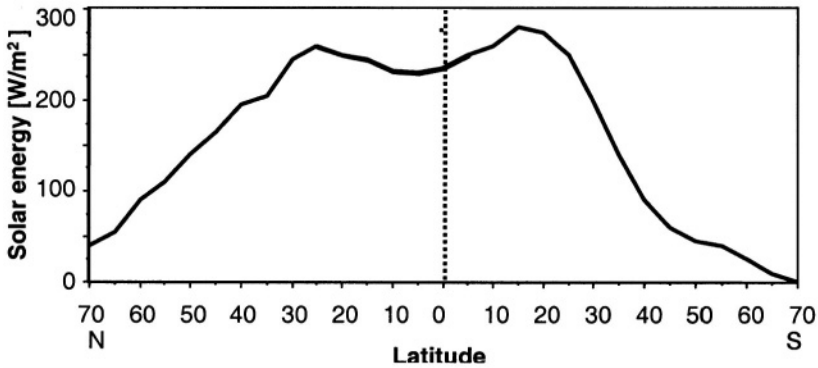

Figure 2.8. Latitudinal distribution of solar energy intercepted at the Earth's surface (long-term annual average)

Furthermore, the imbalance of heat is enhanced by the fact that the Earth loses energy at all latitudes through infrared cooling, whereas solar warming is confined to the daylight side of the Earth on a diurnal basis and to the seasonal migration of the zone of maximum energy located between the tropics. Figure 2.8, by analogy with Figure 2.3, shows the distribution of solar energy intercepted at the surface, as a function of latitude. As expected, the energy is on average minimum at the Poles, due to the fact that the surface is tangential to the path of solar radiation at high latitudes. Solar energy exhibits a double maximum around the tropics and a relative minimum close to the Equator. This is related to the fact that much of the equatorial zone is covered by clouds that reflect part of the radiation that would otherwise be at its maximum here, as it is at the top of the atmosphere. The tropics, on the other hand, are associated with arid zones and related cloud-free skies that thereby enable more incoming solar energy to reach the surface than around the Equator.

2.2. HEAT TRANSPORT FROM EQUATOR TO POLE

The net energy at the surface, i.e., the balance between solar energy intercepted at the surface, the infrared energy emitted from the surface, and the infrared energy re-emitted from the atmosphere back to the surface, exhibits a peak in the equatorial zone and a minimum at the Poles, as illustrated in Figure 2.9.

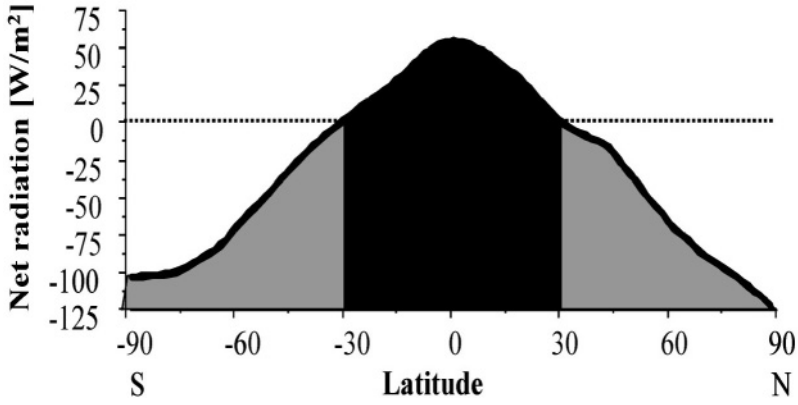

Figure 2.9. Net energy profile at the Earth's surface as a function of latitude. Black shading: regions where there is an excess of energy; gray shading; regions where there is an energy deficit.

Net energy R can be quantified through the following relationship:

$$R = (Q + q)(1 - \alpha) - I \qquad (2.7)$$

with Q and q defined in equation 2.6 as direct and diffuse solar radiation, respectively, α is the albedo, and I the effective infrared emission emitted to space by the Earth.

Figure 2.9 emphasizes the excess of solar energy over infrared energy loss in between the tropics poleward of about 35° latitude, there is a net loss of energy, whereby solar radiation can longer compensates for terrestrial long-wave radiation to space. Long-term annual values of net radiation around the globe exhibit a seasonal migration of areas of net surface radiation. This reaches maximum values over continents and low-latitude oceans that warm considerably during the summers in both hemispheres, as illustrated in Figure 2.10 for June and December.

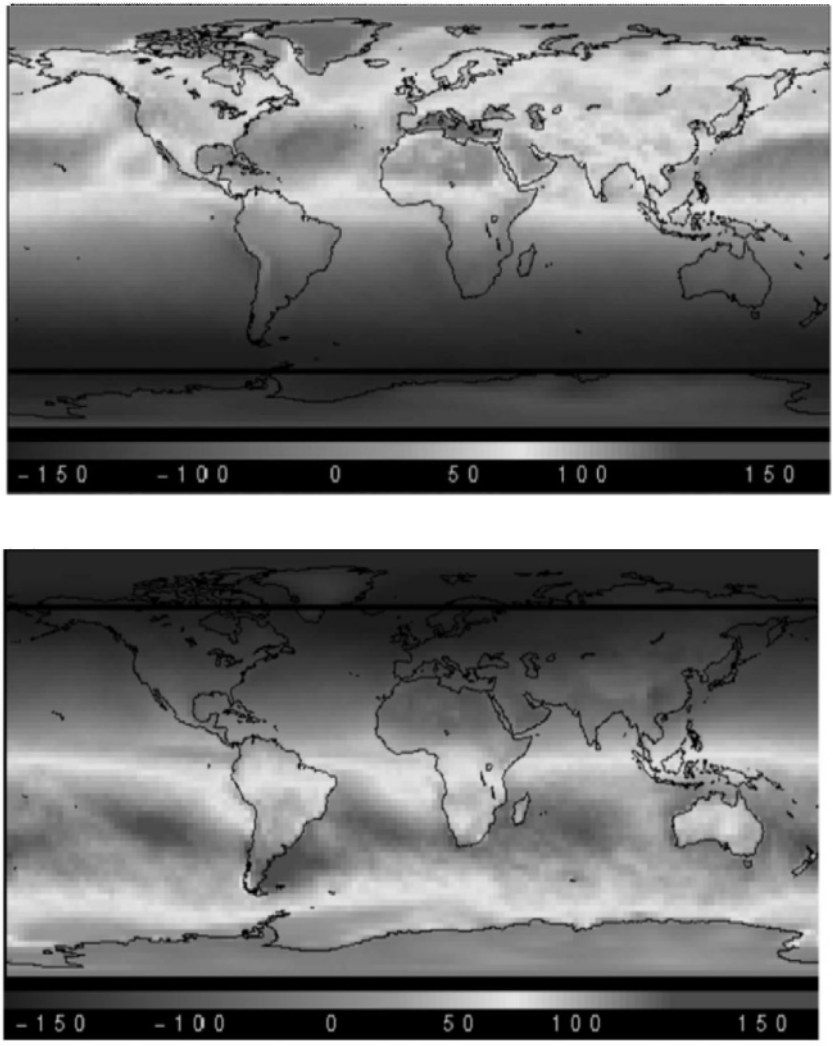

Figure 2.10. Distribution of net radiation for June (upper) and December (lower). Scale in W/m^2 is given at the bottom of each figure (long-term annual averages)

The imbalance in energy needs to be compensated for by an Equator-to-Pole transfer of heat. This transfer is regulated by ocean and atmospheric currents that transport large quantities of heat embedded within the fluid motions in a process known as advection. The advection of heat is estimated at about 6 PW (Petawatts, or 10^{15} Watts), which is roughly 3 orders of magnitude greater than the total annual energy used collectively by the

global economy. Heat transfer mechanisms also include latent heat release associated with condensation and precipitation processes; moisture that condensates releases considerable amount of heat that is then advected by atmospheric flows towards colder regions. Figure 2.11 shows the meridional transport of heat, separated into the three major components, i.e., ocean circulations, atmospheric flows, and latent heat. In contrast to the atmosphere, ocean circulations contribute little to the total meridional heat transport, except in very specific regions. Close to 50% of the meridional heat transport by ocean eddies in the Northern Hemisphere takes place in the Atlantic Ocean (Ganachaud and Wunsch, 2000). Warm near-surface waters are directed from the Caribbean towards the north-east as part of the wind-driven flows in the narrow western-boundary current commonly referred to as the Gulf Stream that extends into Greenland Sea. Heat transfer resulting from latent heat release is most pronounced in the equatorial zone, particularly over the tropical oceans where the large sources of heat and moisture continuously feed cloud systems. In the Northern Hemisphere mid-latitudes, storm systems traveling eastwards act as a relay for exchanging heat polewards across the so-called *"Polar Front",* which is the narrow interface separating warm tropical air from cold air masses of polar origin.

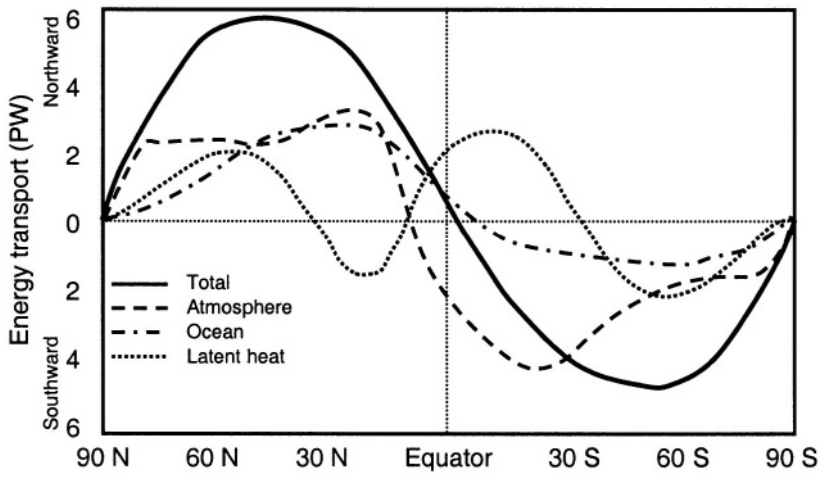

Figure 2.11. Total meridional heat transport and its oceanic, atmospheric, and latent heat components (Following: Bryden and Imawaki, 2001).

A conceptual model that explains the transfer of heat in the atmosphere from the Equator to the Poles was put forward in the 18th century by the British physicist George Hadley. This idealized model suggests that energy

transfer is carried out in the form of circulation cells that, in a 2-D representation resemble those illustrated in Figure 2.12. Each of the three major cells acts to transfer heat polewards in a manner analogous to a series of interconnected conveyor belts.

Close to the Equator, the strong surface heating by the Sun leads to high thermal instability, thereby resulting in the ascent of large quantities of moist air. The rising air condenses and generates deep convective cumulonimbus-type clouds. When these clouds reach the top of the troposphere, the energy they contain is generally no longer sufficient to penetrate higher into the stable layers of the stratosphere. The mass of air transferred by the clouds therefore flows horizontally north and south of the Equator in the vicinity of the tropopause, whose altitude in the equatorial zone often exceeds 15 km.

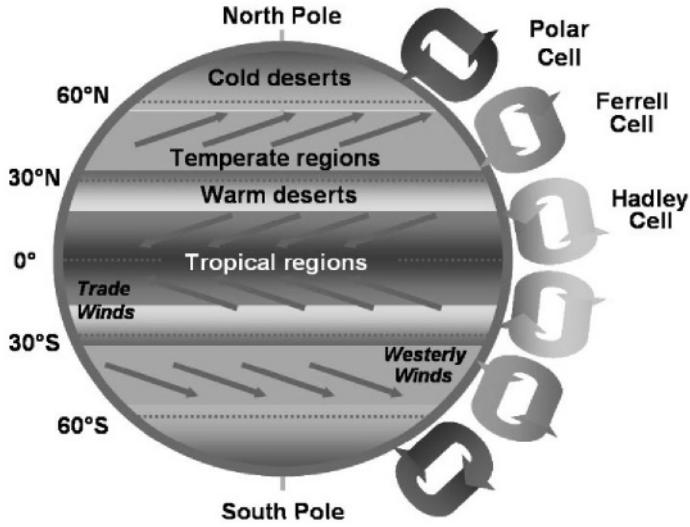

Figure 2.12. A conceptual view of poleward heat transfer in the form of circulation cells. Dominant flow direction in the tropics and mid-latitudes are also shown, as are the principal climatic zones associated with these circulations.

At these high elevations, the air cools and becomes progressively denser as it moves away from the Equator. Close to the tropics, in a band situated roughly 25-30° latitude north and south of the Equator, the dense air subsides and begins to warm by adiabatic compression; at the surface, the generally arid or semi-arid environments of continental areas located in these latitudes are intimately related to the subsiding branch of the Hadley Cell. In order to satisfy continuity principles, flow returns towards the Equator in order to close the circulation cell.

In the temperate latitudes, the Ferrell Cell acts to transfer warm air masses of tropical origin towards higher latitudes, where it ultimately encounters the Polar Cell. The interface between the two cells (the "Polar Front") is characterized by perturbed atmospheric systems that are accompanied by significant storm activity, the formation of clouds and precipitation systems, and associated latent heat release, which is then communicated to the Polar Cell for the final segment of the poleward heat transfer.

The concept of circulation cells also helps to explain the presence of the major climatic zones of the globe as a function of the location of these circulations. Warm, moist, and rising air with associated abundant year-round precipitation is responsible for the presence of tropical vegetation, while on the contrary, subsiding air close to the tropics serves to explain the presence of arid or semi-arid zones. In the mid-latitudes, the principle source of moisture resides in storm activity that transports large quantities of humidity from the oceans to the continents, while in the high latitudes, the air masses associated with the Polar Cell are essentially cold and dry. This simple scheme can be completed by including further climatic zones at the interface of the principal regions highlighted in Figure 2.12, such as Mediterranean climates located between the tropical and the temperate zones, or other more subtle distinctions related to the degree of continentality of a particular geographical location.

Although an oversimplified and theoretical view of the world, the conceptual framework of the Hadley circulation has a physical basis. In reality, the circulation patterns that enable Equator-to-Pole heat transfer is rendered more complex by numerous factors, such as the influence of the rotation on the Earth on atmospheric flows (the *"Coriolis Force"),* surface heterogeneities that include the uneven distribution of continents and oceans, the presence of topography, and local heat sources or sinks related to the nature of the underlying surface.

2.3. ELEMENTS OF THE CLIMATE SYSTEM

Figure 2.13 provides a schematic illustration of the different components of the climate system that are important for its evolution on time scales ranging from minutes to millennia. Each of the individual elements depicted in this figure have their own complex behavior, and the interactions between them can take place at widely varying time and space scales.

2.3.1. The atmosphere

The atmosphere is the most rapidly reacting element of the system, because of the high level of dynamics associated with atmospheric motion. It is here that the radiative exchange takes place, and where most of the high-frequency changes related with day-to-day weather occur

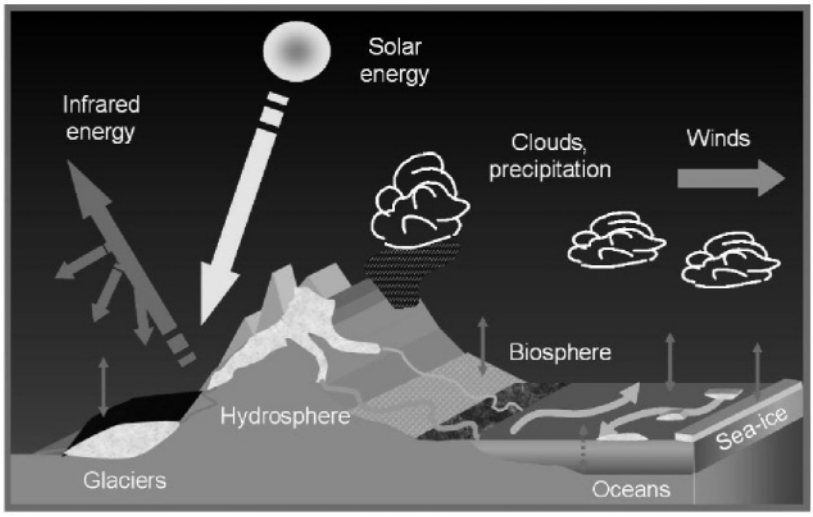

Figure 2.13. A schematic illustration of the climate system.

As mentioned in the preceding section, the atmosphere transports a large amount of heat polewards through atmospheric motion and elements such as clouds that allow additional heat to be injected into the atmosphere through condensation processes. The atmosphere reacts to numerous forcings in addition to the exchange of solar and terrestrial radiation mentioned earlier in this chapter. The Earth's surface acts as a physical boundary to atmospheric dynamics and as a source of complex sources and sinks related to spatial and temporal heterogeneities in roughness, heat, and moisture. These are reflected for example through land-use characteristics where surface-induced friction effects are a function of the type of land cover, in particular urban areas, vegetation surfaces, bodies of water, or snow and ice. The thermodynamic structure of the atmospheric boundary layer (ABL) is also a function of surface temperature and moisture heterogeneities linked to vegetation type and the presence of rivers, lakes or oceans.

Many flows occurring in nature and in engineering applications are turbulent and with the exception of very stable thermal conditions, the ABL is inherently turbulent. It should be noted that turbulence is not a feature of fluids but of *fluid flows.* One major characteristic of turbulent flows is their irregularity, or random nature, that makes a deterministic approach to the problem intractable. Turbulent flows are always dissipative, since viscous shear stresses perform deformation work, thereby increasing the internal energy of the fluid at the expense of the kinetic energy of the turbulence. Turbulent motion within atmospheric flows can have profound consequences for features embedded within these flows, in particular the diffusion (or dispersion) of heat, moisture, momentum, and gaseous compounds and aerosols. The intensity of turbulence can be related to purely dynamic factors, such as the roughness of the surface and its interactions with atmospheric flow above, the vertical deformation of the flow (or *wind shear*). It may also be influenced by thermal processes related to atmospheric stability or, obviously, by a combination of both dynamic and thermal features.

Cloud formations, especially the turbulent cumulus type, are capable of generating significant dynamic and thermodynamic modifications in the atmosphere. The formation of cloud condensation droplets is accompanied by the release of latent heat; at the cloud edges and cloud top, evaporation of liquid droplets leads to latent heat absorption and corresponding cooling of the neighboring cloud-free air. In dynamic terms, a cumulus-type cloud is an unstable and turbulent phenomenon that acts to restabilize the vertical thermal stratification of the atmosphere. Exchange of air at the cloud boundaries can result in secondary circulations that perturb atmospheric flows from the surface through to the upper troposphere.

Stratiform clouds exert an influence on the atmosphere through interactions with radiative fluxes rather than through turbulent exchange of heat and moisture. The high reflectivity of the upper boundary of these clouds reduces the incoming solar radiation at the surface, while the base of these types of cloud are relatively opaque to outgoing terrestrial radiation and thus trap heat in the lower atmosphere. The interaction between clouds and radiation in the atmosphere is still a subject of intense research because of the uncertainties that still subsist as to the net global effect of clouds on the climate system, i.e., warming or cooling.

Precipitation processes are closely linked to cloud formation and in a cumulus-type cloud, for example, precipitation is the sign of a stabilization or decay of cloud growth, and therefore an attenuation of the cloud dynamic and thermodynamic influence on its atmospheric environment. As rainwater exits its saturated cloud environment, it partially or totally evaporates,

thereby cooling the layers beneath the clouds and thus stabilizing the sub-cloud atmosphere. In the case of moderate to heavy rain, the combined thermodynamic effects of evaporation cooling and dynamic effects of rainwater fallout lead to a reversal of vertical motion, cutting off the cloud from its low-level dynamic and moisture sources and leading to its ultimate decay. The different characteristics of precipitation can significantly modify the structure of the ABL and its influence on the evolution of the larger-scale atmosphere.

2.3.2. The oceans

The oceans are certainly the most important element of the climate system on time scales ranging from decades to centuries, because of the large thermal capacity of water compared to land, that serves to act as a thermal modulator of climate. The diurnal and annual ranges of temperatures in a maritime climate are markedly less than in regions far removed from the oceans. Because the ocean represents a large source of moisture, there is also more precipitation in a maritime climate than in a continental one, provided the dominant wind direction is onshore.

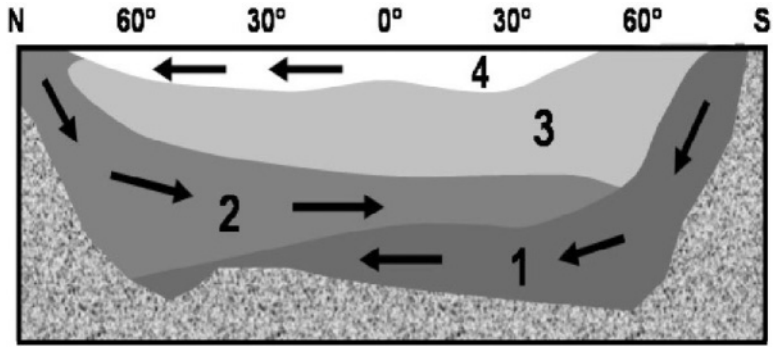

Figure 2.14. Schematic illustration of deep-water formation in the Atlantic. 1: Antarctic Bottom Water, very cold and nutrient rich; 2: North Atlantic Deep Water, cold and nutrient rich; 3: Intermediate Water; 4: Surface Water, warm and nutrient poor. Direction of flows are indicated by arrows.

Ocean circulations are complex flows that determine current climate and major shifts in climate that have occurred in the past. They consist of surface gyres that are driven by atmospheric flows, and deep water currents that are the consequence of sinking water masses in specific regions of the global

ocean. In the Northern Hemisphere, the only location where deep-water formation occurs is in the northern North Atlantic Ocean, where cold air outbursts originating in the Arctic and storm activity associated with frontal systems crossing the Atlantic are capable of extracting sufficient amounts of heat from surface waters for these to become dense enough to sink. Furthermore, because the surface waters originating in the warm Caribbean region are laden with salt, this salinity further augments the density that has risen because of lower temperatures. Figure 2.14 provides a schematic view of the formation of North Atlantic Deep Water (NADW) off the coast of Greenland (e.g., Gordon, 1986; Schmitz, 1995).

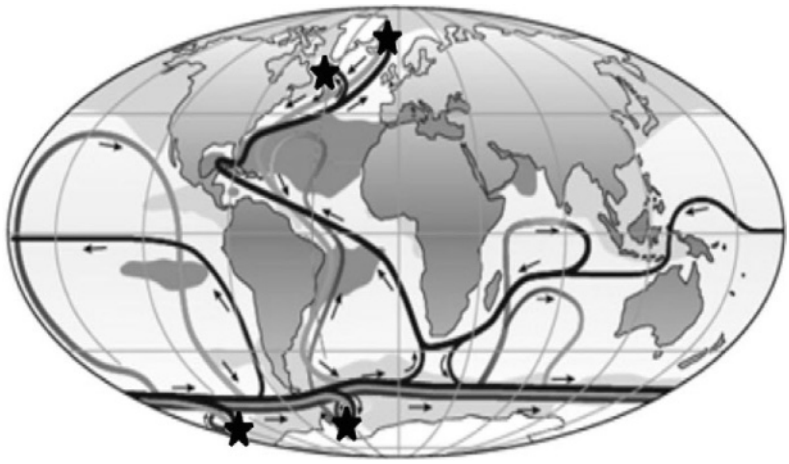

Figure 2.15. A sketch of the atmospheric thermohaline circulation, following Rahmstorf (2003). Dark lines represent surface currents, while lines with increasingly lighter shading refer to deep and bottom currents, respectively. Light gray shading on the oceans indicates regions of low salinity (<34 °/oo) and dark gray shading represents high salinity (> 36°/oo) Dark stars mark the sources of deep water formation in the Greenland and Labrador Seas, and the Ross and the Weddell Seas around Antarctica.

The dual control of temperature and salinity on ocean current densities has led to the notion of the *"thermohaline circulation"* (i.e., salinity *and* temperature driven currents), where an intricate set of interconnected surface and deep ocean currents circumvent the globe in what is sometimes referred to as the *"ocean conveyor belt"*. The North Atlantic Ocean is unique in its contributions to deep water formation (Figure 2.14), because although the Pacific and Indian oceans have similar surface gyres, their surface waters are never saline enough to lead to sinking. The amount of heat transported in the

mid and high latitudes is thus greater in the North Atlantic than at similar latitudes in the Pacific, resulting in the generally mild conditions that western and central Europe experience. In the Southern Hemisphere, waters in contact with the sea ice in the vicinity of the Antarctic cool sufficiently to sink here also, thus contributing to an important part of the deep-ocean circulations south of the Equator. The thermohaline circulation is thus a consequence of gradients of sea surface density in which waters are warmed in the tropics and cooled at high latitudes. Turbulent mixing enable heat to be mixed into deeper layers of the oceans, and as a result the effective heating source is located deeper in the ocean and thus at higher pressures than the cooling that occurs at high latitudes. The differential heat and pressure between the warm and cold parts of the ocean provides the mechanical energy to drive the currents that make up the ocean conveyor belt. Figure 2.15 provides an illustration of the intricacies of the thermohaline circulation.

2.3.3. The cryosphere

The cryosphere includes snow, continental ice caps such as Antarctica and Greenland, mountain glaciers, and sea ice. The interactions between snow, ice and the atmosphere influences the net energy balance due to the high albedo, low thermal conductivity, and large thermal inertia of these surfaces. The cryosphere contributes to instabilities in the atmospheric general circulation as a result of temperature differences between the Poles and the Equator. The intensity of feedbacks between elements of the cryosphere and the climate system is in direct proportion to the surface area covered by snow or ice. Snow affects continental heating and sea ice is critical in determining the upper ocean mixing and the energy exchange between the surface and atmosphere. Snow and sea ice have a marked seasonal cycle, and therefore the signal generated by the presence of cold, reflecting surfaces in the atmosphere varies during the year according to changes in the areal extent of snow and ice. Over continental areas, the interaction of snow surfaces with the atmosphere are more pronounced in the Northern Hemisphere because of the much larger area covered by land masses here compared to the Southern Hemisphere.

Sea ice is a fundamental component of the cryosphere because it controls heat, moisture, and salinity fluxes in the polar oceans. Sea ice insulates the relatively warm ocean waters from the much colder atmosphere of the polar regions, with the exception of cracks in the ice that enable a direct ocean-atmosphere exchange of energy and vapor.

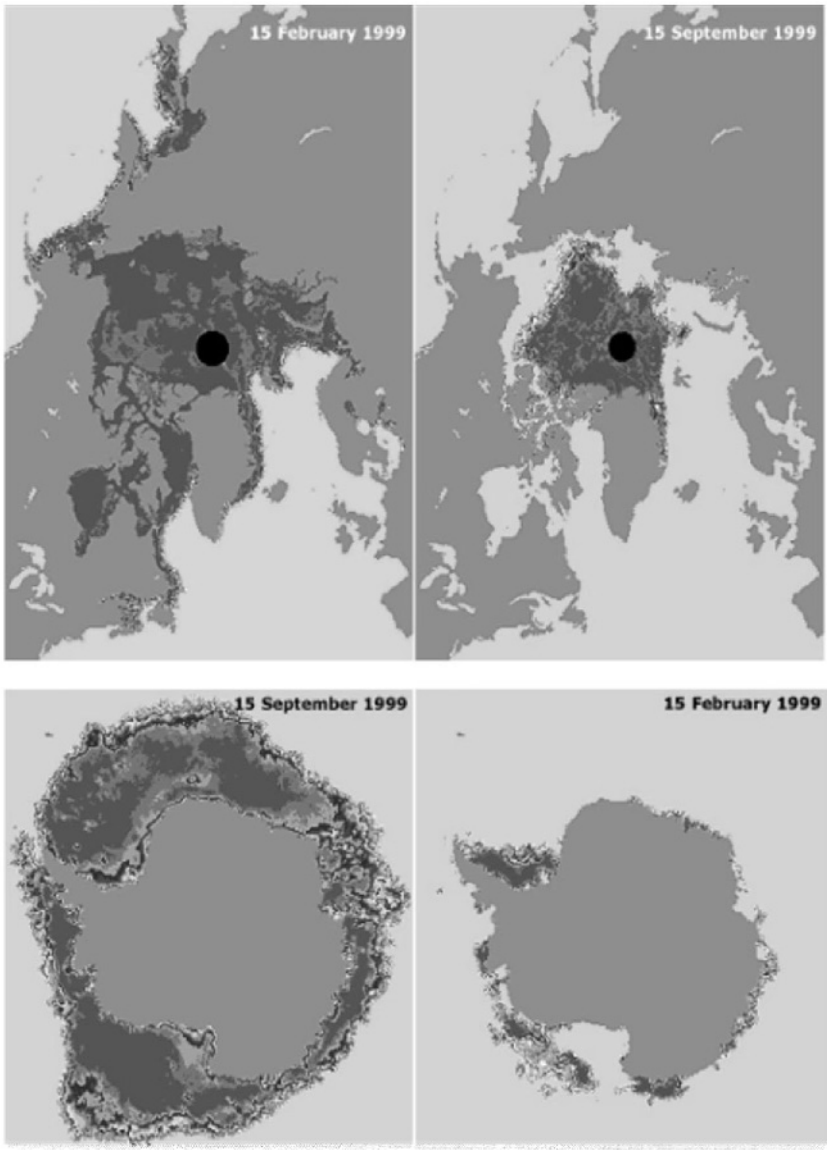

Figure 2.16. Contrasts in sea-ice extent in the Arctic Ocean basin (upper) and around Antarctica (lower), for winter and summer. Examples for 1999 based on satellite imagery Gray shading offshore from the continents indicates presence and thickness of sea ice. (Images courtesy of the National Snow and Ice Data Center, University of Colorado, USA).

In addition, sea-ice has a relatively high albedo value (e.g., Grenfell and Maykut, 1977), so that useable solar energy at the surface, already small in

the high latitudes, is very low because of the added effect of surface reflectivity when the sun is above the polar horizon.

The total surface area of sea ice and its mean thickness, as well as the fraction of open water within the ice pack responds very sensitively to climatic conditions. The total area of sea ice typically ranges from 14-16 million km^2 in the Arctic and 17-20 million km^2 around the Antarctic. The seasonal fluctuation of sea-ice extent is much greater in the Antarctic than in the Arctic. Typical sea-ice extent in winter and summer are illustrated in Figure 2.16 for a particular year (1999). The maximum and minimum extent of sea ice changes from year to year according to annual and seasonal climate characteristics. Serreze et al. (2003) have shown that the reduction in Arctic sea ice reached record proportions in 2002, a conclusion that is certainly consistent with recent global warming trends.

2.3.4. Water and the hydrological cycle

Water and associated hydrological processes form an integral part of the climate system. Water is present in abundance in the oceans (97.3% of all water in the Earth system), while the remaining 3% represents the availability of fresh water. Of this minor fraction, 77.4% is stored in the form of ice in the continental ice caps, mountain glaciers, and snow, while ground water accounts for about 22.1%. Surface water makes up only 0.4% of available freshwater, and water in the atmosphere represents a mere 0.04%. In view of this seemingly minor fraction of water in the atmosphere, it is remarkable that so many key processes which take place within the atmosphere are related to the presence of moisture and the energetics related to the phase changes of water.

The hydrological cycle represents the balance between water masses that are evaporated from the surface (85% over the oceans; 15% over land) and those that are returned to the ocean via precipitation and surface runoff or ground-water. Part of the solar energy that is available at the Earth's surface is consumed by evaporation processes in the oceans, lakes, rivers, and vegetation. The water that thus enters the atmosphere in vapour form can undergo substantial thermodynamic transformations, whereby phase changes of water allow it to exist in the forms of vapor, liquid, or ice. When changing phase, water molecules absorb or release large quantities of heat, which is then transported by atmospheric flows. Moving air masses transfer moisture and its thermodynamic properties to areas far removed from those where the initial surface evaporation takes place. Precipitation over the continents in the form of rain or snow will ultimately return to the oceans through river

systems; seasonal snow-pack at high latitudes or altitudes melts in the spring and supply water to many rivers. Part of the precipitation that falls on land surface filters into the ground and recharges the ground water table.

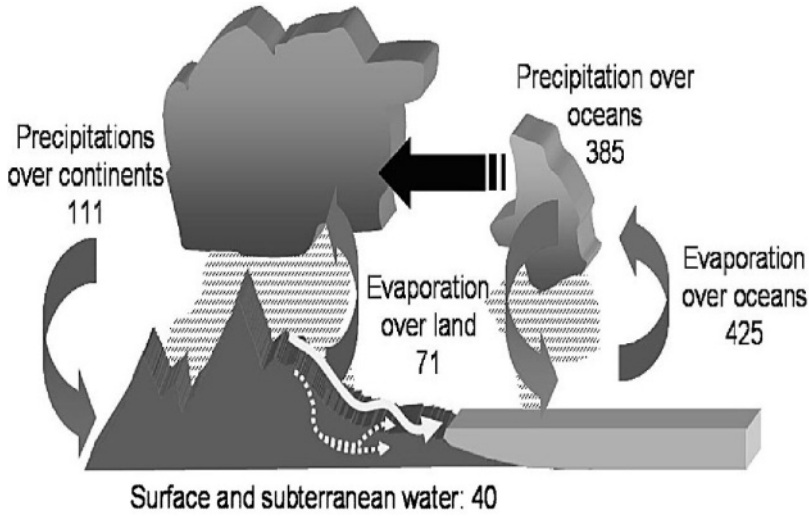

Figure 2.17. Elements of the hydrological cycle. Figures are in thousands of km^3 per year.

According to the geological characteristics of the substratum, ground water may have long residence times, sometimes of the order of millennia. By transporting moisture over large distances that feed into hydrological basins around the world, the atmosphere contributes to particular processes such as freshwater fluxes into the oceans that are capable of modifying the density of sea-water and thereby modulating the delicate balance of the thermohaline circulation. Moisture transports to high latitudes or high altitudes supplies precipitation in the form of snow that allow snow and ice to play their crucial role in surface-atmosphere interactions. Figure 2.17 provides an overview of the components of the hydrological cycle and the quantities of water that are associated with each part of the cycle.

2.3.5. The biosphere

The terrestrial and marine biosphere interacts with the climate system in a number of complex and subtle ways. One of the primary effects of the biosphere is on surface albedo, and according to the surface area covered by a particular biome, the feedback between a vegetation surface and the

atmosphere can be quite marked. Forests have relatively low albedos compared to deserts (30%) or ice caps (up to 80%), ranging from 15% for deciduous forests to about 10% for evergreens (Barry and Chorley, 1992). Tropical forests of the Amazon, equatorial Africa, or SE Asia even have reflectivities as low as 7%. The vast forests of the boreal zone and those close to the Equator play a major role in the surface energy balance.

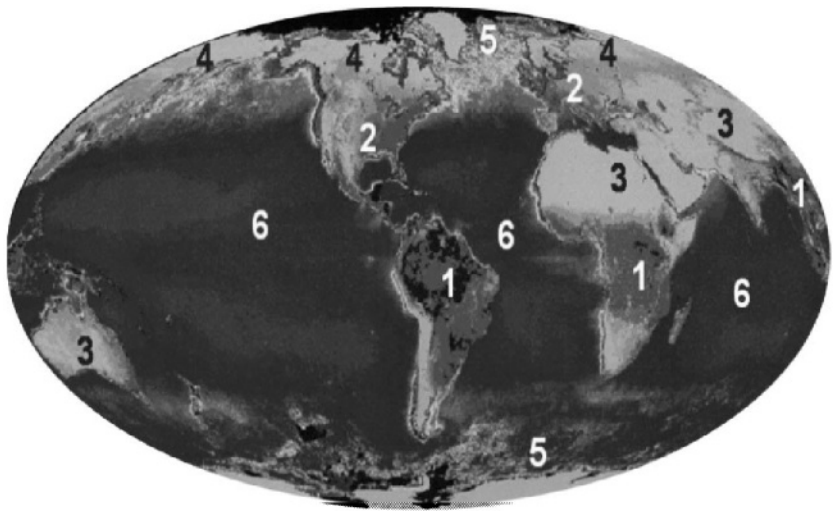

Figure 2.18. A simplified chart of the distribution of terrestrial and marine biomes and their influence on surface albedo as seen in this composite satellite image. A very succinct breakdown of biomes includes 1: Tropical forests; 2: Temperate forests; 3: Deserts; 4: Boreal vegetation; 5: High marine productivity of cold waters; 6: Low marine productivity of warm waters.

Agricultural practices have also modified the natural vegetation in many parts of the world, including the albedo of the surface. Natural vegetation and crops are influenced by the seasonal cycle in the mid and high latitudes, thereby adding a degree of complexity to surface albedo through seasonal changes in reflectivity that act to enhance or reduce feedbacks with the atmosphere. Figure 2.18 shows a composite satellite view of the average distribution of terrestrial and marine biomes; these latter are seen to be concentrated in cold waters of the northern and southern oceans, where nutrients are most abundant.

The fluxes of many greenhouse gases such as carbon dioxide and methane are regulated by both the terrestrial and the marine biosphere. Plankton in the surface oceans utilise the dissolved carbon dioxide for photosynthesis. There is thus a flux of carbon directed from the atmosphere

towards the oceans; the oceans thus act as a carbon sink. When marine organisms, the carbon they contain sinks towards the deep ocean, where it accumulates in the sediments on the ocean floor. The carbon cycle within the ocean significantly modulates the atmospheric concentrations of carbon dioxide (Broecker, 1982). Solid particles (aerosols) of organic origin are emitted by the biosphere through numerous biological processes (e.g., pollen, spores, or by-products of biomass combustion), thereby scattering incoming solar radiation, at least on local and regional scales as seen in Figure 2.19.

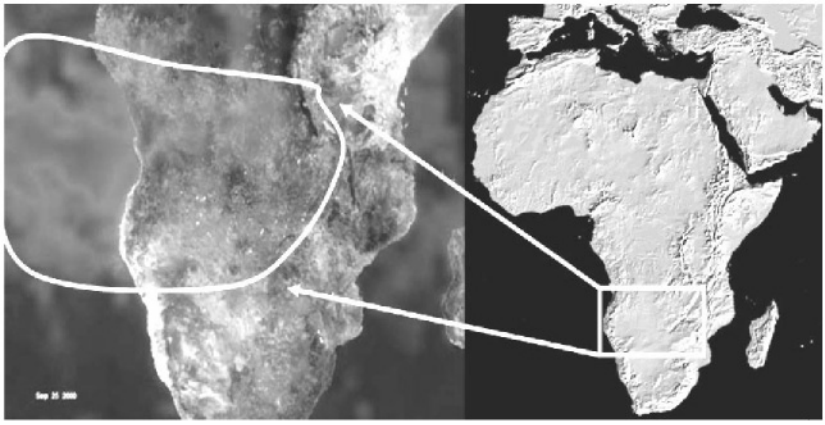

Figure 2.19. Satellite view of aerosol loading in the atmosphere during a spate of forest fires in southern Africa. The spatial extent of aerosols provides an estimate of their potential influence on the net energy budget at the Earth's surface.

Primary productivity in the oceans results in the emission of a number of compounds such as DMS (Dimethyl sulfides), which can act as condensation nuclei that enhance the efficiency of cloud formation (Charlson et al., 1987). Marine emissions of DMS and other aerosols produced by the terrestrial biosphere thus indirectly affect the thermal balance of the atmosphere through their influence on cloud formation and distribution (e.g., Charlson et al., 1992).

Additional feedbacks between vegetation and the atmosphere include the modulation of turbulence in the lowest layers of the atmosphere, through differential roughness elements at the surface, and the flux of water vapour to and from the surface. Evapo-transpiration processes in vegetation canopies act to transfer moisture from the soils to the atmosphere; this effect can be quite significant in many parts of the world and, for example, the Amazon rain-forest pumps large quantities of moisture from the surface to

the atmosphere that are subsequently transported over large distances through atmospheric dynamics.

2.3.6. The lithosphere

A final component of the climate system that exerts an influence mainly over geological time scales is the geosphere, consisting of the various tectonic elements of the Earth, and lithospheric elements such as rocks and sediments. Continental drift has modified the relative distribution of oceans and land masses, and the positioning of continents in past geologic ages compared to today, has modified climate to a very large degree (e.g., Ruddiman and Kutzbach, 1991) by controlling energy exchange between land, oceans, and the atmosphere.

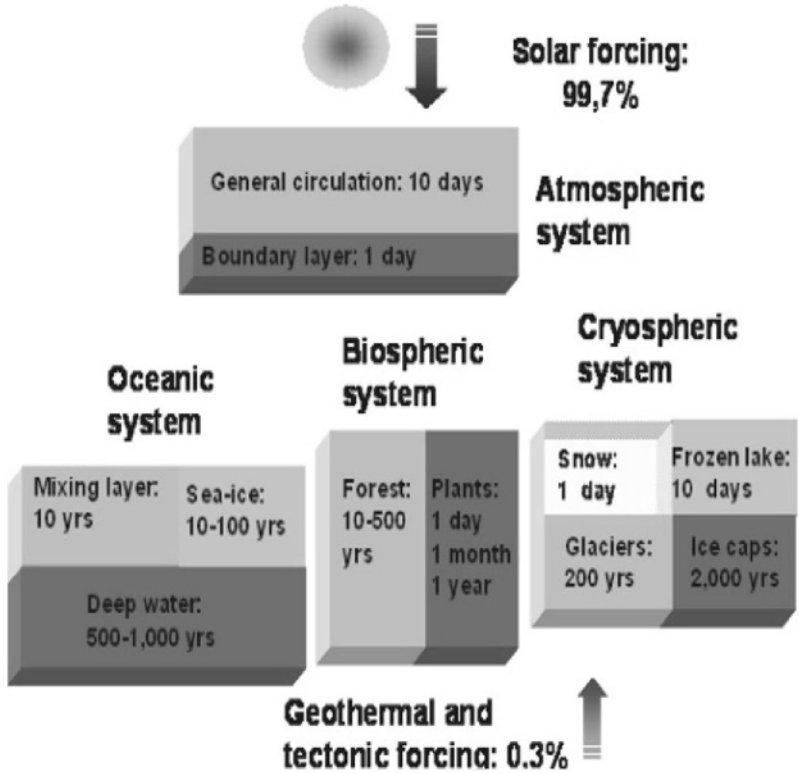

Figure 2.20. Typical response times of elements of the climate system to a perturbation.

On shorter time-scales, volcanic activity as part of a number of geospheric processes emits large quantities of aerosols and greenhouse gases into the atmosphere, thereby changing the radiation balance over much of the globe for a few months to a few years (Sear et al., 1987). Processes such as weathering can affect the albedo and moisture characteristics of soils, as well as the vegetation that is related to particular soil types; over time, such changes can influence the quantities of greenhouse gases that are exchanged between the atmosphere and the terrestrial biosphere (McBean and McCarthy, 1990).

The response or adjustment time of an element of the climate system to a perturbation varies widely from one element to another, as summarized visually in Figure 2.20. Because of its high dynamics, the atmosphere responds rapidly to a forcing, while adjustment times to a given level of perturbation range from decades in the upper layers of the oceans to millennia in the deep oceans. The range of temporal responses in the cryosphere is even more extreme, from less than a day (in the case of a shallow layer of snow exposed to sunlight, for example) to millennia (in the case of the partial or total melting of polar ice caps, notably). These highly variable time responses between individual elements of the system make a full understanding of the exchange processes, and their modeling, extremely complex.

Chapter 3

NATURAL FORCING OF THE CLIMATE SYSTEM

3.1. EXTERNAL FORCING OF CLIMATE

The climate system is in perpetual evolution as it responds to a range of forcing factors. It is possible to distinguish between *external* and *internal* forcings of the system. External forcings are essentially linked to changes in the orbital parameters of the Earth that control the intensity and location of incident solar radiation, and fluctuations in solar energy.

Internal forcings comprise all those that occur within the Earth system itself, in particular volcanic activity, fluctuations in ocean circulations and large-scale changes in the marine and terrestrial biosphere or in the cryosphere. Over the past two centuries, since the beginning of the industrial era, an unprecedented forcing has been added by human activities in a range of socio-economic sectors, in particular energy, industry, agriculture, and land-use/land-cover changes.

3.1.1. The astronomic forcing of climate

In the course of its 4.5 billion-year history, Earth's climate has been relatively warm for about 90% of the time. Climate has changed on long time scales in response to the evolution of the Sun and to changes linked to tectonic activity that has marked various geological eras and volcanic activity that has influenced the chemical composition of the atmosphere. Ice ages that are a sign of particularly cold conditions at the global level have been relatively rare and geological evidence suggests that the first signs of glaciation appeared about 2.3 billion years ago (Berger, 1978; 1992). Prior to

that period, the Earth was apparently free of ice, despite the lower solar luminosity that is characteristic of the life-cycle of a star such as the Sun. Lower levels of solar energy were probably compensated for by an enhanced greenhouse effect in an atmosphere containing far more carbon dioxide than today. Between 900 and 600 million years before present (BP), there is geological evidence of at least three glacial periods that affected the low latitudes, with a further two major glacial epochs occurring between 600 and 100 million years BP. The subsequent 50 million years appear to have been globally warm and the planet generally free of ice. From 50 to 3 million years BP, a slow but steady global cooling trend took place, with the appearance of the Antarctic ice sheet around 30 million years BP that attained its current configuration roughly 14 million years ago. In the Northern Hemisphere, the first unequivocal signs of repeated glaciations begin 3 million years BP, at which time the Earth entered into the Quaternary Era, with a quasi-cyclic sequence of glacial and interglacial periods that each lasted around 100,000 years. During these cycles, it is estimated that it takes about 90,000 years to accumulate sufficient ice over the continents to form the ice-caps common to all glacial epochs. These ice ages terminate relatively rapidly, and are replaced by the warmer interglacial periods such as the contemporary epoch. The build-up and termination phases of the ice ages are thus highly asymmetric, with a corresponding asymmetry in the response of climate to glacial and interglacial period.

The current interglacial period, known as the Holocene, began about 10,000 years ago following the termination of the last ice age and the last glacial maximum that occurred about 21,000 years ago. At that time, there was probably an additional volume of ice of around 50 million km^3 compared to today, in particular over northern Eurasia and North America. The water stored in the ice was pumped from the oceans, whose level was about 120 m lower than current mean sea level. Despite the extremes of cold that resulted in the formation of continental ice caps, the average surface temperature of the globe was only 5°C less than its present value. Figure 3.1 shows a climate-model estimation of global temperature distribution during the last glacial maximum.

The coldest regions where the ice caps developed, are seen to be located over northern and eastern North America, and northern Europe, with temperatures up to 25 °C colder than today. Elsewhere, temperatures were up to 5°C colder than current climate, while the tropical oceans were somewhat warmer as a result of the very different ocean circulations that occur under ice-age conditions.

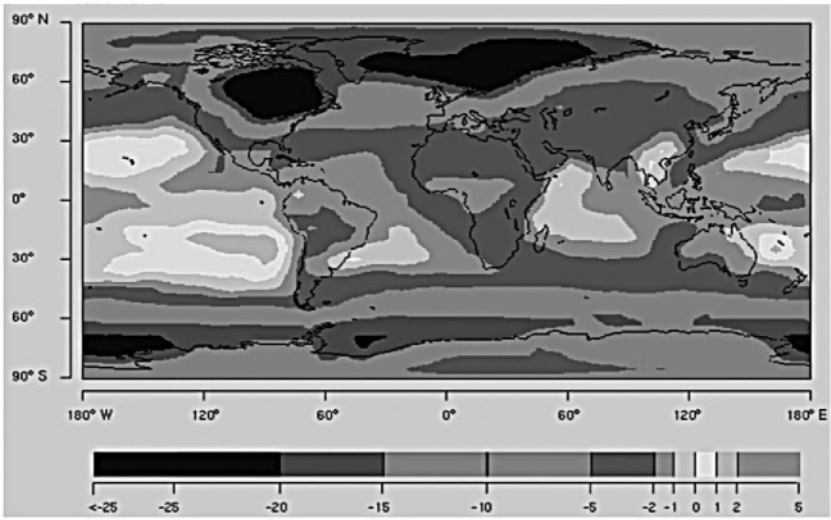

Figure 3.1. Global temperature distribution during the last glacial maximum, based on simulations by the UK Hadley Centre general circulation model (Courtesy: The Hadley Centre for Climate Prediction, the Met Office, UK). Temperature scale is in degrees K compared to current climatic conditions.

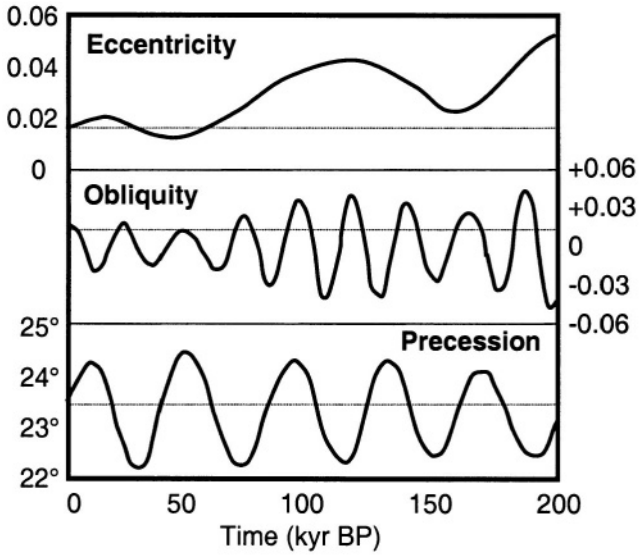

Figure 3.2. Changes in the three principle orbital parameters of the Earth (eccentricity, obliquity, and precession). Dashed lines represent the current values of these three parameters. Adapted from work published by Berger (1992).

In addition to the glacial and interglacial cycles, climate cycles with periods of 41, 23, and 19 thousand years can be identified in the geological record of the past million years. These are related to variations in the astronomic parameters that are responsible for seasonal and latitudinal shifts in incident solar radiation and thereby the manner in which heat is redistributed around the planet both latitudinally and seasonally. The Earth's orbital instabilities include the eccentricity of the Earth's elliptic trajectory around the sun (periodicity of 100,000 years), the obliquity of the axis of rotation that determines the seasons and the geographical location of the tropics (periodicity of 41,000 years), and the climatic precession that is a function of the distance between the Earth and the Sun for a given season (periodicities of 23 and 19 thousand years). The cycles and their irregularities are illustrated in Figure 3.2.

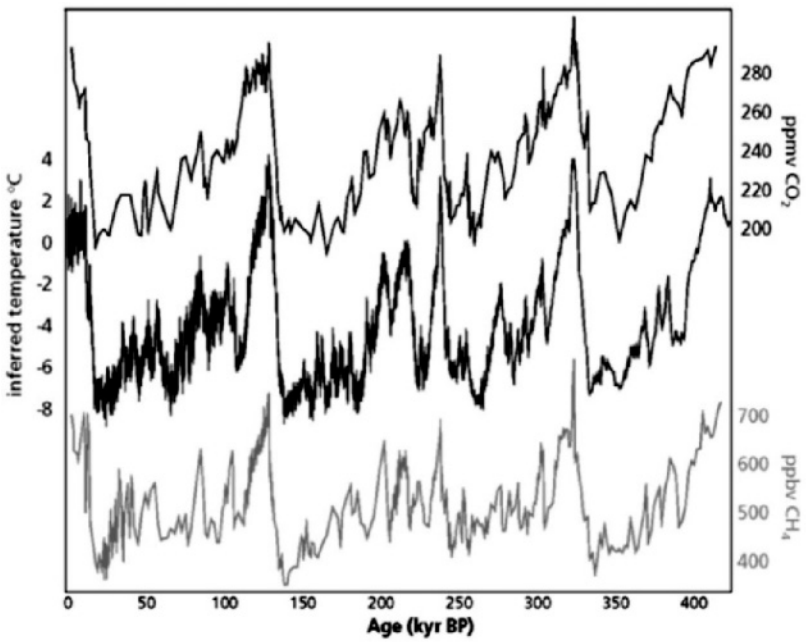

Figure 3.3. Glacial-interglacial cycles over the past 400,000 years as recorded in the Vostock Ice core. Central curve: temperature difference over current climate; upper: CO_2; lower: CH_4 concentrations (Courtesy: IGBP-PAGES Core Office, Bern, Switzerland).

These astronomical cycles (also known as the *Milankovitch Cycles* in honor of the Serb physicist who was the first to quantify the astronomical theory of climatic change) induce feedbacks in the climatic system that act to

amplify the impacts of shifts in incident solar radiation, particularly through water vapor, carbon dioxide and methane, and also surface albedo and vegetation cover. Figure 3.3 illustrates the four major glacial-interglacial periods based on ice-core from the Vostock drilling site in Antarctica, over the past 400,000 years. The asymmetric behavior of temperature (central curve) between the build-up and termination phase of each ice-age can be seen for each cycle, and the shifts in carbon dioxide (upper curve) and methane concentrations (lower curve), that serve to amplify the climate signal, are seen to be well in phase with the temperature cycles (Petit et al., 1999).

Berger (1992) has developed mathematical models based on the Milankovitch cycles that enables an insight into the future evolution of climate forced by astronomical factors on long (millennium and more) time-scales. According to recent work by Berger and co-workers, the duration of the current interglacial period is likely to last much longer than the previous ones shown in figure 3.2, perhaps as long as 50,000 years. This is because the Earth is entering a more circular orbit than in the past, thereby reducing the energy contrasts related to the more elliptic orbits of the past.

3.1.2. Solar cycles

As previously mentioned, the Sun generates 99.7% of all energy available at the surface of the Earth. It is a star of intermediate size whose life-cycle is roughly 10 billion years, and at present the Sun is about half-way through its cycle and has reached peak energy emission rates. Because of its fundamental role in the energetics of Earth systems, any minor fluctuations in energy emitted from the Sun could lead to substantial changes in the Earth's climate. Over the geological era, the so-called "*Weak Sun Paradox"* has shown that despite much lower emitted radiation in the past, the Earth's climate was not excessively different in terms of global temperature from those of today. This is best explained by the fact that while the energy emitted by the sun was at least 30% lower than current emissions about 3 billion years ago, as can be inferred by the study of stars similar to the Sun but in a more juvenile state, there was a far greater abundance of carbon dioxide and other greenhouse gases. This resulted in lower infrared radiative loss from Earth to space and as a result a compensation of lower solar radiation levels through this sharply enhanced greenhouse effect. As life on Earth began to develop under favorable climatic conditions, carbon dioxide was progressively replaced by oxygen through photosynthetic processes; however, the energy output from the Sun grew at a rate that compensated for

the reduction in the greenhouse effect, thereby maintaining global temperatures within relatively narrow boundaries.

On much shorter timescales, the Sun experiences changes in the emission of shortwave radiation that are related to the sunspot cycles. Sunspots as seen in Figure 3.4 are regions on the Sun's where temperatures are lower than the average 6,000 K of its surface, but where the magnetic field is much more intense.

Sunspot activity is linked to a number of well documented cycles whose periodicities are typically 11, 22 and 240-years. Charged particles known as the *solar wind* are emitted and are directed along the lines of equal magnetic force. The solar wind interacts with the Earth's magnetic field and generates perturbations to the ionosphere (resulting for example in the aurora borealis that are magnetic storms in the high atmosphere) and a fractional change in the amount of energy that reaches the high atmosphere.

During the *Maunder Minimum* period of the late 17^{th} century, solar luminosity was lower than today with almost no sunspot activity and temperatures were among the coldest of the last 1,000 years during a period known in Europe as the *Little Ice Age.* Theoretical models of solar physics enable some quantification of the sunspot activity (e.g., Nemes-Ribes et al., 1994), while Zhang et al. (1994) estimate the increase in solar luminosity between the Maunder Minimum and the late 20^{th} century at roughly 0.5%, a figure that is not sufficient to account for the amount of warming that has actually been measured around the globe.

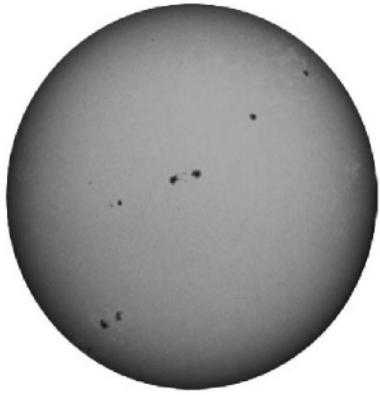

Figure 3.4. View of the solar disc with a number of conspicuous sunspots (Courtesy: NASA).

Friis-Christensen and Lassen (1991) published findings that related climate fluctuations over the past two centuries to sunspot cycles; many of the decadal-scale fluctuations were explained in this publication, but

subsequent calculations showed the original work to contain a certain number of flaws. Sunspot cycles, while one element of external forcing, cannot in themselves explain the complex fluctuations that have been observed since the beginning of the instrumental record.

3.2. INTERNAL FORCING OF CLIMATE

3.2.1. Volcanic activity

Major volcanic eruptions can have a significant influence on climate, for periods ranging from a few weeks to 2-3 years. The 1815 Tambora eruption in Indonesia contributed largely to the cold wave that occurred in the months following the eruption, both in North America and in Europe, to the extent that 1816 has subsequently been referred to as the *"year without summer"*.

Figure 3.5. Clouds of volcanic ash rising above Mt. Pinatubo, Philippines, at the height of the 1991 eruption.

More recent eruptions, such as those of El Chichon in Mexico (1982) and Pinatubo in the Philippines (1991; Figure 3.5), have enabled a quantification of their global influence on climate. Volcanic effects become important when sulfur dioxide (SO_2) in the form of gas is emitted into the stratosphere.

The sulfur dioxide generally mixes with liquid water particles in the atmosphere, creating droplets of weak sulfuric acid (H_2SO_4) that are transported at height by fast-moving atmospheric flows.

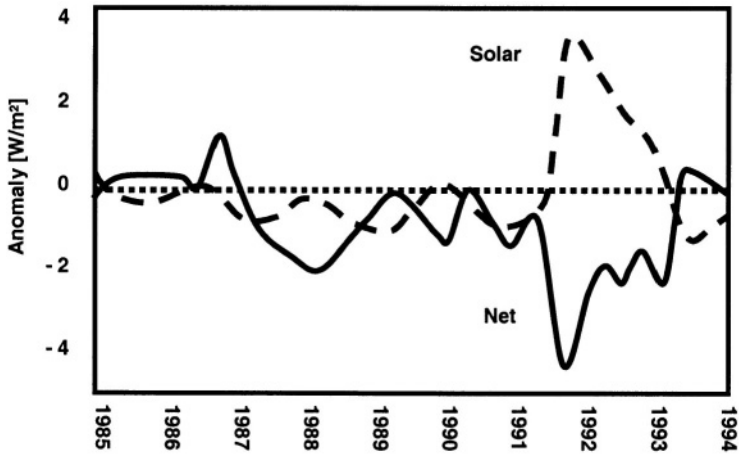

Figure 3.6. Changes in the average reflected solar radiation and the net surface radiation following the 1991 eruption of Mt Pinatubo.

In a relatively short time-span, these droplets circle the globe and act as a screen that prevents a fraction of the solar energy reaching the surface, while reflecting the incoming solar energy at the top of the layer of droplets, as seen in Figure 3.6. The global effect several months after the eruption is highlighted by the reflection of close to 4 W/m^2 more than the long-term average and a decrease by the same amount of net radiation at the surface. This reduction of solar energy at the surface is directly related to the lower temperatures, and the global effect is seen to reach negligible proportions by the middle of 1993, i.e, about 2 years after the eruption itself.

Figure 3.7 shows the aerosol optical depths retrieved from satellite data one month after the 1991 Pinatubo eruption. Estimates of surface cooling due to the presence in the high atmosphere of aerosols of volcanic origin range from a few tenths of a degree to 1°C for major eruptions such as Tambora. The cooling effect lasts as long as there are sufficient aerosols in the atmosphere, but generally no longer than three years when the chemical breakdown of the sulfuric acid droplets is complete and the droplets have dissipated. Volcanic ash and other aerosols have little long-lasting effects on climate because of their mass; the aerosols tend to fall out rapidly by gravity

or are washed out by precipitation, and the residence time is generally not sufficient to contribute to a lasting cooling effect.

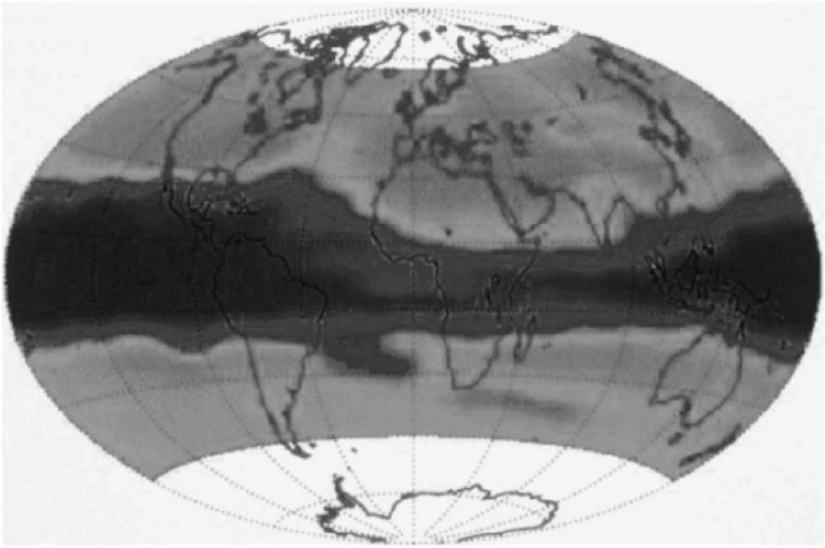

Figure 3.7. Satellite-based retrievals of optical depth one month following the eruption of Mt. Pinatubo in the Philippines (1991). Optical depths in the dark zone encircling the Equator exceed 10^{-1}. The extra-tropical influence of the Pinatubo influence increased for several months after the eruption, leading to a quasi-global influence on climate.

The climatic impact of a volcanic eruption depends on a number of factors, in particular the height at which aerosols are emitted into the atmosphere, the volume of ash and gas emitted and the sulfur content of the eruption. The higher the cloud or aerosols and the greater the sulfur content, the longer the effect of a volcanic eruption on climate will be. The geographical origin of a volcanic eruption is also important; eruptions that occur within the tropics are more likely to have a global effect compared to those that take place in middle or high latitudes. In the former case, the aerosols and droplets first encircle the equatorial and tropical zone, and then are diffused to the north and to the south of the tropics, while in the latter case the material of volcanic origin will remain trapped within the westerly circulations and are very unlikely to affect the opposite hemisphere. Emissions of greenhouse gases by volcanoes, in particular carbon dioxide, are relatively low and thus volcanic eruptions over the past few decades have contributed little to the warming that has been observed.

3.2.2. Ocean-atmosphere feedbacks: El Niño/Southern Oscillation

The dominant influence of the ocean on many elements of the climate system implies that changes in ocean circulation patterns can have strong feedbacks on climate. Changes in the thermohaline circulation have in the past resulted in a marked response of climate, for example about 11,000 years ago during a period known as the *Younger Dryas,* when very cold conditions returned to Europe for several centuries despite the termination of the last ice age. Paleo-climatic investigations suggest that the probable cause of a breakdown of the thermohaline circulation in the North Atlantic that resulted in the Younger Dryas period is related to fresh-water influx into the North Atlantic, that thereby modified the salinity and hence the density of Atlantic waters. The sources of fresh-water influx include ice-sheet melting, sea-ice interactions, and surface runoff from the numerous rivers that feed into the Arctic Ocean from Eurasia and northern North America (Aagard and Carmak, 1989; Bond and Lotti, 1995). There is speculation that the Little Ice Age that affected many parts of the Northern Hemisphere from the early 16^{th} century to the middle of the 19^{th} century may have been triggered by a weakening of the North Atlantic circulations (Broecker, 2000).

On decadal time scales, changes in ocean-atmosphere interactions are brought about by quasi-periodic events such as ENSO (El Niño/Southern Oscillation) in the Pacific Ocean, and the North Atlantic Oscillation (NAO) whose behavior is probably related to changes in interactions between sea-ice, ocean surface temperature, and surface currents.

The Southern Oscillation refers to a large scale, "seesaw" exchange in sea-level air pressure between areas of the western and the south-eastern Pacific. It is has only relatively recently been recognized that the contraction or expansion of the warm waters in the west Pacific and the marked oscillations of the Southern Oscillation are part of a common phenomenon that is now referred to as ENSO. It is a manifestation of a coupled ocean-atmosphere system. Under average or "normal" conditions in the western tropical Pacific, the surface of the sea is consistently close to 30°C, with low pressure and high precipitation occurring over Indonesia and some of the western Pacific islands. The opposite is true on the eastern side of the Pacific close to South America, where the waters are much cooler (21-25°C), with high pressure and low rainfall. Between these two systems separated by over 12,000 km, the marked east-west difference in Pacific Ocean temperature induces what is known as a "thermally direct" circulation loop; this tropical circulation pattern is referred to as the *Walker Circulation.* The Walker Circulation is named in honor of the observations made by a British

administrator in India Sir Gilbert Walker, who was the first to notice certain seesaw mechanisms related to pressure and precipitation in the India-Pacific region. In the late 1960s, Bjerknes provided the first physically-based conceptual framework clearly linking the Southern Oscillation to the oceanographic phenomenon known as El Niño. He laid down the foundations for theoretical predictions of disturbances in temperature and currents, known as Kelvin waves and Rossby waves that are particular to the equatorial ocean (e.g., Philander, 1990).

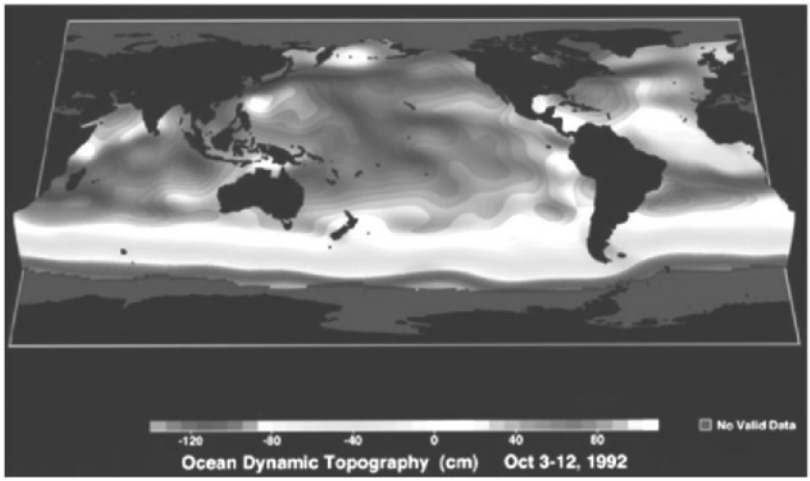

Figure 3.8. Three-dimensional rendering of the dynamic topography of the ocean surface, based on satellite data. Ocean level differences are related to atmosphere-ocean interactions induced by wind stress at the ocean surface.

The Walker Circulation consists of low-level easterly flows that propagate along the equatorial Pacific ocean and a return, upper-level flow whose rising branch is triggered by surface instabilities in the warm waters that of the western Pacific ocean. This atmospheric loop in turn drives a shallow oceanic circulation that is a response to the tilt of the ocean surface from west to east across the Pacific Ocean. The tilt of the surface is due to the fact that the wind stress on the ocean surface induced by the low-level easterlies push surface waters westwards that pile up against the continental land masses to the west (Australia and South-East Asia). Satellite measurements by interferometry methods are today capable of mapping the anomalies of ocean surface water heights, also known as *"dynamic topography",* as illustrated in Figure 3.8.

The excess water mass in the western Pacific needs to be compensated for by surface flows to the north and to the south of the Equator, but also by a vertical circulation pattern that is composed of a descending branch in the west (downwelling of water) and a rising branch of cool waters to the east (upwelling off the coast of South America), as illustrated in Figure 3.9.

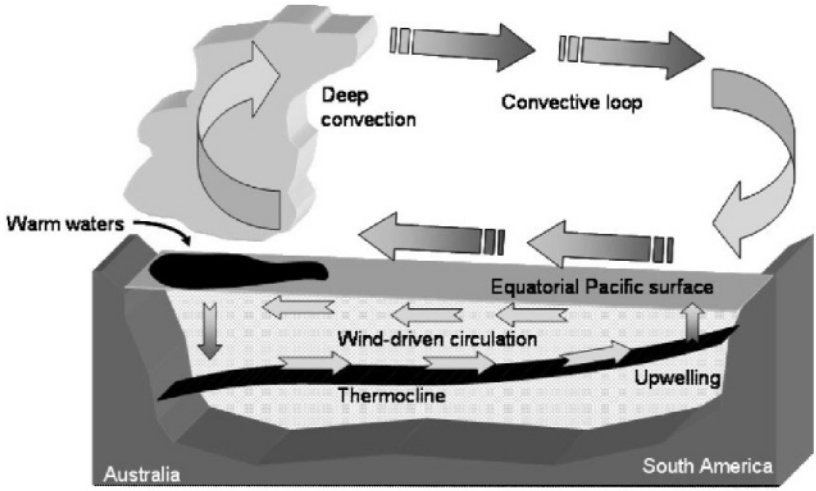

Figure 3.9. Convective loop (Walker Circulation) and associated ocean circulation during normal ENSO conditions across the Pacific.

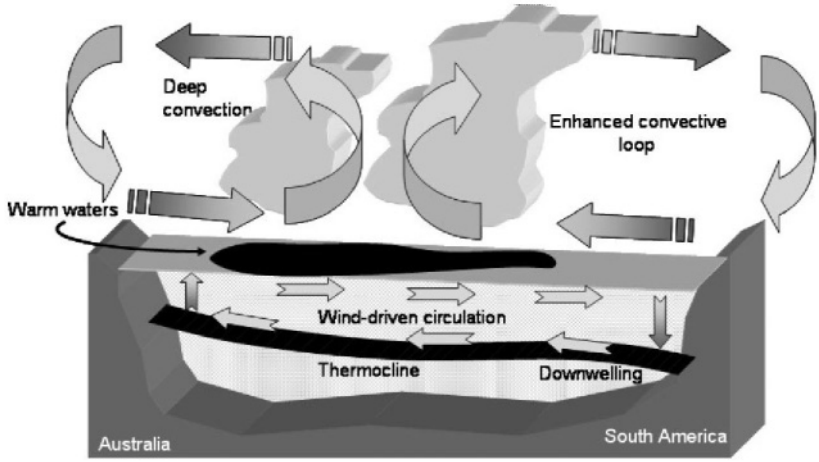

Figure 3.10. Shifts in atmosphere and ocean circulation patterns and associated convection during El Niño conditions.

Warming of the ocean surface during an El Niño year often peaks off the coasts of South America in late December, thereby explaining the origin of the name El Niño, or "The Child", in reference to Christmas. The reflection of Kelvin and Rossby waves at the ocean boundaries trigger changes in the depth of the thermocline that characterize both the warm and cold ENSO phases. The strong easterly Trade winds that characterize normal and La Nina states raise the depth of the thermocline in the east while deepening it in the west, through the actions of Kelvin and Rossby waves. During El Niño, the Trades weaken with a progressive deepening of the thermocline deepens in the east and rise in the west compared to the normal state, as shown in Figure 3.10.

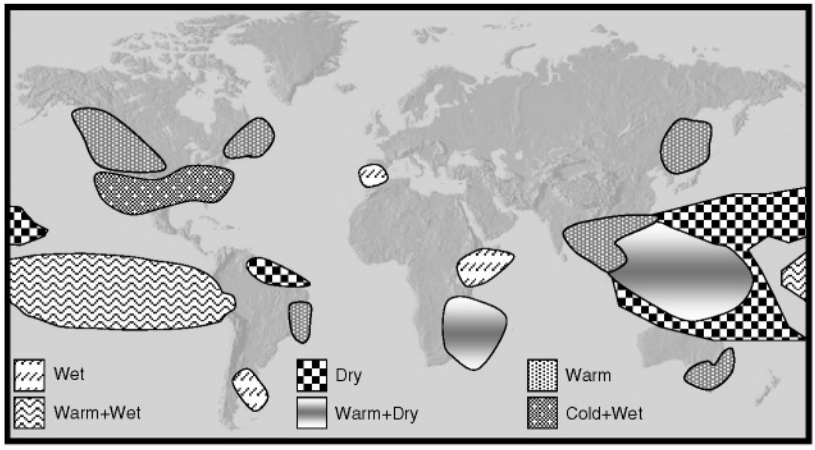

Figure 3.11. Climate anomalies that are frequently associated with El Niño events.

The area of anomalously warm waters at the peak of an El Niño episode can reach 30 million km^2, and as a consequence the sensible and latent heat exchange at the ocean-atmosphere interface is sufficient to perturb climatic patterns globally. The shifts in convective regimes imply that mass, energy, and moisture transfers take place in regions other than those observed during normal conditions. The surface temperature anomaly signal is transferred to the middle and upper troposphere, where it is transported out of the tropics and into the mid-latitudes by upper atmospheric flows. According to the intensity of the El Niño event, there can be major perturbation of climatic regimes in many parts of the world. The map in Figure 3.11 provides an overview of the type of climatic anomalies that are associated with strong El Niño episodes, such as the major 1982-1983 and the 1997-1998 events.

Areas such as Southeast Asia (the Philippines, Indonesia and Papua New Guinea) or Australia frequently experience unusually dry conditions during El Niño. Normally arid regions of Latin America (in particular Peru and northern Chile) as well as North America (Mexico; California) can be subject to extreme precipitation events, with associated mudslides and landslides. Areas of the globe other than the Pacific rim are also affected by ENSO, such as southern and eastern Africa, the Indian subcontinent, Brazil and Argentina. The 1997-98 El Niño was the most intense event of the 20th Century, resulting in massive forest fires from Indonesia to Australia, catastrophic flooding in southern and central California, Peru and Chile, crop failures in the Philippines, Indonesia (rice), Brazil and southern Africa (millet; tropical fruit). It coincides with the warmest period of the century, lending some credibility to the speculation that there may be a link between global warming and increases in El Niño events. ENSO-related phenomena also appear to be associated with epidemics, variations in crop yields, ecosystem disruptions, famines and even market fluctuations whenever there are impacts on economic sectors such as agriculture or enhanced natural hazards such as terrain instabilities or forest fires in regions with significant infrastructure as for example urban areas in California or Australia. The 1982-1983 event cost some 8 billion dollars worldwide, according to Swiss Re (1998).

The cold phase of ENSO, commonly referred to as La Niña, occurs sometimes (but not always) at the end of an El Niño event. Anomalously cold waters invade the tropical Pacific region, and the strength of La Niña can in some instances reverse the previously discussed anomaly patterns, i.e., by enhancing respective precipitation or drought patterns where these normally occur.

Both sea level pressure (SLP) across the Pacific basin and sea surface temperatures (SST) in the Pacific Ocean are indicators of the intensity of ENSO. The SLP difference between Tahiti and Darwin in North Australia has been measured since 1882 and is known as the Southern Oscillation Index (SOI). It is measured in normalized units of standard deviation, and the time series for 1882-2000 are illustrated in Figure 3.12. A negative SOI represents a phase with low pressure in the eastern and high pressure in the western part of the Pacific Ocean and thus characterized the warm El Niño phase (Horel and Wallace, 1981; van Loon and Shea, 1987). The episodes of 1982-1983, 1992, and 1997-1998 are visible in the form of sharp negative peaks in the SOI series. El Niño events have been documented back to the 15th century, and other evidence indicates events occurring since about 700 (e.g., Diaz and Markgraf, 1992).

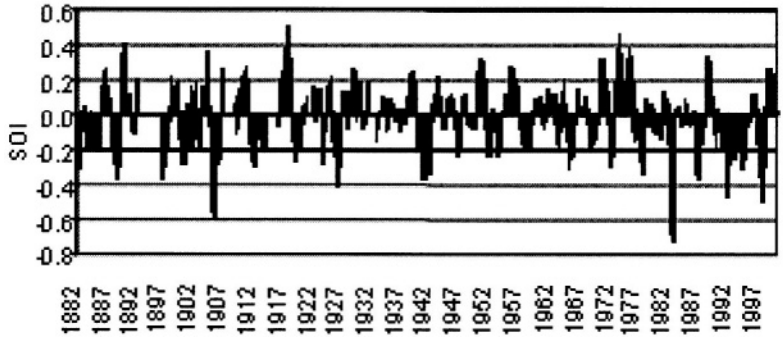

Figure 3.12. Normalized SOI index for the period 1882-2000, with a 5-year filter to remove interannual noise.

There is speculation (Wolter and Timlin, 1998) that global warming may enhance the frequency and intensity of ENSO events. This is based on the observation that since the early 1970s, the return period of the warm phase of ENSO has substantially increased. There is a clear increasing trend in peak temperature anomalies and also a reduction in the frequency of the cold La Niña phase of ENSO. Following the 1992-93 event, the waters of the equatorial Pacific did not return to normal conditions for a number of years. Although this may be unrelated to observed warming and could be explained by natural variability in the highly non-linear processes related to ocean-atmosphere coupling, if a warmer climate were to be accompanied by increases in El Niño events, then the consequences would weigh heavily on many economies, particularly in the developing world.

3.2.3. Low frequency climate variability: the North Atlantic Oscillation

The North Atlantic Oscillation (NAO) represents one of the most important modes of decadal-scale variability of the climate system after ENSO (El Niño/Southern Oscillation), and accounts for up to 50% of sea-level pressure variability on both sides of the Atlantic (Hurrel, 1995). It is observed to strongly influence precipitation and temperature patterns on both the eastern third of North America and western half of Europe; the influence of the NAO is particularly conspicuous during winter months. It has been shown in recent years (Beniston et al., 1994 ; Hurrel, 1995; Rodgers, 1997; Serreze et al., 1997) that a significant fraction of climatic anomalies observed on either side of the Atlantic are driven by the behavior of the

NAO. The behavior of the North Atlantic Oscillation was first documented in the 18th century when a Danish priest (Hans Egede Saabye) observed that when temperatures were above normal in Denmark, they were below normal in Greenland, and vice-versa. This oscillatory behavior is today quantified by the NAO Index, which is the difference in surface pressure between the two major centers of weather activity in the North Atlantic Ocean, namely the Azores high pressure zone and the Iceland low. The sign and magnitude of the index is a measure of the strength of atmospheric flows across the North Atlantic.

As its name indicates, the NAO is centered on the North Atlantic Ocean basin. Here the atmospheric circulation normally displays a strong meridional (north-south) pressure contrast, with low pressure in the northern edge of the basin, centered close to Iceland, and high pressure in the subtropics, centered near the Azores. This pressure contrast drives the mean surface winds and the wintertime midlatitude storms from west to east across the North Atlantic, bringing warm moist air to the European continent. It has long been observed that the monthly and seasonal (particularly wintertime) averaged sea level pressure in stations in Iceland and the Azores, display an out-of-phase relationship with one another. More precisely, there is a tendency for sea level pressure to be lower than normal in the Icelandic low pressure center when it is higher than normal near the Azores and vice versa. This fluctuation is referred to as the NAO. It is related to noticeable changes in monthly and seasonal averaged wind speed and direction over the ocean, and concomitant changes in the paths of wintertime storms and their effect over the ocean and Europe. The NAO is the dominant mode of atmospheric variability in the North Atlantic sector throughout the year, but it is most pronounced during the winter season.

A particular feature of the positive phase of the NAO index is that it is invariably coupled to anomalously low precipitation and milder than average temperatures, particularly from late fall to early spring, in southern and central Europe (including the Alps and the Carpathians), while the reverse is true for periods when the NAO index is negative, as seen in Figure 3.13.

In addition, the position of the storm tracks and the location of the regions of maximum storminess changes according to the sign of the NAO index. The NAO thus exerts a dominant influence on wintertime temperature and precipitation across the North Atlantic basin and thus has major impacts on marine and terrestrial ecosystems. Changes in these climatic factors are of serious consequence to a wide range of human activities, as has been evident from recent scientific and media reports in Western European countries.

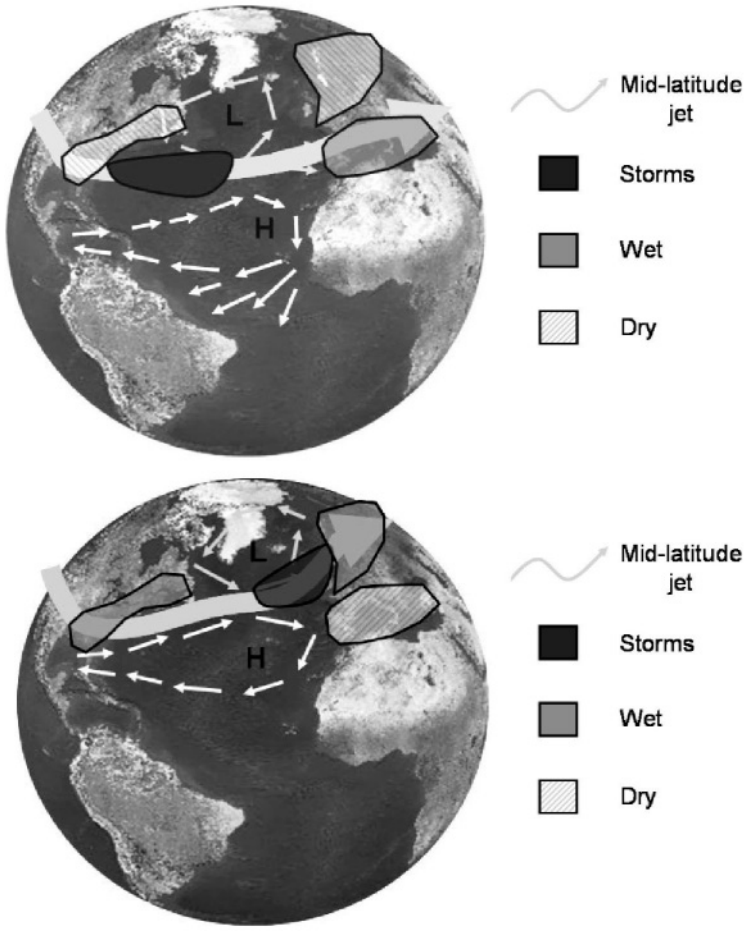

Figure 3.13. Negative or cold phase of the North Atlantic Oscillation (upper) and positive or warm phase (lower). Adapted from M. Widmann, GKSS Research Center, Germany.

Linear regression analysis shows that a considerable portion of the climatic fluctuations in surface temperatures and sea surface temperatures is directly related to the NAO index. Changes of more than 1°C associated with a one standard deviation change in the NAO index occur over the northwest Atlantic and extend from northern Europe across much of Eurasia. Changes in temperatures over northern Africa and the southeast U.S. are also notable.

The changes in the mean circulation patterns over the North Atlantic are accompanied by pronounced shifts in the storm tracks and associated synoptic eddy activity which affect the transport and convergence of

atmospheric moisture and can, therefore, be directly tied to changes in regional precipitation. Hurrell (1995) has shown that drier conditions during high NAO index winters occur over much of central and southern Europe and the Mediterranean, while wetter-than-normal conditions occur from Iceland through Scandinavia. This has been the case for much of the past two decades. In Portugal and Spain, for instance, severe drought conditions throughout Spain have affected olive harvests.

In contrast, increases in wintertime precipitation over Scandinavia may be related to recent positive mass balances in the maritime glaciers of southwest Norway, one of the few regions of the globe where glaciers are not retreating. Widmann and Schär (1997) have found no particular correlation in the Alpine region, although. Beniston(1997a) has shown that snow depth and duration in Switzerland is in phase with the behavior of the NAO. Other studies which decrypt the influence of the NAO on climate parameters have been carried out by Hurrell (1995), who examined correlations between the NAO-index and climate parameters such as temperature and precipitation, and concluded that the behavior of the NAO explains up to 34% of interannual variability in the extratropical northern hemisphere.

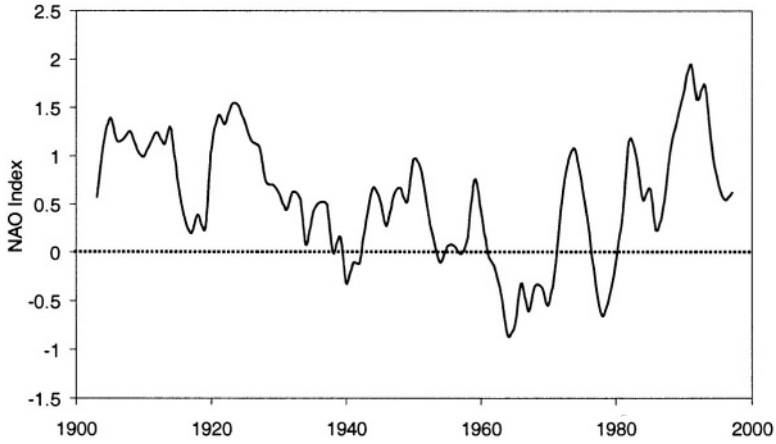

Figure 3.14. Time-series of the North Atlantic Oscillation Index in the course of the 20th century. A 5-point smoother has been used in order to remove interannual noise.

Beniston (2000), among others, has shown that temperature, moisture and pressure trends and anomalies at high elevations stand out more clearly than at lower levels, where boundary-layer processes, local site characteristics and urban effects combine to damp the large-scale climate signals. Climatic

processes at high elevation sites such as in the Alps can thus in many instances be considered to be the reflection of large-scale forcings, such as the NAO. These findings have been confirmed through numerical experimentation by Giorgi et al. (1997), who have emphasized the altitudinal dependency of regional response to large-scale climatic forcings.

The NAO seems not to be a stationary stochastic or deterministic process in the time scales that are common in climate research. Appenzeller et al. (1998) showed by means of wavelet analysis that in a 1400-year simulation with the ECHAM General Circulation Model (GCM) developed at the Max-Planck-Institute in Hamburg, as well as in ice-core data, the dominant frequencies of the NAO-index changes in time. One frequency in the NAO-index of ECHAM could be attributed to a coupled ocean-atmosphere mode which projects into the NAO-index (Timmermann et al., 1998).

Another indication that the NAO can change its regime is the strong positive trend of the index since the late 1960s. During this latter part of the record, an 8-year oscillation may be observed, as seen in Figure 3.14.

Chapter 4

ANTHROPOGENIC FORCING OF THE CLIMATE SYSTEM

4.1. HUMAN INTERFERENCE WITH THE CLIMATE SYSTEM

Human activity, through industry, agriculture, energy generation and transportation, has released significant amounts of greenhouse gases into the atmosphere since the beginning of the industrial era that began in the first half of the 19th century. Today, there is concern that this may be inadvertently modifying the global climate through an enhancement of the natural greenhouse effect. According to the IPCC (2001), global mean temperatures could increase by 1.5 to 5.8°C by the end of the 21st century in response to the enhancement of radiative forcing in the atmosphere. While this may appear to be a minor amount of warming when compared to diurnal or seasonal amplitudes of the temperature cycle, it should be emphasized that the projected global-mean temperature rise is unprecedented in the last 10,000 years. It is not only the amplitude of change but also the rate of warming that is generating concern in the scientific community, especially in terms of the vulnerability and response of environmental and socio-economic systems to climatic change.

There are numerous root causes that explain human interference on the natural environment and the climate system, many of which are embedded in complex economic, cultural, and political systems. However, economic growth and demography can be identified as two broad factors that explain to a large extent the human pressures on a wide range of environmental systems in general and on the climate system in particular. The economic

level of a country determines to a large extent its resource requirements such as energy, industrial commodities, agricultural products and fresh water supply. Demography, on the other hand, is a critical factor in the sharing of the natural and economic resources in a particular country or region.

High economic levels are resource-intensive and thus lead to strong emissions of greenhouse gases into the atmosphere because of demands for energy, commodities, and mobility through transportation. Energy use per capita in the United States is 350 times greater today than in Ethiopia or Rwanda, for example (IPCC, 1998), and though technology has made progress over the past 50 years, it is still to a large degree very much energy-intensive, particularly in the transportation sector where fuel demand for road and air transportation continues to grow rapidly.

High demographic growth is also a cause of high levels of greenhouse-gas emissions, as populations attempt to maintain or improve their standards of living through the exploitation of indigenous resources, often without any long-term planning or management. While in most of the industrialized world, population increase is low (often less than 1%), population growth rates in certain countries of the developing world continue to exceed 4% per annum, with the consequence that economic levels are dwindling as economies are unable to keep pace with demography to supply inhabitants with infrastructure (housing, schools, hospitals), as well as basic commodities such as food and water. Low-cost options are often sought in order to stimulate economies, such as the use of coal as the primary energy source in countries like India and China, but these solutions are often at the expense of the degradation of the environment. Although the contribution by the developing world to overall greenhouse-gas emissions is low in comparison to the industrialized world, emerging countries such as China, India, and Brazil will in coming decades become significant contributors to global greenhouse-gas emissions.

This chapter will cover the salient aspects of the carbon cycle, the anthropogenic emissions of greenhouses gases (GHG) and the reasons for which the global energy sector is a major contributor to the current levels of greenhouse gases in the atmosphere, and will continue to be so in the future.

4.2. THE GLOBAL CARBON CYCLE

Carbon is one of the principle “building blocks” of living organisms, and is found in abundance in a wide range of organic molecules. As many other elements, carbon is exchanged between various components of the environment. A number of “reservoirs” can be identified within the Earth

system that transfer carbon from one reservoir to another according to chemical, physical and biological processes in what is commonly referred to as the *carbon cycle.*

The principle reservoirs for carbon comprise the terrestrial biosphere, namely vegetation and soils, the marine biosphere, the hydrosphere (oceans and freshwater), the atmosphere, and the lithosphere. The time scales associated with carbon cycling through one or other of these systems depends on the processes that absorb or release carbon, and the amount carbon a particular element of the system is capable of storing. The carbon system is a dynamic one that is coupled to climate on seasonal, annual, and decadal time-scales.

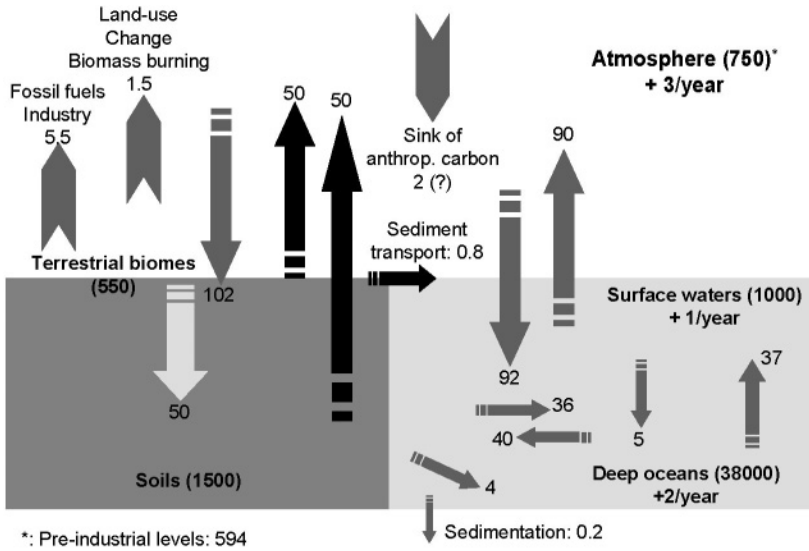

Figure 4.1. The global carbon cycle. Numbers in brackets: carbon storage in GtC, otherwise carbon fluxes in GtC/yr. Arrows with pointed tails represent the human perturbations to carbon sources and sinks. (Following F. Joos, University of Bern, Switzerland).

Figure 4.1 illustrates the various components, the quantities stored, and the fluxes of carbon in GtC/yr (Gigatons, or billions of tons, of carbon per annum), based on observations and on carbon-cycle modeling as reported by Siegenthaler and Sarmiento (1993), Falloon et al., 1998 and Ciais et al., (1995), among others. CO_2 is absorbed from the atmosphere by terretrial vegetation during photosynthesis and released during the decay of dead plant material and organic carbon in soils. Simultaneously, CO_2 is continuously exchanged between the atmosphere and the oceans through gas fluxes at the

air-sea boundary. Figure 4.1 shows that although absolute amounts of carbon in each reservoir are large, and that the fluxes of carbon from one reservoir to another are big in comparison to anthropogenic emissions of carbon, the carbon cycle in the absence of human interference is in a delicate balance between the various sources and sinks. Human activities are thus emitting an additional amount of carbon into the atmosphere that exceed the threshold beyond which other reservoirs are no longer capable of absorbing any additional amount of carbon in the atmosphere.

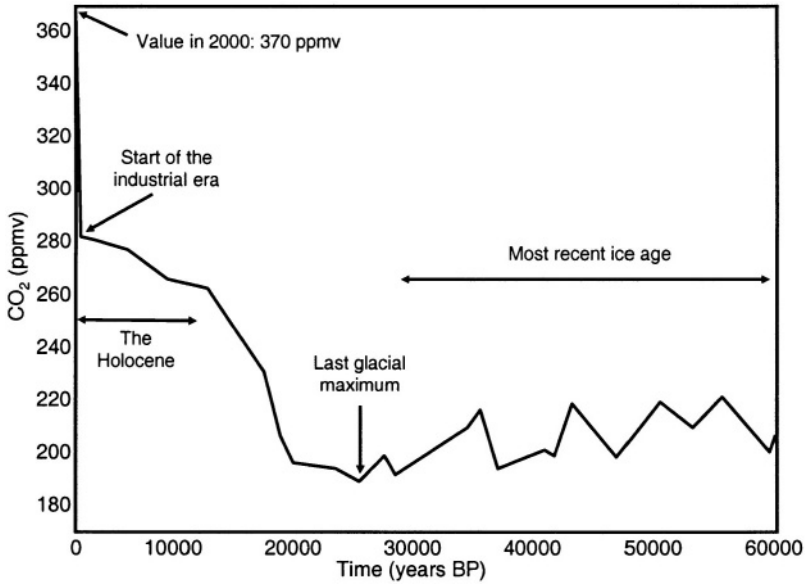

Figure 4.2. Change in CO_2 levels in the atmosphere since the last ice age, based on ice-core records (adapted from Indermühle et al., 2000).

As a result, the atmosphere has increased its levels of carbon since the beginning of the industrial era, and more particularly since the second half of the 20^{th} century when industrialization, energy supply, trade and transportation were steadily becoming global phenomena. Figure 4.2 shows the change in carbon dioxide (CO_2) levels in the atmosphere as reconstructed from paleo-climatic archives for the past 60,000 years, based on ice-core records from a number of drilling sites in Greenland. The curve shown in this figure is a smoothed interpolation between a number of individual data points (Indermühle et al., 2000) that are, however, not particularly dispersed so that the mean curve shown here is a fair representation of CO2 levels during this period.

The discussion on the astronomical forcing of climate (Chapter 3.2; Figure 3.3) showed that changes in CO_2 levels are remarkably in phase with temperature change over a number of glacial and inter-glacial periods. The observed natural CO_2 variations are thus recognized as constituting an important feedback mechanism for climate and climatic change. The Earth's orbital instabilities that drive glacial-interglacial cycles do not in themselves explain the strong climate response, since the energy shifts linked to differential interception of incident solar radiation are not sufficient to generate the climatic changes that are responsible for the start or the termination of a glacial epoch. The astronomical signal therefore is amplified in order to allow the large differences in global temperature and ice volume to take place. Model results suggest that the amplification factor is found in changes in the concentration of carbon dioxide and methane. These explain roughly 50% of the observed glacial-interglacial surface temperature difference, in particular because atmospheric dynamics allow these gases to be well mixed in the atmosphere and therefore to exert a global influence. Indeed, model results show that global warming since the inception of the industrial period and the widespread cold conditions of the last glacial maximum are consistently explained by changes in atmospheric greenhouse gas content and the positive feedbacks that they exert on the climate system when their concentrations are high (e.g., Rahmstorff, 2003).

The measured glacial-interglacial CO_2 variations remains show that terrestrial carbon storage was reduced by about 300 to 700 GtC during the last glacial maximum, implying that the additional carbon during glacial periods was locked in the oceans and not in the terrestrial biosphere. Millenium time-scale changes in the ocean's temperature, salinity, and circulation patterns, a more efficient utilization of nutrients in surface waters by the marine organisms, and interactions between sediments and ocean waters serve to explain the low values of CO_2 encountered during ice ages.

Atmospheric CO_2 has varied slowly and within a very narrow margin during most of the Holocene and up to the beginning of the industrial revolution. Since the end of the 19^{th} century, however, there has been an unambiguous jump in the atmospheric CO_2 content (and a similar jump in methane concentrations) that can only be explained by the human-induced perturbations of the global carbon cycle and the slight excess in carbon emissions over carbon sinks. This has resulted in a 40% increase in CO_2 concentrations and a doubling of atmospheric methane content in the course of the last century. Since 1957, direct measurements of CO_2 have begun in a number of locations, one of which at the Mauna Loa Observatory on the Big Island of Hawaii (Keeling et al, 1996; Keeling and Whorf, 2000) is perhaps the most representative, since it is far removed from any industrial source

that could contaminate the observations. Figure 4.3 shows the increase in CO_2 concentrations at the Mauna Loa site since the late 1950s; the annual fluctuations in the record are related to seasonal changes in photosynthetic rates during the vegetation cycle of many plants.

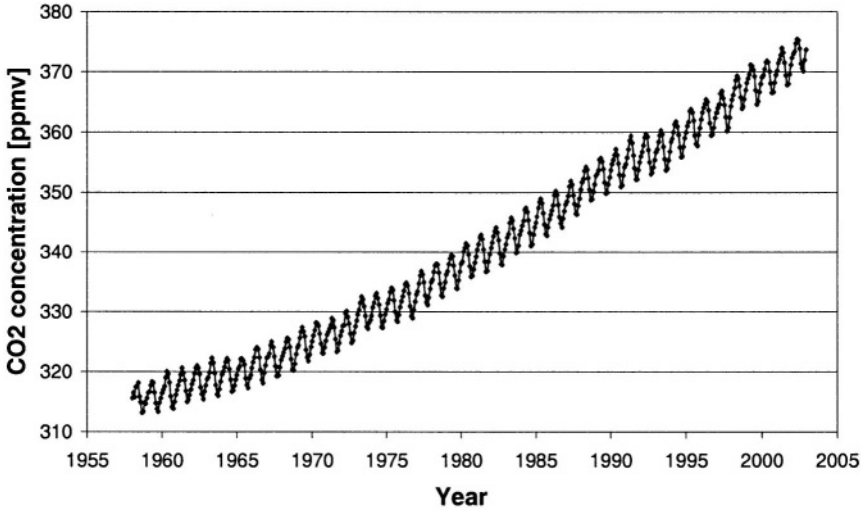

Figure 4.3. Increase in atmospheric CO_2 content as measured at the Mauna Loa Observatory, Hawaii (Source: Keeling and Whorf, 2000).

4.3. THE GLOBAL ENERGY SYSTEM

The anthropogenic sources of greenhouse gases are broadly related to three sectors, namely industry, agriculture, and land-use changes. Under the heading of industry come energy transformations, production of goods, and transportation. Land-use changes, or the shifts in the management of land, harbor a number of issues such as desertification, urbanization, conversion of land from natural vegetation to agriculture, and deforestation. These changes can lead to feedback mechanisms with the climate system, since a consequence of land-use and land-cover changes is its impact upon the physical and biological properties of the surface, such as albedo, surface roughness, temperature and humidity that are exchanged between the ground and the atmosphere. Additionally, changing vegetation and soils can result in shifts in the magnitudes of the sources and sinks of carbon dioxide and methane, and therefore modulate the radiative budget of climate. Over the past few years, there has been a growing recognition that land-use and land-

cover changes may be a more important component of climatic change than previously thought. For example, deforestation contributes about 25% of total anthropogenic CO_2 emissions, through the release of carbon by decomposition of uprooted trees and, far more rapidly, through biomass burning.

The combustion of fossil fuels is by far the greatest single source of anthropogenic carbon emissions, and this sub-chapter will focus upon the global energy sector to highlight a number of the economic and technological issues that explain the current level of emissions.

The global energy system is made up of two key elements, that of supply and that of energy end-use. The supply sector comprises the extraction of the energy resource, its conversion into a useable form, and its transport and distribution to the consumers. Energy end-use includes services such as lighting, heating, refrigeration and air conditioning, transportation and the transformation of raw materials into consumer goods, for example.

Energy sector					
Extraction	Oil well	Coal mine	Uranium mine	Forest	
Sources	Oil	Coal	Uranium	Biomass	Sun
Conversion	Refinery	Power station	Power station	Methanol	Solar cell
Distribution	Pipelines	Electricity grid	Electricity grid	Trucks	Electric cables
Final energy	Gas, petrol	Electricity	Electricity	Methanol	Electricity
Related energy end-use technologies					
	Cars, aircraft	Coal oven	Light bulb	Cars, buses	Water heater
Related energy services					
	Transport	Heat and light	Heat and light	Transport	Heat

Table 4.1. Different components of the global energy system.

Primary energy groups all resources found in nature, in particular the thermodynamic energy supplied by fossil fuels and biomass, the potential

energy of hydropower, the electromagnetic energy of solar radiation, and the fission and fusion of nuclear energy. *Final energy* is that found in an electricity plug, a gas pump, or firewood. *Useable energy* is the energy that is consumed for industrial or domestic purposes, in the form of heat or power. This is ultimately used by various types of machines or equipment that provide the consumer with an *energy service.* Table 4.1 summarizes the different elements that enter into the *global energy system.*

Pricing the different energy services as summarized in Table 4.1 depends on technology, infrastructure and materials, capital investment and human resources. Each of these factors has its own specific price and many are interchangeable. Attempting to price these different services is complex and the energy sector seems to defy the commonly-accepted laws of economics, in part because the energy sector is still very much regulated by state or private monopolies where laws of supply and demand rarely come into play, despite recent moves to liberalize the energy market, particularly in North America. The pricing system for the moment precludes internalization of external costs related for example to environmental degradation or health, and has maintained the costs of fossil fuels artificially low.

Unit	Quantity	Typical consumption
Kilojoule, KJ	10^3 J	-
Megajoule, MJ	10^6 J	Kitchen oven for 30 minutes
Gigajoule, GJ	10^9 J	Average vehicle traveling 100 km
Terajoule, TJ	10^{12} J	Annual energy consumption for a family house
Petajoule, PJ	10^{15} J	Energy potential of 100,000 tons of petrol
Exajoule, EJ	10^{18} J	Annual energy consumption of New York City
-	10^{21} J	Annual global energy consumption

Table 4.2. Typical consumptions corresponding to specific levels of energy. 1 J = 1 W/s.

Despite falling reserves and the higher costs of oil prospection and extraction, the price of oil remains so low as to discourage investments in alternative energy sources. This trend is changing to some extent, and recent statements made by some of the large oil companies on both sides of the Atlantic suggest that new technological solutions are being sought, for example fuel cells and hydrogen-based fuels, to enable these companies to remain the leaders in the field of energy supply. Certain associated industries such as vehicle manufacturers, are also keeping pace with technology and energy issues with the development of new car engines that do not rely exclusively, if at all, on oil as the primary fuel for vehicles.

However, these developments are likely to remain marginal to the main thrust of industries that base their technologies on fossil fuels, in part because of the low price of energy, and also because even if oil reserves may be showing some signs of depletion, other fossil fuels are in abundance. Coal and natural gas, already used as a primary source of energy in numerous countries, will continue to be used well beyond the 21st century even if demand and consumption rises in coming decades, because of the very large reserves of coal in many parts of the world. In terms of energy consumption, Table 4.2 provides a brief reminder of the units and the amount of energy that this corresponds to in everyday life.

Energy *intensity* is defined as the quantity of energy that is required to generate a unit of economic output, generally measured in terms of Gross Domestic Product (GDP) or Gross National Product (GNP). In many countries, structural, technological, and in some instances political changes have served to reduce the energy intensity over time. In the industrialized world, this has been achieved by shifting energy supply from coal to oil and natural gas.

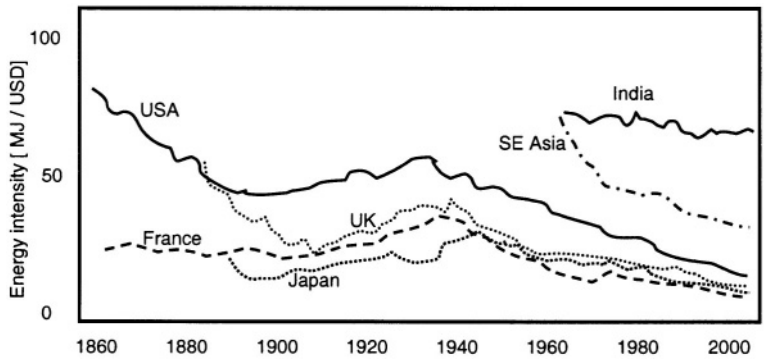

Figure 4.4. Energy intensity for various countries measured in Megajoules per United States Dollars (1980 values) from the mid-19th century to today (Source: IPCC, 2001).

Figure 4.4 illustrates the falling trends in energy intensity in most parts of the industrialized world first at the end of the 19th century and in a second phase from the 1940s. Europe and Japan have a lower energy intensity than the United States because of higher energy costs that increase the incentive towards energy savings. India's principal energy source is coal that is less efficient in energy terms than oil or gas; however, India has its own coal supplies that reduce its dependency on imported energy.

Energy is conserved according to the First Law of Thermodynamics; it can neither be created not destroyed, but can be converted from one form to another; for example, hydraulic energy can be used to generate electricity, while heat is transformed into mechanical energy in a vehicle. However, this energy transformation is rarely optimal and the conversion of primary energy to end-use is accompanied by a net loss of energy. On a global average scale, the conversion of primary energy to final energy is accompanied by a loss of close to 30%, while an additional 60% is lost in the transformation from final energy to useable energy. Hence, the global energy *efficiency* is less than 30%, and much of the 70% of energy that is lost is in the form of heat or acoustic emissions, and in the form of gas and aerosol emissions whenever there is a combustion process involved.

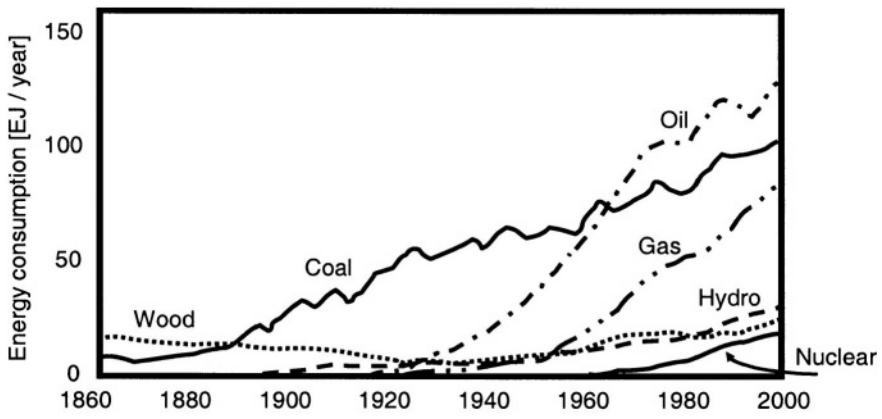

Figure 4.5. Global energy consumption according to energy source (Source: IPCC, 2001).

Combustion of fossil fuels releases the carbon that is contained in coal, oil and, to a lesser extent, natural gas; the carbon that enters into the atmosphere combines with oxygen to form carbon dioxide. Hence a large fraction of the carbon dioxide emitted by human activities is due to the low energy-use efficiency that generates waste by-products such as CO_2. More than 50% of the anthropogenic greenhouse-gas emissions are directly or

indirectly related to the global energy system, in particular because 75% of all energy used currently around the world is based on fossil fuels. Primary energy consumption has increased by over 2% per annum on average since the beginning of the industrial revolution two centuries ago, which represents a doubling of consumption approximately every 30 years.

Figure 4.5 provides an overview of the energy consumption according to primary energy source, since 1860. All fossil fuels exhibit an upward trend that is particularly marked for oil since the 1930s, natural gas since the 1950s, and despite the switch from coal to oil and gas in many industrialized countries, coal consumption still continues to rise as emerging economies consume large quantities of coal to drive their industries and economies. Even though the consumption of hydropower, nuclear energy, and even wood and biofuels has increased in the latter part of the 20^{th} century, these sources represent much less than the fossil fuels themselves.

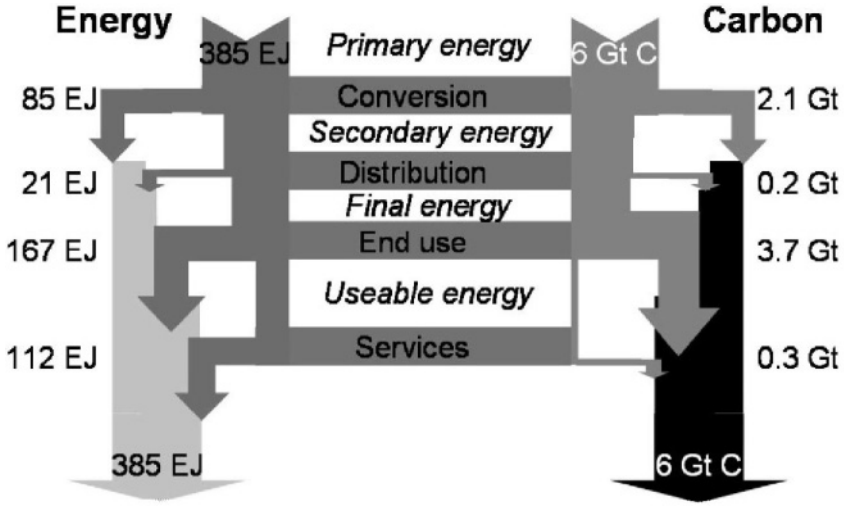

Figure 4.6. Energy and carbon fluxes in the global energy system as a measure of the correspondence between energy consumption and carbon emissions (Source: IPCC, 2001).

While a number of structural changes have resulted in technological improvements that have led to improvements in energy efficiency *and* intensity, these adjustments concern essentially the industrialized world. Emerging markets are often reluctant to use energy-efficient (and hence more environmentally-friendly) production processes, unless there is a clear economic incentive to do so. Currently, the carbon emitted from fossil fuel combustion represents over 6GtC per year, of which 2.3GtC is emitted by

the energy sector in converting from primary energy to useable energy, while the remaining 3.7 GtC are released during end-use consumption. Figure 4.6 highlights the emission of carbon to the atmosphere in direct relation to energy consumption.

4.4. CHARACTERISTICS OF GREENHOUSE GASES

Although the largest contributor to the natural greenhouse effect is water vapor, its presence in the atmosphere is not believed to be directly affected by human activity in the same way as carbon dioxide, for example. Water vapor is likely to increase as a result of global warming, however, because of warmer air can hold more moisture in the form of vapor than cold air. There is thus the potential for an additional positive feedback on atmospheric temperatures, but it needs to be recognized that the interactions between clouds, radiative processes and thermodynamic processes in the atmosphere are still not fully understood, so that the precise magnitude of this feedback remains unknown. In addition, more clouds around the globe would reflect greater quantities of solar radiation, thus constituting a negative feedback for the lower atmosphere.

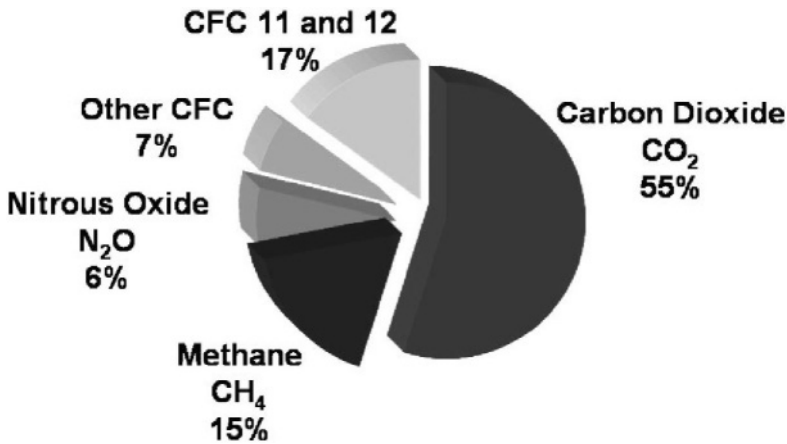

Figure 4.7. Contributions of individual greenhouse gases of anthropogenic origin to the overall warming in the atmosphere (Source: IPCC, 1996).

Carbon dioxide is currently responsible for over 55% of the anthropogenic greenhouse effect, as illustrated in Figure 4.7. Current annual emissions amount to over 7 GtC, which represents a sustained 1% annual

annual CO_2 increase of about 1% in CO_2 concentrations. Methane (CH_4) is a powerful greenhouse gas whose principal sources are of agricultural origin, notably in the tropical regions (rice), livestock (particularly cattle and other grazing livestock), emissions from concentrated organic material such as in waste dumps, and also as by-products from fossil fuel production and use. Methane currently contributes 15–20% of the greenhouse effect and its concentrations have more than doubled since 1900; the IPCC (2001) estimates this increase at close to 150%. Much of the agriculturally-related increase in methane has taken place in Asia, where the area set aside for the cultivation of rice in particular has sharply increased since the 1950s in order to keep up with the pace of population growth. In addition, changes in consumption patterns and consumer demand for a greater variety of products have resulted in considerable increases in livestock levels.

Nitrous oxide (N_2O, also known as "laughing gas"), chloro-fluorocarbons (CFCs), and ozone contribute the remaining 25-30% of the anthropogenic greenhouse effect. N_2O is an agricultural by-product, formed in the digestive tract of livestock and released as a by-product of the chemical decomposition of fertilizers. CFCs are entirely artificial gases that are found in refrigerants, solvents and spray propellants. The concentrations of CFCs have stabilized in the 1990s as a result of stringent emission controls introduced under the 1987 Montreal Protocol designed to address the issue of stratospheric ozone depletion. However, their substitution products (Hydro-fluoro-carbons or HFC), while relatively benign in terms of stratospheric ozone depletion, are potent greenhouse gases and are likely to increase their share of the anthropogenic greenhouse effect in coming decades.

There are a range of other gases that have an influence on the radiative balance of the atmosphere, that are directly or indirectly related to fossil-fuel combustion, such as VOC (Volatile Organic Compounds), tropospheric ozone (O_3) and carbon monoxide (CO); some of these gases may not be greenhouse gases *per se,* but through their chemical reactivity act as catalysors for producing elements that may have a strong radiative effect. Unlike the major greenhouse gases that are chemically stable, thus allowing them to become well-mixed in the atmosphere and exert a genuinely global radiative effect, other gases such as VOCs or tropospheric ozone can be found in abundance but only locally or regionally. Their chemical reactivity is such that as they are transported by atmospheric flows, they will undergo transformations so that the original greenhouse gas molecules may no longer play a role after a certain distance from their source. As a consequence, it is difficult to estimate the global effect of molecules or compounds that essentially have a local impact.

A further problem related to GHGs is their long residence times in the atmosphere, as shown in Table 4.3. Gases such as CO_2 have residence times on the order of 1-2 centuries. Methane is relatively short-lived, on the order of a decade or so, while the CFCs have century-scale lifetimes. These long residence times are the consequence of the strong chemical bonds of molecules that contain carbon and that do not disintegrate rapidly in the absence of strong chemical reactions in the atmosphere. The implication of the figures given in Table 4.3 is that even if all GHG emissions were halted in the near future, their combined influence would continue to warm the atmosphere for a century of more.

Anthropogenic greenhouse gas	**Atmospheric residence time (years)**	**Global warming potential (Carbon=1)**
Carbon dioxide (CO_2)	150-200	1
Methane (CH_4)	10-15	56
Nitrous oxide (N_2O)	150	280
Chloro-fluoro-carbons (CFC)	80-150	5,000-15,000
Hydro-fluoro-carbons (HFC)	10-250	500-10,000

Table 4.3. A comparison of residence times and 100-year time-scale global warming potentials for a number of greenhouse gases.

In its second assessment and subsequent reports, the IPCC (1996; 2001) put forward the notion of *global warming potentials,* i.e., a measure of the relative radiative effects of various greenhouse gases defined in W/m^2. The index is defined as the cumulative radiative forcing between the current reference period and a time horizon, e.g., 50 or 100 years for a unit mass of gas that is emitted into the atmosphere. The warming potential is thus a measure of the efficiency with which a molecule warms its atmospheric environment through the re-emission of infrared radiation, and is different from one GHG to another. Table 4.3 has also included the 100-year warming potentials relative to CO_2 whose warming potential is set to unity for comparison purposes. At present, atmospheric concentrations of all gases other than CO_2 are still very low, thereby explaining why this gas is still the major contributor to the overall anthropogenic greenhouse effect despite its low warming potential. Significant increases in one or other of the remaining greenhouse gases would be necessary for them to play as important a role in

global warming as CO_2 currently does. The estimation of global warming potentials has a certain degree of uncertainty associated with it, in particular because it is necessary to take into account both direct and indirect effects of a given gas; a typical example is ozone, which has both warming and cooling effects according to the level at which it is found in the atmosphere; the global radiative effects of stratospheric ozone and tropospheric ozone are substantially different, mainly because ozone in the stratosphere partially absorbs shortwave solar radiation and thus reduces the amount of incident solar energy at the surface, while tropospheric ozone is a powerful greenhouse gas.

While much of the discussion of climatic change focuses on greenhouse gases and their radiative effects, other influences that are also partially attributable to human activities need to be taken into account. This is notably the case for aerosols that are solid or liquid particles whose optical properties generally act to reduce incoming solar radiation at the surface. This occurs either through the direct reflection of shortwave radiation back to space as it interacts with the particles and through changed optical and physical properties of clouds when cloud liquid droplets combine with aerosols. In general, high aerosol content in clouds acts to increase their albedo and thus reduce incoming solar energy. However, some particles such as soot have a positive feedback on their atmospheric environment because of their low albedo, thus absorbing solar energy and redistributing it as heat into the atmosphere.

Aerosols include dust from bare surfaces that is injected into the atmosphere through turbulent exchange between atmospheric flows and the surface, organic compounds released through the combustion of biomass, organic and inorganic material released from the ocean surface often when waves break and release spray into the atmosphere, ash from volcanic eruptions, and through waste by products of fossil fuel combustion (particularly coal and heavy oils) and industrial processes. Aerosols rarely have a global impact because as non-gaseous particles, they are ultimately removed from the atmosphere through gravity or are washed out by precipitation processes. Their influence is thus confined to the source areas themselves and downwind. According to the altitude at which aerosols are found in the atmosphere, their influence on the atmospheric radiative will differ; particles with a relatively low mass transported into the upper troposphere or the stratosphere, such as fine volcanic ash, have residence times of up to 2-3 years, while heavier aerosols of industrial origin are likely to be deposited or washed out within a few days.

Figure 4.8 shows the relative effects of global warming potentials for a range of natural and anthropogenic factors; despite large uncertainties, the

cumulative effects of anthropogenic greenhouse gases that have been emitted over the past 200 years are clearly a dominant factor today. Error bars provide a measure of the uncertainty, which remains small for the contribution of the combined effects of the major greenhouse gases to climatic forcing.

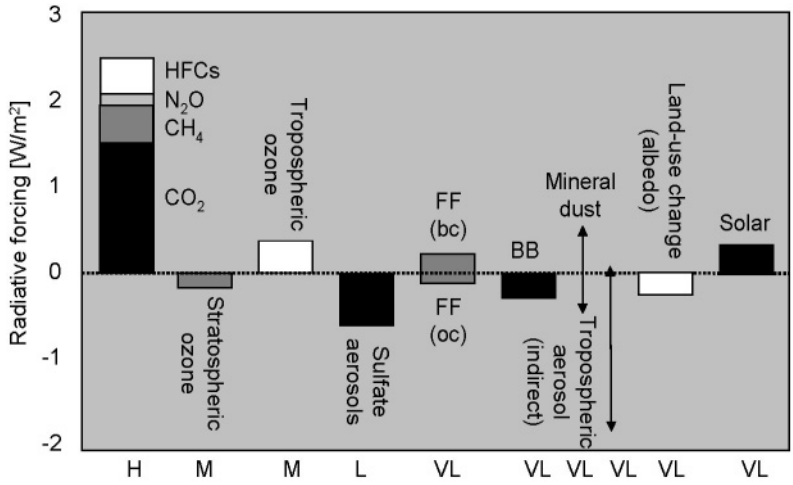

Figure 4.8. Global Warming Potentials of a range of anthropogenic and natural forcings on climate. There are large uncertainties in many of these estimates, as indicated by the coding on the abscissa (H: High level of understanding; M: Medium; L: Low; VL: Very low). FF refers to fossil fuel burning, BB to biomass burning, while bc and oc are black carbon and organic carbon, respectively (Source: IPCC, 2001).

4.5. FUTURE TRENDS IN GREENHOUSE GAS EMISSIONS

The future course of greenhouse gas emissions will be the result of a complex mix of economic, social, political, and technological options, many of which are difficult to quantify within reasonable bounds of confidence. It is for this reason that the IPCC (2001) have developed a range of possible emission futures, or *emission scenarios,* based on a combination of hypotheses governing population increase, economic growth, and technological adjustments to the end of the 21st century Nakicenovic et al. (2000) developed over 40 emission pathways for the 21st century, known as the IPCC SRES Scenarios (SRES: Special Report on Emission Scenarios). The SRES scenarios are based upon four different sets of paradigms related to socio-economic trends that strive to maintain consistency in the links

between emissions and their evolution. A set of 40 scenarios has been established in the IPCC framework that cover the wide range of the main demographic, economic and technological forces that are likely to drive future greenhouse gas and sulfur emissions. The SRES scenarios make no assumptions, however, of whether emission reduction targets as set by the Kyoto Protocol of the UN Framework Convention on Climate Change will be implemented within this time frame.

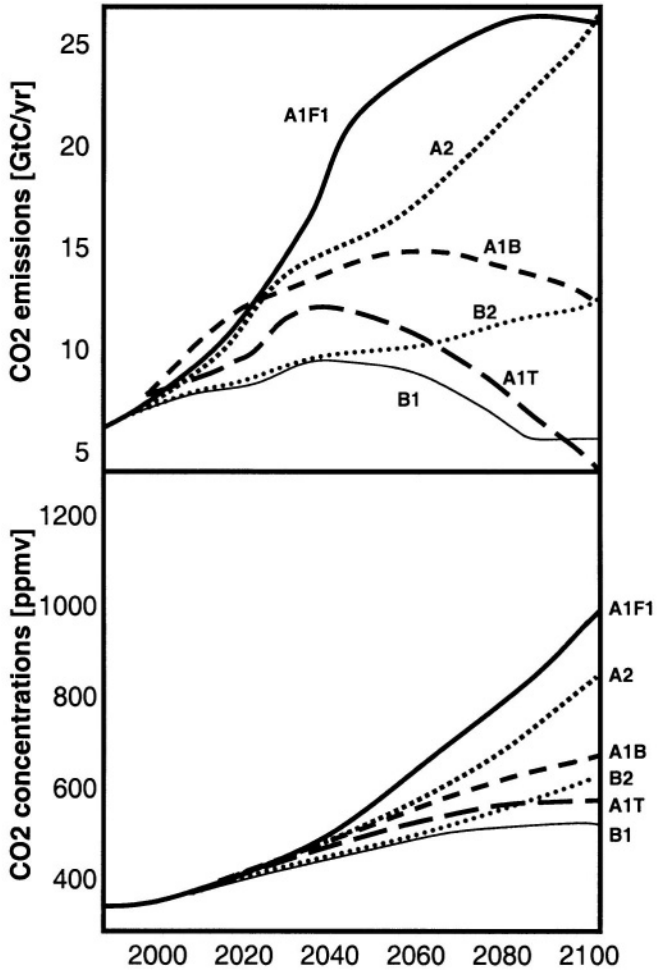

Figure 4.9. IPCC SRES CO_2 emission scenarios until 2100 (upper) and resulting CO_2 concentrations in the atmosphere (lower) in the same time frame. Letters refer to specific SRES scenarios as described in Nakicenovic et al. (2000).

The scenarios developed in 2000 (Figure 4.9) take into account possible changes in population, social and economic development, technology, resource use, and pollution management, each of which contributes to varying degrees to emissions. Each main group of scenarios is as likely to occur as another, and the IPCC has avoided placing a priority on any one particular scenario or set of scenarios. The set of "A1" scenarios, for example, stress the influence of technology change on emissions while maintaining the other driving forces (demography, economics) constant, while the "A2" scenarios assume little change in economic behavior. In addition, rising population levels and relatively little international collaboration on resource and environmental protection exacerbate the problem of emissions; the A2 scenarios are sometimes referred to as "Business-as-Usual", a phrase that was coined for one of the previous sets of IPCC scenarios (IPCC, 1994; 1996).

The "B1" scenarios assume a stabilization of global population by the middle of the 21^{st} century and a slow decline thereafter, with economic and technological adjustments geared towards a society based on services and information technologies that are less energy-intensive than current industrial developments. The "B2" set of futures consists of levels of population growth and economic development that are intermediate between the "A2" and "B1" scenarios.

The total CO_2 emissions that result from the various SRES scenarios, and the corresponding increase in CO_2 concentrations until 2100 are identified in Figure 4.9. It is seen that even under stringent controls on emissions, as the A1T and B1 scenarios, for example, concentrations continue to rise in the future. The salient difference is that the increase in concentrations is somewhat reduced when emissions are strongly reduced. This diagram suggests, therefore, that even when CO_2 emissions are strongly curtailed, the global carbon cycle is still in disequilibrium, with emissions exceeding sinks.

These different scenarios are a necessary component of climate modeling, discussed in the next chapter, because they represent one of the essential forcing factors to which modeled climate systems will respond.

Chapter 5

MODELING AND OBSERVING CLIMATE

5.1. INTRODUCTION

Models are mathematical, computer-based, or conceptual tools that allow a synthesis of the current understanding of particular systems in the realms of physics, chemistry, biology, or economics. In climate research, numerical models attempt to take into account numerous elements of the system that are important for its evolution, in particular the oceans, the cryosphere, and the biosphere. Advanced models enable investigations of certain mechanisms that may ultimately be relevant to a system's evolution, such as feedbacks between its different constitutive elements, and the sensitivity of climate to disturbance. Models also have some measure of predictability for complex non-linear processes, which are the rule in the physical, biological or economic sciences.

There are numerous approaches to simulating climate or components of the climate system. Models can be 1, 2, or 3-dimensional, and be applied to a single physical feature of relevance to climate, or may be designed to simulate fully interactive, three-dimensional climate processes. In order to gain insight into the functioning of climate, the most complex models are not necessarily the most explicit; the type of model to be selected is therefore closely linked to the nature of the problem to be investigated (Henderson-Sellers and McGuffie, 1987; Beniston, 1997b). There are three broad types of climate models, namely the Energy Balance Models (EBM), the two-dimensional zonally-averaged Statistical-Dynamical Models (SDM), and the fully three-dimensional General Circulation Models (GCM). Principles governing both EBMs and GCMs will be briefly reviewed in this chapter.

5.2. ENERGY BALANCE MODELS

As its name implies, an energy balance model (EBM) is a simple conceptual representation of the climate system, based on the balance between incoming short-wave (solar) and outgoing long-wave (terrestrial infrared) radiation, as outlined in Chapter 2. The simplest representation of the Earth's energy balance is a point in space that exchanges solar and infrared energy; more complex renderings of an EBM make use of a two-dimensional representation of the Earth, in which not only radiative heat exchange is involved but also the latitudinal transport of heat to compensate for the imbalance of heat between the Equator and the Poles. Such an EBM is sketched in Figure 5.1; solar energy is reflected according to the mean albedo in a particular latitudinal band, and infrared radiation is partially trapped by an atmosphere in which greenhouse gases are present.

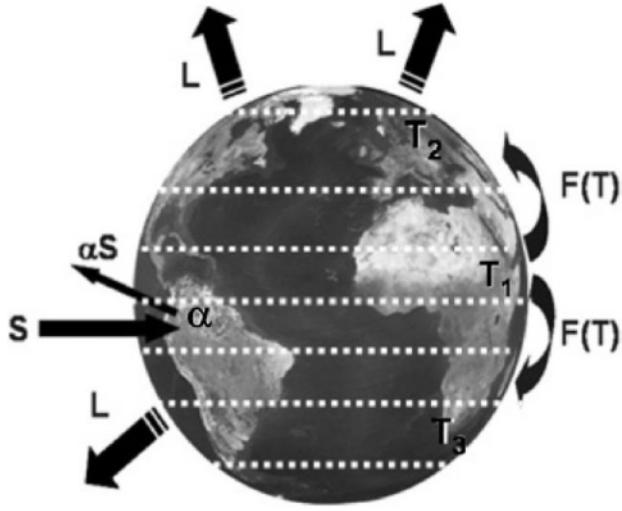

Figure 5.1. A sketch of the main elements that are incorporated into a two-dimensional Energy Balance Model (EBM). S: Solar short-wave radiation; α: Surface albedo; αS: Reflected solar radiation; L: Outgoing terrestrial long-wave (infrared) radiation; F(T): Heat transport from regions of high temperature (T_1) towards those of lower temperature (T_2 or T_3). Dotted lines represent latitudinal bands for which the various components are computed.

A numerical framework that relates the different terms given in Figure 5.1 begins with the global heat balance equation, described by the time-dependent relationship below:

$$c_m \Delta T(t) / \Delta t = R\downarrow(\phi) - R\uparrow(\phi) + Tr(\phi) \qquad (5.1)$$

where c_m is the heat capacity, $R\downarrow$ is the incoming short-wave radiation, is the outgoing long-wave energy, and Tr is the heat transfer from warmer to cooler latitudes. All terms are dependent on the latitude, ϕ, thus enabling the computation of temperatures for different latitudes.

Each of the terms on the right hand side of Equation 5.1 can be expanded in the following manner:

$$R\downarrow(\phi) = (1 - \alpha(\phi))\ S/4 \qquad (5.2)$$

where α is the surface albedo or reflectivity, and S the solar energy at the top of the atmosphere. The factor 4 is included to account for geometry and the fact that only one side of the Earth is illuminated by the Sun at any given time. Equation 5.2 thus states that the useable long-wave radiation is the incoming solar radiation weighted by reflection at the surface or by clouds, aerosols, and molecules in the atmosphere.

Outgoing radiation is represented by:

$$R\uparrow(\phi) = \varepsilon\ \sigma\ T(\phi)^4\ \tau_a \qquad (5.3)$$

This is the Stefan-Boltzmann equation that relates the emission of radiation to the fourth power of temperature. ε is the emissivity (that is ideally 1 for a "black body"), σ the Boltzmann constant (5.67×10^{-8} J/kg/K), and τ_a the transmissivity by the atmosphere. If is τ_a is equal to 1, then the atmosphere is totally transarent, i.e., there are no greenhouse gases present in the atmosphere and all emitted radiation crosses the atmosphere without hindrance. The lower the value of τ_a, the greater the greenhouse effect as the atmosphere becomes more opaque.

If, for a point representation EBM, all conditions are in equilibrium, then the time-dependent term is zero and there is of course no latitudinal heat transport. In this case, the energy balance is simply the exchange of solar and terrestrial radiation; setting an average value for albedo at 0.3 and the transmissivity at 0.62, the computation of temperature from the radiative fluxes yields an average global temperature of 287.6 K (or 14.5°C) that corresponds to the current, long-term value of temperature.

In a two-dimensional representation of the world, the heat transport term $Tr(\phi)$ needs to be quantified; in its simplest representation, heat exchange between different latitudes is assumed to be a function of the temperature difference between one latitude band and the mean global temperature, and

the efficiency with which this transfer is carried out. The transport term is thus described by:

$$Tr(\phi) = K\,(T(\phi) - T_g) \qquad (5.4)$$

where $T(\phi)$ is the mean temperature for a latitude band ϕ, T_g is the mean global temperature, and K is a transfer coefficient that is a measure of the efficiency of latitudinal heat transport.

Finally, the albedo can be specified to be a function of temperature. This allows the albedo to rise to high levels whenever a particular latitude band becomes covered with snow or ice; the reflectivity of the surface thus changes from relatively low values characteristic of bare soils or regions covered by vegetation and forests, to high values that are common for snow and ice. By allowing α to be temperature-dependent, feedback mechanisms involving the appearance or disappearance of snow and ice are incorporated into the EBM. Following Henderson-Sellers and McGuffie (1987), a typical temperature-dependent albedo reads:

$$\begin{aligned} &\alpha(T(\phi)) = 0.6;\ T(\phi) < T_c \\ &\alpha(T(\phi)) = 0.3;\ T(\phi) > T_c \end{aligned} \qquad (5.5)$$

In order to make Equation 5.1 more tractable, the infrared radiation emission term in Equation 5.3 can be linearized through the following simplified representation:

$$R\uparrow(\phi) = A + B\,T(\phi) \qquad (5.6)$$

with A and B constants that represent the combined effects of greenhouse gases, clouds, and aerosols on the transmissivity of the atmosphere.

Using this linearized equation, it is now possible to define a latitude-dependent equation for temperature at equilibrium, that is derived by manipulating the various terms of Equation 5.1 through the use of Equations 5.2, 5.4, 5.5, and 5.6. The diagnostic equation thus reads:

$$T(\phi) = [(1 - \alpha(T(\phi))\,S + K\,T_g - A] / [B + K] \qquad (5.7)$$

In the following, a few examples of the sensitivity of the EBM to changes in one or more of its constitutive parameters are shown by applying Equation 5.7 to different parameter values. In the four figures that follow, the bold line represents the simulation of "current climate" by the EBM, using parameters

such as albedo, atmospheric transmissivity, or the heat transfer efficiency that have been adjusted to represent as closely as possible the present-day world. This is referred to as the "control simulation"; other simulations that are shown here comprise:

1. A 5% increase and decrease of the solar constant, S, which would correspond to changes in the Earth's astronomical parameters allowing the emergence or the termination of an ice age, for example.
2. An increase in surface albedo in the tropical regions and decrease in high latitudes; such a change would correspond to an almost complete loss of tropical forests and their conversion to agricultural land with much more reflection from the vegetation surface. Higher albedo in the polar latitudes would correspond either to a reduction in snow and ice cover or to the deposition of aerosols of volcanic or industrial origin on the ice surfaces, for example.
3. An increase of the heat transport efficiency; this could occur if the major meridional circulations such as the Hadley Circulation or ocean currents were to become more active.
4. An increase in the opacity of the atmosphere; this is typically associated with an enhancement of the anthropogenic greenhouse effect.

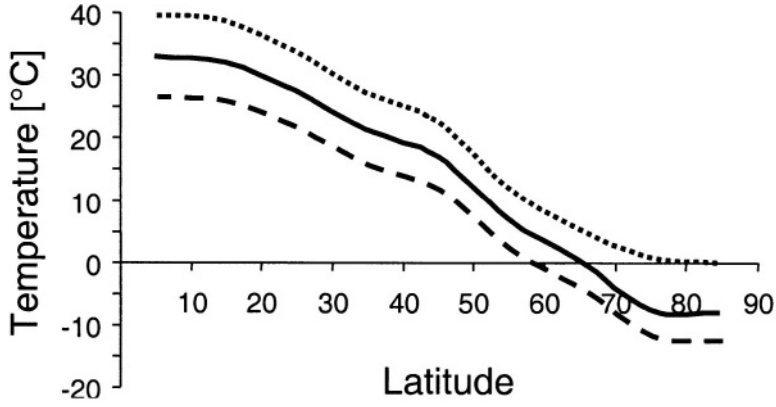

Figure 5.2. Response of latitudinal-average temperatures to a 5% decrease in the solar constant, S (dashed curve, lower), to a 5% increase in S (dotted curve, above), compared to the control simulation for current climate (solid line, middle), as computed by a two-dimensional energy balance model. Only one hemisphere is represented as in this model because energy balance and temperatures are symmetrical in both hemispheres.

Figure 5.2 illustrates the results for the first set of simulations in the list above. The current climate situation, shown only for one hemisphere since the model is symmetric in energy terms between both hemispheres, exhibits a progressive decrease in temperatures from the Equator to the Pole. Temperatures in the polar regions tail off in the last latitudinal band as heat transport compensates to some extent for heat loss. When the solar energy is reduced by 5%, the model enters into a cold mode, with low temperatures and the formation of an additional latitudinal band containing snow and ice. The increase in incoming solar radiation, on the other hand, exhibits warming that is greater in the high latitudes than in the tropics because there is now no longer any significant amount of ice in the polar regions; the high reflectivity associated with ice-covered surfaces is replaced by a lower albedo and a corresponding positive feedback for high-latitude temperatures.

Figure 5.3 shows the results for the second experiment, namely an increase in surface albedo in the tropics and reduction in high latitudes. The response in the tropics is a significant cooling. Because average global temperatures are reduced in the tropical zone, the heat transport term is also substantially modified since it depends on the temperature difference between a given latitudinal band and the global average temperature.

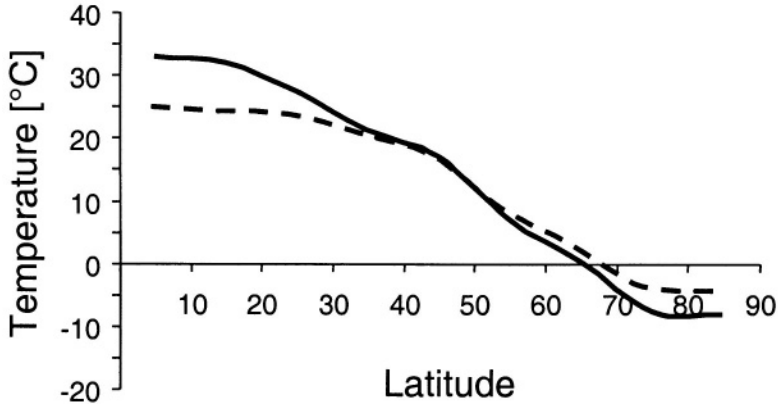

Figure 5.3. Comparison between the control simulation (solid line) and a simulation where there has been an enhancement of albedo in the tropics and a reduction in high latitudes (dashed line).

The polar regions see their temperature contrast reduced compared to the control simulation because of the lower surface reflectivity, thereby serving to raise temperatures in the high latitudes through the additional absorption of solar energy.

In Figure 5.4, the activation of meridional heat transfer benefits essentially the mid-and high latitudes, where sufficient heat arrives in the polar regions to melt the snow and ice that is found in the control simulation. As a result, there is a disproportional warming close to the Pole because of the albedo feedback mechanism already discussed.

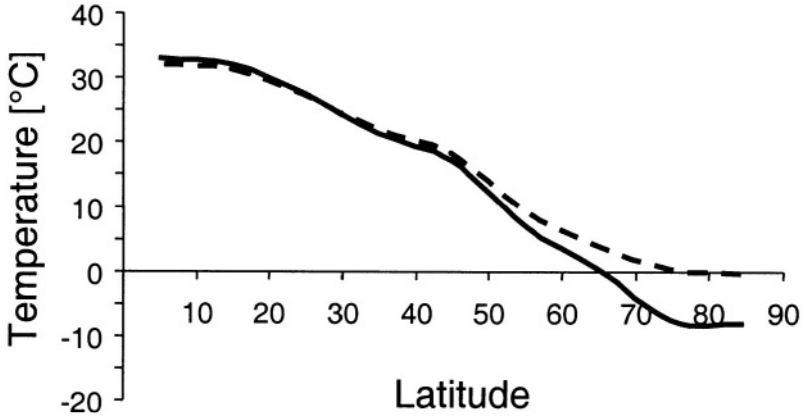

Figure 5.4. Comparison between the control simulation (solid line) and a simulation where there has been an enhancement of the efficiency in the latitudinal heat-transfer term (dashed line).

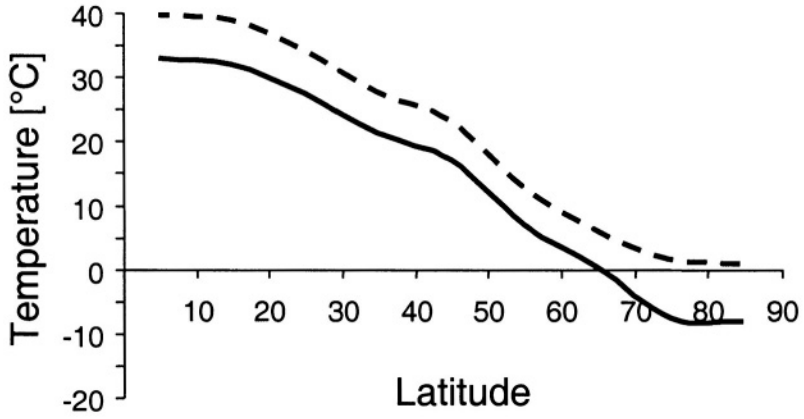

Figure 5.5. Comparison between the control simulation (solid line) and a simulation where there has been a decrease in the transmissivity of the atmosphere (dashed line).

The final example illustrated in Figure 5.5 provides a clear illustration of the enhanced greenhouse effect where, in this simulation, temperatures that are in equilibrium with an atmosphere containing roughly 750 ppmv (i.e., three times the pre-industrial values of greenhouse gas concentrations). Temperatures increase at all latitudes, since the greenhouse effect is global, with the additional high-latitude warming related to the positive feedback resulting from lower surface reflectivity as the surfaces covered by ice are sharply reduced.

These examples serve to illustrate the sensitivity of a simple, model climate to a change in a set of external or internal forcings. These are seen to generate significant changes in temperatures at the global scale, even when the forcings are local. Furthermore, the system can respond strongly even if the change in forcing is modest, because of feedbacks in the system that are included in a simplified manner (e.g., the ice-albedo interactions with the atmosphere).

Energy balance models have the advantage of being computationally-efficient and can be run on PCs; they can highlight areas of change that could be important if one or more of the dominant controls on the energy balance are modified.

However, in many instances EBMs are oversimplified models in terms of the processes they take into account and their representation for a very heterogeneous planet such as the Earth. More complex models are thus required to adequately represent the processes that are responsible for the temporal evolution of the climate system and salient elements of its spatial differences. An in-depth approach to climate simulations thus requires the use of full three-dimensional models that can address many of these issues.

5.3. ATMOSPHERIC GENERAL CIRCULATION MODELS

General circulation models (GCM) are based on the physical dynamic and thermodynamic laws governing the atmosphere. These describe the redistribution of heat, momentum, and moisture resulting from atmospheric motion, radiative transfer and thermodynamics associated with phase changes of water. The governing equations are non-linear partial differential equations that require numerical methods for their solution. These consist in subdividing the atmosphere vertically into discrete layers, and horizontally either into discrete grid-points or by a finite number of mathematical functions as in so-called spectral models. The values of the predicted variables, such as surface pressure, wind, temperature, humidity, and rainfall

are integrated at each grid point (or for each spectral function) with respect to time, in order to obtain a prediction of the future state of these variables. A sketch of the structure of a GCM is given in Figure 5.6.

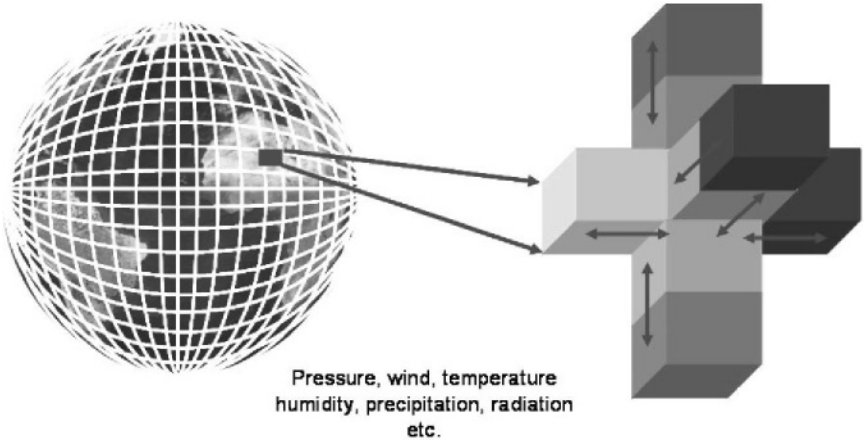

Figure 5.6. A sketch of an atmospheric model grid structure; at right, an individual element as seen on the globe is expanded into a series of adjacent grid-volumes for which, at each intersecting grid-point, computations will be undertaken.

The globe is divided into small volumes consisting of grid-points in three-dimensional space. The solution of the equation systems that govern the atmosphere depends on the interactions and transports between adjacent grid volumes that collectively determine the temporal evolution of the system and its essential components (temperature, moisture, pressure, etc.).

A GCM is essentially a weather-forecasting model that operates at a reduced spatial resolution in order to project further ahead in time (years to decades) than forecast models that are designed to investigate weather changes for up to two weeks. In addition to the atmosphere, global models attempt to incorporate as many elements of the climate system as possible, in particular the oceans, the cryosphere, and the biosphere. A GCM is one of the largest and most demanding scientific applications in terms of computing resources. Such models solve large sets of equations on several million grid-points distributed in three dimensions around the globe, and these computations are repeated 50 or more times per simulated day. Computer time and space requirements are thus extremely large, and GCM simulations operate on the most advanced supercomputers.

There exists an abundant literature describing fluid flow and thermodynamic principles as applied to the atmosphere. Comprehensive textbooks dealing with such issues include for example Holton (1972),

Tennekes and Lumley (1972), Haugen (1973), Pielke (1984), or Trenberth (1991) so that only a summary of the governing equations and a very brief overview of some the issues of parameterization will be provided here.

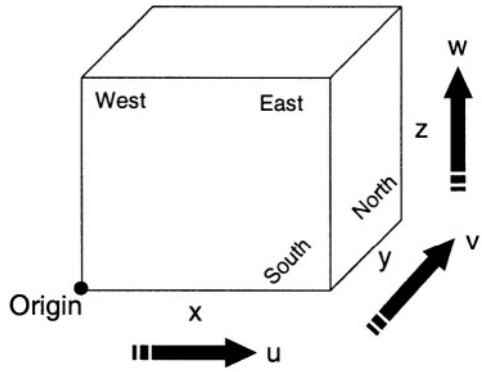

Figure 5.7. Conventional three-dimensional Cartesian representation of space for the x, y, and z axes. Wind vectors u, v, w flow along the x, y, z axes, respectively. Both the space and velocities are, by convention, positive in the direction shown by arrows.

All models make use of conservation principles in their formulation; the governing equations for the atmosphere may be written in a three-dimensional Cartesian representation (whose symbolic and directional conventions are shown in Figure 5.7) as follows:

- Conservation of zonal momentum

$$\partial u/\partial t = - u\partial u/\partial x - v\partial u/\partial y - w\partial u/\partial z - 1/\rho\partial p/\partial x + fv + F_u \qquad (5.8)$$

In this equation, the term on the left-hand side represents the local time-dependent zonal wind velocity, u, which is described by advection processes (i.e., the transport of momentum by the flow) represented by the first three terms on the right-hand side of Equation 5.8, the pressure-gradient term, $1/\rho\partial p/\partial x$, the Coriolis acceleration, fv ($f = 2\Omega \sin\phi$, with Ω the Earth's angular rotation and ϕ the latitude), and the dissipation of wind energy by turbulence and by friction with the surface, F_u.

- Conservation of meridional momentum

$$\partial v/\partial t = - u\partial v/\partial x - v\partial v/\partial y - w\partial v/\partial z - 1/\rho\partial p/\partial y - fu + F_v \qquad (5.9)$$

where v is the meridional velocity.

- Conservation of vertical momentum

$$\partial w/\partial t = - u\partial w/\partial x - v\partial w/\partial y - w\partial w/\partial z - 1/\rho\partial p/\partial z - g + f^{*}u + F_w \quad (5.10)$$

where w is the vertical velocity. g is the gravitational acceleration that acts only in the vertical plane, and $f^{*}u$ is the vertical component of the Coriolis acceleration ($f^{*} = 2\Omega \cos\phi$).

Equations 5.8, 5.9 and 5.10 that are the fundamental relationships governing fluid dynamics are commonly referred to as the *Navier-Stokes Equations.*

- Conservation of heat energy

$$\partial\theta/\partial t = - u\partial\theta/\partial x - v\partial\theta/\partial y - w\partial\theta/\partial z + C_\theta + R_\theta + F_\theta \quad (5.11)$$

Here, θ is a thermodynamic variable known as potential temperature, which is frequently used instead of temperature as the primary variable for the computation of heat exchange in the atmosphere. C_θ, R_θ, and F_θ represent the thermodynamic effects resulting from phase changes of water, the radiative exchange between solar and terrestrial energy, and the turbulent heat flux, respectively.

- Conservation of specific humidity

$$\partial q/\partial t = - u\partial q/\partial x - v\partial q/\partial y - w\partial q/\partial z + C_q + F_q \quad (5.12)$$

with C_q the moisture source and sink term associated with condensation and precipitation processes, and F_q the turbulent transport of humidity

The governing equation set is completed by the equation of state for a perfect gas, which relates pressure, temperature, and density (and thereby links atmospheric dynamics and thermodynamics) through:

$$p = \rho R T_V \quad (5.13)$$

Here, T_V is the virtual temperature ($T_V = 1 + 0.61q$) which takes into account the influence of water vapor on atmosphere on pressure. In many models designed to simulated processes on the larger climatic scales, dynamic processes are assumed to be hydrostatic; the pressure term is then

computed from the hydrostatic equation, one form of which is given below (making use of the equation of state and replacing temperature T by potential temperature θ):

$$\partial p^{R/cp} / \partial z = -g\, p^{R/cp} / cp\theta \qquad (5.14)$$

Conservation of mass is written in the form of a predictive equation for density, which reads:

$$\partial\rho/\partial x = - \partial\rho u/\partial x - \partial\rho v/\partial y - \partial\rho w/\partial z \qquad (5.15)$$

For most models where incompressibility is assumed, however (i.e., $\partial\rho/\partial x = 0$), Equation 5.15 may be simplified to a form of the continuity equation that for shallow atmospheric systems is expressed as:

$$\partial u/\partial x + \partial v/\partial y + \partial w/\partial z = 0 \qquad (5.16)$$

Equation 5.16 takes on an additional importance when the hydrostatic equation (Equation 5.14) is applied to the system; the hydrostatic approximation is a consequence of the simplification of the vertical momentum equation (Equation 5.10) where, for most atmospheric processes outside the range of micro-scale turbulence and cumulus-cloud processes, the dominant forces represent a balance between the gravitational acceleration g and the vertical pressure gradient $\partial q/\partial z$. This implies a loss of the predictive capability of Equation 5.10 (i.e, $\partial w/\partial t \sim 0$), such that the only manner in which the vertical velocity can be computed is through the integration of the continuity equation (5.16) in the vertical.

In the predictive equation set (5.8-5.12), the advective terms, i.e., the first three terms on the right-hand sides of the equations (e.g., $-u\partial u/\partial x - v\partial u/\partial y - w\partial u/\partial z$) are all grid-resolved. This implies that they can be solved directly by a particular combination of a spatial discretization scheme and time integration algorithm at each model grid-point and for each time-step; this is also the case, in Equations 5.8-5.10 for the pressure-gradient and Coriolis terms.

This is not the case for all terms, however, and because they have physical relevance for the time evolution of weather and climate, they cannot be neglected and thus need to be included through procedures known as *parametric schemes.* Parameterization, or the simplification of the equations through physically-coherent approximations, is implemented in numerical models for a number of reasons. Certain physical processes may be acting at

a scale smaller than the characteristic grid interval, as in the case of turbulence, but which nevertheless have relevance to the evolution of the system. Other processes important for the functioning of the climate system, such as the physics associated with cloud formation and precipitation would, if computed explicitly at each time step and at every grid-point, overload the available computer resources. Parametric schemes thus need to be devised in order to take into account subgrid-scale features and complex physical processes in a physically-coherent and computationally-efficient manner. A parametric scheme attempts to relate the variables at unresolved scales to those resolved at model grid-points; the quality of GCM results are directly related to the quality of the parameterized physics. A brief review of the various parametric schemes will be outlined in the following sub-sections, without entering into any particular level of mathematical detail, in view of the fact that there are as many parametric schemes as there are models. The idea in the following paragraphs is simply to provide the reader with a succinct overview of the ideas and principles underlying different types of parametric schemes.

5.3.1. Radiation (R term in Equation 5.11)

The parameterization of radiation is probably one of the most crucial elements in models addressing anthropogenic climatic change issues, because the radiative forcing of greenhouse gases is one of the key drivers of change (Paltridge and Platt, 1976).

A radiation scheme computes the radiative balance of the incoming solar radiation, the outgoing terrestrial radiation, long-wave radiation, and reflection. Absorption and re-emission of infrared radiation are calculated in several spectral bands by taking into account the concentration of different absorbers and emitters, in particular carbon dioxide, water vapor, ozone, and aerosols (Fouquart, 1987; Stephens, 1984). Seasonal cycles form an integral part of radiation schemes, but diurnal cycles are often neglected for reasons of computer economy.

Feedback mechanisms between radiation and water vapor and clouds are also important mechanisms that need to be quantified at global to regional scales (e.g., Beniston and Schmetz, 1985; Schmetz and Beniston, 1986). Cloud-radiation feedbacks are extremely sensitive for long-term climate simulations, and parameterizations of this effect are based either on estimates of cloud amount (dependent on the relative humidity) within a grid volume, or on the variation of cloud optical properties through the water content in clouds. There is still much uncertainty regarding the net radiative

effect of clouds on climate that can either consists in a positive feedback (net warming) through the trapping and re-emission of outgoing infrared radiation, or in a negative feedback through the reflection of intercepted solar radiation.

5.3.2. Clouds and precipitation (C terms in Equations 5.11 and 5.12)

The computational grid of general circulation models is generally too coarse to directly resolve clouds other than stratus-type clouds that may have a considerable horizontal extent; this is a crucial problem in view of the fact that clouds exert a major control on climate dynamics through both positive and negative feedback effects (e.g., Senior and Mitchell, 1993; Yao and DelGenio, 1999).

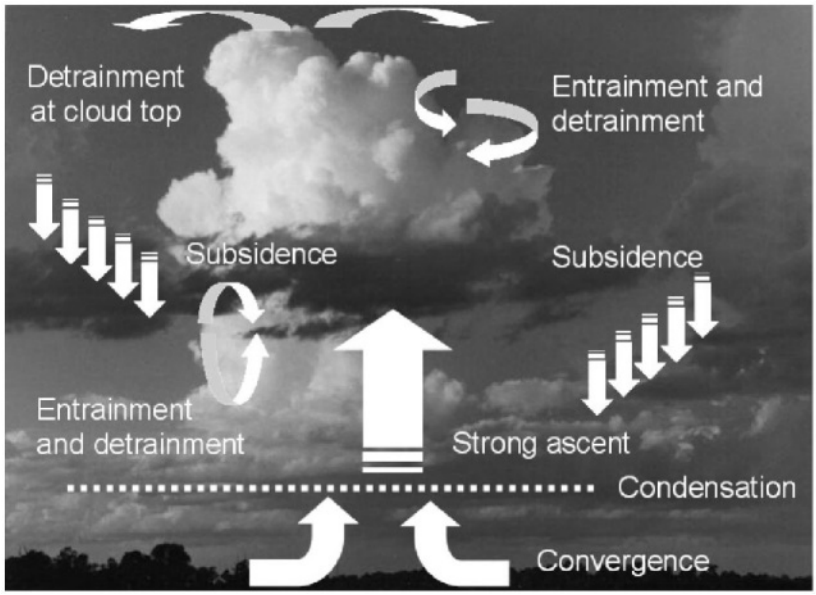

Figure 5.8. Sketch of heat and moisture transfer in the vertical resulting from cloud-related processes in a cumulus-type cloud.

Figure 5.8 illustrates some of the feedback mechanisms that are important in a cumulus cloud scheme; such clouds act as an important pump of heat and moisture in the vertical plane, aimed at re-stabilizing a nominally

unstable thermal situation in the atmosphere. As low-level convergence lifts moist-laden air towards higher and cooler levels, condensation will occur at a certain altitude, thereby triggering the thermodynamic processes associated with condensation. As the cloud pursues its vertical development through rapid ascent in its core, strong turbulence resulting from wind-shear and thermal instabilities will lead to exchange of air between the cloud and its environment in what is referred to as entrainment (intake of air into the cloud) and detrainment (expulsion of air from the cloud into the neighboring unsaturated environment). Entrainment and detrainment processes are one of the principal mechanisms by which heat and moisture are transferred with height due to the cloud itself. At the top of the cloud, evaporation takes place and will lead to cooling of air at the upper levels of the cloud. This cooling increases the air density, leading to compensating subsidence in the vicinity of the cloud, thereby also fulfilling the basic principles of continuity (e.g., Arakawa and Schubert, 1974).

Cumulus-type convection is one of the main heat-producing mechanisms at subgrid scales in a vertically unstable atmosphere. The technique known as *moist convective adjustment* is one of the primary parametric schemes for cumulus convection (e.g., Betts, 1986; Betts and Miller, 1986). The procedure consists in adjusting the temperature and water vapor profiles to a conditionally stable state. Large-scale clouds are allowed to form when the relative humidity within a given grid volume exceeds a certain threshold value of relative humidity (between 80 and 100% according to the model), which sets the cloud cover at between 95 and 100%.

Figure 5.9. Stratiform clouds off the coast of Baja California, Mexico. The clouds in this picture cover an area of more than 1 million km^2 and represent an area of strong reflection of incoming solar radiation (Photo courtesy of NASA).

It should be noted that cumulus-type clouds have a small areal extent but penetrate deep vertical layers, thereby profoundly modifying the dynamic and thermodynamic structure of a large vertical segment of the troposphere, whereas the contrary is true for stratiform clouds (e.g., Klein and Hartmann, 1993). In the case of these clouds, radiative feedback mechanisms, and not direct dynamic or thermal effects, will be the dominant feature. The satellite photograph in Figure 5.9 shows the large surface covered by white, reflecting clouds over the Pacific Ocean close to the Baja California peninsula in Mexico. These clouds form in stably-stratified air that is in contact with a cold ocean surface that favors condensation within the boundary layer. Such vast regions of stratus are found off the coasts of several regions with similar ocean and atmosphere conditions, such as south-west Africa or Chile, for example.

Large-scale rainfall is usually based upon saturation vapor pressure in each model layer, and moisture is allowed to condense out of supersaturated air. If the temperature of the lowest layer is beneath the freezing point, snowfall occurs and snow depth at the surface is incremented accordingly. In the case of surface temperatures exceeding 273° K, precipitation falls as rain and soil moisture content is incremented.

As model grids become finer, cloud parametric schemes need to be more detailed. The necessity for trade-offs between complex cloud physics on the one hand and computational efficiency on the other has generated much interest in the development of convection and precipitation schemes for high-resolution GCMs (e.g., IPCC, 2001; Emanuel and Ivkovi-Rothmans, 1999).

5.3.3. Subgrid-scale turbulent transport (F terms in Equations 5.8-5.12)

A major driving force for the climate system is the heterogeneous distribution of heat at the surface, resulting from differential absorption of solar energy by the different types of surfaceThe *Atmospheric Boundary Layer* (ABL) comprises the lowest 500-2000 m of the atmosphere where dynamic and thermodynamic exchanges between the surface and the atmosphere take place. ABL processes are characterized by small-scale turbulent exchanges of heat, moisture, and momentum that take place at resolutions well below those of the model grid. Most of the momentum dissipation resulting in the deceleration of air in contact with the Earth's surface takes place within the boundary layer.

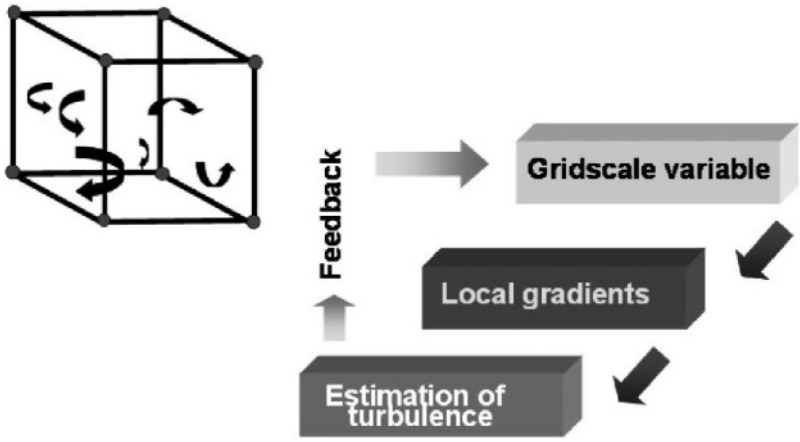

Figure 5.10. Simplified approach to subgrid-scale turbulence parameterization: turbulent eddies are estimated on the basis of local gradients resolved at each grid-point in the three-dimensional grid-box.

Figure 5.10 provides a sketch of subgrid-scale eddied occurring within a model grid volume; the model resolves only the value of the variable at the grid points represented by the circles at each corner of the grid box. Local gradients of velocity, temperature, or humidity are computed on the basis of their grid-point values. Turbulent fluxes are proportional to the grid-resolved gradients, and the use of diffusion coefficients as a measure of the efficiency of turbulent transport under a range of atmospheric stability conditions enable an estimation of the intensity of dynamic and thermodynamic turbulent transports and therefore the feedback of turbulence on the grid-resolved variables.

In order to estimate the exchange of momentum, heat and moisture between the surface and the atmosphere, parameterizations specific to the surface-layer (the first 10-50 m above the surface) are necessary; these are generally based on mixing-layer theory (e.g., Tennekes and Lumley, 1968).

The salient features of surface-layer turbulence are illustrated in Figure 5.11. Turbulent eddies generated by friction with the surface (that acts against the flow) extract energy from the flow and thereby reduce the velocity of air close to the surface. The shear layer shown to the right has mutual feedbacks with the turbulent eddies, that also transfer heat and moisture in both directions between the surface and the atmosphere.

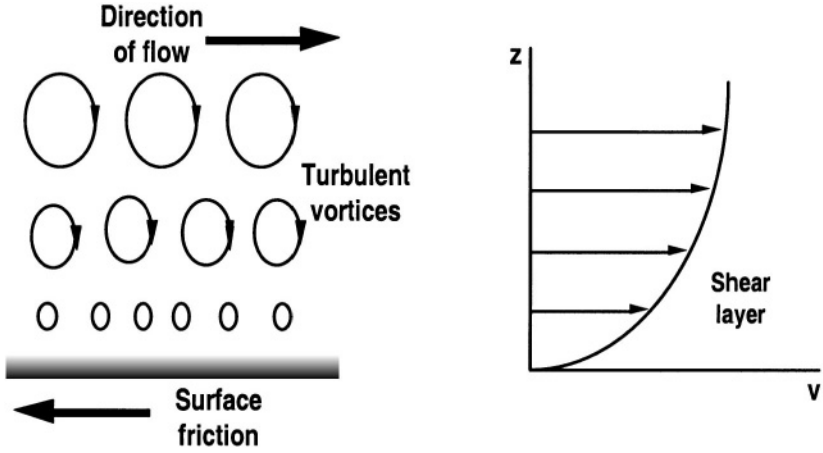

Figure 5.11. Sketch of shear processes close to the surface, that lead to turbulent exchange of momentum, heat, and moisture with the atmosphere.

Type of surface	Roughness length
Calm water	0.001
Flat desert	0.03
Grass	0.1
Mature corn	1.0
Forest	1.5-3.0
Urban area	2.0-10.0

Table 5.1. Values of roughness height (m) according to surface type.

The nature of the surface determines the importance of friction effects and therefore the influence of the surface on atmospheric processes. The larger (i.e., the rougher) the surface elements, the greater the effects of the ground on surface layer processes and above. A dynamic roughness element defined as the *roughness length* is used in the parameterization of surface-layer turbulence (e.g., Businger, 1973); typical values of roughness for various types of surfaces are illustrated in Table 5.1.

A corresponding wind velocity profile with height is given in Figure 5.12, where it is seen that wind speed increases more rapidly with height when the roughness height is smaller.

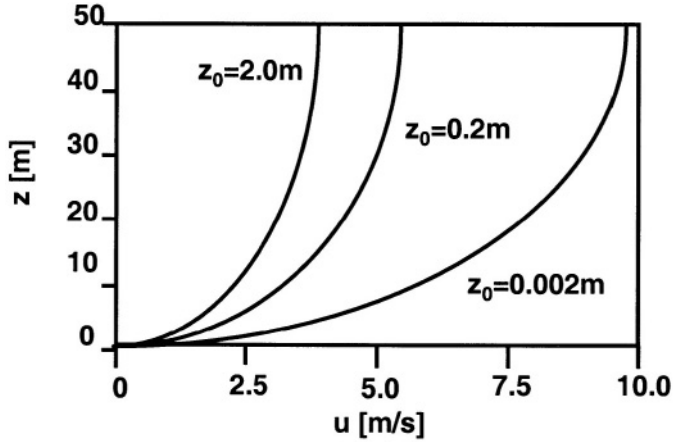

Figure 5.12. Wind-velocity profile with height according to value of the roughness length, z_0.

5.3.4. Gravity-wave drag

The transfer of momentum between the atmosphere and the earth occurs at all scales. At the small end of the scale spectrum, dissipation of energy occurs through friction with the surface. At larger scales, additional processes lead to momentum dissipation, and these are linked essentially to the presence of topography. Mountains that are present over large horizontal distances and with significant heights often generate internal gravity waves which results in gravity wave drag, as sketched in Figure 5.13.

Gravity waves are a dynamic manifestation that reflect the perturbation of stable atmospheric layers of the atmosphere at height by air flowing over a mountain range. The atmosphere attempts to recover its original state through oscillations whose frequency is a function of the thermal stability of the layer. These oscillations propagate and can amplify with height, thus disrupting the dynamics of high altitude flows through gravity wave breaking, thereby dissipating the energy of the flow (Lindzen, 1981; Machenauer, 1977).

Large scale models general resolve rather poorly even important mountain chains, so that mountains need to be included in some parameterized form, such as “envelope topography” which smoothes the real topography over continental areas. Large-scale orographic forcing is then derived by filtering the topography at smaller scales as well as ABL effects. Gravity waves generated by the presence of underlying mountains on the atmosphere are capable of breaking in a similar manner to ocean waves at the

seashore, and in doing so transfer substantial quantities of momentum from the large-scale to the small-scale flows. They also have an influence on the formation of clouds and precipitation close to mountains, which are in turn indirect mechanisms of heat and moisture transfer in the vertical (Palmer et al., 1986).

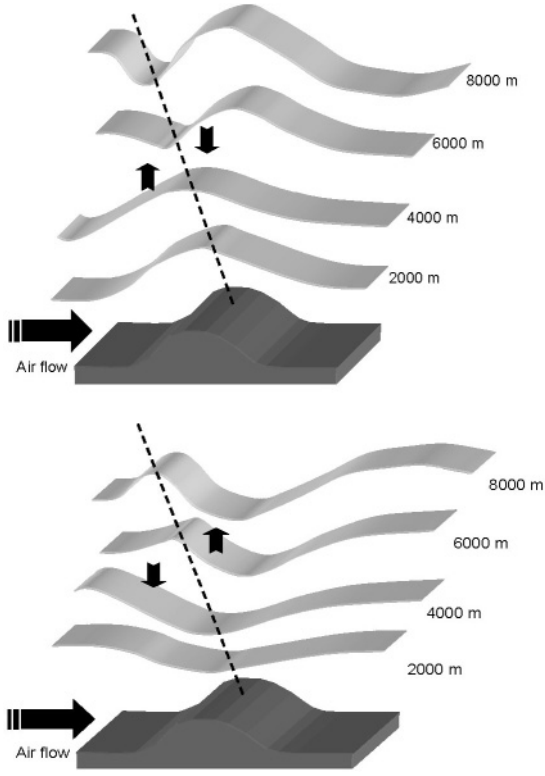

Figure 5.13. An example of the thermal perturbation in the vertical induced by gravity waves as air flows over a mountain. Backward-propagating waves with height induce strong oscillations in stable atmospheric layers represented by isotherm surfaces that oscillate from one time interval (upper) to the next (lower).

5.3.5. Land-surface processes

The exchange of energy, heat, moisture and carbon between the surface and the atmosphere needs to be accounted for in models because significant change in land use and land cover can affect climate in a number of ways

(Bonan, 1995; Dickinson, 1995; Schimel, 1995). For example, tropical deforestation reduces evaporation and simultaneously increases surface temperature through the complete change of the natural vegetation. Photosynthesis processes have also been identified through satellite observations as having an important impact on carbon cycling, water uptake and release and the related efficiency of energy exchange with the atmosphere. Most of these processes act at the subgrid scale in a model, so that soil moisture, runoff, snow cover, and other surface heterogeneities and their changes need to be parameterized, often still in a rather rudimentary form.

It is important in climate models to parameterize not only processes at the surface itself, but the heat and moisture transfer within the soil as well. This involves estimating the surface hydrology balance that includes precipitation, snow melt, ground-water storage, runoff and other processes occurring at the surface.

Anthropogenic climate change may be significantly modulated by changes in soil moisture, because this determines the manner in which local climates may change from moist to dry, or vice-versa, according to significant shifts in the atmospheric general circulation, and the feedbacks from changed soil moisture content on the atmospheric flow patterns.

Soil moisture can be parameterized in the form of a thick soil layer acting as a single reservoir in which moisture increases through precipitation, or decreases through evaporation. Evaporation no longer takes place once all the moisture has been used up. More sophisticated techniques use multiple soil layers, the uppermost one responding most rapidly to precipitation. If the upper layer dries out, some moisture is available for evaporation from the deeper, reservoir, layer. If the model incorporates vegetation as a land-surface characteristic, then moisture in the reservoir layer is taken up by the vegetation during dry periods for evapotranspiration (e.g., Deardorff, 1978; Monteith, 1973).

At any model grid-point over land, a balance between precipitation, evaporation, runoff, and soil moisture accumulation is evaluated. If precipitation exceeds evaporation, then accumulation will occur locally until saturation is achieved. Excess runoff occurring under saturated soil conditions is used for fresh-water input into the ocean, which can have significant local effects in ocean models.

5.3.6. The biosphere

Biospheric processes are a key factor in surface-atmosphere feedback mechanisms; the complexity of biological systems precludes anything more than a very crude parameterization of the presence of different vegetation types and their interactions with dynamic, thermodynamic, and chemical processes. In this latter respect, vegetation on land controls the magnitude of the fluxes of several greenhouse gases, including carbon dioxide and methane. Any changes in gaseous composition will change the response of plant types and the redistribution of greenhouse gases within the atmosphere.

Terrestrial ecosystems are also important in their role on the surface fluxes of heat and moisture, as well as determining surface albedo, both in terms of area extent and seasonality. Evapotranspiration releases vast quantities of moisture which can be taken up within the hydrological cycle, thereby redistributing heat and moisture in the atmosphere. Furthermore, the presence of vegetation exerts a dynamic influence through its roughness characteristics. Flow of air over a tundra region, which consists of sparse and low vegetation will be significantly different from flow over large forested areas, as a result of the different characteristic roughness lengths of these surfaces.

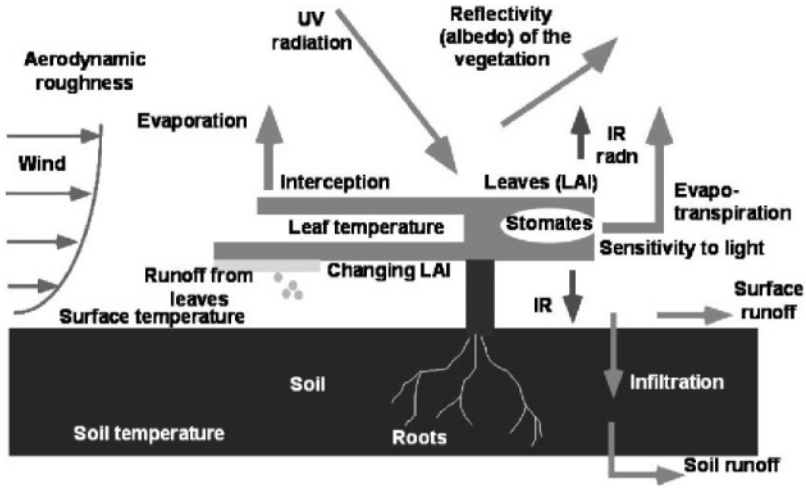

Figure 5.14. Illustration of some of the principle parameters and processes that need to be taken into account in a parametric scheme for vegetation in an atmospheric model. LAI: Leaf Area Index; IR: Infrared Radiation; UV: Ultra-violet Radiation.

Figure 5.14 illustrates the major features of vegetation that are incorporate into land-surface and vegetation schemes. It incorporates albedo and radiative effects, water transfer by the plants from the soil to the atmosphere through the root systems and leaves as a function of their stomatal density. Dynamic effects of plants on air flow are also taken into account; each type of vegetation is associated with a particular roughness length as described in Section 5.3.3.

Parameterization of the biosphere is now a common feature of climate models, using a combined multilayer soil-vegetation surface (e.g., Bonan, 1995; Delage et al., 1999; Sato et al., 1989; Sellers et al., 1989; Xue et al.., 1991). As described above, soils have at least two layers, one acting as a reservoir for plant moisture availability, while the vegetation is parameterized by a canopy layer, surface and root layers, and variable albedo and hydrological characteristics. These latter depend essentially on the leaf-area index (LAI) of the plants, which determine the ratio of transpiring to non-transpiring canopy surface, and the area over which dew formation and precipitation interception occur. More water can be retained by a surface which has a greater LAI, while albedo is determined by the seasonal distribution of this parameter (e.g., LAI will undergo a strong seasonal cycle for deciduous trees in temperate regions, but will be less marked or even insignificant for tropical forests or coniferous trees). In the debate over the influence of massive deforestation in the tropical regions on the carbon cycle and climate change, the necessity of a sophisticated vegetation parameterization techniques becomes crucial.

5.3.7. The cryosphere

The cryosphere is more than a particular case of surface processes. A global model needs to incorporate snow and ice features because of their determining effect on radiation, as well as dynamic mechanisms through Pole-to-Equator temperature gradients. In the summertime, the dominant component of the surface energy balance is solar radiation; small changes in albedo can have large impacts on the response of climate, so that surface albedo requires accurate specification or prediction. In particular, models need to distinguish between sea ice and continental ice surfaces, which have significantly different reflectivity; sea ice albedo is often modeled as a function of latitude and thickness, the latter being determined by the hydrological balance. It is obvious that if a model has difficulty in predicting other variables such as precipitation, then this may reflect upon the accuracy of computations of features such as sea ice.

Similarly, the albedo of surfaces that are snow-covered will be highly different if vegetation is taken into account in a model or not. Snow falling in the Tundra will raise the surface albedo from 0.2 to 0.8, whereas in a coniferous forest, practically no albedo change will be observed as a result of the forest canopy. In a model with no description of vegetation, a sharp rise in albedo would be observed in the region which in reality is covered by forests, thereby feeding into the climate system in a different manner.

5.4. COUPLED MODEL SYSTEMS

Modelers have recognized the need to incorporate as many elements of the climate system within a single numerical framework, though in practice this is exceedingly difficult due to the computational resources involved and the often limited understanding of numerous underlying feedback mechanisms. In addition, an integrated model seeks to simulate processes acting on vastly varying time scales, as seen in Figure 2.19. According to the component considered, the response time to a particular forcing can vary from a few hours to several centuries.

In view of the significant influence of the oceans in terms of heat storage and the absorption of greenhouse gases, long-term simulations of climate require full three-dimensional ocean model systems. For example, if only sea-surface temperatures are prescribed for the ocean component of a climate model, climate predictability in the long term becomes questionable because features such as the quasi-periodic ENSO (El-Niño/Southern Oscillation) phenomenon discussed in Chapter 3.3.2 are not taken into account. Other features such as the formation of deep water also need to be simulated in a physically-coherent manner. Changes in the intensity and location of deep water formation can have profound effects on the atmosphere, and changes in the thermohaline circulation of the oceans have resulted in major climatic responses in the past, such as the cold "Younger-Dryas" period which affected Europe and other regions of the world after the end of the last glaciation (Broecker et al., 1985; Street-Perrott and Perrott, 1990; Salinger et al., 1989).

Coupled models are complex in many ways, because of the differences in the temporal response of the ocean and the atmosphere to perturbations, as already alluded to earlier in this volume. As a result, adjustments are necessary to ensure that the fluxes of momentum, heat and moisture are correctly distributed between the two systems. Bryan (1998) shows that this adjustment can be on relatively short time scales, of the order of less than a decade to half a century, whereby equilibrium is reached by the ocean

following a prolonged change in atmospheric temperature in terms of the atmosphere, land surfaces, the upper levels of the ocean (the mixed layer) and sea ice. There are however residual errors in the mutual adjustment of the ocean and atmospheric components in the surface heat and fresh water fluxes that result in a slower adjustment phase sometimes referred to as *climate drift.* This can take several millennia because of the fact that on these time scales it is also necessary for the deep ocean needs to adapt to forcings occurring at the surface. In order to avoid having to compute climatic change for many processes, coupled models are allowed to reach a state where climate drift is negligible prior to undertaking simulations for assessing the response of the climate system to anthropogenic or natural forcings, as discussed by Stouffer and Dixon (1998). Many model simulations looking into the future have actually been initialised as early as the middle of the 18th century to overcome this problem (e.g., Johns et al., 2003), with an added value that such simulations prior to the current period can be compared to historical and instrumental data.

In many coupled model simulations, it has been necessary to add a correction factor to the fluxes of momentum, heat and water that are transferred from the atmosphere to the ocean in a procedure known as *flux adjustment.* An unfortunate consequence is that these additive terms have no underlying physical meaning; although the flux correction method adds uncertainty to model simulations, the method has enabled models to provide realistic and stable realizations of current climate, both in the atmosphere and at the ocean surface. However, in recent years, coupled model simulations without flux correction have provided reasonable results because of a greater quality of sea-surface temperature data and atmosphere and ocean model parameterizations (e.g., Guilyardi and Madec 1997; Boville and Gent 1998; Gordon et al., 2000).

Recent developments in ocean system models that take into account not only surface processes at the ocean-atmosphere interface, but also those acting at depth (i.e., deep ocean circulations related to the global ocean thermohaline circulation) have resulted in considerable improvements in the quality of climate model results. An oceanic general circulation model requires high spatial resolution to capture eddy processes that are key features of ocean dynamic exchange, and also bottom topography and basin geometry. High-resolution ocean models are therefore at least as costly in computer time as are atmospheric models.

In recent years, there has been a sharp improvement in the simulation of ENSO events with even a certain degree of confidence in the predictability of the onset, if not the intensity, of El Niño episodes such as the 1997-1998

event. Progress in simulating the possibly more complex North Atlantic Oscillation is currently emerging in recent coupled simulations.

Coupled ocean-atmosphere systems in the 1990s represented the first attempt at integrated climate modeling. Today, further integration of other climate system component models include in particular the cryosphere and the biosphere that are now being developed and applied to obtain more realistic simulations of climate on annual to century time scales.

5.5. BOUNDARY CONDITIONS, VALIDATION, AND RANGE OF APPLICATIONS OF CLIMATE MODELS

Theories and models are normally designed to address classes of similar issues. Before they can be used to answer specific questions, they must be adapted to the particular conditions of the problem to be analyzed. This is achieved through the specification of initial and boundary conditions. Model initialization occurs when the state of the system is specified at the beginning of the computation, by setting each of the dependent variables to some reference value obtained from observation or hypothesis. Model initialization is required to specify the state of the system at the beginning of the computation, by setting each of the dependent variables to some reference value obtained from observation or hypothesis. In most models, initialization is not a trivial process, because the information used to initialize a simulation must not only be processed in a manner suited to the internal model structure, but it must also be consistent with the laws and relations which define the model.

Boundary conditions are also a necessary part of a model simulation. These describe constraints on the evolution of the system, or interactions between the system and its environment that are not described explicitly by the model. Since lower and upper model boundaries are artificially enclosed, and additionally at the sides in small and mesoscale limited area models, it is necessary to specify the values of the dependent variables at these boundaries. Boundary conditions generally require updating at each time-step of the integration. For most models, it is convenient to define the top, lateral (for models other than global GCMs) and bottom boundary conditions separately, because the manner in which variables at these surfaces are specified is different for each type of boundary. Furthermore, only the bottom boundary condition has a physical meaning, since it generally coincides with the Earth's surface, whereas the other boundaries are incorporated for computational necessity.

The number of boundary conditions that can be applied to a particular model depends primarily on the form of the differential equations which has been adopted for the model. Model equations that have the correct number are described as *well-posed,* whereas they are *over-specified* if the number of conditions exceeds that actually used. Oliger and Sundström (1976) maintain that over-specification of model boundary conditions can, for certain solution algorithms, lead to physically-erroneous shortwave phenomena which travel across a model grid at the fastest wave speed allowed in the model; these are generated at the boundaries and, if unchecked through mathematical filter functions, are likely to severely contaminate the model physical variables.

Abstract theories and models need to be validated, in order to have some degree of confidence in their projections and analyses. In many cases, the purpose of validation is not so much to prove the absolute accuracy of a model as to define the degree of uncertainty of its results and the limits of applicability. By comparing model results with measurements and observations as far as possible, improvements in model design or recommendations for developing new parameterizations can be suggested.

Confidence in modeling techniques may be reduced for a number of reasons related to the technique itself, a limited understanding of the bio-geophysical mechanisms governing a particular system, or inadequate data for validation purposes.

Models suffer from insufficient spatial resolution and an incomplete description of feedback mechanisms and interactions between various elements of the climate system. Initialization procedures are dependent on a set of physical, biological, economic, and demographic information that contain a wide range of uncertainties to which a model will be sensitive. Computational resources and mathematical algorithms, while in constant development and progress, have difficulty in adequately modeling some of the most complex systems in existence.

Despite these often constraining caveats, however, models have generally reached an advanced level of development. The results of these models, if viewed with sufficient caution, can be used to analyze the functioning and evolution of a number of environmental systems. For example, most climate models are today capable of providing an accurate representation of the broad characteristics of current climate, both in terms of average climatic conditions, as well as seasonal to interannual variability. Such observations increase confidence in model studies of future climatic change based upon a number of socio-economic scenarios, and encourage the commitment of the scientific community to future model development.

5.6. CHAOS IN THE SYSTEM?

Interactions between scales smaller than that of the process under investigation, i.e., generally the grid-scale of a model, need to be addressed in a physically coherent, and numerically efficient manner. The study of scale interaction, however, is no longer trivial when applied to non-linear systems. Fluid mechanics, which are used to describe atmospheric flows, are highly non-linear, essentially because the rate of change of a particular property depends on the transport of that property by the fluid flow, whose velocity V is one of the variables of the problem. The conservation equation for momentum, for example, involves the manifestly non-linear advection terms, such as $V.\nabla V$.

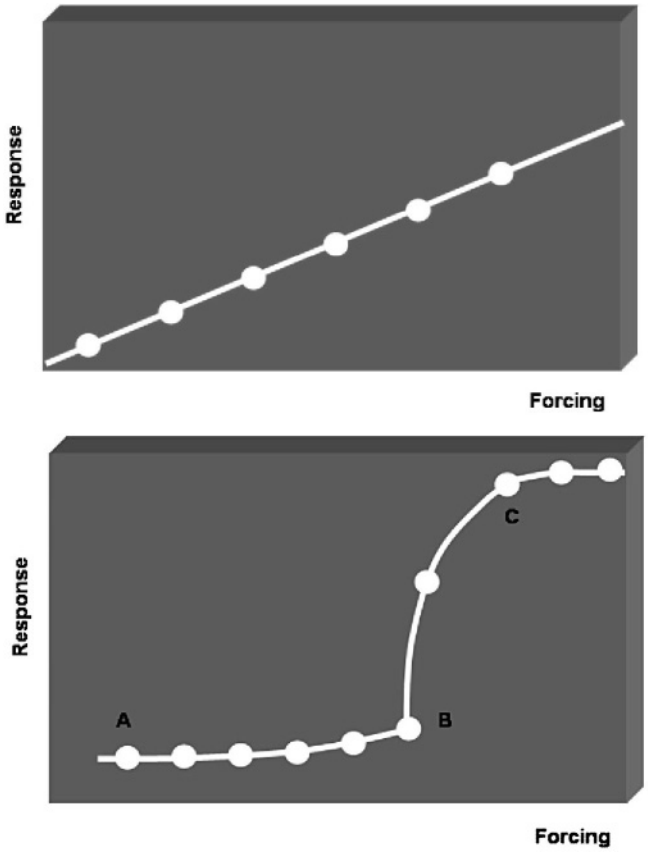

Figure 5.15. Schematic illustration of the difference in behavior between linear (upper) and non-linear (lower) systems.

In a linear system, the ultimate effect of a forcing from the smaller scales to the forcing at the scale of interest is simply the superposition of the effects of each forcing taken individually. In a non-linear system, adding a small cause to one that is already present can induce dramatic effects that may be completely disproportionate to the amplitude of the forcing.

This is illustrated in Figure 5.15, for both linear and non-linear systems. The principles illustrated in these examples serve to emphasize the fact that in non-linear systems, small changes in a particular forcing function can lead to a wide range of responses; in the lower graph of figure 5.15, a large forcing from point A leads to a minor change until point B. Here, a threshold in the system is reached, by which a small additional increase in forcing leads to a large change in response. Finally, a second threshold is reached in this example at point C, where the system no longer responds sharply to further increases in the perturbation to the system.

Lorenz (1963) was one of the first to discover the implications of such considerations for the atmospheric sciences. He developed a nominally simple model of the climate system in which only three modes, each associated with a particular wavelength, were considered.

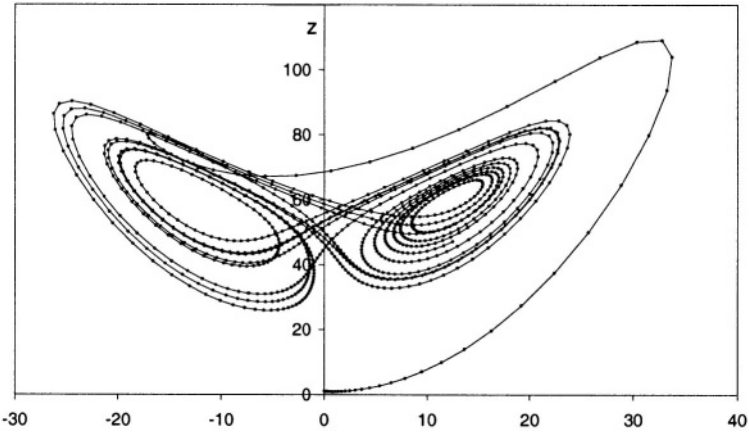

Figure 5.16. The Lorenz Attractor, or a visualization in phase space of the trajectories that represent the response of the system to a particular set of initial conditions. The "climate" in this simple system flips from a cold (left) to a warm (right) climate apparently at random.

The equations in the three-dimensional Cartesian coordinate system read:

$$x_{n+1} = x_n + \sigma (y_n - x_n) \qquad (5.17)$$

$$y_{n+1} = y_n + (\rho x_n + x_n - y_n - x_n z_n) \quad (5.18)$$

$$z_{n+1} = z_n + (x_n y_n - \beta z_n) \quad (5.19)$$

where n refers to the time of iteration, x is proportional to convective intensity, y to the temperature difference between descending and ascending currents, and z to the difference in vertical temperature profile from linearity. σ is the Prandtl Number, ρ the ratio of the Rayleigh Number to its critical value, and β is a geometric factor (e.g., Tabor, 1989).

The solution of the Lorenz equations in phase space shows that the simple climate system he describes can flip from one state to another, apparently at random. In Figure 5.16, the two loops are realizations of the x-component of the equation set (Equation 5.17), where the trajectories in the phase space broadly represent transition from a "cold climate" located to the left of the dividing line, to a "warm climate" located to the right. The trajectories never intersect, nor do they follow precisely the same pathways.

The Lorenz model suggests that weather and climate are inherently unpredictable (Lorenz, 1963; 1968; 1969; 1982; Nicolis and Prigogine, 1989), since they exhibit one of the basic properties of chaotic dynamics, namely the sensitive dependency of the model solutions on initial conditions. Very minor changes in initial conditions can lead to very major differences in the evolution of the atmospheric state after some time, as sketched in Figure 5.17.

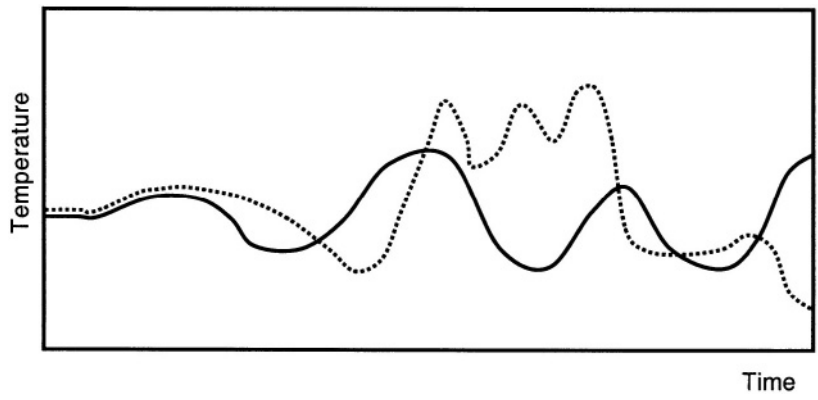

Figure 5.17. Sensitivity to initial conditions: a small difference in the initial conditions at left can lead to strong differences in the evolution of a variable such as temperature after some time, as seen in the difference between the solid and dotted lines.

It is on the basis of this consideration that the well-known "butterfly effect" entered the popular jargon, i.e., the notion that the flutter of a butterfly wing in one location of the globe could trigger major climate phenomena, such as tropical cyclones and other extreme events, in another part of the world. Nicolis and Prigogine (1989) have extensively reviewed systems which exhibit chaotic behavior; chaos in nature reveals the fact that disorder at a certain scale is not incompatible with order at different scale. The apparent randomness of turbulent flow, for example, is not the result of imperfections in an experimental setup or of a complex environment that cannot be controlled, but is indeed embedded in the dynamics of perfectly deterministic systems which may involve only a few variables. In these systems, all scales are important and not simply the largest, most obviously dominant ones. The value in modeling complex environmental systems therefore resides in the possibility of undertaking a large number of sensitivity experiments, in which studies of the response of the system to a particular forcing may be analyzed. Interactions between different elements of the system may also be envisaged in order to further the understanding of the fundamental processes and controls involved. In this sense, models are a powerful analysis tool that not only complement, but often go beyond, the interpretation of observational data.

5.7. OBSERVING AND MONITORING CLIMATE

The advent of satellite imagery over since the early 1970s has largely contributed to the development and understanding of many elements of the climate system and its evolution. However, ground-based measurements and vertical soundings of the atmosphere with instrumented balloons are also an essential component of day-to-day monitoring of the atmospheric environment. More recently, in order to close the data gap in the oceans, systems of buoys have been deployed in certain parts of the oceans, either for routine reporting of temperature or pressure conditions, or in the context of targeted investigations, such as the TOGA-CORE program that was initiated in the late 1980s to monitor atmospheric and oceanic parameters relevant to ENSO in the Pacific Ocean (e.g., Chen et al., 1996; Godfrey et al., 1998).

The World Meteorological Organization (WMO, based in Geneva, Switzerland), has since its inception set up and coordinated a large number of observing stations that enable surface observations and, in many instances, upper air soundings two or more times per day to be made simultaneously. Upper air soundings make use of an instrumented package

that is carried by a helium balloon into the high atmosphere (at least 30 km altitude); the instrumented package emits a signal at regular time intervals to transmit the readings of temperature, humidity, pressure, etc. The WMO upper-air sounding network launches upper air soundings at simultaneous times in order to obtain a "snapshot" of the state of the global atmosphere at a specific time. These surface and sounding data serve primarily for weather forecasting, but the long-term data archives are valuable for analyzing the long-term changes in climate.

Although the understanding of weather and climate phenomena are anchored in their rigorous mathematical formulation, the observation of the Earth from space is an essential element for understanding the system and for providing information of use for specifying climate model boundary and initial conditions and for inter-comparisons between models and observations. The combined techniques of simulation and observation thus enable a framework for predictions of the evolution of the system.

More recently, the GCOS initiative has been set up by WMO with a view of establishing a comprehensive global network of observation points of relevance for climate studies (GCOS, 1992 and more recent reports), in particular the detection of trends in temperature, moisture or radiation at regional to global scales. Figure 5.18 shows the distribution of the network comprising almost 1,000 stations both on continents and on oceans.

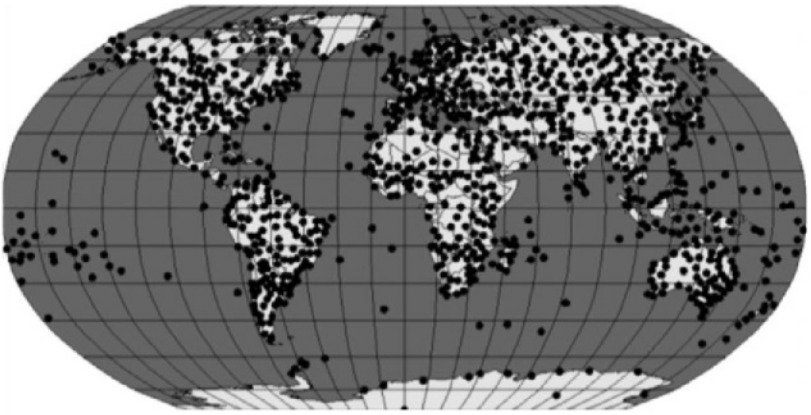

Figure 5.18. The distribution of measurement points of the Global Climate Observing System (GCOS) of the World Meteorological Organization (Courtesy: WMO).

A large number of satellites have been launched since the 1960s, and with the exception of military observations and telecommunications, satellites for observing weather were among the first routine applications of space-borne

remote-sensing in environmental science. Three broad categories of satellite can be identified as a function of their orbit around the globe, namely:

- Low-orbit satellites, whose altitude is typically in the 200-500 km range;
- Heliosynchronous satellites, whose orbits are between 650 and 850 km above the surface;
- Geostationary satellites that are located at 36,000 km above the Equator.

Low-orbit satellites generally yield very detailed images of the planet, but over limited areas at any given time. Repetition of observations over the same site may take time between one set of orbits and the return of the satellite in the same orbital trajectory. Furthermore, the lifetime of such satellites is relatively short because there are sufficient molecules of air at low orbital altitudes to progressively slow down the satellite and ultimately attract it back to Earth.

Heliosynchronous satellites are typically routed on a polar orbit and they circle the Earth from one Pole to another in a plane whose orientation with respect to the Sun remains fixed throughout the year. This configuration has a number of advantages, in particular the systematic observation of the side of the Earth that is illuminated by the Sun. The return period for the satellite above a given area can vary from 1-10 days according to latitude, and the pathways illustrated in Figure 5.19 show the lag between one orbit and another as well as the path width of the sampled surface.

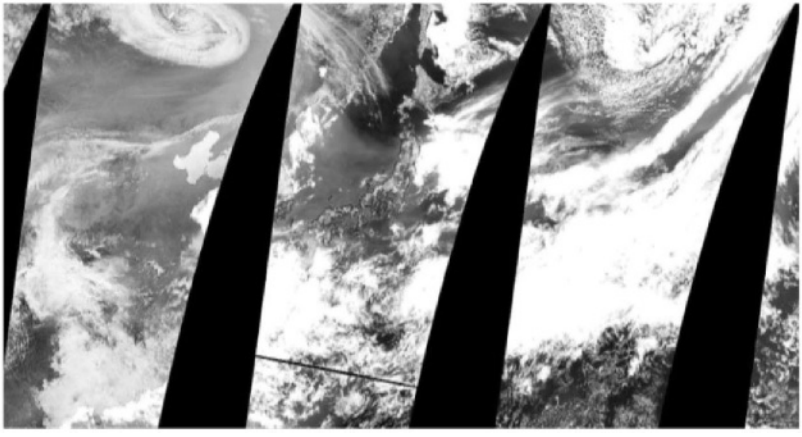

Figure 5.19. Composite image following several successive orbits with a polar-orbiting satellite (SeaWIFS). Band-width at the surface averages 1,000 km (Courtesy: NASA-Goddard Space-Flight Center)

Figure 5.20. Geostationary satellite image of part of the Southern Hemisphere where both Africa and Antarctica are visible (Courtesy: European Space Agency).

Geostationary satellites are locked in orbits that allow them to orbit around the Earth at precisely the same velocity as the Earth's rotation velocity. They are thus always positioned in the same location, which allows them to observe constantly the same part of the world, as seen in the Meteosat weather satellite of the European Space Agency in Figure 5.20.

The platforms that are in orbit around the globe carry one or more instrument systems. In low orbits, the only physical phenomena that can be directly measured are gravity and radiation, this latter parameter being important for climate as already seen in Chapter 2. It is possible to distinguish between passive instruments that measure radiation emitted in various wave-bands from the Earth, and active instruments that emit a signal at a particular wavelength and interprets the return signal modulated by its path through the atmosphere, such as space-borne radar. Satellites that have active instruments on board require an appropriate energy source to operate the instrument. One advantage of this kind of instrument is that it does not depend on reflected sunlight for its measurements but can retrieve data both day and night or, according to the instrument, independently of whether clouds are present or not.

Earth observation instruments can also be classified as a function of the wavelengths at which they operate. Optical instruments analyze the properties of sunlight reflected from the surface or the atmosphere in the visible or near-infrared wavebands, while thermal instruments sample

infrared radiation emitted by the Earth system. Microwave instruments measure in wave-bands typical of radars. Figure 5.21 shows a Meteosat image of water vapor in the atmosphere as measured by the sensor that captures radiation emitted in the water vapor spectral bands. The white regions are associated with high water vapor content, such as in the equatorial convergence zone and in the middle latitudes where the vortex patterns characteristic of frontal systems can be clearly identified.

Figure 5.21. A view with the Meteosat water vapor sensor. Bright regions denote high water vapor content, dark regions are associated with very dry air masses. The satellite does not "see" the Earth's surface as neither oceans nor land emit in the water-vapor bands (Courtesy: European Space Agency).

One of the fundamental problems of remote sensing is to extract useful information on processes and features at the Earth's surface based on radiation measurements at various wave-lengths. The interpretation of satellite data is based upon an understanding of the modulation of the signal received by the satellite that is a function of spherical geometry and physics. The problem of conversion of a signal received by a satellite to a measure of temperature or humidity, for example, is resolved through *inverse modeling* techniques. In a first step, it is necessary to assess the manner in which radiation propagates in the environment and reaches the satellite. Once the radiative transfer processes are known, the inverse problem needs to be solved, i.e., to determine the values of environmental and atmospheric

parameters on the basis of the radiation values measured by the space-borne instrument. Inverse modeling techniques are generally complex because as a rule there may be more than one environmental state capable of explaining satellite measurements.

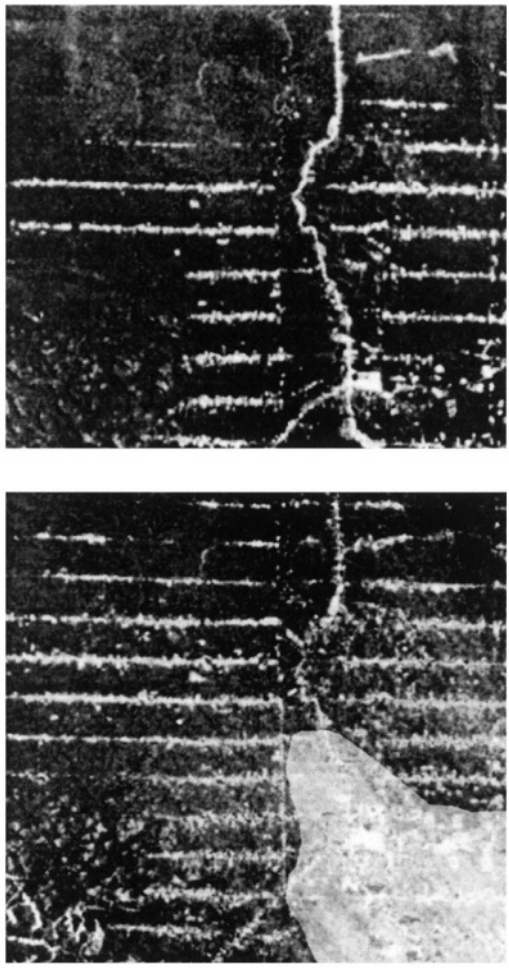

Figure 5.22. Tropical deforestation in Amazonia between 1979 (upper) and 1986 (lower). Straight lines are roads penetrating into the forest. Shaded area at bottom right in the lower figure highlights the zone where a small town has been built (Courtesy: NASA).

It is thus necessary to use detailed models of environmental processes and to have access to other sources of information in order to identify the most

likely set of processes that govern the intensity of the signal received by a satellite. There exists today a wide range of mathematical algorithms capable of handling large amounts of satellite data in a short time and at reasonable cost. The accuracy of space measurements and derived products depends entirely on the degree of precision and the quality of the methods used for analyzing and converting the signal measured by the space-borne instruments.

Remote-sensing products are often represented in the form of maps showing the geographical distribution of one or more variables. When these data are collected on a regular basis in time and space, they allow an assessment of changes that may have occurred between one set of observations and another. In Figure 5.22, for example, the surface area of tropical forest that has been removed over two specific time periods allows to estimate the rate of deforestation. The two satellite pictures, taken in 1979 (upper) and 1986 (lower) highlight the direct interference of human activities with the tropical rainforest. In the 1979 view, a main highway (vertical line) has allowed penetration into the forest through a network of side roads. In 1986, the number of side-roads and their penetration into the forest has significantly increased; in addition, a community has been set up at the junction of two highways (shaded area in the lower figure), with a considerable spread of deforested land radiating out from the small town.

Chapter 6

CURRENT AND FUTURE CLIMATIC CHANGE

6.1. EVIDENCE FOR CLIMATIC CHANGE AND THE EMERGENCE OF THE ANTHROPOGENIC FACTOR

In view of the observational evidence regarding changes in atmospheric chemistry that are related to human activities, it is of interest here to provide a brief summary of changes in climate that have been observed in the past that may be related to the increased radiative forcing in the atmosphere.

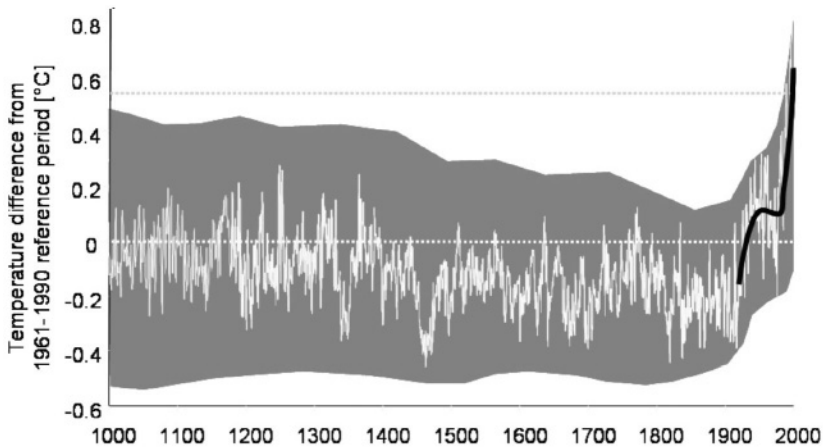

Figure 6.1. Reconstructed time-series of Northern Hemisphere temperatures. Gray shading represents the uncertainty range of the data; the black curve from 1900 onwards is based on the instrumental record, and the dotted line highlights the record 20^{th} century mean global temperature (Adapted from Mann et al., 1999).

Mann et al. (1999) have summarized the investigations based on a number of different proxy records, including tree-ring data, ice cores, historical archives and, since the middle of the 19th century, from instrumental data in the graph given in Figure 6.1. The figure shows that despite the large error spread especially towards the beginning of the record, temperatures throughout the past millennium and up to the middle of the 20th century were consistently lower than they have been at the end of the 20th century. Indeed, a cooling tendency is observed until the early 1900s at which time temperatures rise in an unprecedented manner.

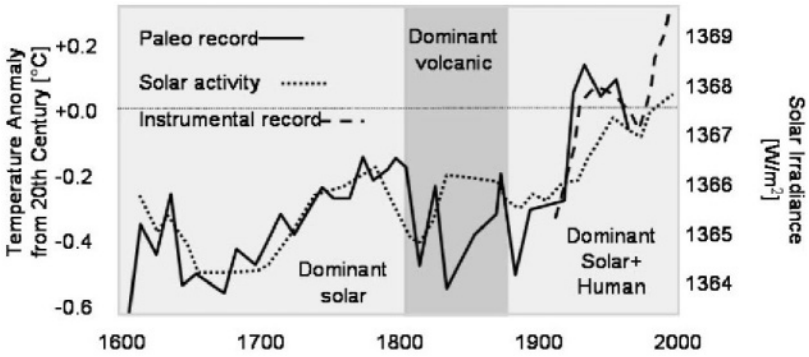

Figure 6.2. Possible physical mechanisms explaining the low temperatures in the second half of the millennium and the rise in global temperatures following the termination of the Little Ice Age around the middle of the 19th century.

There are several hypotheses that can explain the fluctuations seen in Figure 6.2. Paleo-climatic and paleo-environmental research, as well as astronomical reconstructions of solar cycle point to three major root causes for climatic change over the last 500 years, namely a period where solar activity (or a weaker phase of solar luminosity) appears to be responsible for the Maunder Minimum period at the end of the 16th century and the subsequent "Little Ice Age" that affected many parts of the Northern Hemisphere until the mid-18th century; a period dominated by strong volcanic activity during the 19th century, associated with strong reductions in incident solar radiation at the surface due to aerosols at high elevations, and the most recent part of the record that involves both increased solar activity and the greenhouse effect (Bradley, 1999; Crowley and Lowery, 2000; Mann and Bradley, 1999; Mann et al., 1998; 1999).

According to the most recent findings of the IPCC (2001), the global average surface temperature has increased since the middle of the 19th century. In the course of the 20th century the increase has been 0.6 ± 0.2°C.

The estimates are based on a combined average of temperatures close to the surface over the land and at the sea surface, and include adjustments to remove the bias of urban heat island effects, for example.

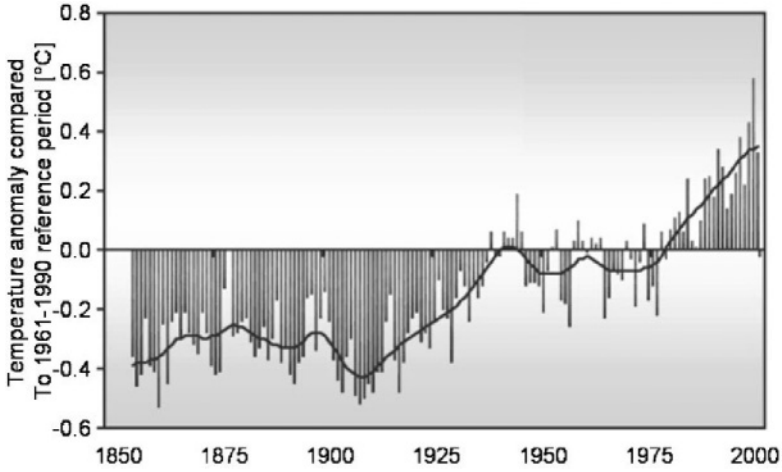

Figure 6.3. Trends in Northern Hemisphere computed as departures from the 1961-1990 climatological average reference period. A 5-year smoother has been applied to the bold line to highlight trends in the absence of interannual noise (Data: Courtesy of the Climatic Research Unit, University of East Anglia, UK).

As seen in Figure 6.3, the record exhibits much variability and most of the 20th century warming occurred has taken place in two broad periods, namely 1910-1945 and 1976-2000, with the 1990s showing an even greater rate of warming than preceding decades.

In addition to mean temperature rise, there has also been an asymmetric change in the trends of minimum (nocturnal) and maximum (diurnal) temperatures, with the former increasing at more than twice the rate of diurnal temperatures, thereby decreasing the diurnal temperature range and lengthening the duration of frost-free periods in the winter (Karl et al., 1993). The increase in nocturnal temperatures is consistent with the enhancement of greenhouse gas concentrations, where infrared energy loss to space is curtailed and night-time temperatures do not fall as low as when there is more infrared radiation emitted from the surface. The increase in sea-surface temperatures has also been measured since the beginning of the 20th century, although this increase is only about 0.3°C because of the larger heat capacity and higher density of sea water compared to air.

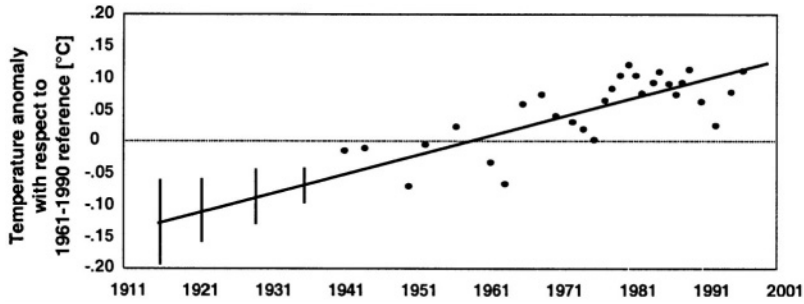

Figure 6.4. Temperature anomalies at intermediate depths (1,500-2,500 m) in the Atlantic Ocean close to Bermuda. Vertical lines show the uncertainty associated with sparse measurements prior to the 1940s.

Measurements conducted at depths of 1,500-2,500 m in the Atlantic Ocean close to Bermuda constitute one of the most unique long-term records of temperature trends at intermediate depths (e.g., Michaels and Knapp, 1996). Figure 6.4 shows that here also, a warming trend of about 0.3°C is apparent at the century time-scale; however, a single record of this nature cannot be considered as proof of a global warming tendency, but is nevertheless consistent with warming trends around the globe.

Perhaps one of the most unequivocal signs of change, however, is to be found in the glacier record of many mountain regions of the world. The annual glacier mass balance, that is dependent on both temperature and precipitation, has been measured for several decades for about 50 glaciers located essentially in the Northern Hemisphere. In addition, the changes in the length of an additional 1000 glaciers provide a supplementary measure that helps to confirm the results from the limited number of direct mass balance measurements. An assumed step change in the equilibrium line altitude of a glacier, i.e., the level where accumulation processes by snow are in balance with ablation processes, induces an immediate step change in specific mass balance.

The resulting shift in specific mass balance is the product of the shift in equilibrium line altitude and the gradient of mass balance with altitude, weighted by the distribution of glacier surface area with altitude (hypsometry). Hypsometry represents the local or topographic part of the glacier sensitivity to changes in weather and environmental conditions, whereas the mass balance gradient reflects principally the regional or climatic part (Kuhn, 1990). Because the mass balance gradient increases in the presence of enhanced humidity (Kuhn, 1981), the sensitivity of glacier

mass balance is generally much higher in areas with humid and maritime climates than those with dry, continental conditions (Oerlemans, 1993).

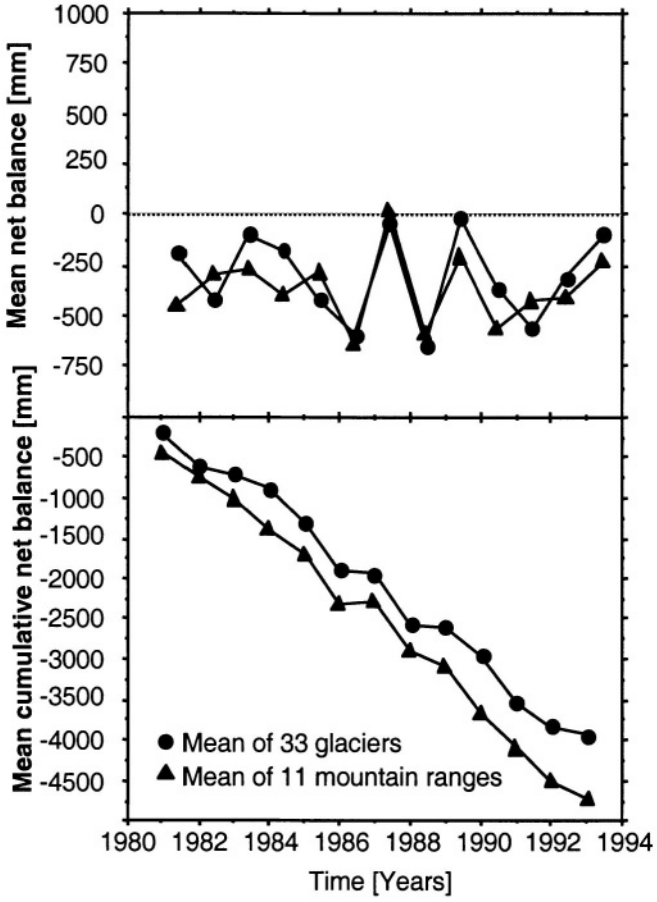

Figure 6.5. Mean net balance (upper) and cumulative mean net balance (lower) measured from 1980 to 1993 on 33 glaciers in 11 mountain ranges (From: IAHS/UNEP/UNESCO, 1994).

Results from continuous mass balance observations during the period 1980-1993 in North America, Eurasia and Africa are summarized in Figure 6.5. The mean of all 33 glaciers investigated here is strongly influenced by the great number of Alpine and Scandinavian glaciers. A mean value was therefore also calculated using only one single value for each of the 11 mountain ranges involved. The mean specific net balance that has been

computed for these glaciers, approximately a loss of 30 cm of water equivalent over the 14 years of this record, correspond to an additional energy flux of 3 W/m^2. This is close to the estimated radiative forcing resulting from anthropogenic greenhouse gas emissions.

Decadal to century-scale trends are comparable for numerous mountain regions, with continentality effects being a major controlling factor on glacier sensitivity (Letreguilly and Reynaud, 1990) along with individual hypsometric effects (Furbish and Andrews, 1984; Tangborn et al., 1990).

Glaciers in the Southern Alps of New Zealand have lost 25% of their area over the last 100 years (Chinn, 1996), and glaciers in several regions of central Asia have been retreating since the 1950s (Fitzharris et al., 1996; Meier, 1998). The seven-year average rate of ice loss for several glaciers monitored in the US Pacific Northwest was higher for the period since 1989 than for any other period studied (Hodge et al., 1998)

In the tropical mountain zones, glaciers have also experience sharp retreats over a relatively short period of time, emphasizing the global nature of temperature increases that have affected almost all mountain glaciers of the world.

Accelerated retreat has been reported for the tropical Andes (Thompson et al., 2000). High altitude ice cores reflect significant increases in temperature over the last few decades with glaciers and ice caps disappearing altogether in some places such as in the Venezuelan Andes (e.g., Schubert, 1992). At Quelccaya, in the Ecuadorian Andes, temperatures in the last 20 years have increased to the point that by the early melting observed in the early 1990s had reached the summit at an elevation of 5,670m (Thompson et al., 1993). In the entire 1,500 year ice-core record from Quelccaya, there is no comparable evidence for such extensice melting at the highest elevations. Similarly, at Huascarán, in northern Peru, isotopic evidence shows that temperatures have increased markedly, from a Little Ice Age minimum in the 17^{th} and 18^{th} centuries, to a level for the last century which was higher than at any time in the last 3,000 years. Ice cores from Dunde Ice Cap, China, also show evidence of recent wanning that is higher in the last 50 years than in any other 50 year period over the last 12,000 years. Evidence from other high altitude sites (Hastenrath and Kruss, 1992) including the glaciers of Mt Kenya and the ice crown of Kilimanjaro in eastern Africa point to a dramatic climatic change in recent decades; Mt Kilimanjaro has lost over 60% of its ice cover in the last century (Hastenrath and Greischar, 1997).

In snow at the temperatures well below the freezing point that are common in the high latitudes, but also in regions of continental climate and at very high altitudes, atmospheric warming does not directly lead to mass

loss through melting and runoff as for temperate glaciers, but rather acts to warm the compacted snow layers (Blatter, 1987; Haeberli and Funk, 1991; Robin, 1983). Sublimation processes, i.e., the conversion of ice directly to vapor in the atmosphere, can also be important in certain regions where relative humidity is extremely low.

Snow cover in the Northern Hemisphere has diminished on average, according to satellite measurements, and the thawing of lakes and rivers at the end of the winter season intervenes currently about two weeks earlier than at the beginning of the 20th century in middle and high latitude regions (IPCC, 1998).

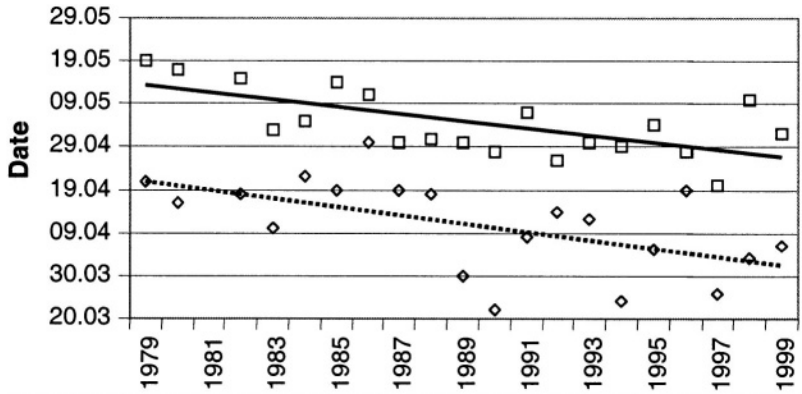

Figure 6.6. Beginning (lower line, dotted) and end (upper line, solid) of the birch pollen season in Geneva (From: Clot, 2003)

Phenology, or the study of the timing of particular vegetation cycles such as blossoming of trees, is increasingly used as an indicator of long-term trends in climate. Some plants in the temperate and high latitudes respond to seasons through hormonal clock mechanisms, while others are sensitive to a particular temperature threshold that will set the annual vegetation cycle in motion. The release of pollen into the atmosphere is linked to blossoming, with a corresponding increase in the sensitivity of persons allergic to certain pollens. The phenology of allergenic plants has been closely monitored in view of the different, and in the course of the second half of the 20th Century, it has been possible to identify shifts in the seasonality of pollen outbreaks (e.g., Clot, 2003; Emberlin et al, 2002; Teranishi et al., 2000; Walther et al., 2002; among others). There has been a trend towards earlier release of certain types of tree pollen into the atmosphere, even though for many species, there has not been a significant extension of the pollen season itself,

implying a symmetric shift in the beginning and end of the season, as seen in Figure 6.6 for the birch tree family (Clot, 2003), for example. Other species have seen their season extended as well as an earlier timing for blooming and pollen release, as described by Frei and Leuschner (2000), Leuschner et al. (2000), Spieksma and Nikkels (1998), and Voltolini et al. (2000) for example.

Not all parts of the world have experienced systematic warming trends, however, and these include southern Greenland and parts of the Southern Hemisphere oceans and some areas of Antarctica. There are also no definite trends in extreme events, other than in some specific regions where local land-use practices such as deforestation may have exacerbated risk-prone situations. In addition, the greenhouse effect is not the only forcing factor for climate, and the influence of features such as ENSO or the NAO on decadal time-scales make it difficult to identify changes in extremes and attribute these exclusively to the anthropogenic greenhouse effect.

While many of the issues discussed in this section clearly show that climate has changed considerably in the 20^{th} century, and that there is on the basis of various figures of greenhouse gas concentrations and rates of warming since the beginning of the industrial era at least circumstantial evidence of a human influence on the climate system, it is still difficult to assess the fraction of warming that is the result of human activities compared to perturbations to the system that are of natural origin. As a result, the IPCC in both its second (1996) and third (2001) assessment reports, has addressed the issue of *detection* and *attribution.*

The IPCC defines detection as "the process of demonstrating that an observed change is significantly different (in a statistical sense) than can be explained by natural internal variability", while attribution is the identification of a clear cause-to-effect relationship between anthropogenic forcing of the climate system and its response in terms of changed circulation, temperature and precipitation regimes. In order to carry out the combined detection and attribution procedures, it would be necessary to assess the principal forcing on an individual basis in order to test the sensitivity of the system to each forcing factor taken in isolation, such as solar or volcanic forcing, ENSO variability, and enhanced greenhouse gas concentrations in the atmosphere. This approach would prove to be momentous, because not all forcings would be necessarily taken into account or even fully understood, thereby resulting in an element of doubt as to an unequivocal cause-to-effect relationship between human interference with the climate system and its response.

Approaches to the detection and attribution problem thus make use of statistically-based investigations of some of the most important climatic

forcing factors in order to show that the changes that have monitored over the past century or more are beyond changes that could be expected from internal climate variability. Observations and models have shown that climate is capable of changing on different time scales as a result of its inherent internal variability linked to ocean-atmosphere feedback mechanisms, for example. Methods of attribution need to ensure that the rate and amplitude of warming is physically coherent with the quantities of greenhouse gases in the atmosphere and their evolution since the 19th century. For example, the fact that the warmest years on record have occurred since the 1990s at a time when carbon dioxide and methane levels have never been so high is one indirect confirmation of the coherence of links between anthropogenic forcing and atmospheric temperatures. Further care has been given by the IPCC (2001) to ensure that other plausible mechanisms do not explain the observed changes.

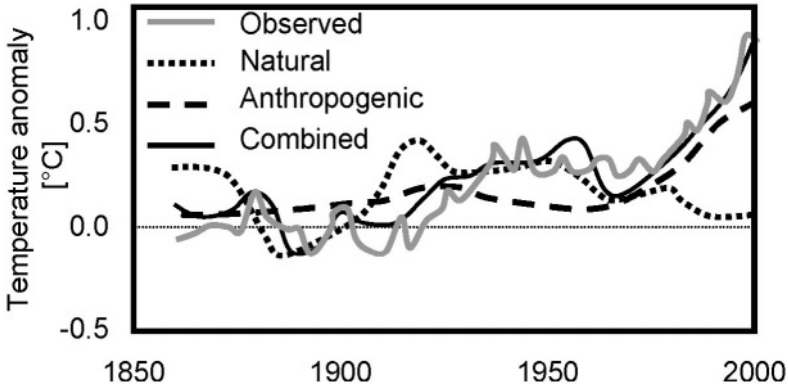

Figure 6.7. Schematic overview of a set of model ensemble simulations that force the climate system from 1850 onwards with natural forcing only, anthropogenic forcing only, and a combined natural and anthropogenic forcing. This latter forcing combined comes closest to the observations of mean global warming shown by the gray curve (Adapted from the IPCC; 2001).

The most convincing results shown by the IPCC in its 2001 assessment report involve three global model ensemble simulations that have investigated the time evolution of the climate system over the last 150 years. The first set of simulations considered solar and volcanic forcing only, the second anthropogenic forcing only (i.e., greenhouse gas increases and aerosol loading of the atmosphere from industrial sources, deforestation, and land-use practices), and the third the combined natural and anthropogenic forcings. Figure 6.7 provides a schematic overview of the model results

based on the original IPCC (2001) figures. When compared to the observational record from 1850-2000, the natural forcings diverge during the second half of the 20th century and no longer seem capable of explaining the sharp global-average temperature increase since the 1970s, while the simulations that involve only anthropogenic forcing come closer to the observed curves but with some inconsistencies compared to observations at particular times of the 20th century. It is only when natural *and* anthropogenic forcings are combined that the model simulations come very close to the observations, as shown in Figure 6.7.

The model results clearly highlight the fact that average temperatures in the second half of the 20th century are on a course that natural forcing cannot explain but that anthropogenic forcing largely seems to contribute to. It is on the basis of these sets of experiments, upheld by other detailed statistical studies, that one of the strongest statements of the IPCC was published in its 2001 report, to the effect that: "there is new and stronger evidence that most of the warming observed over the last 50 years is attributable to human activities", which is a considerably more affirmative statement than in the 1996 report that stated "the balance of evidence suggests a discernible human influence on global climate", and reflects the progress in science that has emerged in the intervening 5-year period related to these issues.

6.2. PROJECTIONS OF FUTURE CHANGE AT THE GLOBAL SCALE

In Chapter 4, the future course of greenhouse gas emission scenarios according to different combinations of social, political, economic and technological factors was seen to yield a range of concentrations by the end of the 21st century of between 450 and 1,100 ppmv, i.e., roughly 2-4 times the pre-industrial values that were the norm during much of the Holocene.

As the climate change debate began in the late 1980s, estimates of the amplitude of warming according to scenario suggested that global average temperatures could rise by 1.5–5°C by the end of the 21st century. Over a decade later, and with climate models that have become much more detailed (including the essential coupling between ocean and atmosphere processes), the plausible range of global atmospheric temperature increase remains essentially unchanged (1.5-5.8°C according to the IPCC 2001 third assessment report). It is also remarkable to note that in 1897, Svante Arhenius, a distinguished Swedish chemist, carried out the first calculation of the effect of greenhouse gases on the temperature of the earth and came to the conclusion that a doubling of CO_2 in the atmosphere would lead to a 4°C

warming, a figure that is still well within the bounds of the most sophisticated climate model results. As will be seen further on, however, there have been substantial improvements in the simulation of climate variability both at the global scales and, more recently, at the regional scales through regional climate modeling techniques as briefly discussed in the preceding section of this chapter.

In the various suites of IPCC reports (1996; 1998; 2001), a range of models has been applied to assess the response of the climate system to anthropogenic forcing in the 21st century; these include fully-coupled ocean-atmosphere models, atmospheric general circulation models, and simpler models designed to investigate a particular element of the system such as the global carbon cycle, or to integrate much further ahead in time than the more computationally resource-intensive general circulation models. In order to capture the limits of uncertainty of the model results, and to investigate the variability inherent to the climate system, *ensemble simulations* have been undertaken. Ensemble simulations involve the use of a set of different models that employ the same forcing scenario (e.g., those described in Chapter 4) but with slightly different initial conditions (e.g., Brankovic and Palmer, 2000; Doblas-Reyes et al., 2000; Derome et al., 2001). Small perturbations to initial conditions result in an internally-generated climate variability that produces different results for the different members of the ensemble simulations. These can be considered to reflect to some extent the natural variability of the system, upon which the strong anthropogenic signal is superimposed. As no single model can be considered to be providing a unique or best set of results, it is necessary to make use of all results from a set of ensemble simulations. The ensemble approach provides a more coherent strategy to climate simulations and has shown skill in reproducing the observed distributions of pressure, temperature and pressure under current climatic conditions, as reported by Lambert and Boer (2001).

Figure 6.11 shows the probable global warming rate in response to a number of the IPCC SRES emission scenarios developed by Nakicenovic et al. (2000) and described in Chapter 4.5. According to the scenario, the response of climate ranges from an increase in global mean temperatures of 1.5°C to 5.8°C. The range illustrated in this figure is not simply a result of the uncertainty in climate model simulations, but reflects the range of socio-economic futures. Each one of the SRES emission scenarios is as likely as another one, with the result that there is no single response curve in Figure 6.8 that is more probable than another. However, the area shaded in dark gray highlights the median range of warming that is likely to be encountered in the course of the 21st century.

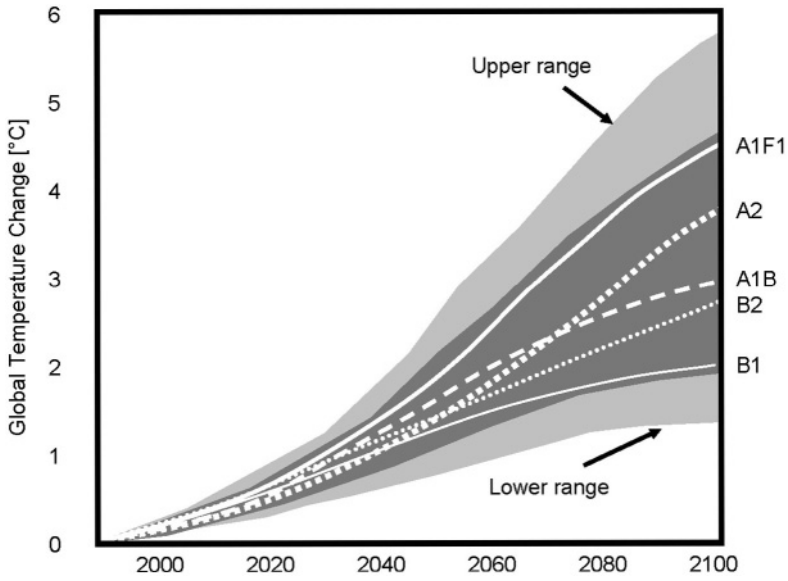

Figure 6.8. Global warming futures according to various greenhouse gas emission scenarios developed by the Intergovernmental Panel on Climate Change (Source: IPCC, 2001).

Results from coupled ensemble ocean-atmosphere general circulation models allow the geographical distribution of change to be mapped. Of the range of possible emission scenarios, only results based on the IPCC SRES A2 scenario (Nakicenovic et al., 2000) are discussed here in order to emphasize the strongest response of the climate system to greenhouse gas forcing.

The A2 assumes a high level of emissions in the course of the 21^{st} century, resulting from low priorities on greenhouse-gas abatement strategies and high population growth in the developing world. The A2 scenario leads to atmospheric CO_2 levels of about 800 ppmv by 2100, i.e., about three times their pre-industrial values) and provides an estimate of the upper bound of climate futures discussed by the IPCC (2001). An ensemble simulation of the SRES A2 scenario has been presented by the IPCC and is highlighted in a simplified view for temperature change between current (1961-1990) and future (2071-2100) climates in Figure 6.9 and for precipitation in Figure 6.10.

The change in temperature is strongest in the high latitudes than over the equatorial region. The changes that are expected in terms of snow cover and sea-ice in the Arctic Ocean would modify very substantially the energy balance at the surface, in terms of albedo in particular. High latitude regions

would therefore exert a very strong positive feedback with the system compared to the tropics where the essential characteristics of the surface are not expected to change as substantially. One exception to this is tropical deforestation, where the albedo and the thermal and humidity characteristics of the ground are modified by the presence of the vegetation (managed crops and trees) that replaces the areas previously occupied by rainforests.

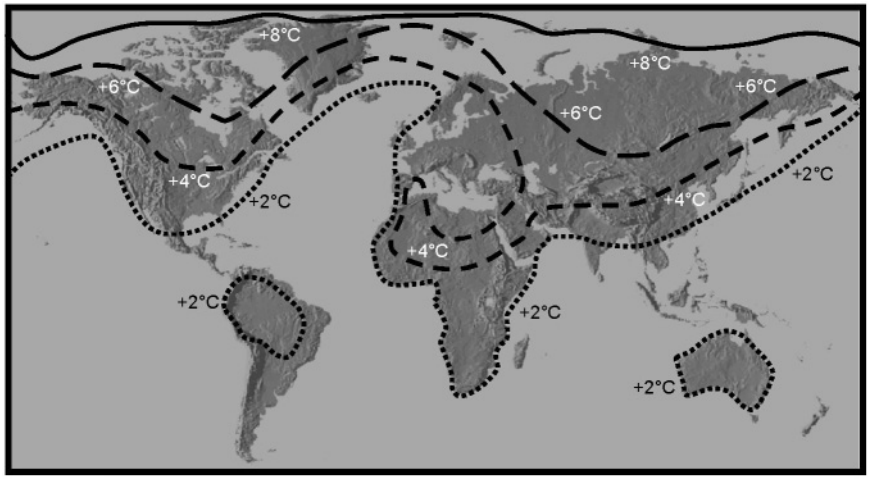

Figure 6.9. Changes in temperature between current (1961-1990) and future (2071-2100) climates based on ensemble model simulations. (Adapted from the IPCC, 2001).

Temperature change is also of greater amplitude over the continents than over the oceans, because of the much higher heat capacity of the oceans that require more energy per unit volume to warm than an equivalent volume on continental areas.

Precipitation changes exhibit broadly exhibit a dual mode, as shown in the simplified figure (Figure 6.10) compared to the original IPCC (2001) illustration; the figure here highlights only those regions that are expected to experience either an increase or a decrease of average annual precipitation by 10% or more compared to today.

The two distinctive features are the drier conditions on average over the mid-latitude ocean areas and the boundaries of the continents concerned. The Mediterranean Basin also experiences substantial reductions in average precipitation levels in the future climate, from North Africa into central Europe and beyond to the Middle East. The principal mechanism that can explain these drier conditions is the reduction of the equator-to-pole temperature gradient seen in Figure 6.9; this gradient is one of the major

drivers of storm systems as they cross the oceans from west to east, and with a reduction in the temperature difference between low and high latitudes, the activity of frontal systems diminishes. This in no way precludes, however, the possibility that short-lived but very intense systems may increase in the future, despite the tendency towards an average reduction of mid-latitude storm activity.

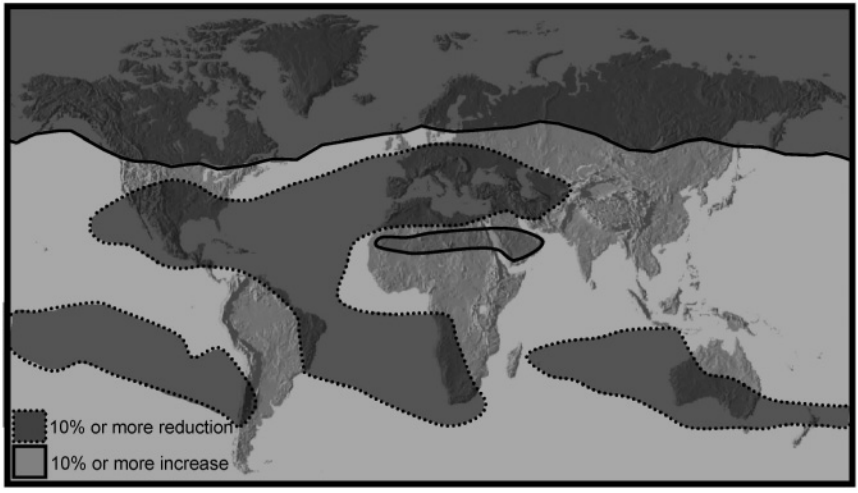

Figure 6.10. Changes in precipitation between current (1961-1990) and future (2071-2100) climates based on ensemble model simulations. (Adapted from the IPCC, 2001).

At higher latitudes of the Northern Hemisphere, increases in precipitation are simulated by the models, in response to the enhancement of the hydrological cycle in a warmer climate and the shift in storm trajectories. Other areas where an apparent increase is mapped include some of the more arid regions of the world, such as the Arabian Peninsula. Any increase of a small quantity will give a large change in terms of percent, so that the apparently strong increases as mapped in Figure 6.10 represent low amounts of precipitation change in absolute terms.

These simulations include not only the response of climate to enhanced atmospheric greenhouse gas concentrations, but also the low-frequency variability of elements such as El Niño/Southern Oscillation (ENSO) and the North Atlantic Oscillation (NAO) discussed in Chapter 3. Indeed, the configuration of precipitation in the North Atlantic area is very reminiscent to conditions that prevail during the positive (warm) phase of the NAO that may be a common feature of a future, warmer climate (e.g., Osborne, 2002).

One of the more immediate consequences of climatic change is sea-level rise, that is brought about by the combined effects of thermal expansion of water and the additional influx of freshwater to the oceans from melting mountain glaciers and ice sheets. According to the amplitude of warming, estimates of sea-level rise are in the range of 50-100 cm by the end of the century. If the two largest planetary ice-caps, Antarctica and Greenland, were to melt in the immediate future, the world oceans would rise by over 120 m. This is not likely to take place in coming decades because of the very long lag-times involved in cryosphere-climate interactions and, especially, because Antarctica is expected to expand in volume in coming decades. This is because there may be additional precipitation falling on the Antarctic continent, exclusively in the form of snow even in a warmer climate; Antarctica over coming centuries will buffer the consequences of global warming for sea-level rise, although there are signs that the Greenland ice cap is losing mass along its coastal boundaries and thus contributing to some of the sea-level changes observed in the past century.

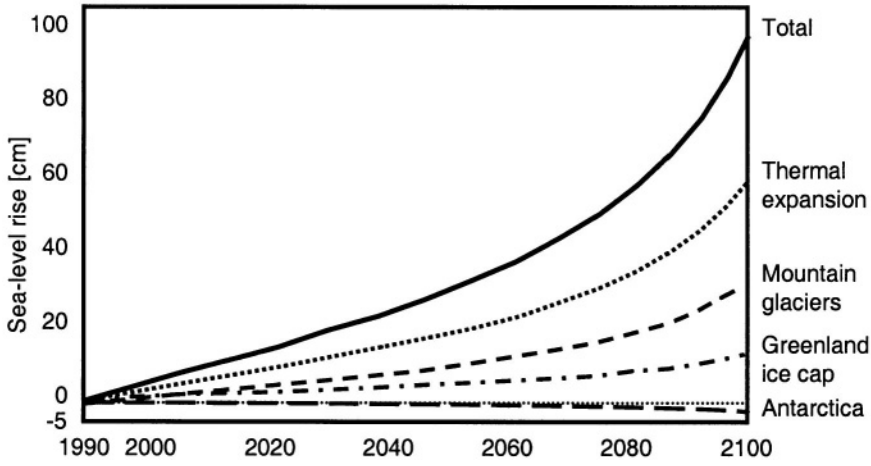

Figure 6.11. Changes in sea-level according to the SRES A2 scenario, as suggested by the IPCC(2001).

The essential contributions to melt-water, however, come from mountain glaciers which, with very few exceptions, have been losing large amounts of mass since the end of the Little Ice Age, and even more so in the latter part of the 20^{th} century, as illustrated in Figure 6.11.

The consequences of sea-level rise for many low-lying coastlines may represent one of the most important impacts for societies and economies. A major fraction of world population lives on or close to a sea-shore, often

within the critical 1 m above sea-level as in island states such as the Maldives in the Indian Ocean, the Marshall Islands in the Pacific, certain parts of Bangladesh in the Ganges delta, or Indonesia to name but a few examples.

Feedbacks between the ocean and the atmosphere could take a dramatic turn in the future if the thermohaline circulation as described in Chapter 2 were to weaken significantly or even collapse due to the combined effects of strong fresh water inflow into the North Atlantic from glacier melt water and enhanced river flows in the high latitude, and the reduced extent of sea-ice in the Arctic Ocean. The radical changes in the Atlantic Ocean circulation patterns would result in a rapid change in climatic conditions on both sides of the Atlantic, in particular a sharp drop in temperature that could intervene within a few years. Paleo-climatic reconstructions have shown that the thermohaline circulation has been disrupted in the past. Manabe and Stouffer (1993) and Stocker and Schmittner (1998) have addressed the issues of thresholds in the levels of atmospheric CO_2 that could lead to the breakdown of the thermohaline circulation. Although the results are in part contradictory, these studies basically come to the conclusion that the thermohaline circulation may be affected for greenhouse gas thresholds between 2 and 4 times their pre-industrial levels (Alley et al., 2003). This suggests that, even if many specialists believe that a breakdown of the North Atlantic oceanic circulations is a low probability event that can have high levels of impact, models suggest a weakening of the thermohaline circulation in the course of the 21^{st} century; abrupt change is not to be excluded, especially in view of the fact that the critical threshold of greenhouse gas concentrations, if correct, may well be attained before 2100. The predictability of the time horizon and the exact threshold is, however, still low in view of the numerous non-linearities that enter into these processes (Knutti and Stocker, 2002).

Impacts of a breakdown of the thermohaline circulation entail a drop of average temperatures in Europe by several degrees, resulting in very short adaptation times of natural environmental systems in particular, and many socio-economic systems, thereby significantly disrupting large sectors of the environment and national economies.

6.3. REGIONAL CLIMATE MODELS: LINKING THE GLOBAL AND THE REGIONAL SCALES

Regional-scale climate information is important for climate impacts research and policy making, where the resolution of climate information

must be at scales much finer than those at which general circulation models normally operate. Furthermore, processes acting on local or regional scales often feed into the climate system, so that investigations of scale-interactions are crucial to furthering our understanding of the climate system and the role of the smaller scales in its spatial and temporal evolution.

One technique that was pioneered by Giorgi and Mearns (1991) and has since become commonplace in the climate modeling arena (e.g., Giorgi and Mearns, 1999), to address the scale problems related to insufficient grid resolution in GCMs is that of "nested modeling". Results from a GCM are used as initial and boundary conditions for a regional climate model (RCM) that operates at much higher resolution and with generally more detailed physical parameterizations. A regional model is in this case an "intelligent interpolator", since it is based on the physical mechanisms governing climatic processes rather than a mathematical interpolation technique, and serves to enhance the regional detail lacking in global climate models.

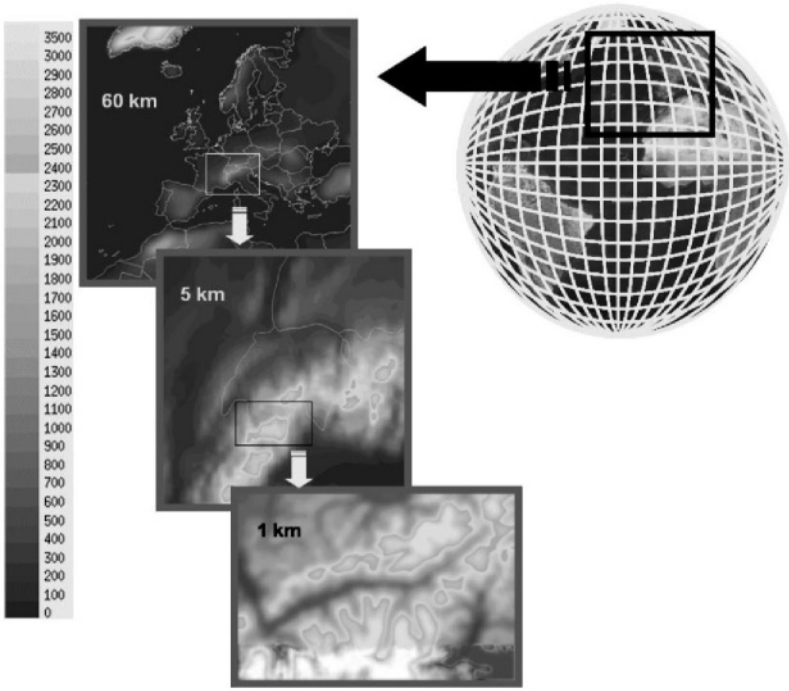

Figure 6.12. Coupling between a general circulation model and a regional climate model. Scale shows the topography height in meters as seen by the models. The self nesting procedure in this example is centered on the European Alps at a 60-km scale, and to a specific alpine valley in south-west Switzerland at the 1-km resolution (Courtesy: S. Goyette, University of Fribourg).

Such a procedure becomes particularly attractive for remote regions or those with topographic elements, whose complexity is unresolved by the coarse structure of a GCM grid, and where observational data is often sparse or nonexistent.

Today, RCMs have even the capability of "cascade self-nesting" by which the resolution of the same basic model is refined in order to capture the salient features of an atmospheric phenomenon, such as a storm entering Europe and whose impacts may be important over a relatively small surface area. As seen in Figure 6.12, the example of the Canadian Regional Climate Model CRCM-2 (Laprise et al., 1998) shows that it can function by using data either from synoptic observations or from a GCM grid (upper right) and then enter into its self-nesting mode; the figure shows the domains from which data is used to initialize the regional model at the higher resolutions. As the spatial definition of the grid increases, the detail of topography shown in Figure 6.8 also considerably improves with, at the 1-km scale, details of individual valley and mountain systems emerging. Goyette et al. (2001; 2003) have used this technique to simulate strong winter storm conditions over the alpine area at an initial resolution of 60 km, allowing the model to track the storm as it enters Europe from the North Atlantic Ocean, then at progressively finer resolution down to 1 km in order to assess storm damage in complex topography. Each increase in resolution does not necessarily entail an increase in the number of computational grid points in the horizontal (i.e., the total domain covers a smaller surface area at higher resolutions), but there is generally an increase in the number of vertical levels to take into account in a more precise manner certain processes like cloud convection. In addition, because many interactions and feedbacks that are important for the evolution of the atmosphere at fine scales are short-lived, the computational time-step needs to be reduced (also for numerical stability of the time integrations). Hence fine resolution computations with such a model are generally more resource-intensive than at higher resolution.

In its Third Assessment Report, the IPCC (2001) has extensively used the nested modeling technique in an attempt to improve regional climate information. When driven by analyses and observations, RCMs generally simulate a realistic structure and evolution of synoptic events. Model biases with respect to observations are in the range of a few tenths to a few degrees for temperature and 10 - 40% for precipitation. These biases tend to decrease with increasing resolution or decreasing RCM domain size. GCM-driven RCMs tend to produce less convincing results, however, which is to be expected since GCMs can generate unreliable results in terms of storm tracks and precipitation belts, for example. As a result, the errors of a GCM will tend to propagate into an RCM.

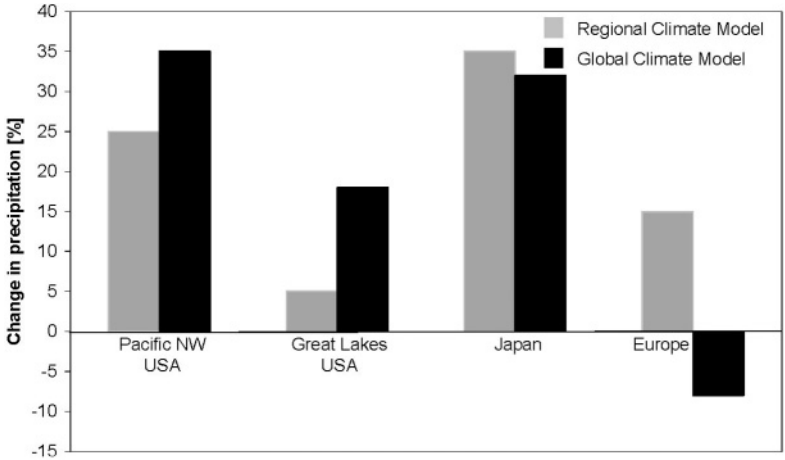

Figure 6.13. Changes in precipitation in a future climate compared to present, as simulated by a global climate model and a regional model for several geographical regions.

Figure 6.14. Sketch of a variable-resolution grid in a general circulation model such as the French ARPEGE model, where sharper resolution is obtained in a region of interest at the expense of lower resolution elsewhere.

RCMs may in some instances provide more realistic information on climatological processes than GCMs, however, because they capture the regional detail of key elements such as topography or large lakes in a far

more realistic manner than GCMs. In the example illustrated in Figure 6.13, results for precipitation have been compiled by Giorgi et al. (1994) for an RCM operating at 50 km resolution nested into a GCM with a 300 km resolution.

An alternative to a system whereby a regional climate model is embedded into a general circulation model involves the use of variable-mesh general circulation models. Such global models increase the horizontal grid resolution over a region of interest at the expense of resolution in the model antipodes. This is a method that has been employed for a number of years by the French modeling group at Météo-France in Toulouse, whose ARPEGE general circulation model (Figure 6.14) has been running successful climate and climatic change experiments with a tight grid over France and western Europe in order to enhance particular features such as coastlines or topography that have an influence on weather and climate in the region.

6.4. PROJECTIONS OF FUTURE CHANGE AT THE REGIONAL SCALE: APPLICATION TO EUROPE

Within the European Union project PRUDENCE (Christensen et al., 2002), a suite of regional climate models have been applied to the investigation of climatic change over Europe for the last 30 years of the 21st century, enabling *inter alia* an insight into possible changes in the extremes of temperature by 2100. When analyzing the results for temperature in Europe, the different model simulations broadly agree on the magnitude of change in mean, maximum, and minimum temperatures; Deque (2003) has highlighted the clustering of model results that constitutes one measure of the uncertainty or reliability of the regional-scale simulations. The HIRHAM4 regional climate model (RCM) of the Danish Meteorological Institute (Christensen et al., 1998) is one such model whose results correspond well with those of the other RCMs used in PRUDENCE. Furthermore, simulations of the reference climatic period 1961-1990 has shown that HIRHAM4 exhibits skill in reproducing contemporary climate, thereby providing some confidence as to its capability for simulating the characteristics of temperatures in the future.

Figure 6.15 shows the shift in summer mean maximum temperatures between the 1961-1990 reference period and 2071-2100. South-western Europe exhibits some of the strongest changes, from the Iberian Peninsula to the south-west quadrant of France, where summer temperatures may increase by over 6°C over the next century. This is possibly related to stronger positive feedbacks from dry soils in the region. The elevated

temperature change in the Baltic Sea is a model artifact resulting from the driving GCM simulations, that "sees" the Baltic as a sea with no connections to the North Sea.

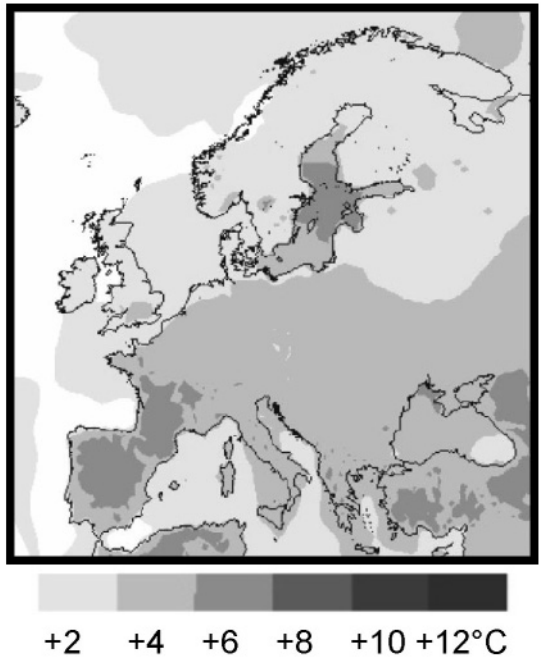

Figure 6.15. Changes in mean summer temperatures (June-July-August means) in Europe between current (1961-1990) and future (2071-2100) climates based on HIRHAM4 regional climate model simulations (Figure: B. Koffi, University of Fribourg).

The changes in the 90% quantile of maximum temperature (Figure 6.16), exhibit an asymmetric increase, i.e., the shifts in the upper extremes of summer temperatures are generally more marked than the changes in means, and can attain 10°C in some parts of western and southern Europe. The change in mean summer maxima is thus accompanied in many parts of the continent by asymmetrical shifts in the extremes. This has significant repercussions for hydrology, ecosystems, and agriculture, where extreme temperatures generally tend to exert stronger controls than mean temperatures on evaporation and desiccation as well as on heat and water stress to plants.

Another manner of viewing the changes in extreme temperatures is illustrated in Figure 6.17, where the change in the number of days with an threshold excess beyond 30°C have been mapped for the reference period

1961-1990 and for the end of the 21st century (2071-2100). The figure suggests that there is a geographical shift of all climatic zones by 400-600 km towards the north. Climate by the end of the 21st century in southern France thus resembles the current conditions of southern Spain, and the summers of the alpine region may tend towards those of southern France within the same time-frame.

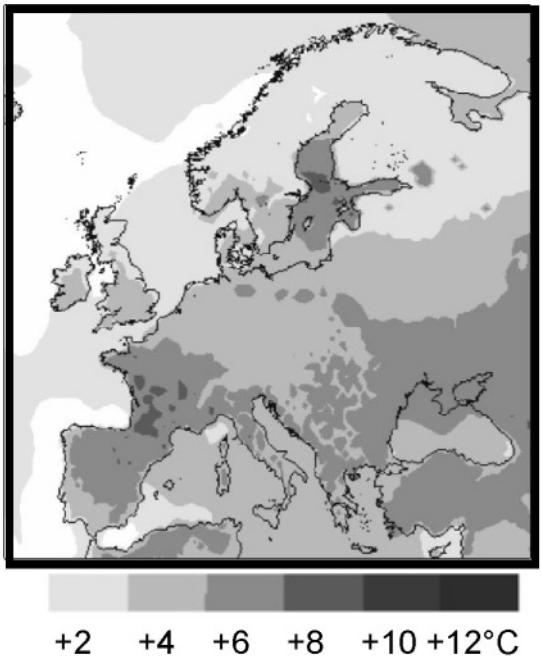

Figure 6.16. Changes in the 90% quantile of summer temperatures in Europe between current (1961-1990) and future (2071-2100) climates based on HIRHAM4 regional climate model simulations (Figure: B. Koffi, University of Fribourg)..

The statistics mapped over Europe for maximum temperatures and threshold excess have implications for the future course of extreme events such as the increase of heat waves and the reduction in cold spells and frost days. According to the baseline used, the very definition of a heat wave could change in a future, systematically-warmer climate, compared today. The climate of southern Spain, for example, that is currently characterized by temperatures exceeding 30°C for about 60 days per year on average may in the future experience over 150 days or more, i.e., close to half the year. Under such circumstances, the notion of heat wave loses some of its value

when a rare or exceptional feature of today's climate becomes commonplace in tomorrow's climate.

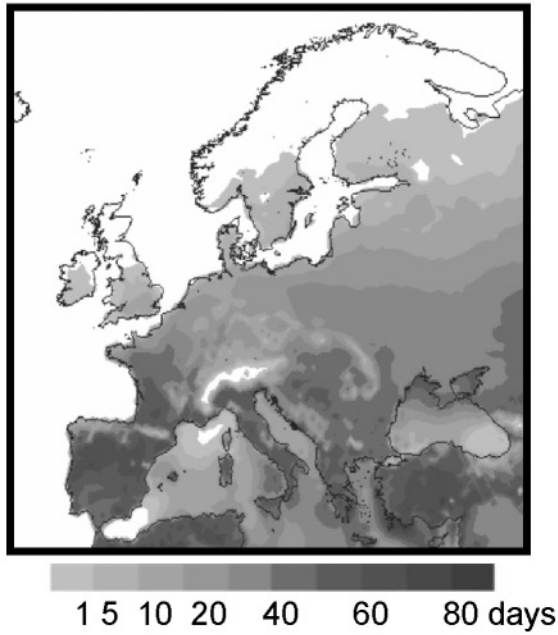

Figure 6.17. Changes in the number of days that exceed the 30°C threshold in Europe between current (1961-1990) and future (2071-2100) climates based on HIRHAM4 regional climate model simulations (Figure: B. Koffi, University of Fribourg)..

Precipitation patterns in Europe reflect those of the global-scale climate simulations, whereby southern and central Europe will experience generally less precipitation than today, but northern Europe may gain in moisture. Christensen and Christensen (2003) have published the results of an investigation on future precipitation regimes based on regional climate simulations by the HIRHAM4 model. They conclude that in a northern Europe, there is likely to be more precipitation on average, while in a large band stretching from France to the Black Sea and beyond (Figure 6.18, upper), summer precipitation is projected to diminish by as much as 40% on average in certain parts. Simultaneously, the HIRHAM4 model results point to a strong increase of the short-lived but very intense precipitation events in certain regions (Figure 6.18, lower) that are prone to such hazards, such as the river systems of central Europe (e.g., the Elbe river basin), southern France, and northern Spain. This apparent paradox of lower average rainfall but more frequent extreme precipitation events is not a feature that is unique

to the European region but has been reported elsewhere, for example in North America (IPCC, 1998).

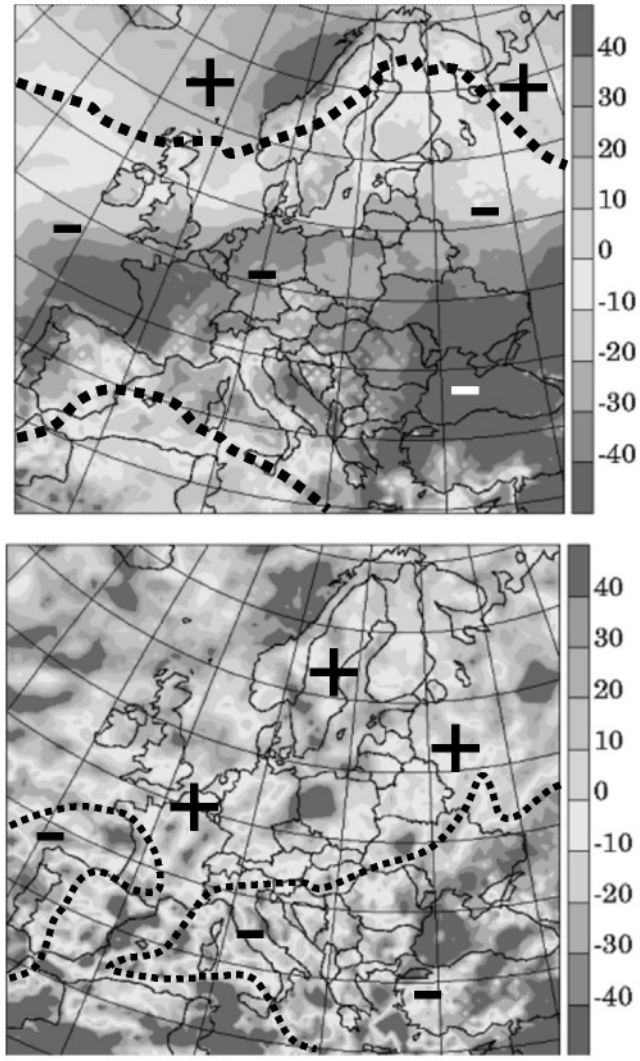

Figure 6.18. Changes in summer precipitation (July, August, September) for mean precipitation in % (upper) and extreme precipitation at or beyond the 99% quantile, also in % (lower). In order to distinguish between the positive and negative color shading, limits between precipitation decreases (-) and increases (+) are delimited by dotted lines (Adapted from: Christensen and Christensen, 2003).

Increased flood hazard is likely to affect many parts of Europe as a consequence, both because of higher overall precipitation in northern Europe or because river catchments may respond to to short-lived but very high-intensity events. When these events occur towards the end of the summer, at a time where soils are dry and have difficulty in absorbing abrupt and large quantities of water at the surface, many river basins will respond through flooding. At other times of the year, flood potential can also increase when precipitation, associated with snow-melt during the winter or early spring, discharges unusual amounts of water that cannot be absorbed by the river catchments. Such situations have prevailed in a recent past along the entire course of the Rhine river basin, for example.

Chapter 7

CLIMATE IN SWITZERLAND SINCE 1900

7.1. INTRODUCTION

This section will investigate aspects of climate during the 20th century that are specific to the European Alps, and will provide an insight into the manner in which climate may change in the latter part of the 21st century in response to global warming.

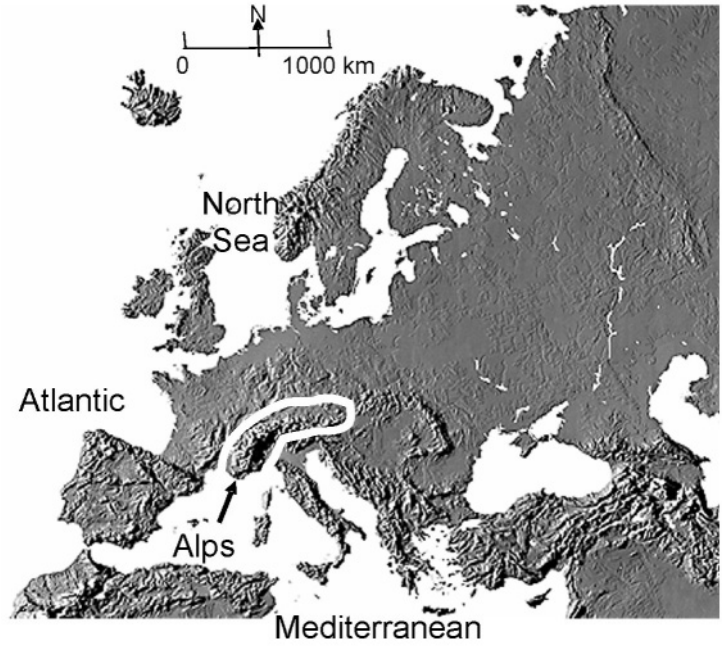

Figure 7.1. Geographical location of the European Alps.

The Alps (Figure 7.1) are a particularly interesting region for many climate and environment studies as a result of their geographical location and morphological configuration that place them at a "climatic crossroads" of competing climatic influences. The Alps consist of an arc that stretches in a north-south direction from the Mediterranean in France, that then curves eastwards through Switzerland and finally stretches in an east-west direction as far as eastern Austria. The Alps are to some extent bounded by the competing influences of the Mediterranean, the Atlantic, and to a lesser extent the North Sea and the Baltic. They are located in one of the warmest areas of the Northern Hemisphere mid-latitudes as a result of the proximity of the modulating influence of the Atlantic Ocean and the heat reservoir that the Mediterranean Sea represents.

The European Alps are by far the best-researched mountain area of the world in terms of weather and climate and related environmental characteristics (Barry, 1994), and as a consequence the wealth of data that is available for the alpine domain makes this a privileged region for climatic and environmental studies.

The alpine arc is subject to the influence of storms that cross the Atlantic or develop in the Mediterranean, but can also influence weather patterns in several ways, such as through lee cyclogenesis (the development of low-pressure systems resulting from the interaction between atmospheric flows and topography), the formation and persistence of blocking high pressure systems, and the triggering of turbulent mountain waves (gravity waves) whose influence can be felt far downstream of the mountains themselves

The Alps simultaneously exhibit characteristics related to continentality and to latitude, as seen in Figure 7.2. Here, monthly-means of temperature (upper) and precipitation (lower) have been plotted for the climatological reference period 1961-1990 at Lugano (located at 290 m above sea-level to the south of the Alps), Zurich (567 m above sea-level, to the north of the Alps), and Säntis, in the north-eastern Swiss Alps at 2,500 m above sea level. The three temperature curves are in phase but shifted as a result of the altitude difference and the generally-warmer Mediterranean influences in the case of Lugano. The precipitation statistics exhibit a wide discrepancy between sites; Lugano has a double peak of precipitation in spring and late summer, associated with convective precipitation, while in Zürich precipitation peaks in the summer and is at a minimum during the coldest months of the year due to continentality effects. Precipitation is highest at Säntis due to the effect of orographically-induced rain and snow, and exhibits much-reduced precipitation in the autumn.

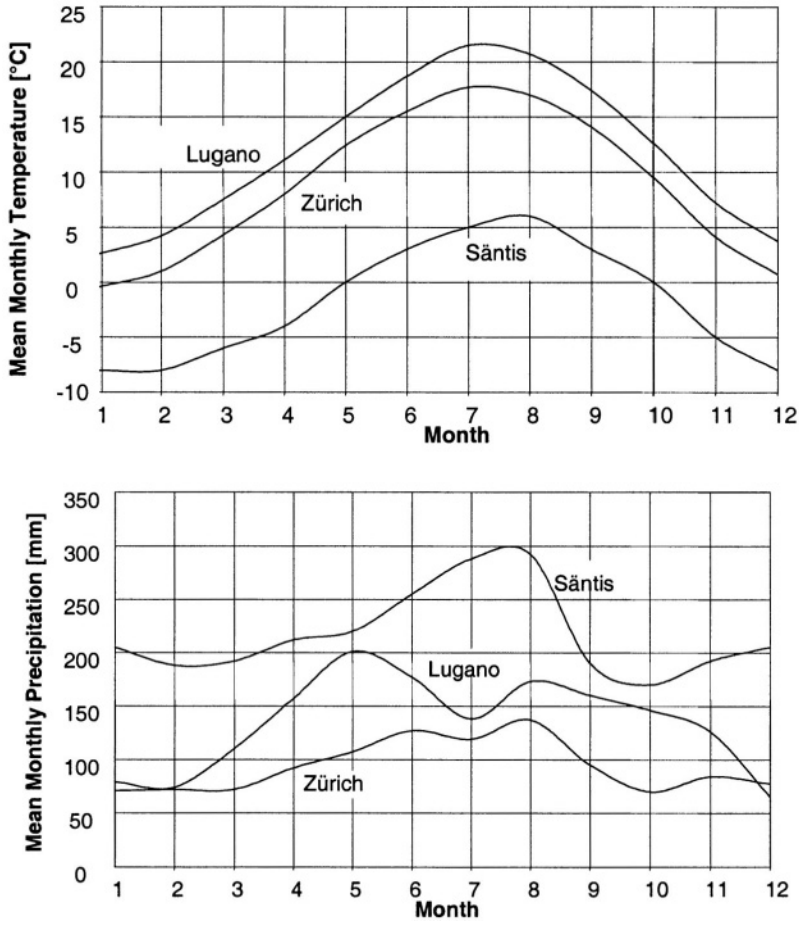

Figure 7.2. Monthly means of temperature (upper) and precipitation (lower) in three locations of the Swiss Alps, namely north of the Alps (Zürich), in the Alps (Säntis), and south of the Alps (Lugano).

7.2. PARTICULARITIES OF ALPINE CLIMATE

Mountain climates in general are governed by four major factors (Barry, 1994), namely continentality, latitude, altitude, and topography. The relative influences of these factors affect the Alps to a greater or a lesser degree. A brief overview of the salient features of mountain climates as the affect the Alps will be given here.

Continentality refers to the proximity of a particular region to an ocean. The diurnal and annual ranges of temperatures in a maritime climate are markedly less than in regions far removed from the oceans; this is essentially due to the large thermal capacity of the sea, which warms and cools far less rapidly than land. Because the ocean represents a large source of moisture, there is also more precipitation in a maritime climate than in a continental one, provided the dominant wind direction is onshore. Examples of maritime mountain climates include the Norwegian Alps, while continental climates affect inner-continental mountains chains and upland regions such as the Tibetan Plateau. The European Alps act as a boundary between Mediterranean-type, Atlantic, and continental climates with, on occasion, even outbreaks of Saharan air masses that transport dust across the Mediterranean and well to the north. While mountains in continental regions experience more sunshine, less precipitation, and a larger range of temperatures than maritime mountains, they are not necessarily harsher environments. For certain ecosystems, the larger amounts of sunshine compensate for lower mean temperatures in continental regions.

Latitude determines to a large extent the amplitude of the annual cycle of temperature and, to a lesser extent the amount of precipitation that a region experiences. In the Swiss Alps, the latitude effect would be expected to be small because of the limited distance across the alpine chain; however, as seen in Figure 7.1, there are some distinct features that differentiate between climates south of the Alps and those to the north, for reasons related more to the proximity of the Mediterranean Sea than to purely the influence of latitude.

Altitude, however, is certainly the most distinguishing and fundamental characteristic of mountain climates, because atmospheric density, pressure and temperature decrease with height in the troposphere. Mountains often sense serve as elevated heat sources, whereby diurnal temperatures are higher than at similar altitudes in the free atmosphere (Flohn, 1968). Diurnal and annual range of temperature tends to decrease with altitude because of the lower heat capacity of the atmosphere at height. The altitudinal controls on mountain climates also exert a significant influence on the distribution of ecosystems. Indeed, there is such a close link between mountain vegetation and climate that vegetation belt typology has been extensively used to define climatic zones and their altitudinal and latitudinal transitions (for example Klötzli, 1991, 1994; Ozenda, 1985; Quezel and Barbero, 1990; Rameau et al., 1993).

Mountain systems generate their own climates (Ekhart, 1948), as a function of the size of the land mass at a particular elevation. Topographic features also play key role in determining local climates, in particular due to

the slope, aspect, and exposure of the surface to climatic elements. These factors tend to govern the redistribution of solar energy as it is intercepted at the surface, as well as precipitation that is highly sensitive to local site characteristics. In many low and mid-latitude regions, precipitation is observed to increase with height; even modest topographic elements can exert an often disproportionate influence on precipitation amount. Precipitation mechanisms are linked to atmospheric dynamics and thermodynamics. When a mass of moist air is forced to rise above the condensation level, the excess vapor is converted to fine liquid water particles that become visible in the form of mist, fog or clouds. If uplift of air continues, at some stage precipitation processes will be triggered.

Precipitation in a mountain region will generally fall on the windward-facing slopes of the mountains because of the dynamics associated with uplift. Because most of the moisture is extracted from the clouds on the windward slopes, the air that crosses over to the lee side of the mountains is essentially dry. An east-west gradient of precipitation is observed in the Alps, with less precipitation falling in eastern Switzerland and Austria on average than in the western part of the Alps when dominant flow patterns are from the Atlantic. This effect would be even more exacerbated were it not for the presence of the Mediterranean to the south that acts as a moisture source for atmospheric perturbation systems that are embedded in flows from a southerly sector.

Solar radiation is intercepted differently according to the orientation of slopes. In the mid- and high-latitudes of the northern hemisphere, slopes oriented towards the south receive more energy per unit area and therefore experience larger thermal amplitude than slopes with different orientations. Differential absorption and distribution of energy at the surface leads to different atmospheric responses, because air in contact with a warm surface tends to rise, as opposed to air in the vicinity of a colder surface. Air at the same elevation in the center of a valley also warms less rapidly than the air in direct contact with the ground, so that the density differences from one side of the valley to another are capable of driving local mountain and valley breezes. Because less dense air moves up the valley slopes, it needs to be replaced by air from lower down in the valley; during the day, therefore, flow close to the valley floor is directed up-valley. The reverse situation occurs at night, when energy at the surface is lost through infrared radiation and cools the air in contact with the surface; continuity principles imply that the air moving downward toward the valley floor needs to be replaced by air from higher elevations; as a result, nocturnal flows are directed down-valley. This cyclic pattern of up- and down-valley air is present in all parts of the Alps, according to the prevailing meteorological situation, and each valley

can be considered to have its own unique microclimate. Mountain and valley breezes are important in industrialized or urbanized valleys, or those with a dense highway network because of their effect on air quality through the recycling and dispersal of pollutants of local origin.

At night, or during periods of persistently stable high pressure conditions, temperature inversions form as a result of high energy loss by infrared terrestrial radiation. Under such circumstances, cold air accumulates at the bottom of a valley floor and tends to stagnate because of the constraining effects of the valley boundaries. The depth of the inversion depends on local weather and topographic characteristics, but in general does not exceed 1,000 meters. Temperatures above the inversion are milder, because the colder, denser air flows to the valley floor and remains there. It is only at much higher elevations that the general rule of decreasing temperatures with height is verified once again. According to local site characteristics, i.e., valley floor, mountain slope, or mountain top, temperatures at equivalent elevations exhibit large differences in the diurnal and annual range of temperatures. Topographically-induced local climates have strong implications for the distribution of climate-sensitive systems, such as vegetation, snow and ice.

7.3. OBSERVED CHANGES IN CLIMATE IN SWITZERLAND

7.3.1. Trends in mean, minimum, and maximum temperatures

For many of the discussions that will follow, climatological data from a number of stations in Switzerland with over 100 years of daily data in digital form has been used. The climatological database is provided by the Swiss weather service, MeteoSuisse (Bantle, 1989), with much of the data in homogenous form (Begert et al., 2003). In terms of Swiss temperature time series, the first decade of the 20^{th} century was on average the coldest, while the warmest was clearly that of the 1990s. Indeed, the temperature record for the last decade of the past century is completely out of the range of the normal secular trends; this is particularly true for winter nighttime minimum temperatures at high altitudes.

These trends have continued into the first years of the 21^{st} century; in terms of record-breaking temperatures, until the 2003 heat wave that affected much of Europe, Basel held the absolute record maximum temperature

(39.1°C in July 1952); this was broken in August 2003 in the Italian part of Switzerland at Grono, with 41°C. The coldest temperature recorded in Switzerland is -40.7°C in the village of La Brévine, in the Jura mountains at 1,047 m ASL in February 1985. If these trends were to continue in coming decades, the ecological and economical consequences resulting from such changes in regional climates would likely be quite substantial. The fact that high altitude sites are generally more sensitive to changing temperatures makes them extremely vulnerable locations. The alpine biosphere, cryosphere and hydrosphere would certainly be strongly impacted upon by rapid change as experienced in the 1990s. The impacts on the natural environment would in turn have consequences for mountain communities that have to cope with an increase in other related side-effects of climatic change, such as natural hazards and their economic repercussions.

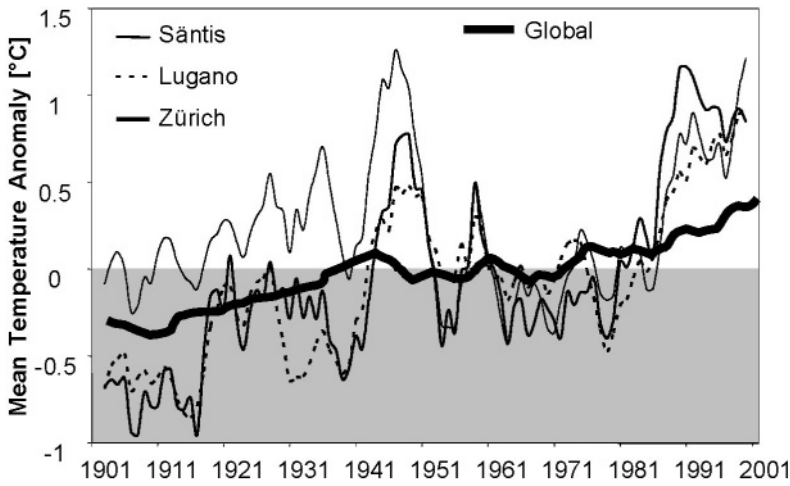

Figure 7.3. Temperature departures from the 1961–1990 climatological mean for three sites in Switzerland compared to global temperature anomalies.

Figure 7.3 shows the changes in yearly surface temperature anomalies during the 20th century at the same three locations as in Figure 7.2, as a representative example of changes that have occurred in the alpine region at various altitudes and to the north and south of the mountain barrier. The anomalies are computed as the difference between daily mean temperatures and the mean daily average for the 1961-1990 climatological reference period and then averaged to provide the annual value that is represented here. In order to remove the noisiness of year-to-year variability, the data has been smoothed with a 5-point filter for the purposes of clarity. All three

curves are in phase, and the anomalies are essentially identical from the middle of the 20th century. The global data described in Jones and Moberg (2003) has been superimposed on this graph to illustrate the fact that the temperature change in the Alps is more marked than on a global or hemispheric scale. The warming experienced since the early 1980s, while synchronous with warming at the global scale, is however of far greater amplitude and exceeds 1.5°C for the Säntis data, which represents roughly a three-fold amplification of the global climate signal (Diaz and Bradley, 1997).

Beniston (2000) has reported on a number of studies related to climate trends this century in the Swiss Alps. Climate change in the region this century has been characterized by increases in minimum temperatures of about 2°C, a more modest increase in maximum temperatures (in some instances a decrease of maxima in the latter part of the record), little trend in the precipitation data, and a general decrease of sunshine duration through to the mid-1980s. Several periods of warming are observed during the instrumental record, with the 1940s exhibiting a particularly strong warming and then a cooling into the 1950s, probably associated with increased solar energy fluxes (Friis-Christensen and Lassen, 1991) that did not, however, offset the warming of the 1940s. The asymmetry observed between minimum and maximum temperature trends in the Alps is consistent with similar observations at both the sub-continental scales, and the global scale. Karl et al. (1993) have shown that over much of the continental land masses, minimum temperatures have risen at a rate three times faster than the maxima since the 1950s, the respective anomalies being on the order of 0.84°C and 0.28°C during this period.

Jungo and Beniston (2001) have shown that for the alpine region, an unprecedented behavior has emerged towards the end of the 20th century in terms of both minimum and maximum temperature trends, with minimum temperatures exhibiting stronger shifts than maxima in the course of the 20th century. At the beginning of the 20th century, the nighttime minimum temperatures were systematically lower at all locations in Switzerland and for every season. Minimum temperatures have exhibited the strongest warming over the course of the last century, and there is a distinct amplification of this warming in the second half of the 20th century, especially at high elevations. Additionally, at low altitudes to the north of the Alps, diurnal summer temperatures have increased significantly during the past 40 years, whereas the autumn temperatures at high altitudes have to some extent diminished during this period. The decadal-scale trend of both minima and maxima has remained positive since the late 1980s for all seasons except autumn.

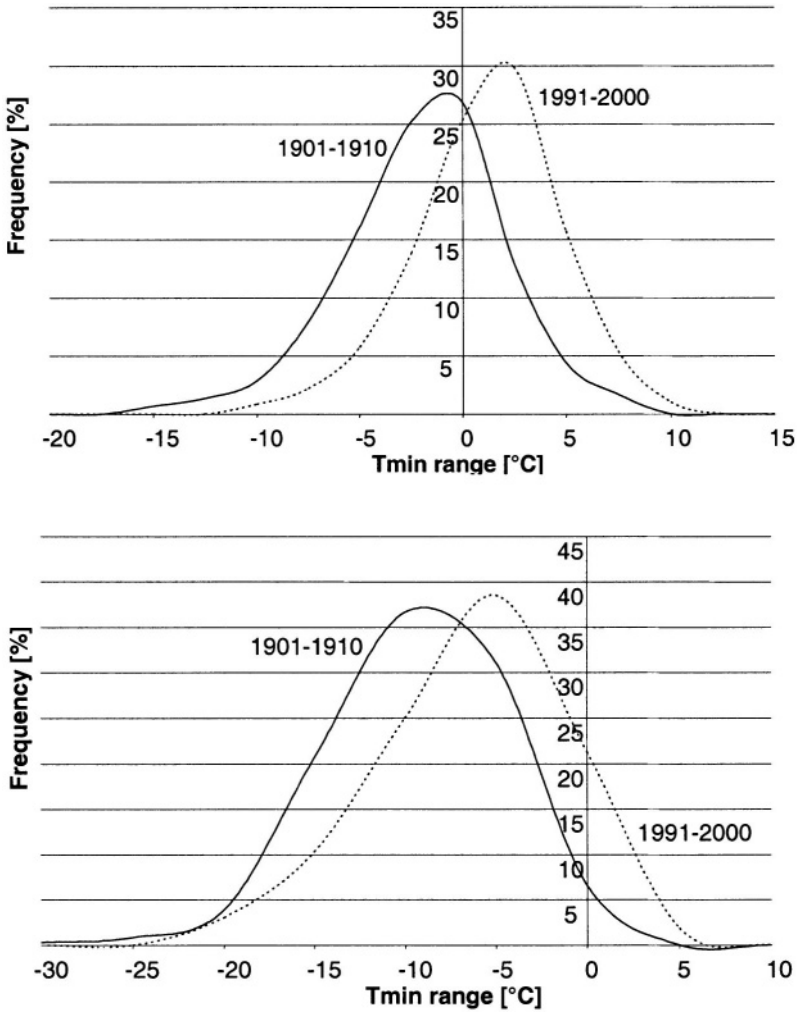

Figure 7.4. Probability density functions of Tmin for Neuchâtel (upper) and Säntis (lower).

A closer investigation of the behavior of minima and maxima allows further insight into the behavior of temperatures in the early and the later parts of the 20th century. Figure 7.4 illustrates the PDFs of winter mean minimum temperatures (Tmin) at Neuchâtel (upper) and Säntis (lower) for the time frames 1901-1910 and 1991-2000.

The winter mean temperature is defined as the average daily minimum temperature for December, January, and February (DJF). While not perfect Gaussian profiles, the two sets of curves nevertheless highlight the fact that

there has been an almost symmetrical shift of the cold and warm extremes of Tmin in response to the 3°C increase that has intervened between the beginning and the end of the 20th century in Neuchâtel (from -3.0°C to -0.1°C) and Säntis (from -11.8°C to -8.9°C). Indeed, the shift of the entire PDF distribution towards higher temperatures, including both the median and the tails, is common to all Swiss observational sites where century-scale data is available.

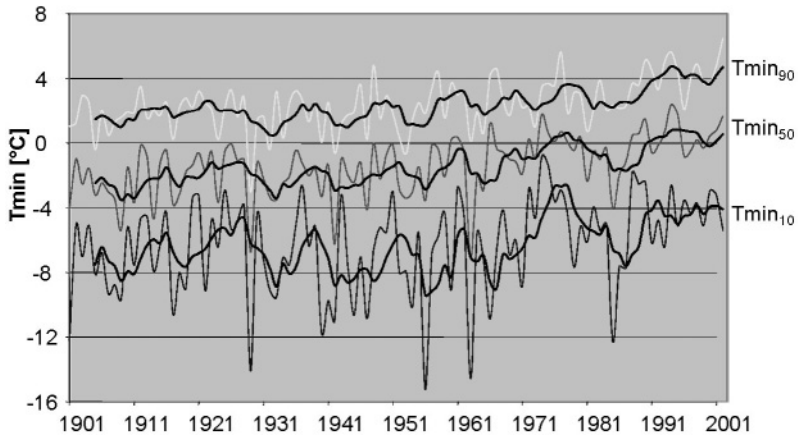

Figure 7.5. Trends in the 10%, 50%, and 90% quantiles of minimum temperatures in Neuchâtel in the course of the 20th century. Smoothed curves use a 5-year filter.

When analyzing the behavior of the quantiles of Tmin, it can be seen in Figure 7.5 that for the selected values of $Tmin_n$ (n=10, 50, 90 percentiles) in Neuchâtel, all curves show an increasing trend during the 20th century, with much of the warming occurring since the late 1960s. The greatest interannual variability is at the cold end of the Tmin distribution (at and below $Tmin_{10}$), and when cold events occur as in 1929, 1956, 1963, and 1985, the median ($Tmin_{50}$) appears more strongly correlated with $Tmin_{10}$ than with $Tmin_{90}$. In addition to the annual data plotted on this graph, a 5-year running mean has been applied to to remove higher-frequency variability, thereby yielding the smoothed curves that have been superimposed upon the annual data. One can readily identify the influence of the long positive phase of the North Atlantic Oscillation (NAO), whose influence on climate on both sides of the Atlantic is dominant in winter (Hurrell, 1995), from the late 1970s onwards in all time-series. Beniston and Jungo (2002) have shown that the reduction of the coldest extremes in the latter part of the record is well correlated with the behavior of the NAO.

About 41% of the variance of $Tmin_{10}$ is explained by the behavior of the NAO, 31% of $Tmin_{50}$, and 23% of $Tmin_{90}$.

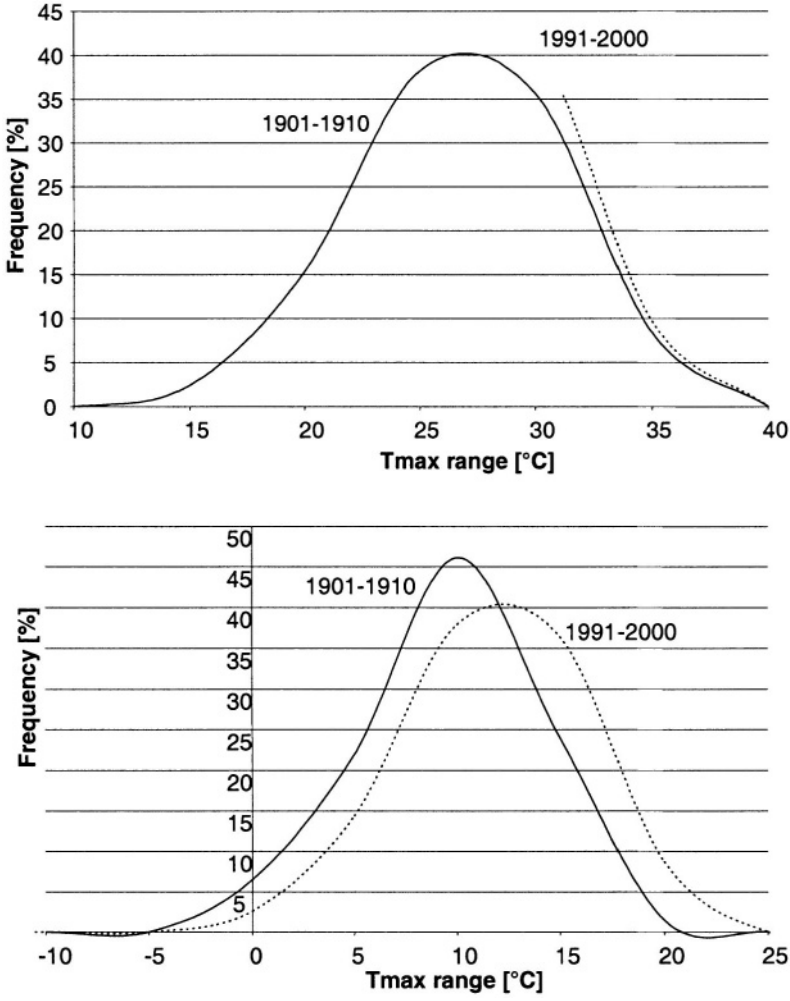

Figure 7.6. Probability density functions of maximum temperatures for Neuchâtel (upper) and Säntis (lower).

The behavior of the NAO thus seems to be more closely linked to changes in the coldest extremes than of those of the warmest extremes of Tmin. At the lower-elevation stations, the greatest warming trends occur in the lower half of the Tmin PDF, and the warming is on average about

0.5°C/century less for the upper extreme ($\geq Tmin_{90}$) than for the lower extreme ($\leq Tmin_{10}$) of the distribution. This is not the case for the high-elevation site of Säntis, where the rate of warming increases with increasing quantile, reaching more than 2.1°C/century for quantiles exceeding $Tmin_{90}$ as opposed to 1.5°C/century for quantiles below $Tmin_{10}$.

This different response of temperature with altitude has been emphasized in the past by Beniston and Rebetez (1996), Giorgi et al. (1997), and Beniston and Jungo (2002), for example. The different behavior of Tmin with elevation is probably linked to the presence of persistent winter inversion layers at lower elevations in the alpine domain that effectively decouple the low-level sites from the free atmospheric processes above.

Similar analyses have been conducted for maximum summer temperatures (Tmax), that have been computed as the June, July, and August (JJA) average of daily maxima. The behavior of the maximum temperatures, their extremes, and their trends, is substantially different from that of the minima as discussed in the preceding paragraphs. The asymmetric behavior of Tmin and Tmax trends have been reported in other studies at the hemispheric scales (e.g., Karl et al., 1993) and regional scales (e.g., Jungo and Beniston, 2001). Using the same procedures as for the previous paragraphs, Figure 7.6 shows the shift in the Tmax PDF from the coldest (1901-1910) to the warmest (1991-2000) decade of the 20^{th} century. The mean decadal summer Tmax at Neuchâtel rises from 24.1°C to 24.8°C, which is substantially less than the average increase in Tmin recorded for these same decades, and confirms other studies related to the reduction of daily temperature range at hemispheric (Karl et al., 1993) and continental (Heino et al., 1999) scales. The shift in means and extremes is more pronounced at high elevations than at low elevations, probably as a result of earlier snow-melt leading to positive temperature feedbacks at these altitudes.

Figure 7.7 illustrates the changes that have occurred in the median and upper and lower extremes of summer Tmax at Neuchâtel. Unlike the corresponding Tmin curves shown in Figure 7.5, the rise in the maxima does not follow the same course as the minima. The mid-century warm period is clearly identified by the peak of temperatures, and particularly the upper extremes, from the mid-1940s to the mid-1950s. There is speculation that this warm period is linked to a particularly intense episode of sunspot activity (e.g., Friis-Christensen and Lassen 1991). Average and extremes of maximum temperatures have risen again sharply only since the early 1980s, after the cooling that intervened in the 1950s. At low elevations such as Neuchâtel (Figure 7), the maximum values of Tmax barely exceed those experienced in the 1940s, and then only for the lower tail of the maximum

temperature PDF. At Säntis, the high values of the 1940s were slightly exceeded in the early 1990s before dropping off at the turn of the century.

Investigating the behavior of Tmax trends for periods prior to the mid-century maximum of 1945-1946 reveals the fact that warming in the first half of the century was stronger than in the second half. Based on two selected periods for linear trend analyses (1901-1945 and 1946-2000, respectively), Neuchâtel in fact exhibits a cooling tendency in the second part of the century, with the strongest cooling taking place at the upper tail of the PDF, whereas the warming in the first half of the 20th century exhibits a strong bias towards warming at the upper range of the PDF. Although there are no cooling trends at Säntis, the warming through to 1945 is stronger than in subsequent decades, and there is the crossover in the behavior of the extremes, with the warming of $Tmax_{90}$ is far greater than $Tmax_{10}$ in the early part of the century as compared to the period from 1946-2000.

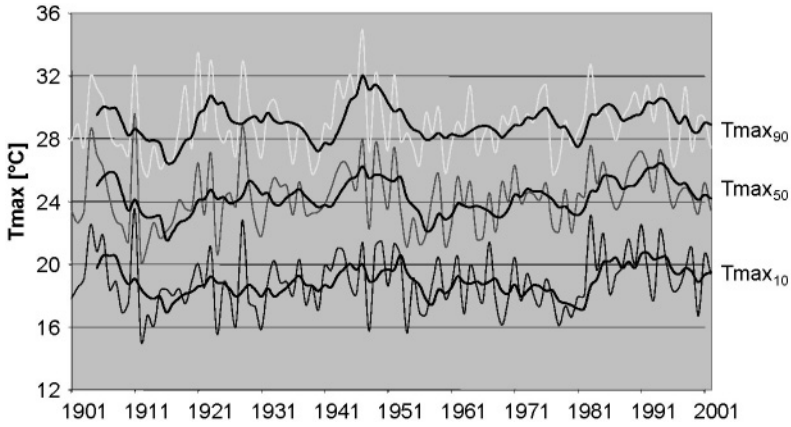

Figure 7.7. Trends in the 10%, 50%, and 90% quantiles of minimum temperatures in Neuchâtel in the course of the 20th century. Smoothed curves use a 5-year filter.

In terms of linear trend analyses, it is clear from the behavior of Tmax that the period of the time series for which the linear trend analysis is conducted will seriously bias the results. The two periods used here nevertheless serve to highlight the contrasting trends between the earlier and latter parts of the 20th century, on the one hand, and the differences that occur between the winter minima and the summer maxima, where the long-term trends of nocturnal and diurnal temperatures are governed by a range of different physical processes, some of them linked to the North Atlantic Oscillation as shown in the section that follows.

7.3.2. Links between climatic features in Switzerland and the behavior of the North Atlantic Oscillation

Since the early 1990s, much interest has focused on the North Atlantic Oscillation, and it is sometimes used as an empirical predictor for precipitation and temperature in regions where climatic variables are well correlated with the NAO index. This is clearly seen to be the case in Northern and Southern Europe, Central Europe and the Alps being generally a pivot around which the forcing of the NAO is amplified with distance north or south of the alpine region. While at low elevations, the NAO signal may be weak or absent in the Alps, higher elevation sites are on the contrary sensitive to changes in NAO patterns (Beniston et al., 1994; Beniston 2000; Hurrell, 1995; Hurrel and van Loon, 1997; Giorgi et al, 1997).

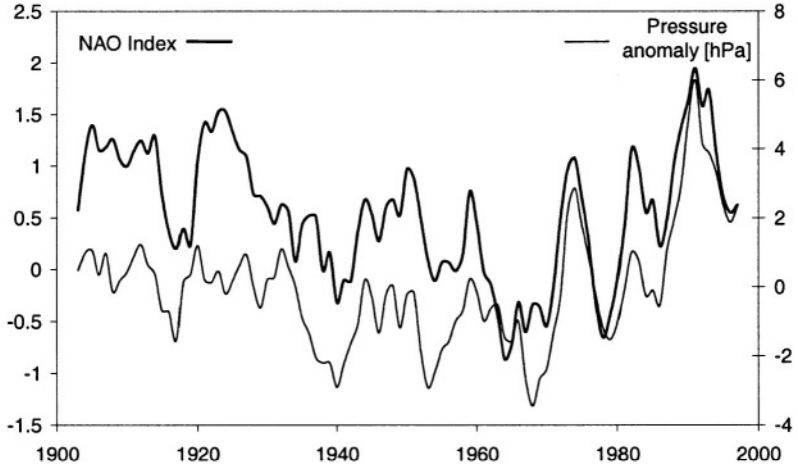

Figure 7.8. 20th Century time series of the wintertime (DJF) NAO index and surface pressure anomalies at Säntis (2,500 m above sea-level). A 5-point filter is used to eliminate high-frequency oscillations in the series.

Because of the exceptional nature of the NAO in the 1990s compared to other periods of the 20th Century (in particular the record high values of the NAO Index observed in the 1990s, and the exceptionally long persistence of the index within the positive range), Beniston and Jungo (2002) attempted to ascertain to what extent these conditions have determined the highly anomalous behavior of temperatures during the 1990s (Jungo and Beniston, 2001). In particular, it is of importance to assess the extent to which changes in the NAO are influencing not only average values of temperature or

humidity, but also their extremes. This is done by investigating changes in the probability density functions (PDF) of climate variables. In the current debate on global warming, there is increasing awareness that shifts in climatic extremes in a changing climate are likely to impact more significantly on environmental and socio-economic systems than simply changes in means.

Figure 7.8 depicts the time series of the wintertime NAO index during the 20th Century, and the associated surface wintertime (December-January-February) pressure anomalies in Zürich, based on the 30-year climatological average period 1961-1990; a 5-point filter has been applied to both curves in order to remove the higher-frequency fluctuations for the purposes of clarity. Here, wintertime refers to the values averaged for December, January, and February (DJF). Average pressure values, even at a single site, can be considered to be a measure of synoptic-scale conditions influencing the Alpine region, as discussed in Beniston et al. (1994).

The pressure measured at Zürich or elsewhere, when averaged on a seasonal or longer time span, is therefore representative of the large-scale pressure field over Switzerland. The very close relationship between the two curves in Figure 7.8 highlights the subtle linkages between the large-scale NAO forcings and the regional-scale pressure response over Switzerland. When computed for 1901-1999, 56% of the observed pressure variance in Switzerland can be explained by the behavior of the NAO. From 1961-1999, this figure rises to 83%, which is considerable bearing in mind the numerous factors which can determine regional pressure fields. Wanner et al. (1997) speculate that the persistent Alpine high pressure observed in the 1980s and early 1990s is linked to rising NAO index values through a northern shift of the polar front jet axis. When this occurs, the Alps lie to the right exit zone of the diverging jet streamlines, and are thus subject to mass influx and hence positive pressure tendencies.

Figure 7.9 illustrates the relation between the wintertime NAO index and the DJF temperature time series for Zürich, where both curves are smoothed as in Figure 7.8. As for pressure trends, the synchronous behavior between temperature and the NAO is striking, particularly in the second half of the 20th Century, where the minimum temperature variance which can be accounted for by the NAO fluctuations from 1961-1999 exceeds 72%.

In order to highlight the possible relationships of high or low NAO index values with shifts in the frequency distributions of climate variables such as pressure, temperature and moisture, two thresholds for the wintertime NAO index have been chosen, namely the lower and upper 10 percentiles of the NAO index distribution during the 20th Century (i.e., the 10% and 90% thresholds, which correspond roughly to index values around –1.5 and +2.0,

respectively). These thresholds are representative of two highly contrasting synoptic regimes affecting the Alps, namely above-average pressure and associated positive temperature and negative moisture anomalies when the threshold is above the 90% level, and lower than average pressure and its controls on temperature and humidity when the index is lower than the 10% level.

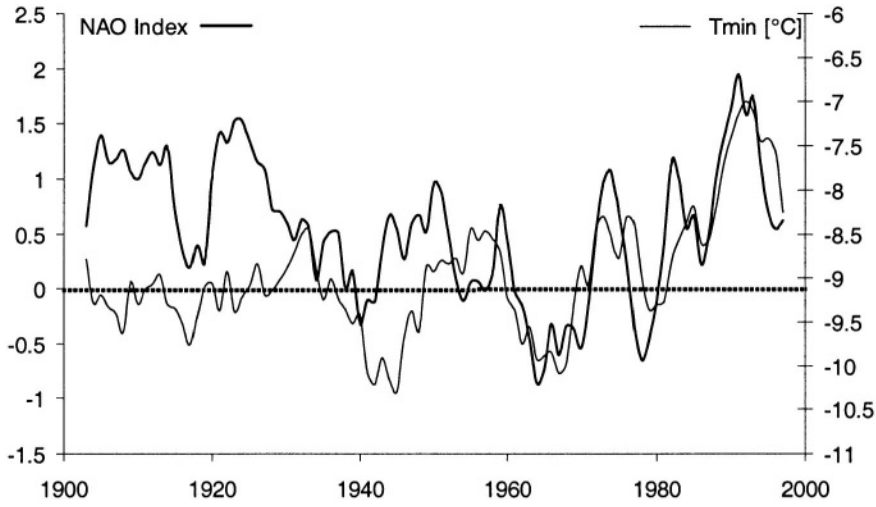

Figure 7.9. 20th Century time series of the wintertime (DJF) NAO index and winter m minimum temperature anomalies at Säntis (2,500 m above sea-level). A 5-point filter is used to eliminate high-frequency oscillations in the series.

The probability density functions (PDF) of pressure, maximum and minimum temperatures, and relative humidity, have been computed for periods where the NAO index is greater than the 90% threshold, and the temperature PDFs for winters where the NAO anomaly index is less than the 10% threshold The discussion focuses here on the high-elevation site of Säntis, a summit in north-eastern Switzerland which culminates at 2,500 m above sea level (asl), and Zürich, located about 70 km to the west, at 569 m asl. The results presented for these two sites are representative of other high mountain and lower-elevation plain locations in Switzerland. The Säntis data are particularly interesting because the high altitude of this site implies that it is closer to free atmospheric conditions, where the data are less likely to be contaminated by local site features, urban effects or atmospheric boundary-layer influences commonly encountered at lower elevations.

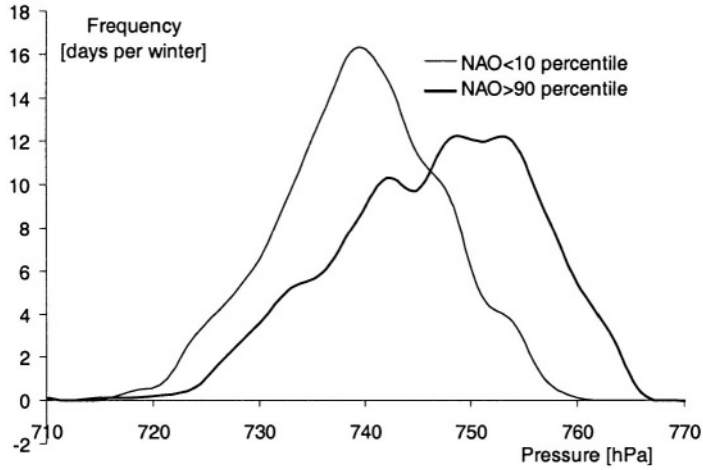

Figure 7.10. Probability density function of pressure at Säntis for periods when the negative and positive NAO index thresholds are exceeded.

Figure 7.10 illustrates the behavior of the pressure PDFs at Säntis, computed for periods of the 20th Century where the NAO index exceeds the upper threshold (90%), or is inferior to the lower threshold (10%). A substantial shift towards significantly higher pressures is observed for periods when the NAO index exceeds the 90% threshold; the PDF curve is shifted to the right of the diagram, with a change in both the skewness and kurtosis of the distribution. Figure 7.11 depicts another manner of visualizing the shifts in the pressure PDF from a strongly negative NAO forcing to a highly positive one, namely by mapping the difference in the normalized distribution between high and low thresholds, at both Säntis and Zürich. A normalized distribution is defined here as the departure of pressure from its central value (i.e., the 50-percentile) in the range observed at the two sites. Using the normalized scale enables a direct comparison to be made, which would otherwise not be possible if the absolute pressure values were used, since the pressure difference between Zürich and Säntis is about 200 hPa. The response of the surface pressure extremes to a switch in the NAO index is observed to be a clear transfer from the lower tails of the pressure distribution to its upper tails. In fact, the central values of the PDF of pressure at both the low and the high elevation site appear to be a « pivotal point » around which the shift occurs. It is seen that the integral of less-than-average pressure is practically identical to that of higher-than-average pressure when the NAO index is positive.

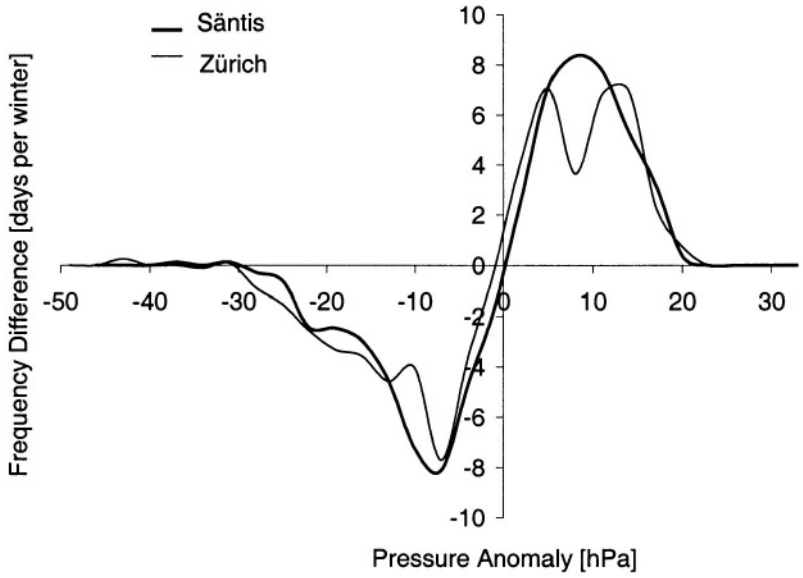

Figure 7.11. Differences in the normalized probability density functions of pressure between periods where the NAO index ≤ **-1.5** and ≥ **+2.0**, for Zurich (569 m above sea-level) and Säntis.

The forcing of the NAO is thus reflected not just in terms of a change in mean pressure as illustrated in Figure 7.9 but, indeed, in terms of the entire pressure distribution itself. The changes are by no means negligible, and represent an average shift on the order of 20 hPa at both Säntis and Zürich. When the NAO index at Säntis ≤10% level, over 15% of the winter months are concerned by pressures which are less than 730 hPa, while less than 10% are affected by pressures exceeding 750 hPa. When the NAO index ≥ 90% level, on the other hand, the respective figures change to 6% and 54%.

Under such circumstances, it is not surprising that temperature distributions and the extremes of these distributions are also strongly influenced by the behavior of the NAO. Figure 7.12 shows the response of the minimum temperature PDF to these two thresholds. It highlights the shift in the normalized winter minimum temperature distribution as a function of low and high index thresholds for both Säntis and Zürich.

Similar to the shifts in pressure PDF illustrated in Figure 7.11, transfers from the extreme low to the extreme high tails of the distribution occur around a "pivotal point" which is at the center of the range of minimum temperatures. The changes are substantial at Säntis, from a peak frequency at

about 12°C below the center of the PDF range when the NAO threshold is low, to about 7°C above the central part of the range when the NAO threshold is high. Comparable shifts in the PDF anomalies are also observed at Zürich; the respective peak frequencies occur for anomalies of –10°C and +5°C, respectively, around the central part of the range of the Zürich Tmin distribution.

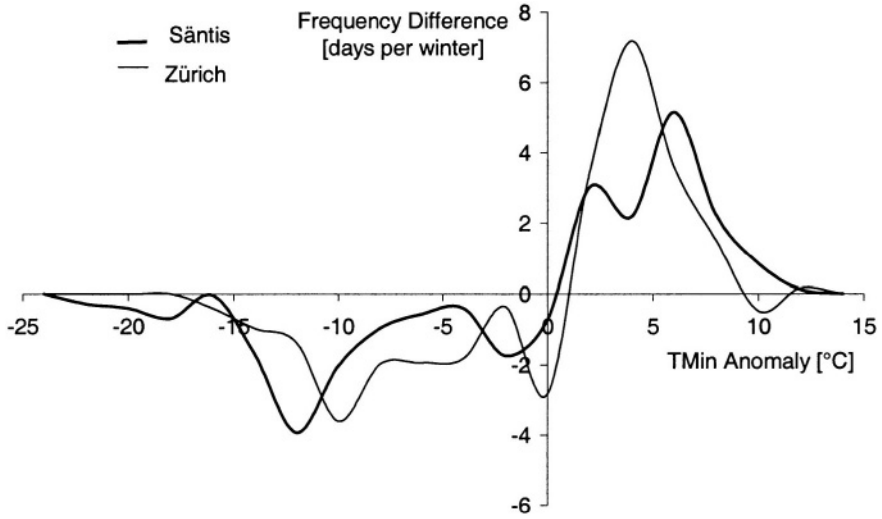

Figure 7.12. Differences in the normalized probability density functions of minimum temperature between periods where the NAO index ≤ **-1.5** and ≥ **+2.0,** for Zürich (569 m above sea-level) and Säntis.

In other words, the extreme low tails of the minimum temperature distribution disappear during periods of high NAO index, in favor of much warmer temperatures. Temperatures below –15°C at Säntis, which account for roughly 30% of the winters where the NAO index ≤ 10% level, are present only 15% of the DJF months for high NAO values, i.e., the periods with extreme cold conditions are reduced by 50%. Conversely, temperatures at the upper end of the distribution, for example above –5°C represent 12% of the winter days for low NAO values and 23% for high NAO values. The duration of milder temperatures at Säntis is thus almost doubled under conditions during which a high NAO index prevails.

Similar conclusions can be reached for the distribution of Tmax (Figure 7.13). This particular figure emphasizes the fact that the number of days in winter in which maximum temperatures exceed the freezing point range from 10 days for the lowermost NAO 10-percentile to 25 days for the

uppermost NAO 10-percentile. This obviously has implications for physical variables such as snow amount and duration, and biologically-relevant factors such as the start of the vegetation period, as will be mentioned later. Temperatures below the "pivotal point" of –5°C, which make up 48 days per winter during low NAO index episodes, drop sharply to only 33 days when the index is high.

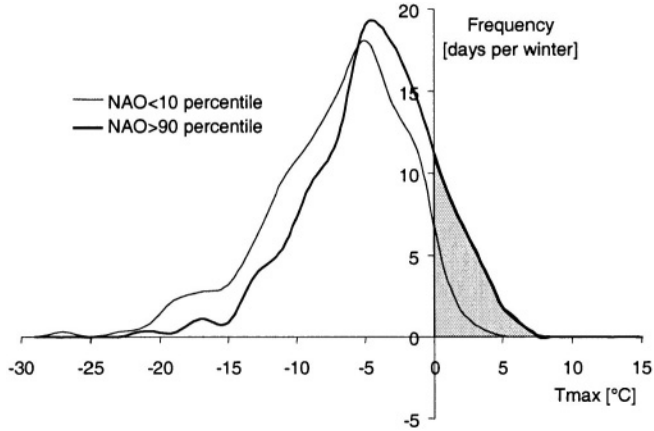

Figure 7.13. Differences in the probability density function of maximum temperature (absolute values) between NAO index ≤-1.5 and ≥+2.0, shown here for Säntis. Gray shading highlights the PDF values beyond the freezing point.

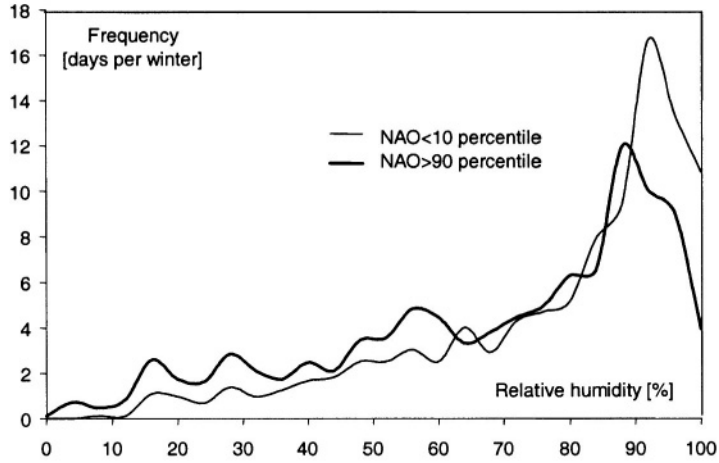

Figure 7.14. Probability density function of relative humidity at Säntis for periods when the negative and positive NAO index thresholds are exceeded

Moisture and precipitation in the Alpine region is also influenced by the behavior of the NAO. As an illustrative example, Figure 7.14 shows the difference in the distribution of relative humidity at Säntis for the two selected thresholds. In the case of the negative index threshold, over 50% of the values recorded in winter exceed 90% relative humidity, while in the case of the positive threshold the 90% relative humidity is exceeded only during 35% of the winter months.

There is thus a clear reduction in ambient moisture at high elevations. Such a substantial drying of the atmosphere is not observed at the lower elevations exemplified by the Zürich observational site; this is because low elevation sites are located within a much moister boundary-layer which, in winter, is often characterized by fog or stratus below 800-1200 m asl when high pressure conditions prevail. The lower levels are essentially decoupled from the higher atmosphere, and as a consequence, the sensitivity of relative humidity to changes in the NAO index is much lower than at higher elevations.

Indeed, the influence of local particularities of climate at low elevations in Switzerland are reflected in Table 7.1, which expresses the changes in the mean of the PDFs of four variables considered here. It is seen that the range of the shift in means is consistently larger at Säntis than at Zürich, whatever the climate variable considered.

Variable	Zürich	Säntis
Tmin [°C]	0.3	1.3
Tmax [°C]	0.1	1.1
Relative Humidity [%]	-0.6	-4.7
Precipitation [mm/day]	-0.4 (-12.8%)	-0.9 (-14.7%)

Table 7.1. Differences in the means of the PDFs of pressure, minimum and maximum temperature, and relative humidity, at Zürich and Säntis, between periods when the NAO index $\leq$-1.5 and $\geq$+2.0.

Although only illustrated here for two sites representative of low and high elevations, respectively, the conclusions from Table 7.1 hold for other locations in Switzerland, according to their elevation, i.e., the sensitivity of climatic variables at low elevations to shifts in the sign of the NAO index is systematically lower than at higher elevations.

The processes associated with periods when the NAO index exceeds the 90% level include frequent blocking episodes, where pressure fields over the Alpine area are high, and vertical circulations induce subsiding air with

associated compression warming. Such circulations invariably generate positive temperature anomalies, and reductions in moisture and precipitation. In addition, diurnal warming at high elevations is enhanced by above-average sunshine, since there is a lowering of cloud amount and duration during periods of blocking high pressures. The reverse is generally true for periods when the NAO index is below the 10-percentile of its distribution. It could be argued that nocturnal cooling should also be stronger in a cloud-free atmosphere, thus leading to lower minimum temperatures; however, in complex terrain, radiative cooling at night will lead to down-slope flow and accumulation of cold air in the valleys. The nocturnal cooling effect is, proportionally, not as strong at mountain summits such as Säntis as further down in the valleys.

Such anomalies are not only reflected in the means of the analyzed climatic variables, but also – and perhaps especially – in their extremes. The previous section has shown that there are clear links between strongly positive or negative modes of the NAO, and extremes of pressure, temperature, and moisture; high NAO values systematically shift the distributions from the lower extremes to the upper extremes.

Since the early 1970s, and up to 1996, the wintertime NAO index has been increasingly positive, indicative of enhanced westerly flow over the North Atlantic. This has led to synoptic situations in recent decades which have been associated with abundant precipitation over Norway, as cyclonic tracks enter Europe relatively far to the north of the continent (Hurrell, 1995). Over the Alpine region, on the other hand, positive NAO indices have resulted in surface pressure fields that have been higher than at any time this century. Investigations by Beniston et al. (1994) concluded that close to 25% of pressure episodes exceeding the 965 hPa threshold recorded this century in Zürich (approximately 1030 hPa reduced sea-level pressure) occured in the period from 1980-1992, with the four successive years from 1989-1992 accounting for 16% of this century's persistent high pressure in the region.

Table 7.2 shows an analysis of mean wintertime values for minimum and maximum temperatures, relative humidity and precipitation at Säntis for four distinct periods of the 20th Century, namely 1901-1999, 1950-1999, 1975-1999, and 1989-1999. In each case, the observed DJF mean is given, followed by the mean which would have occured without the influence of highly-positive NAO index (beyond the 90-percentile threshold). The third column for each variable represents the bias which NAO index $\geq$ 90-percentile has imposed on temperature and moisture variables. It is seen in this Table that the bias is relatively small when considering the entire 20th Century (1901-1999), but then increases as one approaches the end of the 20th Century. In the last decade, from 1989-1999, the bias for minimum

temperatures exceeds 1°C. In the absence of the large forcings imposed by NAO index values ≥90-percentile, this decade would in fact have been slightly cooler in terms of minimum temperature than the average conditions which prevailed from 1975-1999.

Period	Tmin (°C)			Tmax (°C)		
	Observed Mean	Mean without NAO≥90 % level	Bias	Observed Mean	Mean without NAO≥90 % level	Bias
1901-1999	-8.9	-9.0	0.1	-4.3	-4.4	0.1
1950-1999	-8.7	-8.7	0.1	-3.4	-3.6	0.2
1975-1999	-8.2	-8.4	0.2	-2.7	-2.9	0.2
1989-1999	-7.5	-8.6	1.1	-2.2	-2.5	0.3

Period	Relative Humidity (%)			Precipitation (mm/day)		
	Observed Mean	Mean without NAO≥90 % level	Bias	Observed Mean	Mean without NAO≥90 % level	Bias
1901-1999	76	76	-0.4	7.0	7.1	-0.1 (-0.8%)
1950-1999	73	67	6.7	6.4	5.8	0.6 (+9.4%)
1975-1999	69	70	-0.6	6.7	6.9	-0.2 (-2.5%)
1989-1999	66	75	-9.5	8.1	9.7	-1.6 (-20.1%)

Table 7.2. Mean DJF values for minimum temperature, maximum temperature, relative humidity and precipitation for different periods of the 20th Century. The first column represents the mean recorded during each period; the second column represents the mean which would have been observed in the absence of NAO forcing beyond the 90-percentile threshold; the third column represents the bias imposed by NAO index values beyond this threshold (difference between the first two columns).

Indeed, had there not been such a strong positive NAO forcing in the latter years of the 20th Century, minimum temperatures would not have risen by almost 1.5°C (decadal mean for the 1990s minus century mean from 1901-1999) but by less than 0.5°C, as seen in the second column of the minimum temperature analyses. The bias imposed by strongly-positive NAO thresholds on maximum temperatures follows the same trends, but is not as high as for minimum temperatures; even in the absence of the NAO forcing, maximum temperatures would have risen substantially in the latter part of the 20th Century.

In terms of moisture, relative humidity has decreased in winter, with a bias of close to 10% in the period 1989-1999, resulting from the NAO forcing; mean DJF relative humidity would have otherwise remained

relatively constant throughout the century. Precipitation is also seen to be considerably marked by the NAO forcing in the last decade of the 20th Century, with a substantial drop of 20% of winter precipitation linked to the high and persistent NAO index recorded during this period.

Because over half of the NAO index values exceeding the 90-percentile have occurred since 1985, it may be concluded that the NAO is a significant driving factor for the climatic anomalies observed in recent years in the Alps. In particular, the highly anomalous nature of temperatures and then-extremes that have been observed and discussed in Jungo and Beniston (2001) are largely explained by the large-scale influence on regional climate generated by the recent trends of the NAO. Removal of the biases imposed by high NAO episodes would have resulted in relatively modest increases in minimum temperatures and reduced rates of maximum temperature warming, thus leading to Alpine-scale warming comparable to global-average warming (Jones and Moberg, 2003).

In the context of climatic change forced by enhanced greenhouse-gas concentrations, the anomalously warm winters experienced in recent years have been shown to be driven in large part by the high values of the NAO index which has prevailed in the last 15 years of the 20th Century.

The influence of these high values has been to increase the upper tails of the temperature and pressure probability density functions to a significant degree, and to reduce the relative humidity and precipitation amounts at high elevations. Because of the controls which the NAO can exert over much of the winter season, the combination of higher temperatures and lower moisture is likely to have a number of impacts on the natural environment. In particular, the fact that at high elevations such as Säntis (2,500 m asl), the number of days where diurnal temperatures exceed the freezing point can increase by as much as two weeks during the winter season has implications for the timing of snow-melt and the amount of snow which remains on the ground throughout the winter. Earlier snowmelt in turn feeds into the hydrological systems, by increasing river discharge earlier in the season compared to "normal" or negative NAO indexes. Warmer temperatures are also associated with liquid rather than solid precipitation falling at higher elevations; when combined with early snowmelt runoff, this can lead to critical hydrological situations, particularly downstream of the mountains, as was experienced for example in early 1995, when the Rhine River overflowed its banks in Germany and The Netherlands.

Less snow and warmer conditions have taken their toll of glacier mass in the Alps, while at the same time in the late 1980s and early 1990s, Norwegian glaciers were advancing because of the excess precipitation in northerly latitudes associated with high NAO indexes. Earlier snow-melt can

also trigger the seasonal cycle of mountain plants, as much of the high Alpine vegetation is dependent on snow pack amount and duration for its metabolic cycles. The reduction of snow amount, which is closely related to the higher NAO indexes, and generally warmer average temperatures, are coincident with an upward migration of plant species, as reported by Grabherr et al. (1994) and Keller et al. (2000). Plants which survive under warmer conditions are progressively invading areas in which only cold-resistant vegetation was present until recently.

It would be difficult to draw more far-reaching conclusions for climate impacts on the basis of the short series of anomalously warm winters experienced in the Alps; this is *inter alia* the case for ecosystem responses to climate change, which generally occur over longer time-scales. The run of mild winters in the Alps associated with high NAO index values has, however, had a measurable effect on snowline altitude, snow amount and duration, which in turn has influenced flow regimes in a number of hydrological basins originating in the mountains. Perturbations to hydrological regimes in a changed climate will certainly be the norm in the 21st Century (e.g., Gleick, 1987; Krenke et al., 1991; Leavesly, 1994), because of the different timings of the beginning and end of the snow season, and the overall reduction in the duration of the mountain snow-pack. The sparsity of snow has also had significant economic impacts on Swiss mountain communities in the late 1980s and early 1990s, which are largely dependent on winter sports for their income. The conclusion that snow amount and duration has been sensitive to changes in climate since 1985 at altitudes below 1500 - 2000 m is consistent with the rise in average snowline projected under a warmer global climate (IPCC, 1996); these conclusions could already help certain communities in preparing adaptation strategies for the future, for example through diversification of tourism activities rather than relying solely on the ski industry in winter. The conclusions presented here could provide guidance for future environmental and economic planning in the Alps, particularly for activities related to winter tourism, water resource management, and ecosystem studies.

Because of the very significant controls of the NAO on regional climate variables, their means and their extremes, it is vital in the current debate on global warming for general circulation climate models to improve their performance in simulating North Atlantic decadal-scale variability. This would enable an assessment of whether such variability will be as large as during the 20th Century, or whether the system will exhibit systematically positive NAO index values as observed since the 1980s. Climate modelers and climate-impacts specialists would thus be able to quantify the role of the future behavior of the NAO on climatic extremes in Europe.

7.3.3. Changes in extreme weather events

Public awareness to extreme weather hazards has risen sharply in recent years, in part because of instant media attention that serves to emphasize the catastrophic nature of floods, droughts, storms, and heat waves or cold spells.

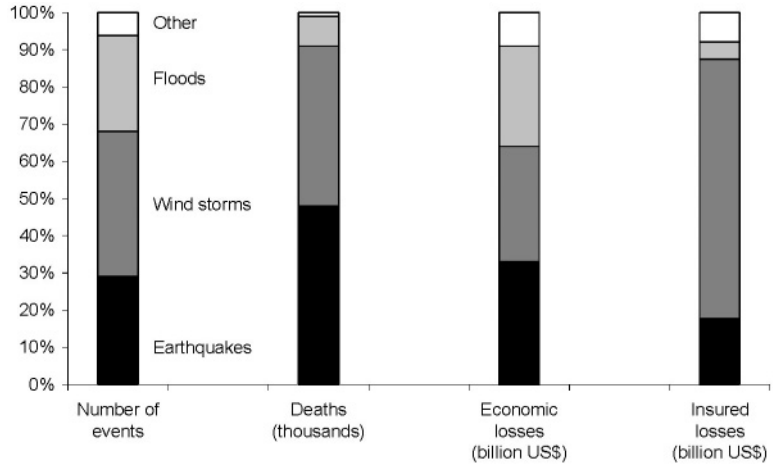

Figure 7.15. Number of extreme climate-related events, death toll, and associated damage costs as a percentage of all natural hazards in the second half of the 20th century (From: Munich Re, 2002).

There is also a general perception that the number of extreme events has increased in the past few decades, based on statistics from the insurance sector as shown in Figure 7.15 (from Munich Re, 2002). These insurance statistics highlight the fact that, with the exception of earthquakes, climate-related hazards are those that take the heaviest toll on human life and exert among the highest damage costs. In the second half of the 20th century, there have been 71 "billion-dollar events" resulting from earthquakes, but more than 170 events with similar costs related to climatic extremes, in particular wind-storms (tropical cyclones and mid-latitude winter storms), floods, droughts and heat-waves.

There is thus an obvious incentive for the research community as well as the public and private sectors to focus on research related to extreme climatic events and the possible shifts in their frequency and intensity as climate changes in the course of the 21st century. However, closer interpretation of the elements of Figure 7.15 suggests that most of the

increase in damage costs resulting from extreme climatic events is related to higher population densities in risk-prone areas than in past decades and a corresponding rise in insured infrastructure, rather than to an increase in the number of events themselves (Swiss Re, 2003).

There is no single definition of what constitutes an extreme event. Extremes can be quantified *inter alia* on the basis of:

- how rare they are, which involves notions of frequency of occurrence; this is the definition that the Intergovernmental Panel on Climate Change has adopted (IPCC, 2001), whereby an extreme is referred to as occurring below the 10^{th} percentile or above the 90^{th} percentile of a particular statistical distribution of temperature, precipitation, pressure, etc.
- how intense they are, which involves notions of threshold exceedance; the intensity of an event has a direct bearing on the associated human and economic damage costs, and can be related to heat waves, excessive wind velocities, or to both ends of the "precipitation spectrum" that can lead to droughts on the one hand and floods on the other;
- the impacts that may emerge from a particular event or set of events, that will also determine the costs for socio-economic and environmental sectors that are related to extremes; impacts-based definitions of extremes are complex because in many instances, many damaging natural hazards can be triggered in the absence of an intense or rare climatic event.

It is thus clear that none of these definitions on their own are entirely satisfactory, however, and each definition corresponds to a particular situation but cannot necessarily be applied in a universal context.

Understanding the mechanisms underlying various forms of climatic extremes is of interest to assess of the manner in which they may evolve in the future, under changing climatic conditions. A better understanding can in turn allow improvements in the ability to quantify the costs associated with natural climate-related hazards and thereby provide the basis for strategies to adapt to climatic change from an economic point of view.

It has been seen in the previous sections that he alpine climate has experienced significant change over the past 100-150 years). It is thus of interest to determine some of the causal mechanisms that are responsible for the rapid rise in temperatures in Switzerland over the course of the 20^{th} century and whether this has had a bearing on the extremes of climate

Heat waves are generally believed to increase when average temperatures are on the rise. This is because if there is a rise in the mean of temperature as given by the vertical arrows in Figure 7.16 (adapted from IPCC,2001), there

can be a symmetrical shift in the PDF of temperature, with the same increase of extreme temperatures at the high end of the distribution (that could be taken as "heat waves") as there is a decrease at the low end of the PDF (that could be considered as "cold spells"), as indicated by the shaded areas. However, the change in mean temperature can also be accompanied by a shift in the skewness and/or the kurtosis of the distribution, yielding a profile that is seen in the lower part of Figure 7.16. In this lower figure, the shift in means is in fact less than in the upper graph, but the asymmetry of the curve yields a disproportionate increase in the extremes of warm temperatures.

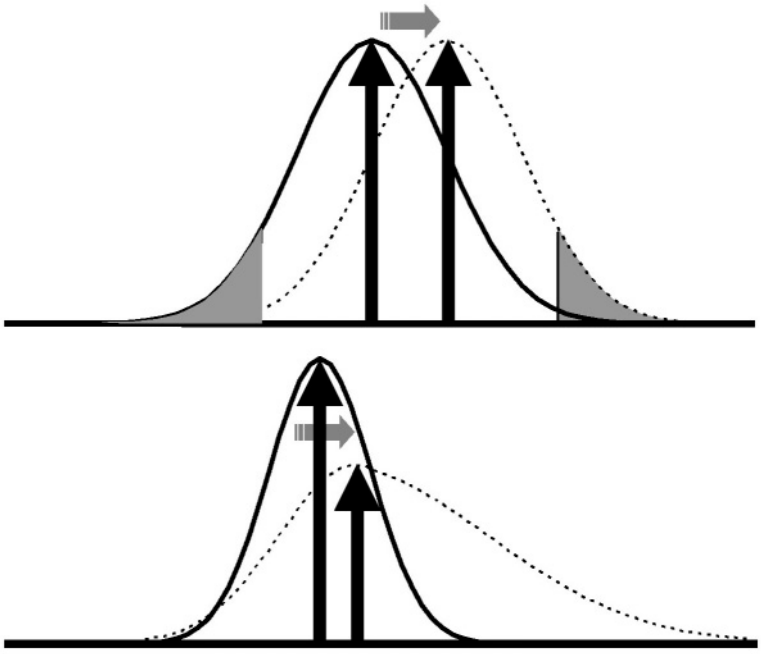

Figure 7.16. Illustrative examples of possible shifts in the probability density function of an atmospheric variable such as temperature. Upper: a symmetrical shift in the entire distribution; lower: an asymmetric shift with a change in both the skewness and the kurtosis of the distribution.

Over the course of the 20th century, observations suggest that there has been a shift in the PDFs of both minimum and maximum temperatures, between the coldest part of the century (1901-1910) and the warmest part (1991-2000), as exemplified in Figure 7.17 for Basel, at 317 m above sea level. The increase in average winter minimum temperatures is 2.2°C between the two periods, from -2.6°C to -0.4°C. The number of days below

freezing has decreased by half, from 26% to 13% of the winter season, while the number of warm winter nights (above 10°C) has increased by a factor of 3, from 2.5 to 8 days per winter.

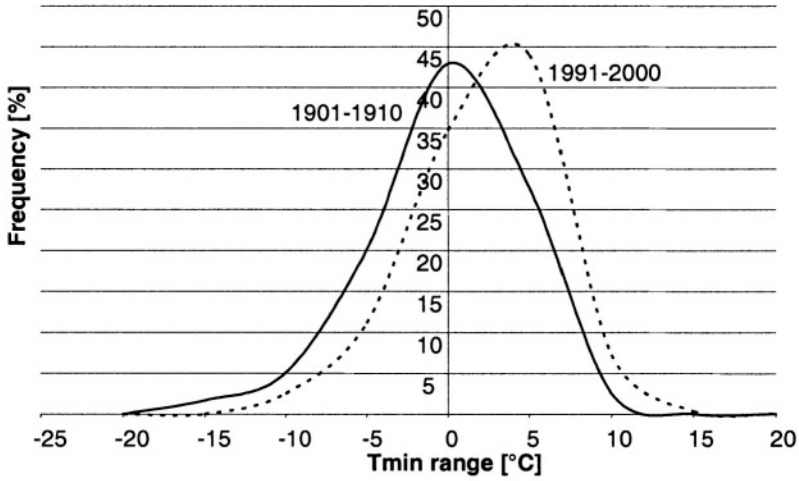

Figure 7.17. Shifts in the probability density function (PDF) of mean annual maximum temperatures at Basel between the coldest (1901-1910) and warmest (1991-2000) periods of the 20th century.

When analyzing threshold exceedance such as the number of days with maximum temperatures above 30°C in Basel, there is a correlation of 0.65 between mean annual maximum temperatures and threshold exceedance; this correlation rises to 0.90 when comparing the number of days exceeding 30°C with mean *summer* maximum temperatures (June, July, and August averages). This is logical in the sense that heat waves will generally occur during the summer, whereas on an annual basis, a cold winter may well be followed by a very warm summer, leading to a moderate annual temperatures and thus a more tenuous link with threshold exceedance. Similar conclusions can be reached for most measurement sites at low elevations in Switzerland.

Other forms of extremes that cause considerable economic damage and, in some cases, loss of life include heavy precipitation events and winter storms. Heavy precipitation seems to have increased significantly in the last quarter of the 20th century, while winter storms of the intensity of the December, 1999 *Lothar* event are still extremely rare events that cannot be linked in any statistically-meaningful manner to long-term global warming.

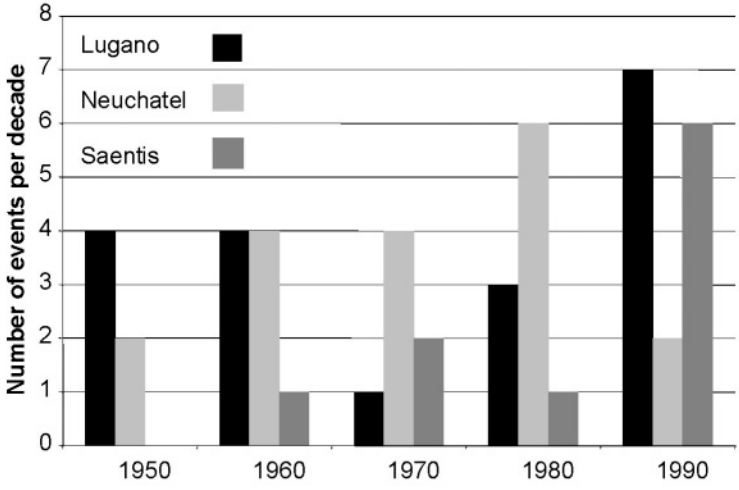

Figure 7.18. Number of extreme precipitation events exceeding thresholds of 100 mm/day in Lugano and Säntis, and 50 mm/day in Neuchâtel for the last 5 decades of the **20th** century.

Figure 7.18 shows the behavior of extreme precipitation events based on selected thresholds in Lugano (south of the Alps), Neuchâtel (north of the Alps), and Säntis (within the alpine domain at high altitude). The thresholds for Lugano and Säntis are 100 mm/day, and for Neuchâtel 50 mm/day. The graph shows that the number of events reached its maximum in Neuchâtel in the 1980s, and at Lugano and Säntis in the 1990s; the sharpest increase is at Säntis where the threshold is exceeded 6 times in the 1990s compared to two or less occurrences per decade prior to the 1990s. In terms of the total amount of precipitation associated with these extremes, Figure 7.19 confirms the trends already seen in the number of events (Figure 7.18), where a three-fold increase in cumulated water amounts from the 1980s to the 1990s for the sites in the Alps and south of the Alps can be observed; Neuchâtel on the other hand shows a decrease in total precipitation that is linked to the decrease in events. At and above 100 mm/day, the potential for flooding and enhanced erosion is high, especially in exposed mountain terrain, as has been reflected in the high costs associated with the Brig catastrophe (September, 1993), the floods of Lake Maggiore in the falls of 1993 and 2000, and the devastating landslides and mudslides in the vicinity of the Simplon (Gondo, October 2000), for example. Attempting to link these events to average warming trends, either on an annual basis or on the basis of the temperatures that prevail during the specific extreme precipitation event, is difficult because there is not necessarily any direct relationship between a given level of temperature at a particular location, and complex physical processes that

are an aggregate of numerous mechanisms occurring at various spatial scales.

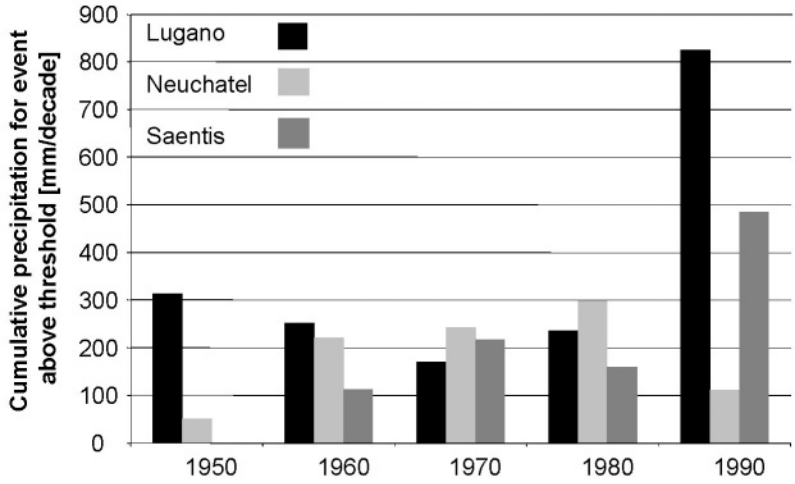

Figure 7.19. Cumulative precipitation for extreme events beyond the 100 mm/day threshold at Lugano and Säntis, and 50 mm/day in Neuchâtel for the last 5 decades of the 20th century.

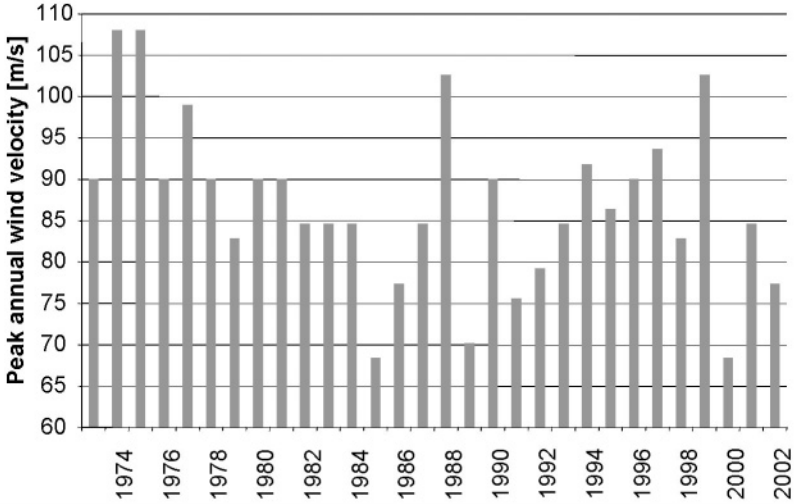

Figure 7.20. Annual peak wind velocities measured at La Dôle (western Switzerland, 1,690 m above sea-level) for the period 1973-2002.

In terms of extreme wind storms, the relationship between these events and warming trends is even more difficult to establish; strong storms are

either generated over the Atlantic, or are associated with föhn-type flows over the Alps, and as such have very little to do with local climatic conditions over the Alpine domain. As shown in Figure 7.20, during the last 30 years of the 20th century, there are no trends apparent in terms of peak wind velocities recorded during each year at La Dôle, a summit of the Jura Mountains exceeding 1600 m elevation close to Geneva, that tends to intercept westerly flows with little interference from topography upstream in France. The record is rather short but nevertheless highlights the fact that there is no significant increase in extreme wind velocities in relation to the increase of close to 2°C in mean annual temperatures that were recorded during this period.

Loss of life and economic damage resulting from strong wind storms, that generally occur during the winter in western Europe and the alpine area, can be significant (e.g., Ulbrich et al., 2000). The December 1999 *Lothar* storm resulted in uprooted or damaged trees equivalent to more than 4 times the annual felling rate in certain Swiss cantons (BUWAL, 2000), and damage to infrastructure that exceeded USD 1 billion in Switzerland alone and over USD 20 billion in the countries affected by the winter storm from France to central Europe, according to SwissRe (2003). Current 20-year return periods of wind velocities associated with winter storms are in the range 30-75 m/s, according to the altitude and the latitude of the site (Goyette, 2003, personal communication).

7.3.4. The 2003 heat wave

The record heat wave that affected many parts of Europe during the course of summer 2003 has been seen by many as a "shape of things to come", reflecting the extremes of temperature that summers are projected in the later decades of the 21st century. The heat wave also affected Switzerland to the extent that previous records for summer maximum temperatures observed in the late 1940s and early 1950s were broken in many locations in August, 2003, according to the Swiss weather service, MeteoSuisse (2003). Research by Pfister et al. (1999), based on written historical archives, indeed suggest that 2003 is likely to have been the warmest summer since 1540.

This sub-chapter will report on trends in average summer maximum temperatures (June-July-August means; hereafter referred to as summer Tmax) at two locations, Basel (367 m above sea-level, in the north-western part of Switzerland close to the French and German border), and the high-elevation site of Säntis (2,500 m above sea-level, in the north-eastern part of the Alps roughly 50 km from the Austrian border). Each of the sites is

representative of temperatures at low and high elevations, respectively, and have been chosen to determine whether the behavior of summer Tmax at these locations are similar or decoupled because of the height factor. The mean and extremes of average summer maximum temperatures have been analyzed to assess whether significant changes have emerged over the past century, and whether there exists a relation between summer Tmax and its extreme values defined by the 90th quantile as suggested by the IPCC (2001).

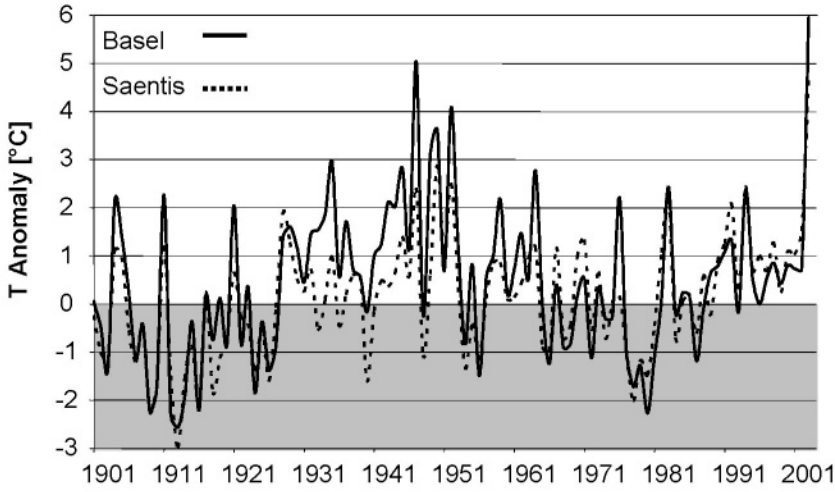

Figure 7.21. Departures of summer maximum temperatures from the 1961-1990 means at Basel (317 m above sea level) and Säntis (2,500 m above sea level), Switzerland.

Figure 7.21 illustrates the anomalies of summer Tmax recorded each year from 1901-2003 at both sites, computed as departures from the 1961-1990 climatological average period (Beniston, 2004). Both series are essentially in phase, with perhaps the exception of the mid-century warm peak at the end of the 1940s that is more pronounced in Basel. The 2003 event stands out as a "climatic surprise", in the sense that it is the first time that average JJA Tmax in Basel has exceeded the 27°C threshold since 1952, the 28°C threshold since 1947, and the 29°C for the first time in this century-long record. The 2003 heat wave comes at the end of a 40-year period during which summers were markedly cooler than the warm summers of the mid-20th century. Positive Tmax anomalies in Basel exceeded 6°C (1°C higher than the previous record of 1947), and 4.7°C in Säntis (almost 2°C more than the 1950 record for this location).

A closer analysis of the persistence of the event based on an exceedance of the 30°C threshold at Basel reveals, however (Figure 7.22, following

Beniston, 2004), that 2003 exhibited fewer days (41) than 1947 (49), for example; furthermore, there were 12 consecutive days in 2003 during which Tmax exceeded 30°C as opposed to 1976 (16) or 1947 (14). The 1940s stand out as a decade in which a clustering of summers with a threshold excess of 20 days or more is not uncommon, whereas such events tend to diminish in the 1970s and 1980s. According to the statistics considered, therefore, 2003 is not seen to have broken all records in terms of extremes; the sudden jump to high exceedance values following over a quarter century where summers never exceeded the 30°C threshold for 20 days or more does, however, constitute a "climatic surprise".

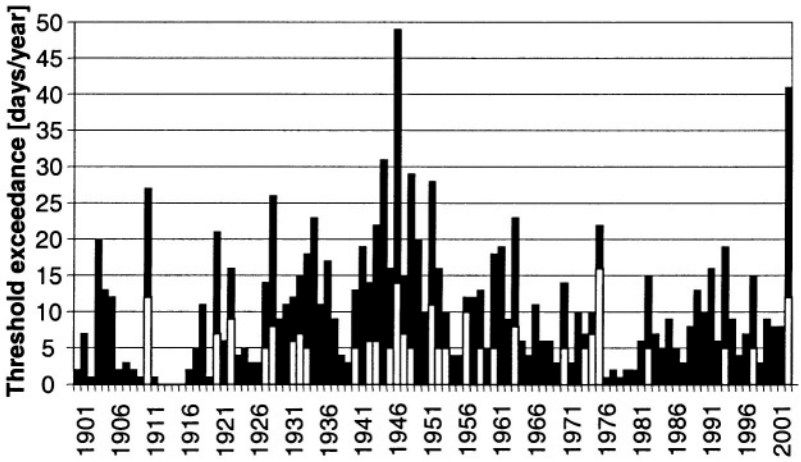

Figure 7.22. Number of days during which temperatures exceed the 30°C threshold in Basel (black) and number of consecutive days of threshold excess (white), from 1901-2003.

The behavior of the 90^{th} quantile of Tmax at both Basel and Säntis, as a measure of changes over time in the upper extreme of the probability density function (PDF) of temperature; exhibits a close resemblance to the anomalies of Tmax illustrated in Figure 7.21 and the extremes of the distribution, suggesting a link between changes in means and shifts in the extremes of the distribution.

This is illustrated in Figure 7.23, where a very significant linear relationship between means and extremes exists at the 99.9% level for both the low and the high elevation sites. The higher-order statistics (variance, skewness and kurtosis) are essentially de-correlated from the average statistics, implying a symmetric shift in the probability density function of summer Tmax, i.e., as the average summer Tmax changes, the upper and lower bounds of the Tmax PDF undergo a similar amount of change. This is

not necessarily the case elsewhere, as has been pointed out by Katz and Brown (1992; also D. B. Stephenson, University of Reading, UK; personal communication; 2003).

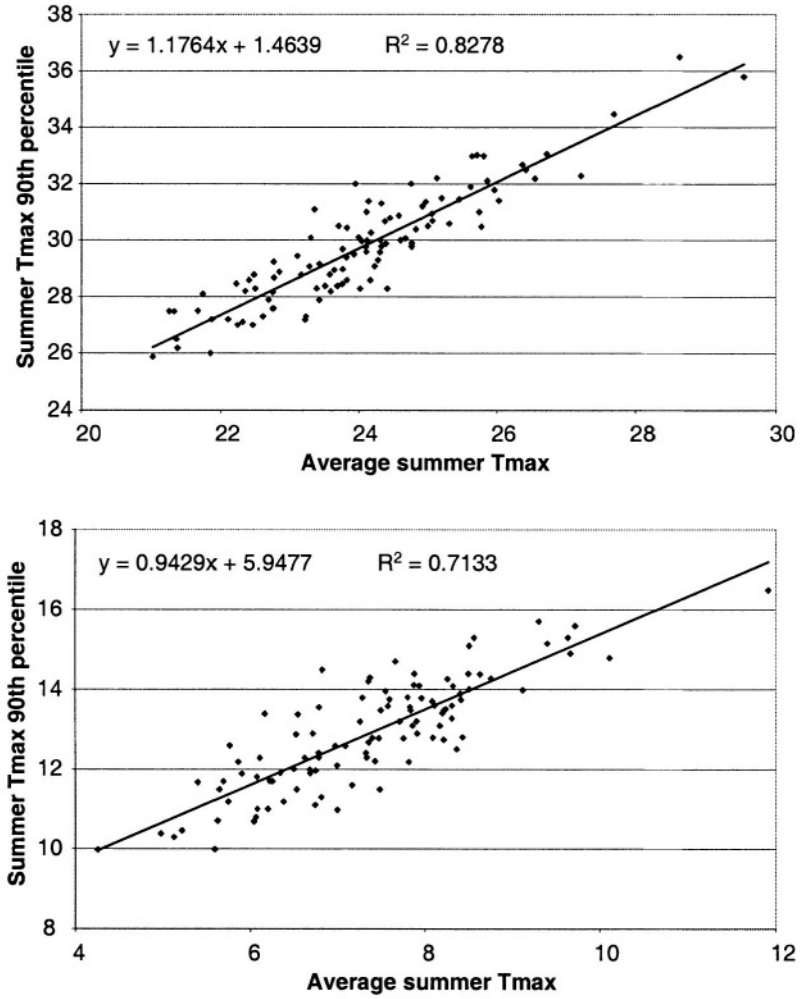

Figure 7.23. Relationship between mean summer maximum temperatures and the 90th quantile of summer maxima at Basel (upper) and Säntis (lower).

There is no salient difference between processes taking place at high elevations compared to low altitude sites, suggesting that the summer temperatures are responding to the same meteorological situations. Altitude

does not appear to be a dominant feature in terms of the behavior of summer temperatures and their extremes, other than the obvious influence of height on the absolute values of temperatures. The conclusions for the two locations selected here are valid for all other Swiss climatological sites analyzed but not discussed here

It was seen in Chapter 6 that the results from simulations with the HIRHAM4 RCM for the IPCC SRES A2 emissions scenario (Nakicenovic, 2000) show a strong warming over much of Europe.

HIRHAM4 model results for contemporary climate (1961-1990) show that the statistics of temperature over Europe are in reasonable agreement with observations, both in terms of the means and the higher statistical moments of mean, minimum, and maximum temperatures, thereby allowing some confidence in the temperature statistics resulting from the A2 scenario simulations. Under future climatic conditions (2071-2100), mean JJA Tmax increases by 5.2°C at Basel, from 23.6°C to 28.8°C, which represents a statistically-significant shift.

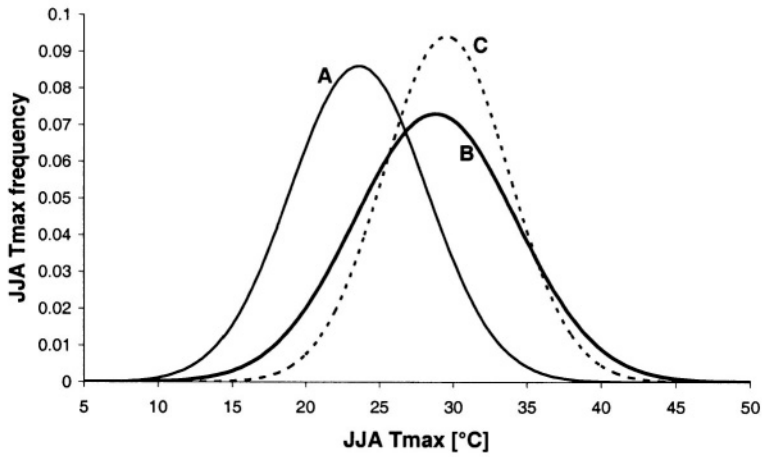

Figure 7.24. Gaussian distributions fitted to the mean summer maximum temperature data at Basel, Switzerland, for A) the 1961-1990 reference period; B) the 2071-2100 A-2 scenario simulation; and C) the 2003 heat wave.

As seen in Figure 7.24, which illustrates the the Gaussian fits to the JJA Tmax data for a number of periods, the change in mean between the contemporary (curve A) and future periods (curve B) is accompanied by a change in the variance of the distribution, which is a feature that has already been observed in other studies (Katz and Brown, 1992). The future climate projections as well as the 2003 event represent a major shift in summer

maxima that is also accompanied by a proportional change in the 90th percentile (about 5.5°C) and a similar shift even at the 99th percentile level. Remarkably, the slope of the linear regression fit between summer mean Tmax and the 90th quantile for future climate is almost identical to that observed for current climate, also with a highly significant correlation coefficient (close to 0.9 in both instances). Mean summer Tmax in Switzerland can thus be used with a high degree of confidence as an empirical predictor of the type of extreme that may occur during a particular summer.

The Gaussian distribution of the 2003 maximum summer temperatures is the only example of a range of summer maximum temperatures that is located entirely within that of the 2071-2100 period and with an almost identical median value, albeit with a much variance. This is to be expected, since the Gaussian curve is fitted to data for a single summer, as opposed to the 30 summers of the future climate scenario where interannual variability naturally results in a wider spread. In terms of individual years in the future climate simulation, 2093 exhibits similar statistics to 2003 in terms of means and variance.

While all the statistics of the 2003 and the 2071-2100 summer maximum temperatures are not in perfect accord, the fact that the JJA Tmax PDF for 2003 lies entirely within the future range projected by the HIRHAM4 model suggests that the recent event may be considered as a close analogue to the summers that may occur in the future as the atmosphere responds to increases in greenhouse gases under the IPCC SRES A2 scenario. Although only the Basel observational site has been presented here, the conclusions remain identical for other low-level locations studied in Switzerland.

Period	A	B	C	D	E	F	G
1961-1990	23.6°C	29.6°C	4.6°C	8	June 19	Aug. 19	61
2003	**29.5°C**	**35.6°C**	**4.2°C**	**41**	**June 2**	**Aug. 30**	**89**
2071-2100	28.8°C	35.9°C	5.5°C	38	June 7	Sept. 5	90

Table 7.3. Statistics of summer (JJA: June-July-August) maximum temperatures in Basel for the reference period 1961-1990, future climate 2071-2100 and, in comparison, the 2003 heat wave.
Column A: mean JJA Tmax; Column B: 0% quantile of JJA Tmax; Column C: standard deviation of JJA Tmax; Column D: Number of days per year where Tmax exceeds 30°C; Column E: Average day in the year when Tmax first exceeds 30°C; Column F: Average day in the year when Tmax last exceeds 30°C; Column G: Duration of the season during which Tmax can be expected to exceed 30°C.

Table 7.3 provides a comparative assessment of current and future climate statistics for Basel, and places 2003 against the backdrop of current and future climates. The characteristics of the 2003 heat wave in Europe bear a far closer resemblance to those of the simulated future climate than to the statistics for 1961-1990 in terms of means, the 90^{th} quantile (i.e., the upper extreme of temperature as defined by the IPCC, 2001), threshold exceedance, and the duration of the season during which temperatures may rise above 30°C for a number of separate or consecutive days. For reasons already alluded to, the standard deviation of summer Tmax during the 2003 event are lower than for the 30 years of future climate.

Between 1961-1990 and 2071-2100, the period during which threshold exceedance can be expected is extended by close to one month, beginning on average almost two weeks earlier and ending more than two weeks later than under current climatic conditions. The total number of days during which the 30°C threshold is exceeded increases almost 5-fold in the future, as it did during the 2003 heat wave. The spread of record summer maxima from one year to the next may range from 35-48°C in the future

The 2003 heat wave, by mimicking quite closely the possible course of summers in the latter part of the 21^{st} century, can thus be used within certain limits as an analog to what may occur with more regularity in the future. The physical processes that characterized the 2003 heat wave, such as soil moisture depletion and the positive feedback on summer temperatures, the lack of convective rainfall in many parts of the continent that generally occur from June-September, are projected to occur with greater frequency in the future. In view of the severity of the impacts related to the persistence of elevated temperatures and drought conditions, such as excess deaths recorded in France and Italy (WHO, 2003), crop failure and sharply reduced animal fodder for the winter in many countries (CLIVAR, 2003), and strongly-reduced discharge in many rivers, the recent heat wave as a "shape of things to come" can help both scientists in assessing the course of future climatic impacts, and decision makers in formulating appropriate response strategies.

Chapter 8

CLIMATE TRENDS AND IMPACTS IN SWITZERLAND IN THE 21ST CENTURY

8.1. ESTIMATES OF CHANGES IN MEANS AND EXTREMES IN SWITZERLAND

The more recent work conducted within the context of EU Framework Program 5 projects alluded to in Chapter 6 has served to confirm earlier simulations of climatic change in the alpine region conducted by Marinucci et al. (1995) and Rotach et al. (1997). These studies concluded that the Alps would within decades experience a shift towards a Mediterranean-type climate, i.e., one that is characterized by a wet winter season and a long, dry and warm summer season. The northward progression of climatic zones that are currently located to the south is, as seen in Chapter 6, expected to be of the order of 500 km within 100 years. The climate of the western part of the Alps may therefore resemble, in terms of its temperature and precipitation characteristics, a type of climate that is currently found in the Mediterranean Alps of southern France.

Both Marinucci et al. (1995) and Rotach et al. (1997) have focused on high-resolution simulations for January and July under both current climate and a climate with a doubled CO_2 concentration. These were undertaken by applying the RegCM2 regional climate model of the National Center for Atmospheric Research (NCAR, Boulder, Colorado, USA) to a domain covering the Alps. The climate scenarios were initialized by using simulated data provided by the ECHAM-4 general circulation model developed at the Max-Planck Institute for Meteorology (MPI, Hamburg, Germany).

Based on the global information provided by the GCM during a five-year time window for both the present and future climates, RegCM2 simulated detailed climatologies over Switzerland. To analyze the model performances, the results from these simulations were compared with two

observed climatological data sets, namely the 0.5° resolution gridded data of Legates and Wilmott (1990) and a dataset from close to 100 observing stations distributed throughout Switzerland.

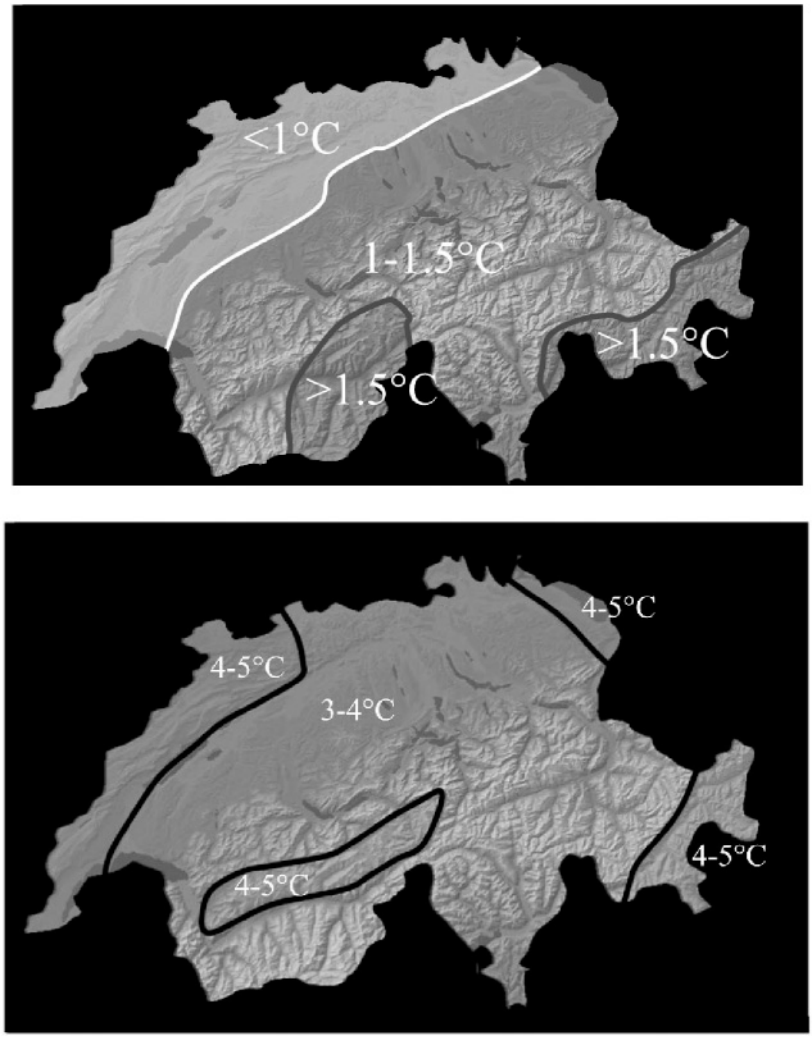

Figure 8.1. Temperature change in °C between current climate and a doubled-CO2 climate in Switzerland for winter (upper) and summer (lower) seasons.

The nested model RegCM2 reproduced several aspects of the Alpine temperature and precipitation climatology but also showed significant

deficiencies which that were identified to be related to failings in the initial and boundary conditions provided by the ECHAM-4 model.

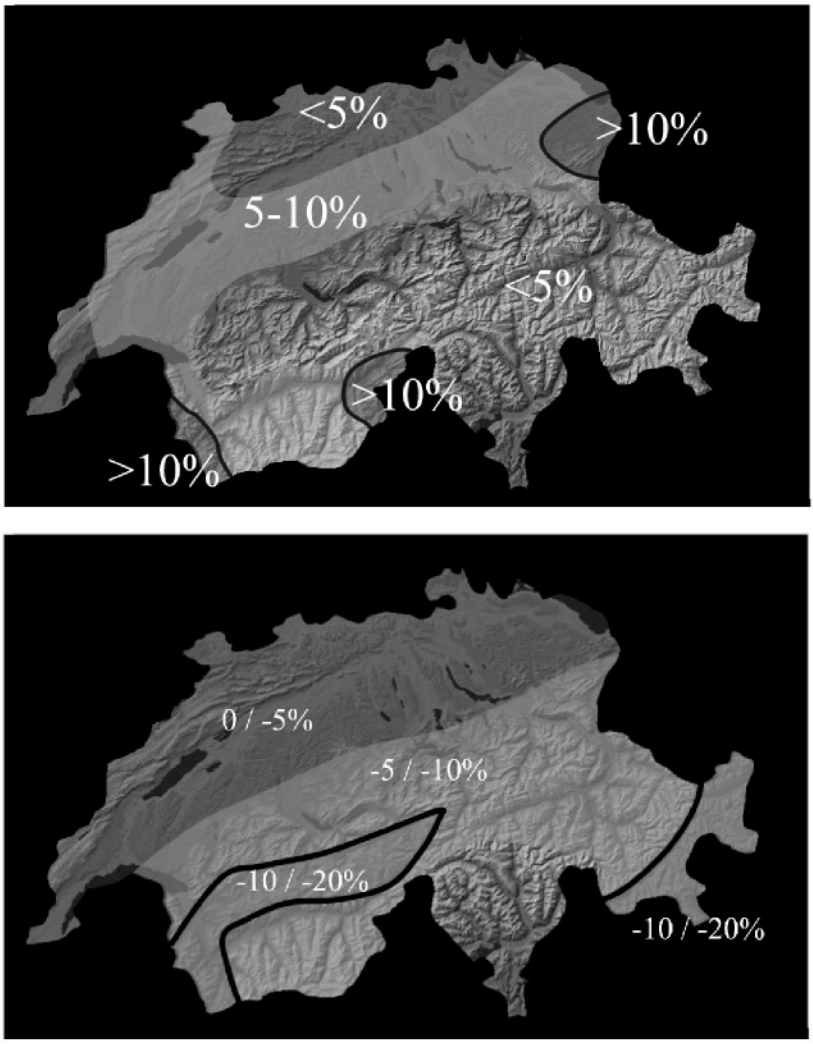

Figure 8.2. Precipitation change in % between current climate and a doubled-CO2 climate in Switzerland for winter (upper) and summer (lower) seasons.

In the climate forced by doubled CO_2 concentrations in the atmosphere, generally higher winter temperatures and a more marked increase in summer temperatures shown in Figure 8.1 appear to be consistent with other studies

on global climate change; there are indications that there is a greater temperature increase at higher elevations compared to lower altitudes (Rotach et al., 1997).

Precipitation is also higher and more intense in winter, but much reduced in summer. While the temperature and precipitation changes are within the range of model errors when compared to observational data, the comparison of model simulations for present and future climates reveals trends in temperature and precipitation that are consistent with what can be expected from the atmospheric forcing by enhanced greenhouse gas concentrations. The sharp reduction in precipitation in summer seen in Figure 8.2 explains the much stronger warming than in winter as observed in Figure 8.1. Cloudiness is reduced and therefore more incoming solar energy is available to warm the surface; in addition, soil moisture diminishes, thereby exerting a positive feedback on the lower atmosphere.

Enhanced winter precipitation, on the other hand, implies perhaps more snow accumulation but at higher altitudes than today, but more rainfall at or below 1,500-2,000 m above sea level (Beniston et al., 2003). Figures 8.1 and 8.2 show quite clearly that, even bearing in mind the large uncertainties related to such simulated results, the more elevated parts of the Alps seem to be more sensitive to future warming and changes in precipitation regimes than lower elevations, i.e. the more fragile and sensitive parts of the mountains are being exposed to the largest climate forcings. This is an extension into the future of disproportionately high increases in temperature at height compared to the lowlands already observed in the 20^{th} century (Beniston et al., 1994; Beniston and Jungo, 2002).

It is not expected that the increase in winter precipitation seen in the upper part of Figure 8.2 would compensate to any large extent the direct influence of more elevated temperatures. As a result, snow and ice will be most sensitive to the particularly strong changes in temperature and precipitation regimes at high elevations, In addition to snow and ice, these shifts in climate will be accompanied by strong changes in hydrological regimes and the distribution of vegetation patterns, as will be discussed in sub-chapter 8.3.

In Chapter 7, a small parenthesis was opened on future climate trends in the discussion regarding the 2003 heat wave and the possibility that summers in a future climate would frequently resemble that experienced during the 2003 event. The subject is revisited here by investigating regional climate model temperature statistics for Neuchatel, located at 489 m above sea-level at the foot of the Jura mountains in western Switzerland

The analysis of the probability density function of maximum daily temperatures illustrated in Figure 8.3 emphasizes the strong shift in

temperature extremes between the 1961-1990 reference time-frame and the future 2071-2100 period as simulated by the HIRHAM model for both current climate and the IPCC SRES A2 scenario (see Chapter 4.6).

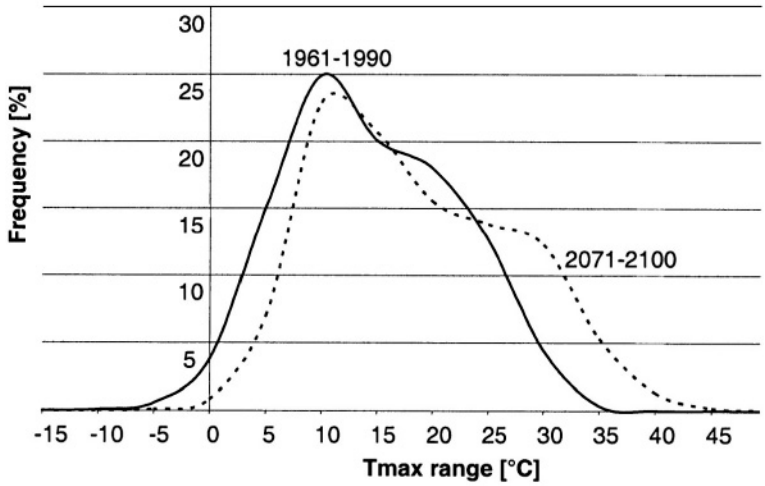

Figure 8.3. Shift in the probability density function of maximum daily temperature at Neuchâtel as computed by the HIRHAM regional climate model for current (1961-1990) and future (2071-2100) climatic conditions using the IPCC SRES A2 scenario.

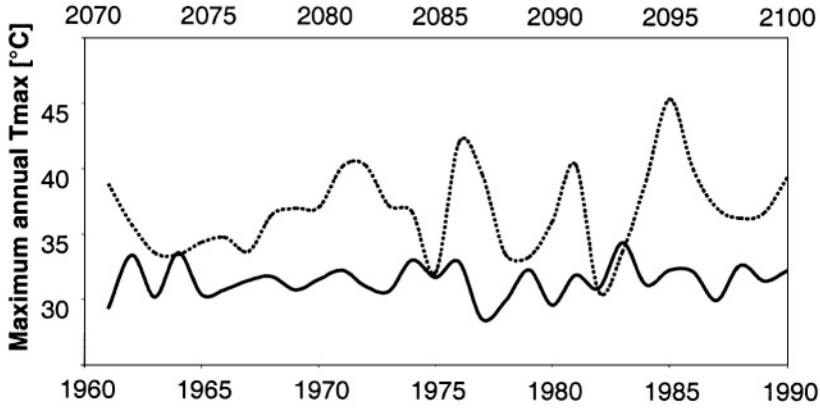

Figure 8.4. Comparison between observed record high maximum temperatures during the 1961-1990 reference period (solid line and lower abscissa) and for the 2071-2100 scenario climate (dotted line and upper abscissa).

The number of days where maximum temperatures remain below the freezing point are almost totally absent in the future (3 days per year on average as compared to 16 days per year on average during the 20th century reference period), while the 30°C threshold is exceeded on average 70 days per year in the future compared to a range of 15-25 days today, i.e., a 3-5 fold increase in the warm extreme range of temperature. Maximum annual temperatures are seen to attain 45 °C in some years of the 2071-2100 period (dotted line of Figure 8.4) as opposed to about 33-36°C currently (solid line).

Simulations of future daily precipitation trends over the Swiss Plateau suggest that both ends of the precipitation "spectrum", i.e, very dry conditions or those associated with strong precipitation events, are likely to increase, shows a dual trend, i.e., a general reduction in *average* annual precipitation, and an increase in *extreme* precipitation events. Episodes with little or no rainfall in the HIRHAM model are seen to increase by about 33% in the future, while the number of days with precipitation exceeding 25 mm/day or more may increase by 25%. The tendency of a dual increase of drought and heavy precipitation in the mid-latitudes in a warmer climate has been reported elsewhere, notably for North America (e.g., IPCC, 2001; Trenberth, 1999) and for Europe (e.g., Christensen and Christensen, 2003). In some parts of the Alps, heavy precipitation could increase by as much as 30% for a 2°C warming according to Frei et al. (1998).

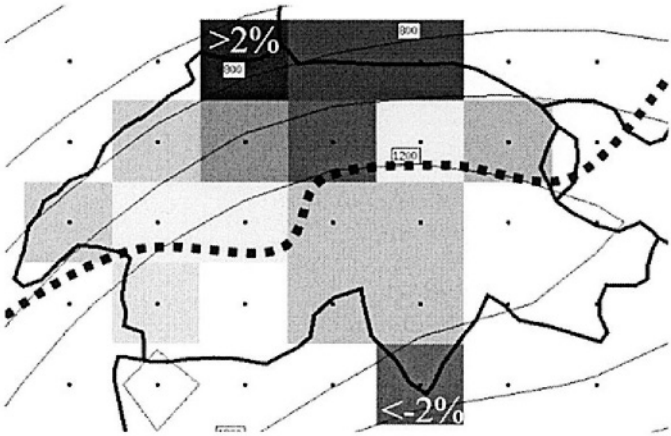

Figure 8.5. Changes in the frequency of strong wind events between current and future climates. To the north of the dotted black line, regional climate model simulations suggest a slight increase in storms originating in the Atlantic and a similar decrease of storms originating south of the Alps. Gray scale is an indication of the magnitude of the change for the 50-km resolution grid-cells of the HIRHAM regional climate model (Courtesy: S. Goyette, University of Fribourg, Switzerland).

Very preliminary results from modeling studies of extreme winter storms, based on model studies of events such as the 1990 *Vivian* storm (Goyette et al., 2001) or the 1999 *Lothar* storm (Goyette et al., 2003), suggest an increase in the frequency of strong winds originating in the Atlantic at the expense of föhn-type storms related to southerly flow across the Alps (Figure 8.5). There is a strong probability that the alpine zone will experience at least one event with similar intensity to the 1999 *Lothar* "storm-of-the-century" by 2020. While this may not appear to be significant, it should be borne in mind that the insured infrastructure is likely to increase over the next decades, thus leading to a strong rise in damage costs in the event of such a wind storm affecting the region.

8.2. IMPACTS ON THE ALPINE ENVIRONMENT

8.2.1. Issues related to impacts assessments

Impacts assessments pose a number of challenges, particularly in mountain regions where the complexity of the terrain and gaps in information may be greater than in other regions. Many of these challenges are related to the dominantly regional or local characteristics of the systems upon which climatic change may have an influence. There is the added complexity due to the fact that patterns of anthropogenic climatic change are superimposed upon those of natural climate variability.

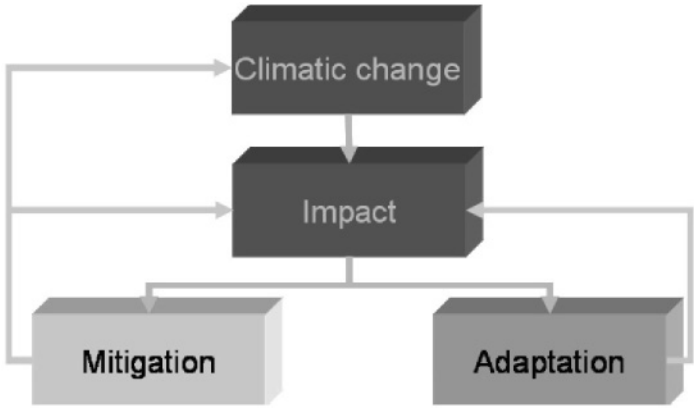

Figure 8.6. A classical approach to climate impacts studies that is based on a sequential concept that assumes an unequivocal "cause-to-effect" relationship between climatic change and the response of an environmental or socio-economic system to change.

Early approaches to climatic impacts assessments were carried out in a sequential manner, i.e., estimates of climatic change were taken up by impacts models to attempt to quantify a cause-to-effect relationship between climate and an environmental or socio-economic sector that may be influenced by climatic change, as schematized by the flowchart in Figure 8.6. The procedure illustrated in this figure then assumes that once the severity of the impact is known, it allows adaptation and/or mitigation strategies to be adopted. The consequences of these strategies could then feed back into the climate and impacts sectors to limit severity of the impacts and/or the amplitude of climatic change.

This procedure is overly simplistic and in many respects illusory, because with few exceptions, there is rarely a single cause-to-effect relationship between climate and natural or managed systems. When analyzing the potential effects of change on a particular system, it should be borne in mind that environmental change comprises a range of stresses. For example, the IPCC (1996) emphasized in its Second Assessment Report that human-induced climatic change represents an *additional stress* on systems that are already threatened by *other changes.* These include diminishing biodiversity, overexploitation of natural resources, numerous forms of air, water and soil pollution, as well as ozone depletion in the stratosphere. Because of this complex inter-linkage of stresses, it is exceedingly difficult to attribute impacts on natural or economic systems to just climatic change.

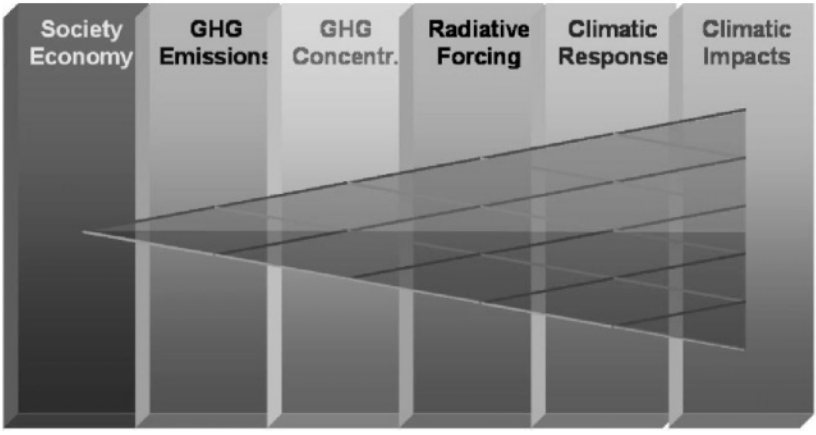

Figure 8.7. The "explosion of uncertainty", or an example of the manner in which uncertainty can propagate in the set of issues that are addresses in an end-to-end climatic impacts assessment investigation (GHG: Greenhouse gases).

Figure 8.7 shows how impacts assessment procedures in the past have overlooked numerous uncertainties associated with the various components that enter into such assessment. As seen in this figure, there is a "cascade" or an "explosion" of uncertainty that cannot be ignored at each stage of the impacts (Viner, 2002). There is a range of uncertainty inherent to the processes or paradigms present in each step shown in Figure 8.6; as the assessment moves on to the next step (towards the right), the range of uncertainties are seen to be cumulative because of the lower and upper bounds that are present at each step. Uncertainty thus propagates in this end-to-end investigation, from left to right, to the extent that the conclusions related to the impact itself may have little use, particularly for policy. It needs to be emphasized here that this diagram is for purposes of argumentation, and should not be interpreted in the sense that societal and emission issues are linked to less uncertainty than radiative forcing or climatic response, for example.

More recent approaches that have been adopted for certain types of impacts studies make use of a "what if" approach as opposed to a "cause-to-effect" paradigm. In the former case, the issues that need to be given close consideration include the sensitivity of a given system to a change in its environment, the vulnerability of that system to change, and its capacity for adaptation. *Sensitivity* of a system is an issue that requires adequate knowledge of its current conditions for sustainability, and the range of stresses that it can withstand without significant damage. *Vulnerability* of a system is the extent to which it may be damaged by changing environmental stresses; this may include not only the magnitude but also the rate of change. *Adaptability* of a system describes the degree to which ecological and socio-economic systems may adjust to changes in their environment; in many cases, natural and social systems have the capability to resist the adverse consequences of new climates or to benefit from new opportunities that environmental change may provide.

8.2.2. Impacts on alpine snow cover

Snow is an essential component of earth system physics, both at high altitudes and at high latitudes, and any changes in the amount, duration, and timing of the snow-pack can have long-lasting environmental and economic consequences as numerous authors such as Beniston (2000), Dettinger and Cayan (1995), Haeberli and Beniston (1998), and other have shown.

Snow determines the timing of peak river discharge during the melting of the snow-pack in the spring and, in many instances, maintains river flows

even during warm and dry summer periods. The timing of snow melt is also a major determinant for initiating the vegetation cycle of many alpine plant species, and hence its quantification is necessary when assessing the response of vegetation to climatic change (Keller and Körner, 2003; Myneni et al., 1997; Prock and Körner, 1996). Körner (1994) has shown that for mountain regions, the length of the snow season and minimum temperatures are the most important factors for high alpine vegetation because they determine the growth and survival rates of numerous species at high altitudes. Furthermore, and especially in the Alps, snow is intimately linked to tourism based on winter sports, on which numerous mountain resorts depend for a substantial part of their income (Abegg and Froesch, 1994; Beniston, 2003).

A quantification of the amount of snow in the mountains and the changes that occur with shifts in climate is therefore crucial for assessing the amount of water that will ultimately runoff and be routed into the numerous river systems originating in the Alps in the spring and early summer. The Alps in general and Switzerland in particular, have in the past been referred to as "the water tower of Europe" (Mountain Agenda, 1998). Any substantial changes in the mountain snow pack would have a significant impact on the flow of many major river basins, not only because of changes in the amount and timing of runoff, but also because of the potential for enhanced flooding, erosion, and associated natural hazards. Such issues would in time require new strategies in water resource management as recommended inter alia by the IPCC (2001), particularly in a country like Switzerland that relies on hydro-power for over 60% of its energy supply.

The two principal determinants of snow are temperature and precipitation; as climate changes, subsequently modifying temperature distributions and precipitation patterns so does snow amount and duration. In mountain regions, an average rise of 1°C is accompanied by a general rise of about 150 m in the altitude of the snowline (Haeberli and Beniston, 1998). Regional studies of climatic change in Switzerland (Marinucci et al., 1995; Beniston et al., 1996; Rotach et al., 1997; Maisch, 1998) suggest that Alpine temperatures could rise by as much as 3°C by 2050, with possibly increased precipitation in winter but a substantial decrease in summer. For the Swiss Alps, a warming of this amplitude would push the snowline upward by at least 400 m in winter. This implies that the surface area with a significant winter snow pack could be reduced from an average of 18,000 km^2 currently (Baumgartner and Apfl, 1994) to less than 14,000 km^2 by 2050, i.e., a reduction in snow-covered surfaces of close to 25%. Results from other investigations confirm the high sensitivity of snow pack and duration to

climate variability (e.g., Cayan, 1996) and observed 20th Century warming (e.g., Dettinger and Cayan, 1995).

It therefore seems appropriate, in view of the central role snow plays in many natural and economic systems, to assess the changes that could intervene in the mountain snow-pack in a changing global climate. At present, however, it is difficult to quantify with any precision the possible changes that may intervene in the Alpine snow-pack in coming decades. Orographic precipitation in general, and snowfall in particular, are among the most difficult variables to simulate in climate models, even at the high spatial and temporal resolutions of current regional climate models (Giorgi and Mearns, 1991). Some attempts to address this problem have been undertaken on the basis of statistical downscaling techniques (e.g., Gyalistras et al., 1994; Zorita and von Storch, 1999, for example), with limited results. Snowmelt models have been developed (e.g., Martinec et al., 1983) for use in hydrological runoff modeling systems, and tested in numerous geographical and climatic regions (e.g., Rango, 1992). However, these models have no predictive capability, as they are based on observation and use Geographic Information Systems (GIS) techniques that link snowmelt to runoff.

More recently, Martin et al. (1994) have developed a statistical snow model in a computer-based expert system, and incorporated this to the French general circulation climate model ARPEGE. Interesting results on future snow-pack trends in the French Alps were reported by Martin and Durand (1998). However, this system has a number of limitations in its long-term predictive capabilities, as the authors themselves point out.

The study and prediction of an important component of the natural environment is clearly constrained by the limits imposed by the spatial resolution of current climate models. Observational data can help overcome such problems, by linking changes in snow pack behavior that are systematically related to specific shifts in climatic conditions, e.g., mild and moist winters, cold and dry winters, etc. Satellite remote sensing provides an estimate of the areal cover of snow and its changes over time, as shown for example by Wunderle et al. (2002), Ranzi and Grossi (1999), amongst others. However, satellite observations at the resolution required for studies of snow span only the last 20 years or so. There have been a number of studies that relate snow to climate more at the hemispheric scales (e.g., Frei and Robinson, 1999), or to large areas of North America or Russia (e.g., Brown, 1998; Clark et al., 1999; Hughes and Robinson, 1996; Ye, 2000), than to mountain-specific conditions. Some studies have addressed issues of snow pack at the regional scales (e.g., Beniston, 1997a; Cayan, 1996; Hantel et al., 2000; Harrison, 1993; Whetton et al., 1996), but these investigations

have focused more upon the duration rather than upon the seasonal accumulation of snow during the winter season.

It is unfortunate that the future evolution of a key parameter capable of exerting major controls on numerous of elements of the earth system cannot be accurately predicted for the time being, particularly at the scales required by the climate-impacts community. One possible manner of addressing the issue of snow-pack duration resides in an approach that is based on a statistical and historical analysis of snow in the Swiss Alps. The behavior of snow as a function of temperature, precipitation, and altitude for a number of Swiss climatological sites will be discussed in this chapter, with a view of establishing a temperature-precipitation matrix upon which snow cover is superimposed. It will be seen that this matrix can be applied not only to current but also to future climatic conditions, at the very local scales required for ecological and hydrological impact studies.

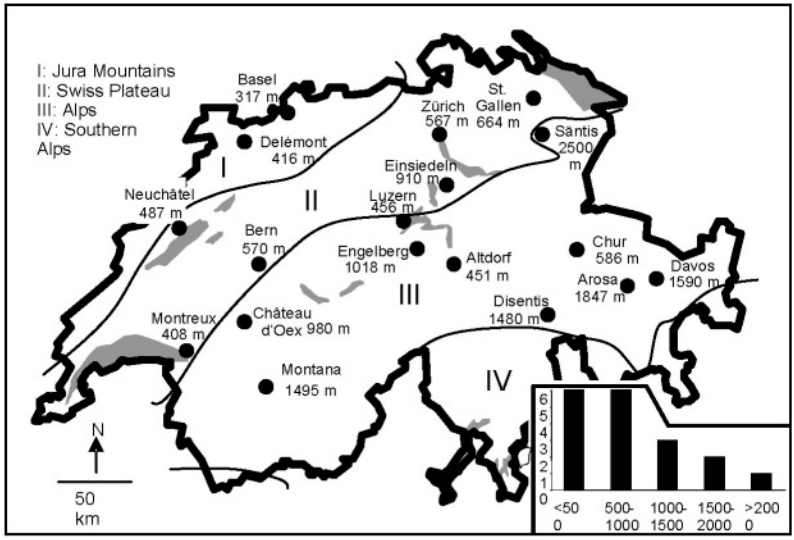

Figure 8.8. Map of Switzerland showing the location of the 18 climatological observing sites used in this study. The inset shows the altitudinal distribution of the 18 sites, for 500 m intervals ranging from 500 to 2,500 m above sea-level.

Human perception of climatic events such as the frequency of "white Christmas" or the fact that "in the past, snow was more abundant than today" are biased by a relatively short collective memory. In addition, it is often the case that one particularly notable event (e.g., a severe snowstorm or an unusual accumulation of snow) triggers the perception that these events are

the norm. Another popular belief is that there has been a shift in the seasonality of snow in the Alps, with the season beginning later in the year, but also ending later in the spring. A genuine shift in the timing of the snow season or a decrease in the quantity of snow would indeed have significant repercussions upon many natural and socio-economic systems. Indeed, if the general perception of stakeholders is based on misconceptions rather than on facts, then certain long-term economic or policy decisions (for example, regarding investments for ski-lift infrastructure) may be taken in an inappropriate manner.

Data from 18 separate sites has been used to investigate snow amount and duration in the Alps under current climatic conditions and are identified in Figure 8.8.

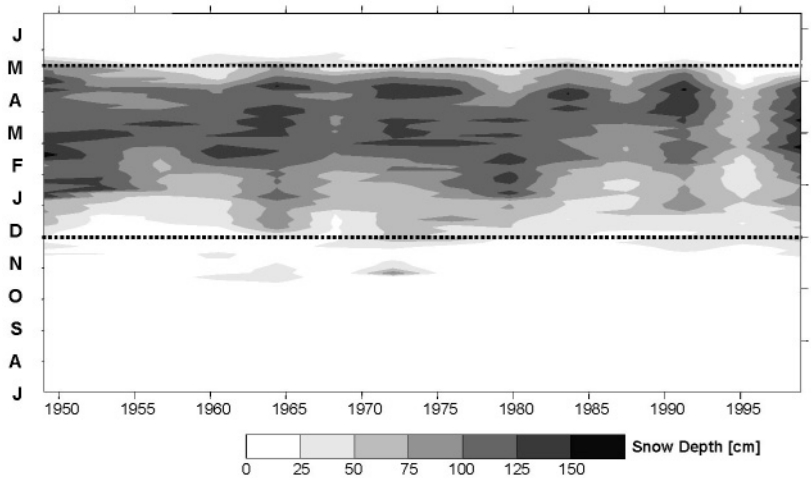

Figure 8.9. Hövmöller-type diagram illustrating the seasonal distribution of snow amount in Arosa (1,846 m above sea level) from 1949-2000. The diagram allows a monthly representation of the quantities of snow over a long time-period.

An example of the distribution of snow amount on a seasonal basis is given for the site of Arosa in Figure 8.9, which uses a Hövmoller type rendering. The large variations in snow amount and duration exhibited in the diagram have been shown by Beniston (1997a) to be closely linked to the behavior of the North Atlantic Oscillation (NAO). During strongly-positive phases of the NAO, the presence of persistent high pressure fields over the Alpine region from late fall well into the winter are accompanied by large positive temperature anomalies and low precipitation, both of which are unfavorable for seasonal snow accumulation. This implies that large-scale

forcing, rather than just local or regional factors, plays a dominant role in controlling the timing and amount of snow in the Alps, as evidenced by the fluctuations illustrated in Figure 8.9 Since the mid-1980s and up till today, the length of the snow season and the snow amount, based on a 20-cm threshold, have been reduced by 2-3 weeks as a result of unusually high and persistent pressure over the Alps. This situation is associated with the highest positive anomalies of the NAO index recorded during the 20th century. Part of the reduction in snow amount and duration is, in addition, the result of the significant warming that has taken place in the 1990s, as will be shown later. Figure 2 also shows that on the whole, however, the snow season in Arosa begins essentially towards the end of November and ends towards mid-May, even if the end of the season has been earlier in recent years. This relative constancy of the beginning and end of the season in Arosa, within ± 2 weeks is principally linked to the cycle of direct solar energy; in late April and early May, solar energy is close to its annual peak and becomes the dominant factor in the snowmelt process.

This particular site does not exhibit any significant shift in the snow season, as frequently perceived by the general public. The snow season at similar altitudes remains constrained principally between the limits highlighted by the dotted lines on the diagram. The quantities of snow, on the other hand, can and do vary widely from one year to another, as a result of shifts in precipitation patterns and distribution that can be partially attributed to the behavior of the NAO.

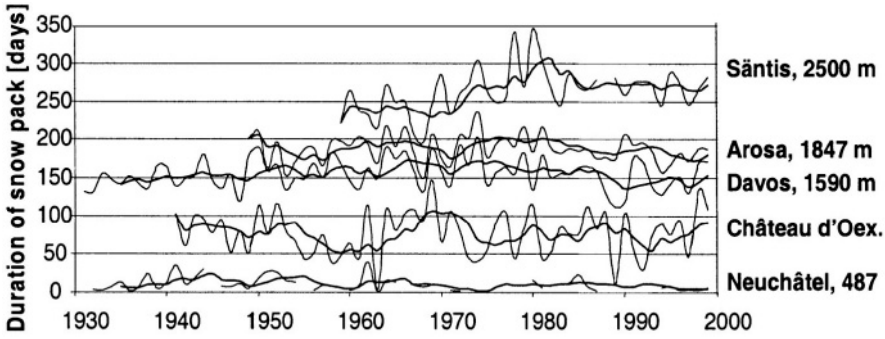

Figure 8.10. Time series of the duration of the snow season for a number of Swiss observing sites located at different altitudes, for a threshold of snow depth of 10 cm or more. Bold lines are smoothed series where a five-year filter has been applied.

A closer investigation for a number of stations confirms the fact that the length of the snow season has tended to decrease at many locations since the

early 1970s, as seen in Figure 8.10. However, the duration of continuous snow cover exceeding 10 cm exhibits high interannual variability; for example, at Château d'Oex in the western part of the Swiss Alps, snow cover with at least a 10-cm snow-pack ranges from 10 days in 1961/62 to 110 days the following year. Davos, on the other hand, exhibits generally the same duration of the snow season towards the end of the 20th century as in the 1930s. One notable exception to the tendency towards a reduction in the length of the snow season is the high-altitude site of Säntis, in the north-eastern Swiss Alps, where snow has on average increased since the 1960s. As will be discussed later, the trends illustrated in Figure 8.10 are consistent with the tendency towards an increase of solid precipitation at high elevations, and an increase in liquid precipitation at low to medium elevations, as suggested by a number of studies related to global warming (Beniston et al., 1996; Martin and Durand, 1998; Parry, 2000). The altitudinal dependency of snow duration is also highlighted in this figure, and so is the synchronism of major events between the different stations, such as the lack of snow in 1961/62 or the peak snow amounts in 1968/69 and 1998/99. In other instances, however, the curves are out of phase, particularly between the lower-elevation sites and the set of three higher-elevation stations. This is a reflection of the fact that in some years, a certain proportion of precipitation falls as snow in Davos and Säntis, and as rain at lower elevations such as Château d'Oex. When taking long-term average values, however, there is a strong linear relation between snow duration and height for the 18 selected Swiss sites, as seen in Figure 8.11 (the correlation coefficient, r=0.97). The fact that most stations lie very close to the regression line, including the Säntis site that is subject to strong winds and interference by buildings close to the summit, give added confidence that the data used here is of sufficient quality and representativity.

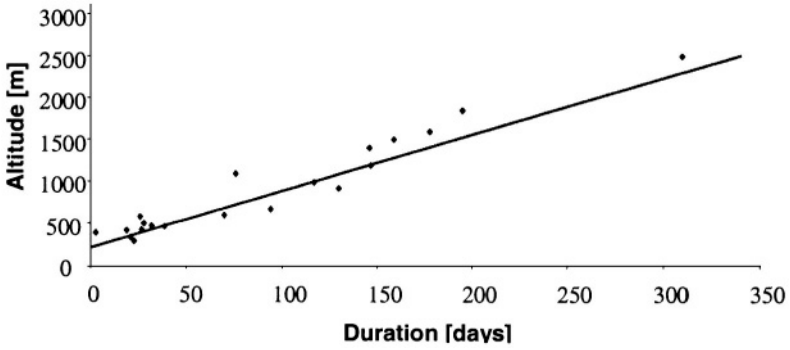

Figure 8.11. Relationship between mean (i.e., 30-year average of the 1961-1990 period) snow-cover duration and height for the observing sites considered.

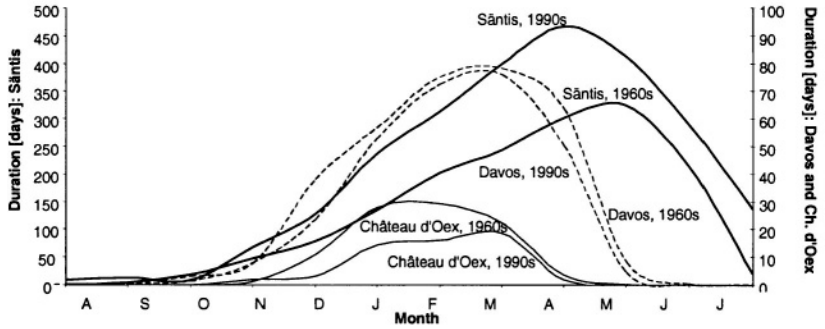

Figure 8.12. Seasonal evolution of snow cover at Château d'Oex (980 m above sea level), Davos (1,590 m) and Säntis (2,500 m) averaged for the decade of the 1960s and that of the 1990s. The left-hand ordinate is scaled for Säntis, while the right-hand ordinate is scaled for Château d'Oex and Davos (a factor of 5 between the two sets of scales), in order to increase the resolution of the latter two curves.

Figure 8.12 provides additional information on the seasonal evolution of the snow-pack at three sites (Château d'Oex, Davos, and Säntis), averaged over the 1960s and the 1990s. It is observed that at the lower elevation site of Château d'Oex, the snow depth is reduced by 45% between the 1960s and the 1990s, based on the figures for total seasonal snow accumulation. Much of the shortfall in snow amount occurs in the early part of the season, where snow does not accumulate as in earlier years as a result of warmer temperatures and the fact that when precipitation falls, it is more often in the form of rain than snow in the early winter. The snow season in Château d'Oex begins later and ends marginally earlier in the 1990s than in the 1960s. Over this same 30-year interval, Davos experiences a reduction of average total accumulation from 330 cm to 288 cm, i.e., a loss of about 12% of snow depth. The beginning and end of the snow season at Davos are essentially the same in both periods, as already mentioned. At the high-elevation site of Säntis, however, the trend is reversed, both in terms of snow amount and duration of the snow-pack. Total accumulation over the season has increased from an average decadal-scale value of 1590 cm in the 1960s to over 2475 cm in the 1990s, i.e., an enhancement of snow depth of 35%.

In parallel, winter minimum temperatures (the average temperature for December, January, and February, or DJF) have increased significantly over this period, and in particular DJF temperature minima, which are an important determinant on snow amount and duration. On a century-scale basis, based on simple linear regression analysis, the warming rates are all significant and range from 1.8°C/century in Neuchâtel to 3.7°C/century at the summit of Säntis. Since the late 1980s, minimum temperatures have

systematically remained above their long-term mean values at all stations. The general rise of winter minimum temperatures began in the early to mid-1960s at all sites, and underwent a cooling in the early to mid-1980s before warming rapidly since, as seen in Figure 7.1 of the previous chapter. In the case of Säntis, however, DJF minima entered the positive anomaly range in the early 1970s and have never reverted to cooler-than-average conditions since, even though there is a relative cooling as at the other sites in the 1980s. The strong trends in minimum temperatures have been reported in the literature, notably by Karl et al. (1993) for Northern Hemisphere observations, and by Jungo and Beniston (2001) for Switzerland. Furthermore, the increasing temperature trends with height were first reported by Beniston and Rebetez (1996) and later confirmed through modeling studies by Giorgi et al. (1997).

The DJF precipitation anomalies, on the other hand, exhibit much more statistical noise than the corresponding minimum temperature anomalies (not shown here). By far the most outstanding increase and overall positive winter precipitation anomaly, with respect to the 1961-1990 reference period, is to be found at Säntis, with a century-scale increase of 3.3 mm/day; this is close to a doubling of precipitation during the 20th century. Since the mid-1980s, the precipitation anomalies have been consistently positive. Other sites do not exhibit any particularly significant trends; some show an overall decrease, especially in the 1990s, others a modest rise that may be due more to the fluctuating nature of the signal rather than to any significant trend. Although the rise in temperature and precipitation are both most pronounced at Säntis, it is difficult to affirm that this combined increase is indeed related to the observed 20th century warming and a consequent enhancement of the hydrological cycle. However, this considerable increase of high-elevation precipitation in an environment where temperatures remain below the freezing point (despite the general rise in temperature since the 1960s), explains much of the change in the snow-pack statistics at Säntis seen in Figure 8.12 compared to lower elevations. At the lower-level sites, warmer conditions have substantially reduced the number of days with minima below the freezing point.

In order to investigate more closely the behavior of snow in terms of different mean winter conditions, the 5 ("cold"), 50 ("average") and 95 ("mild") percentiles of the DJF minimum temperature distributions have been selected. Figure 8.13 shows the manner in which precipitation changes with height according to cold, average, or mild winters. The general increase with height is seen in all three sets of data, but the precipitation-height gradient is considerably enhanced when progressing from cold to mild winters. This implies that precipitation is more abundant during warm

winters than during average or cold winters, and furthermore, that the precipitation excess increases with height. For example, at an altitude of 1,000 m, average daily winter precipitation ranges from 1.5 mm/day during cold conditions to 4.5 mm/day during warm conditions, i.e., an average range of 3 mm/day. At 2,500 m, the respective amounts are 4.5 and 11.0 mm/day, i.e., an average range of 6.5 mm/day.

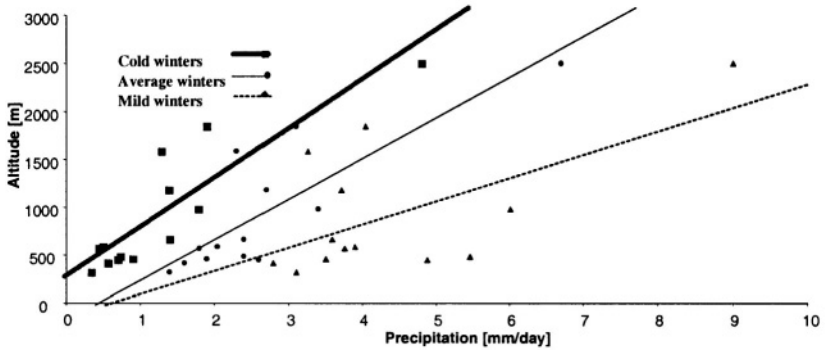

Figure 8.13. Precipitation changes with height for "cold" (5% quantile in terms of temperature), "average" (50% quantile) and "mild" (95% quantile) winters.

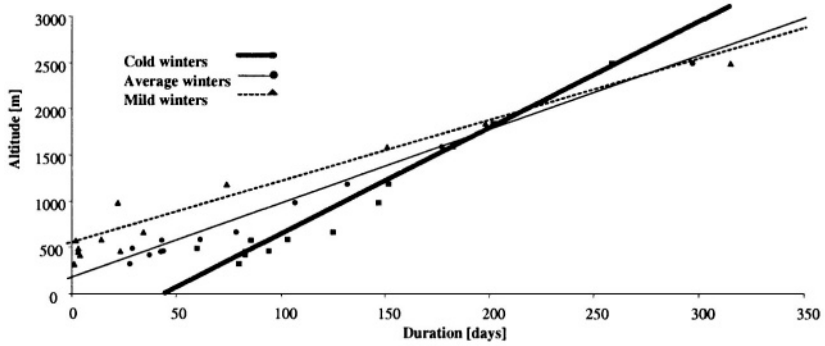

Figure 8.14. Snow cover duration changes with height for "cold" (5% quantile in terms of temperature), "average" (50% quantile) and "mild" (95% quantile) winters.

These changing characteristics of precipitation have obvious repercussions on the amount and duration of snow in the Alps. Using the same definitions for cold, average, and mild winters, Figure 8.14 illustrates the manner in which snow duration changes with height as a function of the type of winter. At low to medium elevations, below about 1,500 m above sea level, mild winters are accompanied by reduced snow amounts and duration,

while the reverse is true for cold winters, because of the transition from liquid to solid precipitation at these altitudes. However, at elevations above 2,000 m, the more abundant precipitation associated with mild winter conditions falls as snow and in much larger amounts than during cold winters. At an altitude of 1,000 m, there is are on average about 135 days with continuous snow cover during cold winters, but only 65 during mild winters. The respective figures at 2,500 m altitude are 250 and 350 days.

The results discussed here can be used as an analogy to what may happen in a warmer climate. The statistics lend some credence to speculation that warmer conditions in the Alps, associated with enhanced precipitation, are likely to lead to more abundant snowfall in the higher reaches of the mountains, but much reduced snow at lower levels where precipitation is more likely to fall in the form of rain. From the statistics outlined in previous paragraphs, the "crossover" level where snow becomes more abundant under milder conditions is located between 1,700 and 2,000 m above sea level. This result is closely related to a previous study by Beniston (1997a), where it was seen that above about 1,700 m in the Swiss Alps, there has been little significant change in snow variability, i.e., whether under warm or cold winter conditions, there is always snow on the ground throughout the winter season, whatever the depth of the snow-pack.

The relationship between mean winter minimum temperature, precipitation, and snow duration can be graphically summarized, for all the climatological sites studied, in the two-dimensional plot given in Figure 8.15, where the abscissa is the DJF mean minimum temperature and the ordinate DJF mean daily precipitation. The 2-D surfaces represent the snow-cover duration, with a contour interval of 25 days. Figure 8.15 suggests a dominant influence of temperature on snow duration, with small shifts in mean winter temperature leading to substantial changes in the length of the season. There is also a secondary influence of precipitation amount on snow duration, where for a given temperature, snow duration changes according to the amount of precipitation.

For a given winter mode (i.e., "cold", "average", or "mild"), any displacement within the contour surfaces is associated with altitudinal shifts, i.e., moving up or down the temperature scale is essentially analogous to moving up or down height levels in the mountains. On the other hand, displacement within these surfaces can also be related to warmer or cooler, wetter or drier climatic conditions.

As a result, this type of diagram can be used empirically to estimate, for a particular site, the changes in snow duration that may occur under shifting climatic conditions. As an example, the high-altitude Säntis site (2,500 m above sea level) is characterized in this diagram by a long-term mean DJF

minimum temperature of –7.1°C and precipitation of 6.3 mm/day, with a corresponding average snow-cover duration of close to 300 days. A rise of mean winter minima of 2°C with no change in precipitation would lead to a 50-day reduction of the snow season (250 days in total at –5°C).

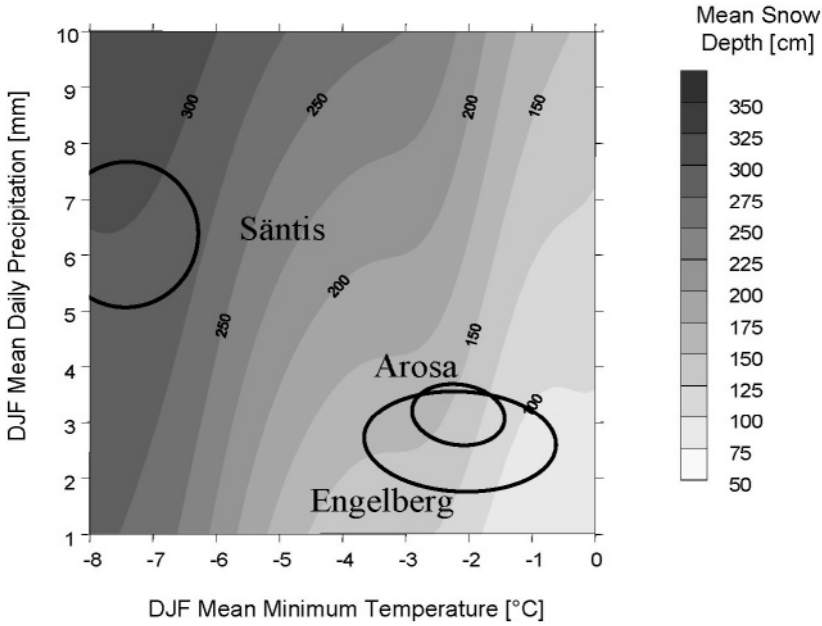

Figure 8.15. 2-D contour surfaces of snow-cover duration as a function of winter (DJF) minimum temperature and precipitation for all selected climatological sites; ellipses show the 2σ range of DJF minimum temperature and precipitation, and corresponding spread of snow-cover duration for Engelberg, Arosa, and Säntis. The slopes of the ellipses depend on the covariance of temperature and precipitation.

With such a rate of warming, precipitation would need to increase from the current average of 6.8 mm/day to over 10 mm/day, i.e., an increase of almost 50%, in order to maintain the current number of days with continuous snow cover. Such an increase is plausible, as seen in the previous discussion pertaining to precipitation/height relationships under differing winter conditions; furthermore, certain climate model results (e.g., Rotach et al., 1997) for the Alpine region suggest a significant rise in winter precipitation. At lower elevations, such as Arosa (about 700 m lower in elevation than Säntis), long-term DJF minimum temperature is –2.2°C and precipitation is 3.1 mm/day, with a corresponding 140 days of continuous snow cover. A rise in temperature of 2°C without any precipitation change would result in a reduction in seasonal snow cover down to about 90 days in total. A 50%

increase in precipitation with the same 2°C increase would to some extent compensate for the temperature rise; in this case, winter snow-pack duration in Arosa would be roughly 110 days.

The empirical analysis outlined here has been constructed on the basis of the long-term averages of the variables considered, and focuses on a number of sites that span a significant altitudinal range. This approach was already suggested by Whetton et al. (1992), but for a single site in Australia; the advantage of the present study is that the snow-duration statistics could have a much wider range of applicability.

The ellipses in Figure 8.15 show the spread of temperature and precipitation on the basis of their 2σ (standard deviation) levels around the mean value, located at the center of the ellipse. The inclination of the ellipses are functions of the covariance between temperature and precipitation. It is seen that at Engelberg, for example, snow duration currently ranges from 80 days to 160 days with a 2σ temperature spread of almost 3°C. The current 2σ range of precipitation, from 2.1 to 3.8 mm/day does not exert such a strong influence on the duration of snow-cover; for example, this increases from 120 to 130 days if the mean minimum DJF temperature is held constant at -2°C.

Figure 8.15 thus emphasizes an additional problem related to estimating changes in snow cover duration under changing climatic conditions, namely the fact that already under current climatic conditions, the year-to-year variability of the snow-pack is extremely high. The contour surfaces provided in the figure may certainly be of value in estimating changes in average snow duration as a function of shifts in winter temperature and precipitation. However, it would also be important to assess the possible future changes in the extreme range of snow duration, represented by the ellipses of Figure 8.15. In order to make the best possible use of these diagrams, information from regional climate models would thus need to include not only the average changes of temperature and precipitation with height, thereby allowing to use the 2-D plots to estimate decreases or increases in snow-cover duration at particular heights or locations, but also the statistical spread of temperature and precipitation in a changing climate.

The physical processes governing the state of a snow pack and its evolution are well described using equations that describe the exchange of energy and water between the land surface and the atmosphere (Coughlan and Running, 1997; Gustafsson et al. 2001). The energy aspects associated with snow melt processes require an accurate treatment of the thermodynamics of the snow pack. Such processes, expressed in terms of water and energy budgets are computed in a physically-based surface energy balance model (SEBM) called GRENBLS (GRound ENergy Balance for

naturaL Surfaces). A description of the model equations, and their application to alpine snow cover was first presented by Keller and Goyette (2003), with examples of simulations at specific alpine locations also in Beniston et al. (2004).

GRENBLS has shown genuine skill in reproducing the observed snow pack characteristics in the Swiss Alps, such as depth and duration. GRENBLS is a semi-prognostic numerical model driven by hourly input data of screen-level (2 m) air and dew-point temperatures, anemometer-level wind velocity, liquid-water equivalent precipitation flux, and surface pressure. The model computes the solar and infrared radiative fluxes, although incoming solar radiation may also be prescribed from observations, the turbulent sensible and latent heat fluxes, as well as the heat flux within the snow pack and its underlying surface. The precipitation determines the amount of snow that falls whenever the air temperature is below freezing. Snow is modeled as an evolving one-layer pack characterized by a particular temperature, mass, and density. The snow temperature is computed in a prognostic manner from the energy balance of the pack. Total runoff is the result of bottom drainage and soil saturation. The former is generated when the soil moisture exceeds the field capacity and the later is related to the level of soil moisture saturation. The melting snow directly enters the underlying surface and thus contributes to the soil moisture budgets.

Beniston et al. (2003) have shown that, according to the type of winter, the response of snow in terms of the duration of the season varies considerably with altitude. Wunderle et al. (2002) have quantified, on the basis of satellite imagery analyses, that the elevation of the snow-line below 2500-3000 m asl varies substantially according to the type of winter. Martin and Durand (1998) were also able to ascertain through modeling techniques that changes in snow duration in the French Alps are very sensitive to temperature at low to medium elevations (below 2000 m asl), whereas at much higher elevations (above 3000 m, for example), there is almost no change under warmer conditions. This is basically due to the fact that at high altitudes, warmer conditions will not raise temperatures beyond the freezing point, so that the controlling factor on snow amount and duration is not temperature but rather the quantities of precipitation that occur during the winter season.

In order to emphasize this point, Figure 8.16 illustrates the observed behavior of a modest snow pack in the Swiss Alps for a low-elevation station (Château d'Oex, at 981 m asl) and a more extensive snow pack at a higher-elevation station (Arosa, at 1847 m asl). Although lower elevations than Château d'Oex could have been selected, it is interesting here to analyze the behavior of snow that has a truly seasonal, continuous character rather than

an episodic character that is typically found at sites such as Bern (570 m) or Basel (317 m). At these low levels, snow will appear or disappear intermittently according to cold or warm cycles associated with frontal systems affecting the Alps during the winter.

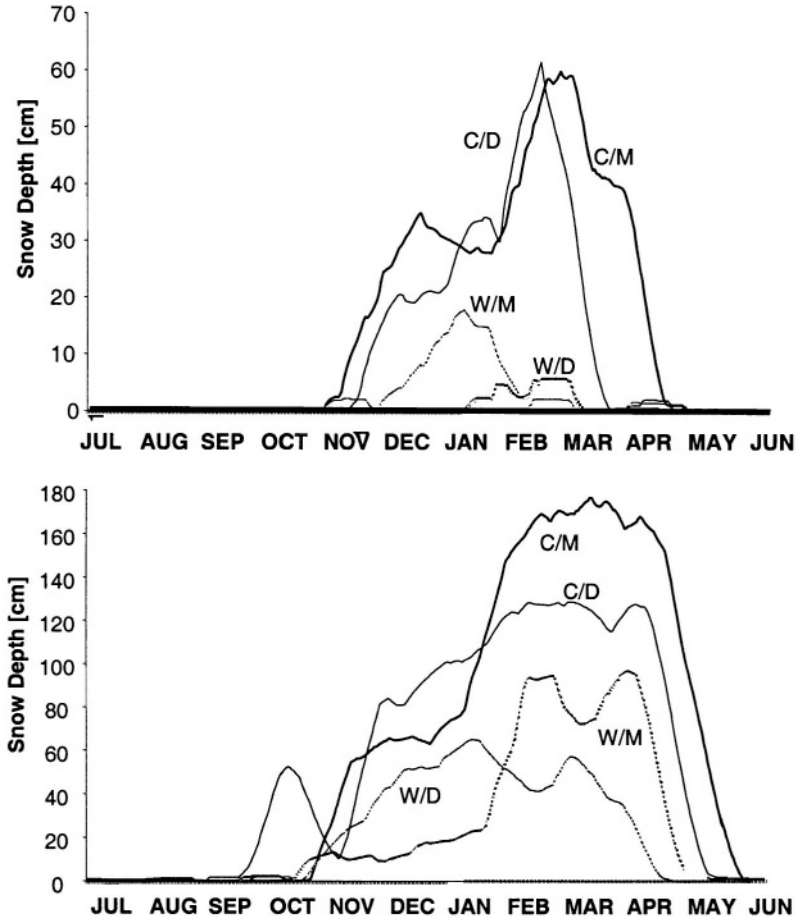

Figure 8.16. Seasonal snow accumulation curves at Château d'Oex (981 m asl; upper) for four different winter modes (C/D: cold/dry; C/M: cold/moist; W/D: warm/dry; W/M: warm/moist) and for Arosa (1847 m asl; lower). Note the difference in scale for the ordinates in the two figures.

The present study focuses on four climatic winter modes, namely cold/dry, cold/moist, warm/dry, and warm/moist. The selection of these modes is based on a combination of winters that are below the lower quartile (i.e., 25% quantile) or above the upper quartile (i.e., 75% quantile) of mean

winter precipitation and temperature. The use of quartiles rather than finer percentiles allows capturing the four basic modes more readily. Here, winter refers to the mean of the three months of December, January, and February (DJF); it was shown in Beniston et al. (2003) that the DJF average minimum temperatures and precipitation provide a reasonable measure of the seasonal snow behavior, and are well correlated with duration and accumulation of snow even if the snow season at high elevations lasts longer than just the three months of winter. All curves have been smoothed to remove the noisiness of day-to-day variability in snow cover. Total (also referred to as seasonal) snow accumulation, as discussed below, is defined as the integral of daily snowfall amounts during the winter; this estimate does not take into consideration morphological transformations of the snow resulting from ambient temperature and moisture conditions during the season. The curves provided here are thus somewhat different from those that would be obtained from simply integrating daily snow accumulations, but nevertheless provide a basis for the subsequent discussion.

It is seen that the greatest snow abundance occurs for cold/moist winters at both sites, while the least abundance is associated with warm winters in Arosa, as could be expected intuitively. Warm and moist winters at Château d'Oex are frequently associated with DJF precipitation in the form of rain, so that the extent of the winter snow pack is rapidly reduced through surface runoff. At higher elevations, on the other hand, the warm-moist winter mode leads to greater total snow accumulation than the warm-dry mode, but does not offset the negative influence of the higher temperatures compared to cold winters. It can also be seen that the duration of the snow season is strongly modulated by the various combinations of temperature and precipitation, the longest being related to the cold-moist winter mode, the shortest to the warm modes (dry at high elevations and moist at low elevations). Although there is much variability in the behavior of the snow pack, in the sense that similar winters modes may exhibit different responses in the shape of the snow total snow accumulation curves, the general pattern discussed here is nevertheless confirmed for most stations.

In a climate that is changing as a result of enhanced greenhouse gas concentrations, the separation into different winter modes can be used as an indication of the type of snow cover that could be expected in the future, by analogy with current conditions. Table 1 lists typical statistics of DJF mean temperature and precipitation associated with each mode for the two stations illustrated in Figure 8.16.

Winter mode	Average DJF temperature (°C)	Average DJF precipitation (mm/day)	Duration of snow pack (days)	Seasonal snow accumulation (cm)
Château d'Oex				
C/D	-3.8	2.5	125	322
C/M	-3.8	4.3	155	520
W/D	0.5	2.4	67	138
W/M	1.0	4.8	22	94
Arosa				
C/D	-6.4	1.9	215	959
C/M	-6.4	3.3	237	1150
W/D	-1.3	2.1	183	562
W/M	-0.7	3.8	198	552

Table 1. Statistics of snow duration and total snow accumulation in the winter season for the four winter modes, namely cold/dry (C/D), cold/moist (C/M), warm/dry (W/D), and warm/moist (C/M).

A rise in temperature of over 5°C at Arosa and a 40% reduction in precipitation, i.e., a switch from the cold/moist to the warm/dry modes, leads to a reduction of 54 days in snow cover and almost a 50% reduction in the seasonal snow accumulation. For an equivalent rise in temperature and reduction in precipitation at the lower site of Château d'Oex, there is a reduction of over 100 days of snow cover, from 125 days to 22 days, and an 80% reduction in snow cover. As can be expected intuitively, the characteristics of the snow pack are substantially more sensitive to changing temperature and precipitation patterns at low elevations as compared to those at higher elevations.

Figure 8.17 shows the relation that exists between average snow total seasonal accumulation and average snow duration as a function of height for the 18 sites; the curves illustrated here can be considered to be representative of the alpine domain of Switzerland. The data for wetter-than-average and drier-than-average winters have been disaggregated, thus also allowing the diagram to be interpreted in terms of the sensitivity of snow duration and total accumulation to precipitation amounts. The correlation coefficient for the regression lines is high, on the order of 0.96 for both curves. The non-linear nature of the best-fit curves reflects the fact that there is a non-linear

increase in seasonal snow accumulation for a linear increase in snow duration. For example, in the case of wetter-than-average winters, an increase in snow duration by 60 days, from 30 to 90 days is accompanied on average by a rise in snow accumulation of 225 cm, from 50 – 275 cm. The same increase of 60 days, but from 240 to 300 days, results in an average additional accumulation of 315 cm, from 960 – 1275 cm. The duration/accumulation relationship can also be viewed in terms of altitude, since the level at which snow falls in the mountains is the major determining factor for the subsequent behavior of the snow pack.

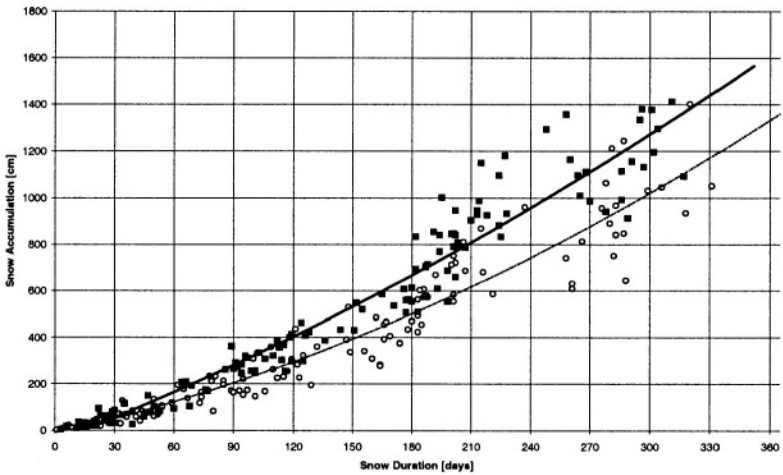

Figure 8.17. Relation between snow duration and total seasonal snow accumulation for wetter-than-average (closed squares) and drier-than-average (open circles) winters. Bold and dashed lines represent the regression curves for both sets of data, respectively.

This type of analysis enables the possibility of assessing the average quantities of snow that accumulate at different altitudes in the Alps as a function of shifting climatic conditions. While the following is based on average quantities of snow at various elevations in the mountains, and does not enter into any particular detail on local site characteristics (south- or north-facing slopes, for example), the results yield interesting estimates that are not far removed from observed snow amounts.

In order to compute snow volume, which is a key snow-related variable for assessing peak flow from snow-melt in river systems originating in the Alps, it is necessary to know the surface area of Switzerland that is associated with a particular height class. Dividing Swiss topography into 44 intervals of 100 m each, it is seen that 55% of the country is located above

the 1000 m level, 24% above 2000 m, and 2.5% above 3000 m. Using the current values of average snow-cover duration, which as shown in Beniston et al. (2003) are a linear function of altitude, it is thus possible to assign the average volume of seasonal snow accumulation for each 100-m interval, using the information provided in Figure 8.17 for both dry and moist winter modes.

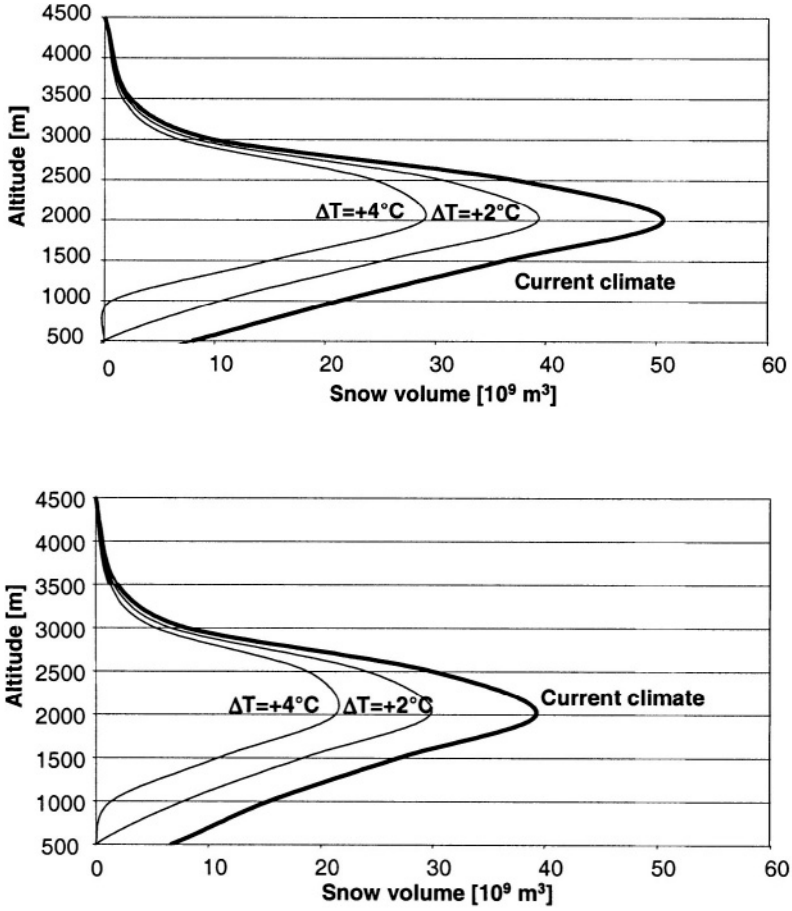

Figure 8.18. Altitudinal distribution of maximum snow volume for wetter-than-average winters (upper) and drier-than-average winters (lower), under current climatic conditions (bold line), and for warming scenarios of 2°C and 4°C, respectively.

This yields the bold curves of Figure 8.18. The shape of the curve reaches a maximum at about 2000 m asl, and represents the combination of snow

depth and surface area that yields the greatest volume of snow. Below that level, even though the surface area considered is greater, the amount of snow that accumulates during the season is much less, and thus the snow pack volume is reduced. Conversely, above 2000 m, even if the total snow accumulation is much greater, the volume is lower because deep snow accumulates on increasingly smaller surface areas. The other curves in Figure 8.18 for snow volume in a warmer climate will be revisited later in this chapter.

With the available empirical approaches that have been developed here, it is possible to estimate the mean changes in snow volume that may intervene with a mean rise in temperature. As was seen in Beniston et al. (2003), changes in snow duration are associated with combinations of shifts in temperature and precipitation (Figure 8.15). Preliminary findings from the analysis of the HIRHAM4 Regional Climate Model (RCM; Christensen et al., 1998) simulation results used in the context of the EU 5th Framework Program "PRUDENCE" project (Christensen et al., 2002) introduced in Chapter 6 suggest that mean minimum winter temperatures will rise in response to greenhouse forcing by up to 4°C and more in the Swiss Alps by the end of the 21st century.

The shifts in temperature and precipitation for Switzerland, averaged over the decades 2071-2080, 2081-2090, and 2091-2100 are given in Table 2. The HIRHAM4 simulations are of course one possible future course of climate, and cannot be considered to be a prediction; the model results do provide, however, a plausible set of scenarios upon which impacts analyses can be constructed.

Period	Average DJF Tmin change (°C)	Average DJF precipitation change (mm/day)
2071-2080	3.6	1.1
2081-2090	4.2	0.9
2091-2100	4.6	1.0
2071-2100	4.1	1.0

Table 2. Average decadal change in winter (DJF averages) temperature and precipitation in the alpine domain in a future climate compared to the 1961-1990 mean climate, based on Regional Climate Model simulations by the HIRHAM model. The 30-year average change is also indicated in the last line of the table.

Superimposing the future climate data in the temperature-precipitation space shows that the expected winter minimum temperature warming of over 4°C by the end of the 21st century is likely to lead to a reduction in snow duration by more than 100 days at both Säntis and at Arosa, the two sites that were used in Beniston et al. (2003). The increase in winter precipitation that intervenes during this period only slightly modulates the dominant effect of the +4°C warming, as seen in Figure 8.19. This figure is an extension of Figure 8.15 applied to current climatic conditions. The "migration" of the Arosa and Säntis statistics can be considered to be highly significant, because the location of snow duration in the temperature-precipitation space, under future climatic conditions, is well outside the range of natural variability of current snow duration.

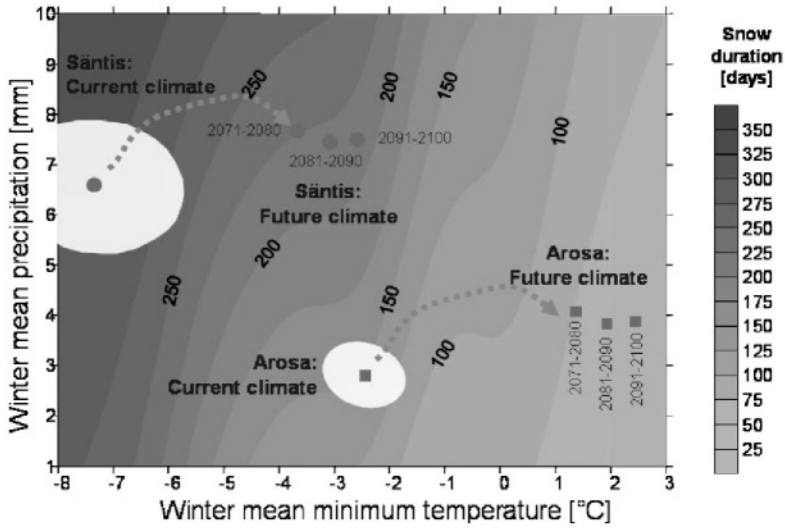

Figure 8.19. 2-D contour surfaces of snow-cover duration as a function of winter (DJF) minimum temperature and precipitation, based on the data extracted from all climatological sites used in this study. Superimposed on this figure is the temperature-precipitation-snow duration data for the Arosa and Säntis sites, for current climatic conditions, and for the three last decades of the 21st century (see text for details). The ellipses show the 2σ range of DJF minimum temperature and precipitation, and corresponding spread of snow-cover duration for Arosa, and Säntis. The orientation of the ellipses is related to the covariance of temperature and precipitation. The figures on the isolines identify the length of the snow season.

On the basis of shifts in snow duration, estimated from the chart in Figure 8.19 and using the snow depth/snow duration relationship illustrated in Figure 8.17, it is possible to generate snow-volume curves for two scenarios of 2°C and 4°C warming of winter minimum temperatures, for drier-than-

average and moister-than-average conditions (Beniston et al., 2004). As shown in Figure 8.18, the overall volume of snow under warmer conditions is significantly less than under current climate, irrespective of the winter precipitation context.

The maximum volume of snow remains in all cases at 2000 m, but the reduction in volume corresponds to at least 10% per degree Celsius of warming. At the 1000 m level, the reduction in snow volume for the wetter-than-average winter season is 50% for a 2°C average winter minimum temperature rise, and over 95% for an average 4°C rise in DJF minimum temperatures, whereas at 4000 m, the respective volume changes are 8% and 14%. In other words, strong warming at low elevations will lead to the removal of almost all the snow pack, while the change at very high elevations will be small. This is mainly because even in a warmer world, temperatures at height will remain cold enough to sustain snow for much of the year. Similar conclusions can be reached for the drier-than-average winters (Figure 8.18, lower), where it needs to be emphasized that for current climate, the volume of snow is reduced by 20% or more compared to wetter-than-average winters. At all elevations, the sensitivity to warming is somewhat greater than in the case of wetter-than-average winters. This is because there is less precipitation during dry winters that can compensate for the warming effect on total snow accumulation. Hence, at 2000 m, for example, a 2°C warming is accompanied by a 40% reduction in snow volume, while a 4°C warming drives a 60% reduction (compared to 20% and 40%, respectively, for moist winters).

8.2.3. Impacts on alpine glaciers

The volume of ice in a glacier, and correspondingly its surface area, thickness, and length, is determined by the balance between inputs (accumulation of snow and ice) and outputs (melting and calving). As climate changes, this balance may be altered, thereby modifying the equilibrium line altitude of the glacier (the altitude at which accumulation and ablation are in equilibrium) and resulting in a change in thickness and the advance or retreat of the glacier. Most of the alpine glaciers with the exception of those at very high altitudes (above 3,500-4,000 m above sea level) have surface and internal temperatures very close to the freezing point, so that any small rise in temperatures beyond the 0°C threshold can result in a very sharp response of the glaciers.

Since 1850 the glaciers of the European Alps have lost about 30 to 40% of their surface area and about half of their volume (Haeberli and Beniston,

1998), a feature that has been observed in numerous other mountain glaciers of the world, both in the mid-latitudes and in the tropics as discussed in Chapter 4 that serves to emphasize the truly global nature of climatic warming to be ascertained. Figure 8.20 provides a dramatic view of the change in morphology in the Glacier du Trient, a medium-sized glacier in the Swiss sector of the Mt Blanc range in south-western Switzerland that has retreated by 500 m in a 15-year period from 1988-2003, at a time when the rate of temperature increase has been the most rapid of the past 150 years.

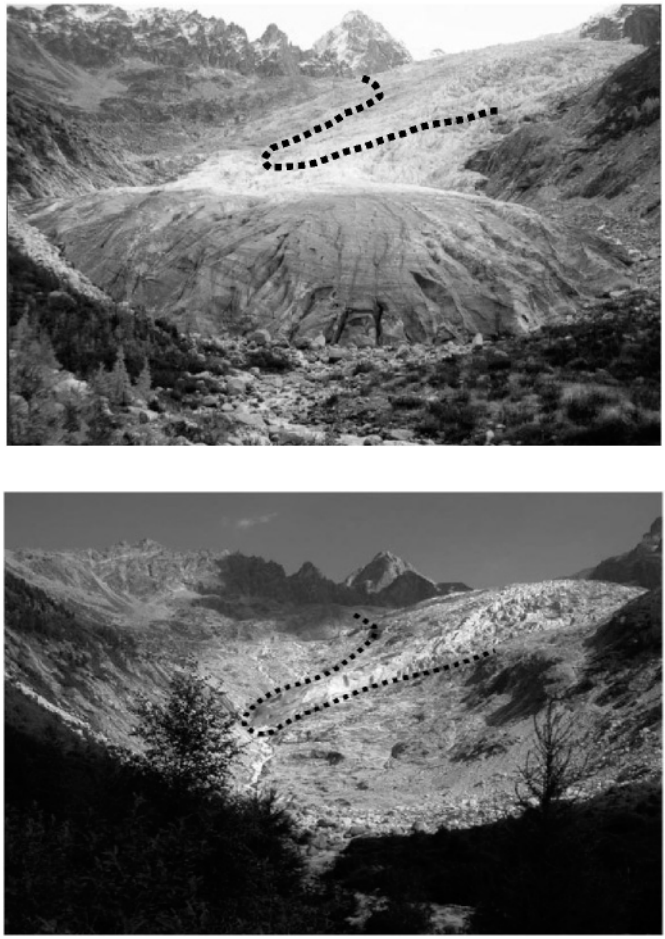

Figure 8.20. Views of the Trient Glacier in the Swiss sector of the Mt Blanc range, in 1988 (upper) and 2003 (lower). Dotted line shows the position of the glacier front in 2003 in a picture taken from roughly the same location as the 1988 view, where the glacier front filled the bottom of the valley 500 m ahead of its 2003 position.

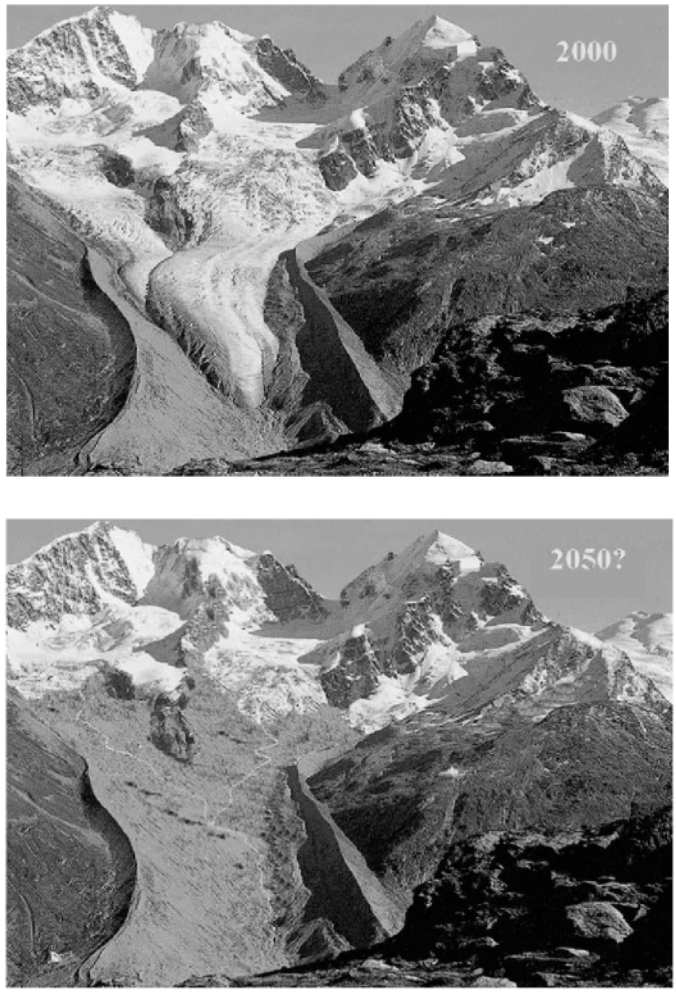

Figure 8.21. Views of the Tschierva Glacier (Bernina Range, south-eastern Switzerland) in 2000 and as it may appear in 2050 following a 3°C average warming (Courtesy: Max Maisch, University of Zürich, Switzerland).

Empirical and energy-balance models indicate that 30 – 50% of existing mountain glacier mass could disappear by 2100 if global warming scenarios in the range of 2-4°C occur (Fitzharris et al. 1996; Haeberli, 1995; Haeberli and Beniston, 1998; Kuhn, 1993). The smaller the glacier, the faster it will respond to changes in climate. For most mountain glaciers in the temperate parts of the world, there exists a close linear relationship between the

equilibrium line altitude of the glacier and the precipitation and temperature controls on glacier mass. Funk (2003; Swiss Federal Institute of Technology, personal communication) estimates that in order to maintain the equilibrium line altitude of a glacier, roughly 300 mm of additional precipitation per degree of warming would be necessary. Projections from regional climate models suggest that in the alpine region, warming will be accompanied by an average reduction of annual precipitation, thereby implying rapidly waning glaciers until they find perhaps another equilibrium at much higher elevations and with substantially reduced volume and surface area; some may disappear entirely as the equilibrium line altitude may be above the glacier catchment area.

With an upward shift of 200–300 m in the equilibrium line altitude, the reduction in ice thickness of temperate glaciers could reach 1-2 m per year in terms of water equivalent. As a result, many glaciers in temperate mountain regions would lose most of their mass within decades (Maisch, 1992). Shrinking glaciers will lead to changes in the hydrological response of certain regions compared to today; as glaciers melt rapidly, they will provide enhanced runoff, but as the ice mass diminishes, the runoff will wane.

Based on a warming scenario of 3°C by 2050, Maisch (1992) has computed the rise in the equilibrium line altitude for several glaciers in the Swiss Alps. Using computer imaging techniques, he has provided a visual rendering of what a typical glaciated region may look like following the extensive glacier retreat that would occur for the Tschierva Glacier (Bernina range) in south-eastern Switzerland, as illustrated in Figure 8.21.

These conclusions are relevant to hydrology, another important impacts sector in the alpine region that will be visited following in the next sub-chapter.

8.2.4. Impacts on hydrological regimes and associated natural hazards

The Alps are the source region for many of western and central Europe's river systems. On average, Switzerland receives close to 1,500 mm of precipitation per year, of which one-third is lost through evaporation and close to two-thirds contribute to surface runoff; a small fraction is stored in lakes, dams, and serves to recharge groundwater reserves.

Within a 30-km radius in the Gotthard region of central Switzerland, surface runoff feeds river systems that flow into the North Sea (Rhine river basin, representing about two-thirds of total water exported from Switzerland), the Mediterranean (Rhone river basin, with about 18% of water

exports), the Adriatic (Ticino that converges with the Po river in Italy and represents 10% of runoff from Switzerland) and the Black Sea (via the Inn that converges with the Danube in Germany, and accounts for about 5% of surface runoff).

Alpine water resources are strongly influenced by mountain climates that govern soil moisture, groundwater recharge, evaporation and runoff. As seen in Figure 8.22 for a river such as the Rhone runoff is controlled by evaporation, precipitation, storage of water in artificial reservoirs, and melt water from snow and ice. The figure combines in one single view the input of water in the system in the lower segment of the graph with the inverse scale, and the loss of water in the form of evaporation, runoff and storage in dams and in the seasonal snow-pack in the upper part of the graph.

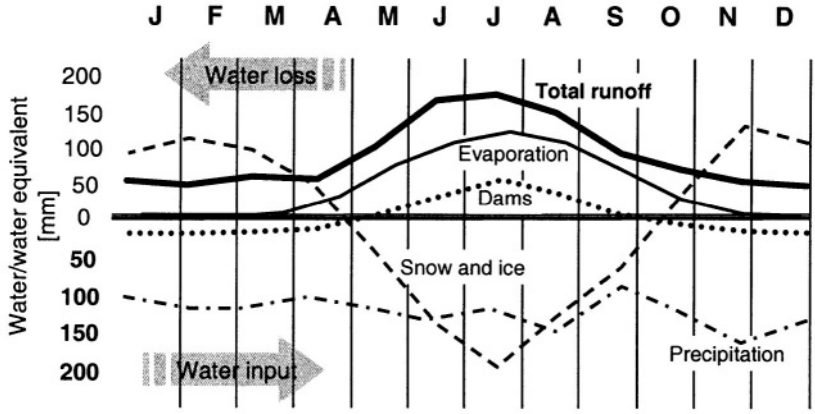

Figure 8.22. Components of the hydrological cycle of an alpine river measured in terms of water and water-equivalents. Average monthly figures are given here for the Rhone River as it enters the Lake of Geneva.

Figure 8.22 can be interpreted in the following manner: precipitation throughout the year, and snow and ice melt waters from May to October provide input to the river basin; in addition, hydro-power utilities release water into the catchments and tributaries of the Rhone during the winter half-year in order to generate power and heat during the peak energy demand period of the winter. In the upper half of the graph, water is locked in the winter snow-pack from November to May and hence is not considered as an input of water to the system but rather as a sink. This is because winter snow accumulation in the mountains removes water from precipitation that would otherwise directly feed into the river itself. Evaporation is a function of temperature and water availability and reaches a maximum during the summer months; and finally, dams retain a small part of snow-melt and

precipitation during the summer months and store this water to prepare for supplying energy later in the year; this storage removes water from the system that would otherwise contribute directly to runoff.

Because precipitation is fairly evenly distributed throughout the year and storage of water in dams represents a small fraction of the total amounts of water involved, the most important seasonal signal in terms of runoff is determined by the alpine snow-pack, in particular the timing of snow-melt and the amount of melt-water associated with the accumulation of snow during the preceding winter. As a consequence, the implications of shifts in the snow-pack in a changing climate that were introduced in the previous sub-chapter are likely to have a strong influence on river flows.

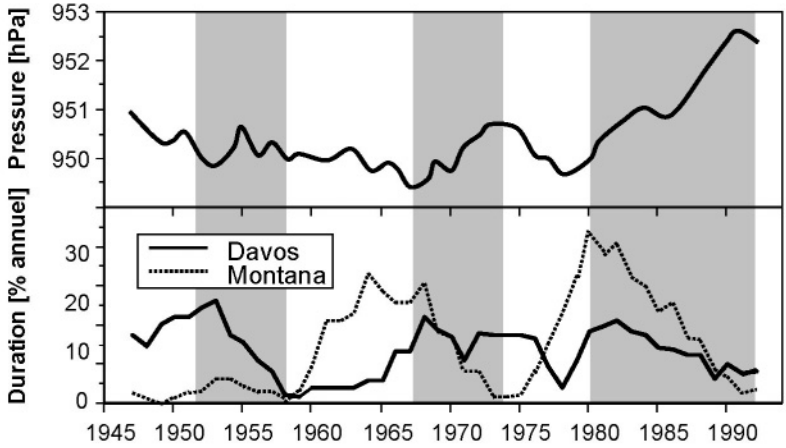

Figure 8.23. Changes in the duration of the snow-pack beyond a 50-cm threshold in Davos and Crans-Montana for periods of strongly positive anomalies of the North Atlantic Oscillation index (highlighted by gray shading). The upper curve shows the average winter surface pressure field in Zürich that is closely linked to the behavior of the North Atlantic Oscillation.

In addition to atmospheric warming and modified precipitation regimes, low-frequency variability associated with the behavior of the North Atlantic Oscillation (NAO) may be superimposed upon the global warming signal. During positive phases of the NAO the response has been an almost systematic and persistent reduction of precipitation and snow accumulation, as shown by Beniston (1997a), for example. Figure 8.23 highlights in grey periods with strong positive NAO anomalies that have resulted in marked decreases in the duration of snow above a given depth threshold (50 cm) at two medium-elevation locations (Crans-Montana, 1,495 m above sea-level

and Davos at an elevation of 1,590 m), as persistent high-pressure settles over the alpine area (upper curve).

Intuitive reasoning based on the foregoing discussion enables a quantification of changes in the components of the hydrological cycle in response to climatic change, as illustrated in Figure 8.24. Compared to Figure 8.22, the changes in the various elements contributing to total runoff are quite substantial. Precipitation itself undergoes seasonal shifts that are related to the increase of winter precipitation and marked decrease of summer and fall rainfall illustrated in Figure 8.2. The contribution of snow and ice changes considerably in a "Mediterranean-type" climate, with a shorter snow season and lower overall snow-pack accumulation, contributes earlier in the year to river runoff with sharply reduced amounts of water. As a consequence, the water storage in dams is accomplished in the spring months as opposed to the late summer under current climatic conditions. Evaporation is enhanced throughout the year and removes water from the system even during the winter compared to today's climate.

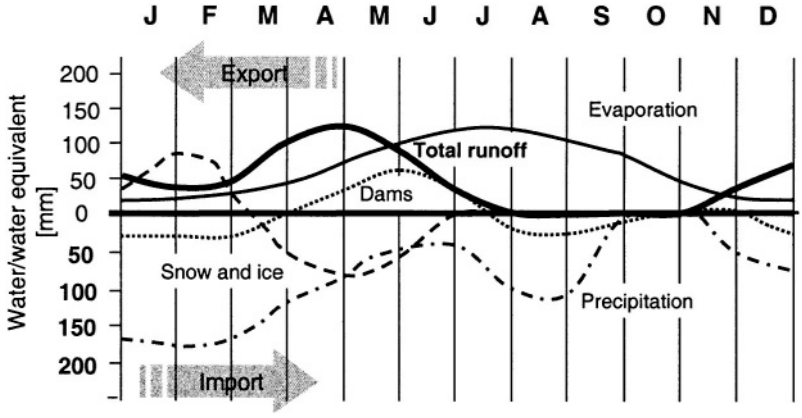

Figure 8.24. Possible changes in total runoff in an alpine river such as the Rhone as a result of climatic change, according to the different sub-components illustrated in Figure 8.22.

Combining the different contributing elements, runoff is seen to change in seasonality and amount compared to Figure 8.22. Peak discharge is shifted forward in the year by 2-3 months, and maximum flow is reduced because of the smaller contributions by the melting of the snow-pack. Furthermore, the hypothetical example illustrated in Figure 8.24 suggests that as a result of the sharply curtailed glacier mass in the mountains and possibly long and dry summers, glaciers will no longer be sufficient to feed water into river catchments at a time of the year when precipitation amounts are low and the

snow-pack has melted. Consequently, some rivers may dry up partially or completely towards the end of the summer and into the early fall. The characteristics of river runoff shown in this figure are common to rivers that are currently found in the Mediterranean parts of the Alps as in south-eastern France and in parts of the Italian-facing slopes of the alpine arc, for example.

In terms of natural hazards in the Alps, the cumulative effect of additional intense rainfall in low to middle altitude regions may lead to high rates of slope erosion. Climatic change could alter the frequency and the magnitude of a wide range of geomorphologic processes related in particular to the projected enhancement of extreme precipitation events that could increase the frequency and severity of floods. When these events occur towards the end of the summer, at a time where soils are dry and have difficulty in absorbing abrupt and large quantities of water at the surface, many river basins are likely respond through flooding. At other times of the year, flood potential can also increase when precipitation, associated with snow-melt during the winter or early spring, discharges unusual amounts of water that cannot be absorbed by the river catchments. Such situations have prevailed in a recent past along the entire course of the Rhine river basin, for example.

Extreme precipitation events would in addition contribute to more erosion, discharge and sedimentation rates. Large rock falls in high mountainous areas are often caused by groundwater seeping through joints in the rocks. If both average and extreme precipitation were to increase, as regional climate models suggest may be the case in winter, then groundwater pressure would rise, providing conditions favorable to increased triggering of rock falls and landslides. Large landslides are propagated by increasing long-term rainfall, whereas small slides are triggered by high intensity rainfall. In a future climate, where both the mean and the extremes of precipitation are projected to rise in certain areas, there would be a corresponding increase in the number of events related to slope instability.

Other trigger mechanisms for rock falls are linked to pressure-release joints following deglaciation; such rock-falls may be observed decades after the deglaciation itself, emphasizing the long time lags involved. A further factor responsible for decreased slope stability in a warmer climate is the reduced cohesion of the soil through permafrost degradation. With the melting of the present permafrost zones at high mountain elevations, rock and mud-slide events can be expected to increase in number and, possibly, in severity.

Deglaciation can in some instances lead to problems of water accumulation behind unstable moraines of isolated blocks of ice that have broken off from the leading edge of a retreating glacier. Under rapidly changing conditions, such as in the event of extreme precipitation, sudden

overspills or outbursts can result in intense flooding and debris flows that can put communities and infrastructure at risk. In the early 1990s, under the threat of a glacier lake outburst in the upper Saas Valley (canton of Valais, southern Switzerland), major civil engineering works were undertaken to divert waters from the lake that formed ahead of the retreating Gruben Glacier, thereby averting a potential disaster for the village of Saas Balen and downstream in the Saas Valley.

Hanging glaciers also pose a threat that is taken seriously in many alpine valleys, for example in the Canton of Valais where several retreating glaciers are located above villages and communication routes. In their retreat, these glaciers reveal a large quantity of unstable rubble and, in some instances, masses of ice that have broken off from the main part of the glacier. This situation could result in severe downslope flow of material, with significant damage potential. Glaciers such as the Bisgletscher close to Zermatt or the Griesgletscher on the Italian border are currently closely monitored. There is a constant fear that catastrophic events may repeat themselves with increasing frequency, such as the Mattmark event where a portion of the Allalin Glacier broke off above the Saas Valley in 1965, killing 88 persons working on the construction site of the Mattmark Dam.

Whatever the nature of change in the hydrological characteristics of many rivers originating in the Alps, shifts in climatic regimes in the mountains will have impacts that may reach far beyond the mountains themselves in populated lowland regions that depend on mountain water resources for domestic, agricultural, energy and industrial purposes. The fluctuations in levels of the Rhine River, for example, have in the past had economic repercussions, particularly when the transport of goods along the river is disrupted during periods when flow levels are either too high (as during the floods of February, 1995) or too low (as during the heat wave of the summer of 2003).

Not only water quantity but also water quality may change with climate, thereby requiring attention by authorities in order to avoid risks associated with the proliferation of toxic algae beyond a certain temperature threshold, for example. Other changes in hydrological regimes will have implications for hydro-power resources, and the potential for altered frequencies of floods and drought, or enhanced sediment transport during floods, may have serious financial consequences for infrastructure, industry, agriculture, and domestic water supply.

8.2.5. Impacts on alpine vegetation

Because temperature decreases with altitude by 5-10°C/km, it could be expected that vegetation would respond to warmer climatic conditions by an upward migration in order to remain within the same "bandwidth" of environmental and climatic conditions as currently (e.g., McArthur, 1972; Peters and Darling, 1985). The simplest view regarding climatic change in the Alps is that it would entail the loss of the coolest climatic zones at the mountain tops and a spread of the vegetation belts upslope. Because mountain tops are smaller than their bases, vegetation currently at high elevations would occupy increasingly smaller areas with a corresponding reduction in plant distribution and an enhancement of species' vulnerability to genetic and environmental pressure (Peters and Darling, 1985; Hansen-Bristow et al., 1988; Bortenschlager, 1993).

This paradigm may in many cases be overly simplistic, however, because of the different climatic tolerance of species involved, including genetic variability between species, different longevities and survival rates, and the competition by invading species (Dukes and Mooney, 1999). In essence, plant life at high elevations is primarily constrained by direct and indirect effects of low temperatures, radiation, wind and storminess or insufficient water availability (Körner and Larcher, 1988). Plants respond to climatological influences through morphological and physiological adjustments that include small leaves and low thermal requirements for plant survival.

Grabherr et al. (2001) note that alpine plants are in many respects good ecological indicators for the detection of climatic changes, particularly those that are close to the lower limits of temperature for their survival, since any small change in temperature may result in large response by vegetation. Guisan et al. (1995) expect that the response of ecosystems in mountain regions will be most important at ecoclines, i.e., gradual ecosystem boundaries, or ecotones, i.e., boundaries where step-like changes in vegetation types occur). Ecological changes at ecoclines or ecotones may be amplified because of changes in vegetation species that take place within adjacent ecosystems. In steep and rugged topography, ecotones and ecoclines increase in quantity but decrease in area and tend to become more fragmented as local site conditions determine the nature of individual ecosystems. The most vulnerable species at the interface between two ecosystems will be those that are genetically poorly adapted to rapid environmental change. Those that reproduce slowly and disperse poorly, and those which are isolated or are highly specialized, will therefore be highly sensitive to seemingly minor stresses (McNeely, 1990). Even though the

timberline is not a perfect ecocline in many regions, it is an example of a visible ecological boundary that may be subject to change in coming decades, although some boundaries may exhibit low sensitivity to climatic change (Körner, 1998; Bugmann and Pfister, 2000) while others may respond with very long lag times (Davis, 1989). There are instances where ecotones are the result of disturbance rather than climate. This is the case for many forests in the Alps, for example, where the current timberline in many parts of the alpine domain is lower than its potential limit because of pastoral practices; in such cases, ecotones may be the drivers of local climatic gradients rather than the contrary (Becker and Bugmann, 2001). Another interesting example from the southern part of Switzerland that represents a combination between human interference and climatic change is the invasion of tropical palm species (Carraro et al., 1999) in the chestnut and deciduous forests on the slopes above Locarno and Lugano in the canton of Ticino. The invasive species were imported as ornamental plants in the gardens or parks of individual trees or mansions in the 19th and early 20th centuries. The seeds of these plants spread into the neighboring countryside over time, but it is only since the 1970s and 1980s that the exogenous species have been able to reproduce and take hold on their local environment; this is because of the strong reduction in the number of frost days that has favored the establishment of these species outside of their initially-allocated areas and in an environment that has never witnessed these species naturally (Carraro et al., 1999).

In the absence of direct anthropogenic interference, species may respond to environmental pressures through a number of strategies that include genetic adaptation, invasions resulting from the competition between species, and extinction (e.g., Huntley, 1991). In terms of adaptation observations in the Alps (Grabherr et al., 1994; Keller et al., 2000) suggest that certain plants are already responding to observed 20th century warming by a progressive replacement of the currently dominant species by more thermophilous (heat-requiring) species. Further adaptation mechanisms include the replacement of dominant species by pioneer species of the same community that have enhanced adaptation capability (e.g., Halpin, 1994). A third possibility is that environmental change may favor less dominant species, which then replace the dominant species through competition (Street and Semenov, 1990). These multiple adaptation strategies can function only if other limiting factors such as soil type or moisture will remain relatively unaffected by a changing environment. In regions where climatic change may lead to warmer and drier conditions, for instance, mountain vegetation could suffer as a result of increased evapotranspiration. This is most likely to occur in mountain climates under the influence of continental and

Mediterranean regimes. Kienast et al. (1998) have applied a spatially-explicit static vegetation model to alpine vegetation communities. The model suggests that forests which are distributed in regions with low precipitation and on soils with low water storage capacity are highly sensitive to shifts in climate. Under conditions of global warming, the northward progression of Mediterranean influences would probably be important, and it is estimated that 2-5% of currently forested areas of Switzerland could undergo a steppe-like transition, particularly on the Italian (south-facing) side of the Alps and in the drier intra-alpine valleys.

Körner (1999) and others (Ozenda, 1985; Burrows, 1990) have emphasized the crucial role of the snow-pack in the Alps and its behavior on the timing of the start of the annual vegetation cycle for many species. The length and depth of snow cover is often correlated with mean temperature and precipitation, as shown by Beniston et al. (2003) and summarized earlier in this chapter. Snow cover provides frost protection for plants in winter, and water supply in spring. Alpine plant communities are characterized by a very short growing season (i.e., the snow-free period) and require water to begin their growth cycle.

Keller and Körner (2003) have subjected over 30 high alpine plant species to scrutiny in their laboratory investigations of the response of plants to different exposures of day-length (or *photoperiod*). This study was conducted to assess the manner in which plants would respond to a shorter season that leads to conditions potentially favorable for an earlier and longergrowth season of high alpine plants. Keller and Körner (2003) found that there was not an identical response to the photoperiod in all the plants studied. Some opportunistic species were able to commence their annual growth cycle as soon as the ground was free of snow, while other responded to hormonal stimuli *(hormonal "clocks")* whereby growth would commence only at a specific time of the year even if there was no longer any snow on the ground. These latter types of plants would in certain respects be more vulnerable than those whose vegetation cycle has already begun and which as a consequence are potentially more robust.

Applying the GRENBLS energy balance and snow model (Keller and Goyette, 2003) to a very localized domain close to the summit of Säntis in eastern Switzerland, Keller and Goyette (2003) and Keller et al. (2004) were able to show that the distribution of many species would change according to the conditions of snow on ridges, slopes or in hollows. In addition, inter-species competition would also be modified as plants adapt differently to the changing snow and environmental conditions.

Figure 8.25 provides examples of the sensitivity of snow exposed to different slope angles and orientations on Säntis according to various

temperature and precipitation scenarios. In this instance, the snow depth in the vicinity of the summit of Säntis is mapped for mid-May under an observed winter (1998) and for a rise of 4°C in winter mean temperatures as seen in Chapter 6 for the EU-PRUDENCE simulations.

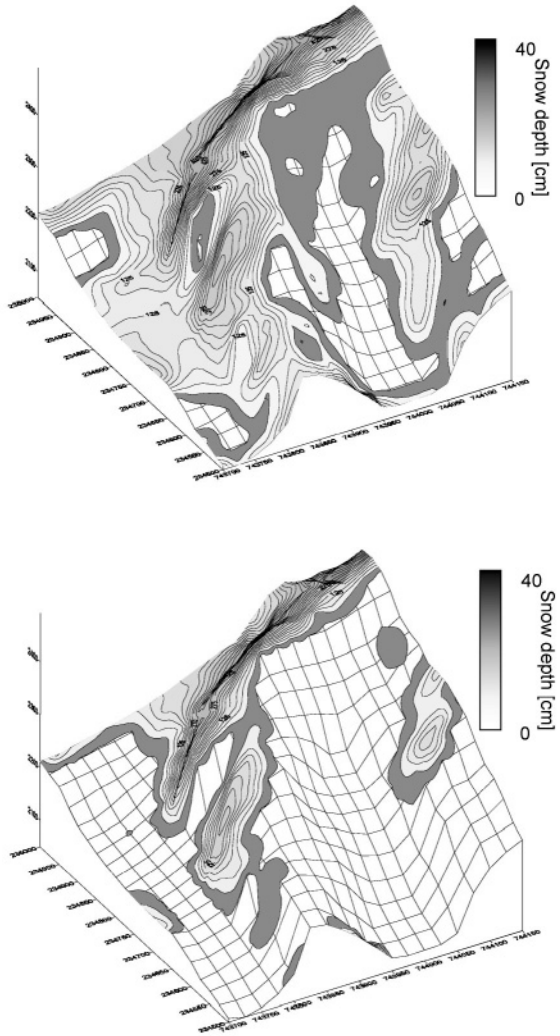

Figure 8.25. Illustration of possible changes in snow cover in mid-May at Säntis (2,500 m above sea-level in the eastern Swiss Alps), for a typical observed winter (1998; upper) and with a 4°C rise in mean winter temperatures (lower). Potential shifts in vegetation would involve adaptations to new snow conditions on crests and in hollows (Following Keller et al., 2004).

The shifts in vegetation that these changes in snow entail if they are sustained over time would involve species' adaptations to snow-free conditions on ridges and in hollows.

Changes in the frequency and intensity of strong wind storms, floods, or drought would in the future impact alpine forests that are already subject to multiple stresses such as acidification of soils, air pollution (in particular tropospheric ozone and other precursor gases), parasite attacks, and also to forest management practices. Isolated or rare extreme events would take their toll of trees in certain parts of alpine woodlands, but if these events were to become more frequent, the damage to forests would be highly non-linear because of the weakening effect on forest stands of the previous extreme event.

Figure 8.26. Zone of forest damage in the Swiss canton of Bern, following the December 1999 *Lothar* winter storm. The surprising configuration of damaged areas within a crown of undamaged trees is a characteristic signature of that particular winter storm.

To date, few investigations of the future sensitivity and vulnerability of forest stands in the Alps to climatic change and environmental stress have been undertaken. Zierl (2001) has developed a water balance model that is used for the assessment of the effect of prolonged droughts in the Alps on tree mortality, and new studies are under way to investigate the regions most vulnerable to wind storms such as those that led to considerable damage to European and alpine forests (the February 1990 *Vivian* storm and the December 1999 *Lothar* storm in particular). According to the intensity of turbulent gusts, associated with slope and orientation of the forest stands,

trees subjected to severe wind storms are observed to be either uprooted or the trunks may be snapped off at some distance above the ground, while other parts of the same forest may remain relatively unaffected. Figure 8.26 shows a view of the heterogeneous nature of forest damage following the *Lothar* storm on the Swiss Plateau, where destruction of trees during the 12-hours storm event represented up to 6 times the annual felling rate in certain Swiss cantons (Figure 8.26).

As with many other systems, the direct cause-to-effect relationships are often difficult to highlight, because of the multiple factors that are responsible for tree growth and survival, and the temporal dimension of multiple stresses that can reinforce the vulnerability of woodlands to a particular extreme event.

8.3. IMPACTS ON SOCIO-ECONOMIC SECTORS

The environmental impacts of climatic change in sensitive regions such as the Alps that are also relatively densely settled and industrialized may have a number of consequences for economic activities taking place within the mountains. Energy and tourism are two sectors that are likely to be influenced by changes in temperature, precipitation, snow amount, and glacier surfaces.

In both the mountains and the lower elevations of Switzerland, there will be consequences for agriculture, although the very large subsidies and direct payments to Swiss farmers will, if sustained over the next decades, partially offset any negative impacts on Swiss farm products. Climatic change changes the external conditions for agricultural economics, in particular plant production (e.g., Riedo et al., 2001). With a projection of a warming of 0-3-0.5°C per decade over the course of the 21st century, the vegetation period will be extended compared to current climatic conditions. In Switzerland, this will influence the production of fodder and, indirectly, animal husbandry. In cropland areas, the seasonality of planting and harvesting will also be modified because of earlier spring and summer conditions, and the reduction of the number of frost days that currently limits the growth season. Warming may provide new opportunities for the cultivation of additional crops compared to today (e.g., Riedo et al., 2000), although the risk of increased parasites and weeds will be an increasing problem. During the warmer and drier summers that could affect many parts of the country, evapotranspiration and reduced soil moisture would need to be compensated for by an increase in irrigation of plants; if water supply

were to be disrupted then the thresholds for plant failure would be reached more quickly under future climatic conditions than today.

Such risks require a forward planning of appropriate adaptation strategies, such as the type of crops to be planted (e.g., drought and/or heat resistant species), the optimal time of the year for planting, and the allocation of soils for specific crops or crop rotation. Additionally, there is an enhanced risk in certain parts of the country of soil erosion that would require better erosion control measures.

Despite a number of potentially adverse climatic impacts on Swiss agriculture (e.g., Fuhrer, 2003), a substantial amount of research is currently under way to assess the potential for grasslands as a carbon sink, allowing Switzerland to use this means of partially attaining its commitments to the Kyoto Protocol on greenhouse gas reductions.

The tourism industry has exhibited the most sustained growth of any global industry in the last 25 years. It accounts for 10% of the world's net financial output, with many countries in the developing world dependent on tourism as their main source of income (Perry, 2000). Figures released by the World Tourism Organization (WTO, 2000) indicate that the number of international tourists has increased 25-fold in the second half of the 20th Century. In Switzerland, the tourism sector is within the first five sources of revenue for the national economy

Global warming is likely to have both direct and indirect impacts on tourism in Switzerland. Direct impacts refer to changes in the climatic conditions necessary for specific activities. Indirect changes may result from both changes in mountain landscapes (referred to by Krippendorf, 1984, as the "capital of nature)", and wider-scale socio-economic changes such as patterns of demand for specific activities or destinations (Price, 1990). Using scenarios derived from GCMs, a number of investigations have been carried out to examine the possible implications of climate change for skiing in Switzerland (Abegg et al., 1997; Koenig and Abegg, 1997). Abegg and Froesch (1994) showed in their study of the Swiss ski industry that if temperatures were to rise by about 2-3°C by the year 2050, the low to medium elevation resorts located below 1,200 – 1,500 m above sea level would be adversely affected. Warmer winters bring less snow at these low elevations, and the probability of snow lying on the ground at peak vacation periods (Christmas, February and Easter) would decline. A general rule for the viability of the ski season in Europe is a continuous snow cover of over 30 cm depth for at least 100 days. Based on these figures, Koenig and Abegg (1997) have shown that whereas in the late 20th Century, 85% of ski resorts have had reliable amounts of snow for skiing, a 2°C warming would bring this figure down to 63%. Regions such as the Jura Mountains in the west of

the country, whose average altitude lies between 900 – 1,200 m, would experience much-reduced periods with adequate snow-cover, whereas the elevated ski resorts in the central and southern Alps would remain relatively unaffected. Such impacts might be partially offset by new opportunities in the summer season and also by investments in new technology, such as snow-making equipment, as long as climatic conditions remain within appropriate bounds. Mountaineering and hiking may provide compensation for reduced skiing, and thus certain mountain regions would remain attractive destinations. However, global climate change has wider implications for traditional holiday breaks, with destinations other than mountains in winter becoming at least as competitive if not more. Higher temperatures may imply longer summer seasons in mid-latitude countries, and Perry and Smith (1996) suggest that a new range of outdoor activities may emerge as a consequence.

Switzerland relies on hydro-power for over 60% of its primary electricity supply, and the Canton of Valais alone accounts for over two-thirds of the total production (10,000 GWh per annum, i.e., a quantity sufficient to supply power to 1.5 – 2 million persons), with the presence of numerous dams including the Grande Dixence that remains to date the largest of its kind in the world. In financial terms, energy production in Valais represents 40% of the added-value in the industrial sector of the canton. Switzerland is a net exporter of electricity through the European grid network, resulting in substantial foreign exchange income for a strategic industrial sector.

Hydropower has both advantages and disadvantages. Its principal advantage resides in the renewable nature of water and the energy potential that it represents; a well-designed dam and forward planning for future infrastructure represents a potential "lifetime" of 600-2,000 years, taking into account the sedimentation and other environmental fluctuations that can influence the functioning of the major dams in the Alps. A further beneficial side-effect is that dams can buffer the effects of severe precipitation by retaining the waters that could otherwise lead to flooding, at least if the dams are not full at the time of a heavy precipitation event. The dams in Valais have the combined potential of retaining up to 30% of the peak flow in the Rhone river; if a heavy precipitation event is short-lived, the dams can make the difference between moderate and catastrophic flooding. The drawbacks of hydropower infrastructure include the ecological impacts of flooded valleys and the reductions in stream flows downstream of the dams, although recent legislation requires the dam operators to ensure a minimum level of flow in the streams and rivers originating in the catchment area of the dam itself.

Mountain runoff (electricity supply) and electricity consumption (demand) are both sensitive to changes in precipitation and temperature. Long-term changes in future climate will have a significant impact on the seasonal distribution of snow storage, runoff from hydro-electric catchments and aggregated electricity consumption. According to the future climate scenario used the seasonal variation of electricity consumption may be less pronounced than at present, with largest changes in winter which is the time of peak energy use for heating. The sensitivity of mountain hydrology to climate change is a key factor that needs to be considered when planning hydro-power infrastructure.

The impact of climate on water resources in alpine areas has been examined by Gleick (1986, 1987) and Martinec and Rango (1989). Similar studies have related electricity demand to climate (Warren and LeDuc, 1981; Maunder, 1986) but few, however, have attempted to integrate these impacts of climate change by considering both electricity supply and electricity consumption (Jaeger, 1983). Changes in flow regimes, induced either by changes in total precipitation, the amount of snowmelt, or a combination of both, would affect hydropower potential. Thermal, nuclear and hydropower stations rely on the supply of water for cooling or for the direct generation of electricity. The sensitivity of some thermal and nuclear power generating stations to shortfalls in water for cooling purposes may increase in the future, particularly during the summer months. Lack of water can lead to reducing or halting energy production, for security reasons. There may be a real risk of increases in such reductions in energy production in coming decades, particularly in those areas which are likely to become drier in the future.

Current difficulties in implementing water resource development projects will be compounded by uncertainties related to the response of hydrological systems the amplitude and speed of projected climatic change. Among these, possible increases in sediment loading would perturb the functioning of power generating infrastructure.

Chapter 9

CONCLUSIONS

9.1. ADDRESSING CLIMATIC CHANGE

This book has attempted to provide in the first section an up-to-date overview of the physics of the climate system and its observation and modeling of. In the second section, issues related to regional climate change and impacts on Switzerland, as a particularly interesting case-study region, have been addressed.

It was seen throughout the volume that climatic change involves a complex set of issues and a subtle mix of social, economic, political, and technological driving forces. In view of the potential severity of the impacts of global warming in many parts of the world, the overarching question that can be posed in this context relates to the apparent inertia in decision-making.

This question is difficult to answer, in part because of conflicting time-scales related to economic policies, that are on the short term (days to months), and the management of the planetary environment, climate, and resources, that by essence needs to be planned on the very long term (decades or more). Collective human behavior is a key factor that seems to govern numerous human endeavor related to environmental perception and management, and only recently has there been a focus on such aspects in the social and behavioral sciences (e.g., Jochem et al., 2000).

One example of collective behavior is related to the fact that, in a world where most physical, biological, social and economic systems are in a state of perpetual evolution, humans generally think in static terms. They see the world at a particular instant in time and do not consider its past evolution that has resulted in the current state of the system, nor do they think of its possible future evolution. When the time scales involved are decades or more, human perception has difficulty in envisaging long-term futures of

environmental or economic systems. Short-term decision-making is thus perceived to be simpler when problems that are of apparently immediate importance, with very little consideration for the fact that there may be longer-term consequences involved. An illustration of short term decisions that have long term consequences is the policy of forest fire suppression in many parts of the world and particularly in North America, that was long considered to be a laudable attempt at environmental and biodiversity protection. Decisions related to fire suppression were in fact addressing only one part of the overall problem of forest protection, and many major forest fires occurred *because* of the accumulation of large quantities of dry wood that was a consequence of fire control. The excessive amount of dry wood fueled events such as the devastating 1988 forest fires in Yellowstone National Park, resulting in impacts that turned out to be more severe than would have occurred in the absence of any fire suppression policy. Fire has since been recognized as being an integral part of the forest ecosystem, providing enrichment to soils and allowing new generations of trees to grow in zones where limited forest fires have cleared the old trees to make room for young saplings.

This example of a sectorial view of the world as opposed to a holistic approach is characteristic of many human enterprises. A holistic approach normally attempts to assess the consequences of a policy aimed at resolving a problem in a particular system, in terms of possible secondary effects – positive or negative – on other elements of the system under consideration. When addressing issues of climatic change and climate-related impacts, this can be a daunting challenge in view of the highly non-linear nature of each of the numerous interacting elements of the climate system that were introduced in Chapter 2.

There are further explanations to the apparent inertia in decision-making related to climatic change. Because of the numerous uncertainties that still remain in the prediction of the evolution of climate, these uncertainties have often been interpreted by many policy makers as a sign that additional scientific proof would be necessary prior to taking any binding decisions. This is a point of view that has been widely supported in the past by many segments of business and industry, which consider any action to address climatic change as a hindrance to business. The decision by the Bush administration in the United States and more recently by the Russian Federation (at the time this book went to press) not to ratify the Kyoto Protocol (discussed in Section 9.2 below) and its commitments to greenhouse gas reductions, was justified in economic terms, in the sense that implementing the Kyoto Protocol could be harmful to the national economy. While greenhouse gas abatement strategies will inevitably have a cost, it is

far from certain that the consequences of such measures would be economically detrimental on the long term. For example, accompanying measures such as energy savings, and the beneficial effects for human health related to reduced air, water and soil pollution that greenhouse gas emission reductions would entail, are certainly likely to have a beneficial influence on large sectors of national economies.

In the present economic context, however, long-term forward planning and the convergence of economic and environmental interests are, with few exceptions, still far from reality. However, some timid signals seem to suggest that solutions to the problem of climatic change may be forthcoming from the industry sector itself rather than from the policy-making sphere. Many industries no longer explicitly deny the reality of climatic change and are learning to cope with the problem and adapt to it as time goes by. Certain oil companies that are keen on remaining leaders in the field of energy supply but aware of the limited global oil reserves are investing heavily in alternate energy sources and technologies such as hydrogen. This has in turn sparked interest by vehicle manufacturers to develop new engine designs that do not rely exclusively on oil as the primary fuel; fuel-cell and hydrogen technologies are today being tested by some of the leading automobile manufacturers. Energy savings can be implemented at little or no cost (especially when estimating the return on investment over several years to a decade or two), that can substantially reduce greenhouse gas emissions.

These first steps are not necessarily motivated by a particular environmental conscience by industry, but the technological solutions that are being considered may be indirectly beneficial in terms of climatic change through the reduction of the dependency on fossil fuels, one of the essential contributors to greenhouse gas emissions in the atmosphere, as discussed in Chapter 4. Such positive steps are urgently required and need to be economically viable and accessible to emerging economies such as China and India, which currently rely heavily on CO_2-intensive coal as their principal energy source for industry and energy. Without any curtailing of this use of coal, these two highly-populated nations will in a very near future become major contributors to global greenhouse-gas emissions.

9.2. THE KYOTO PROTOCOL

The UN Framework Convention on Climate Change (FCCC) was negotiated by over 160 countries during the UNCED-1992 “world summit” (UN, 1992). The FCCC only contains general obligations for the signatory parties to reduce greenhouse gas emissions. The Convention neither quantifies

emission reductions nor does it recommend a calendar for action; this is where the Kyoto Protocol discussed below becomes an important instrument in collective action aimed at climatic change and its impacts. By setting up a process through which governments can meet regularly, the FCCC have put into place an appropriate technical, scientific, legal and institutional framework to address these complex issues.

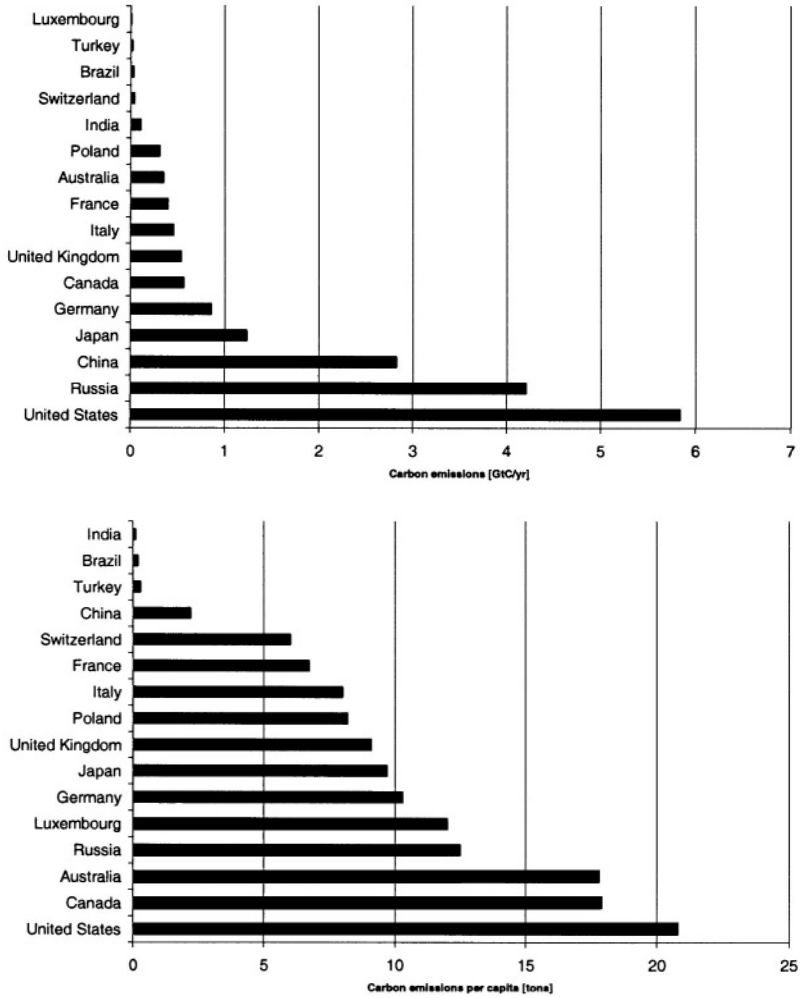

Figure 9.1. Carbon emissions per country (upper) and per capita (lower) for a selected number of countries. (Source: IPCC, 2001).

The 1990 emission levels for a selected number of countries in the developed and the developing world are illustrated in Figure 9.1 and are quantified both in terms of total emissions per country in GtC per annum (GtC: Gigatons of Carbon; Figure 9.1, upper) and of emissions per capita (in tons per person and per year; Figure 9.1, lower). The latter approach to quantifying carbon emissions clearly illustrates the cleavage that exists between the rich, industrialized nations and the poorer developing countries. China comes third in terms of its total carbon emissions, but in 40^{th} position when weighted by population; the United States, which is in both cases the first contributor to emissions, consumes about 50 times more than India in global terms, and 200 times more per capita; the respective populations are 270 million and close to 1.1 billion inhabitants. Luxembourg has a surprisingly high per capita contribution to carbon emissions although its total levels of emissions (5 million tons per annum) are negligible on a global scale. This is because Luxembourg is an important supplier of fuels to its neighbors France, Belgium and Germany, and the trade of oil is credited in terms of emissions to Luxembourg as the exporting country. France's low per capita emission in comparison to other industrialized nations is the result of its national policy of relying heavily on nuclear power for its electricity supply; the same can be said for Switzerland, where 60% of its electricity is generated through hydro-power and 40% through nuclear power.

The FCCC contains a certain number of articles that are of relevance to many of the foregoing discussions. In particular, Article 2 stipulates that:

"...The ultimate objective of the FCCC... is the stabilization of greenhouse gas concentrations in the atmosphere at a level that would prevent dangerous anthropogenic interference with the climate system...Such a level should be achieved within a time-frame sufficient to allow ecosystems to adapt naturally to climate change, to ensure that food production is not threatened and to enable economic development to proceed in a sustainable manner..."

The Kyoto Protocol was negotiated by more than 160 nations in December 1997 in the Japanese city that gave its name to the Protocol. It is a compromise agreement whose principal objective is to reduce greenhouse gas emissions by 5-8% according to country within the time frame of 2008-2012; furthermore, the Kyoto agreements at the time of their negotiation placed the essential burden of reductions on the industrialized world. The governing texts of the Kyoto Protocol include explicit reference to six greenhouse gases that include in addition to carbon dioxide (CO_2), methane (CH_4), laughing gas (N_2O), halo-fluoro-carbons (HFC), perfluoro-carbons (PFC), and sulfur hexafluoride (SF_6). Emissions from air and ocean transportation are excluded from the obligations of the Protocol. Each

industrialized country that has ratified the Protocol is authorized to use a portfolio of economic mechanisms to fulfil its Kyoto commitments.

There are numerous aspects of the Kyoto Protocol that have received much media attention, in particular the requirement for a reduction in the emissions of greenhouse-gases within the coming decade. There are several pathways to lowering the quantities of greenhouse gases in the atmosphere, the most obvious one being a reduction of emissions at the source. These can be encouraged through voluntary reductions on the part of business and industry, fiscal abatement measures for enterprises that significantly curtail carbon emissions, carbon taxes (Switzerland is the first country to have prepared a law authorizing the use of such a deterrent tax by 2004-2005), joint implementation, emission permits and, for developing countries, the so-called "clean development mechanism". The Kyoto Protocol is scheduled to enter into force when it has been ratified by at least 55 states that globally represent over 55% of carbon dioxide emissions (based on their 1990 levels).

Another approach to carbon abatement is to attempt to use carbon sinks as a means of removing carbon in the atmosphere; this is particularly the case of the terrestrial and marine biosphere, where the metabolism of organisms can recycle carbon in living matter through photosynthesis, for example. However, while the current anthropogenic emissions of carbon are relatively well known, within certain limits of uncertainty, the uptake of carbon in a variety of sinks found for example in forestry and agriculture is far less well understood and quantified

The use of carbon sinks as one approach to achieving the objectives of the Kyoto Protocol requires considerable research efforts in order to bring the quantification of these sinks to the same level of accuracy as those related to anthropogenic carbon sources. In compliance with the objectives of the Protocol, reporting on national inventories of carbon sinks is required by each member of the Conference of the Parties having ratified the Kyoto Protocol. This implies accurate knowledge of the processes taking place beneath, at, and above the Earth's surface in terms of carbon fluxes, according to different types of surface and vegetation. Such quantification can be achieved on the basis of *in situ* observations, remote-sensing data, and modeling techniques.

According to the agreement negotiated in Japan in 1997, the European Union committed itself to an overall reduction of 8% spread among the member states (a target that Switzerland also adopted). Other national emission reductions include 6% for Japan, 5% for Canada, between 6 and 8% for Eastern Europe and the Russian Federation and 7% for the United States. This latter commitment was rejected by the Bush administration, which took over from a more environmentally-conscious Democratic

administration led in particular by Al Gore. At the time this book went into press, there was uncertainty regarding the ratification of the Protocol by Russia, whose government suggested in July 2003 that it may also renege on its Kyoto commitments. Ratification by Russia would remove the final obstacle to the entering into force of the Protocol, as the presence of Russia would ensure that the group of countries that have ratified the protocol would collectively account for more than 55% of global carbon emissions.

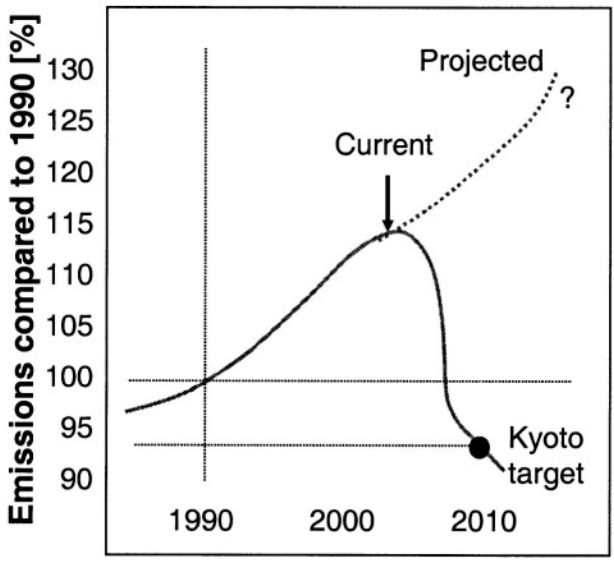

Figure 9.2. Emission pathways for the United States with and without commitments to the Kyoto Protocol.

A problem that also needs consideration is related to the fact that the Kyoto Protocol refers to *1990* emissions levels, and not the *current* emissions that, for many countries, are significantly higher than in 1990. This is particularly the case for the United States, whose long cycle of economic growth in the 1990s resulted in an increase of close to 15% in energy consumption and carbon emissions (UNEP, 2003). This implies that if the United States, or other countries that have increased their emissions since 1990 were to commit themselves to reductions according to the Kyoto agreements, they would need to cut back not only by the 5-8% negotiated in 1997, but also by the difference in emissions since 1990. The emissions pathways shown in Figure 9.2 for the United States, where the Kyoto target is unlikely to be met because of current climate policy, shows that the

increases in emissions are likely to exceed 30% compared to 1990 values by 2010 (UNEP, 2003).

Other countries, particularly those with economies in transition (essentially the former Soviet Union and Central and Eastern Europe) have already largely met their Kyoto commitments because of the collapse of an industrial system based on low-quality fuels and highly polluting production processes. Countries such as Poland or the Czech Republic have seen their carbon emissions reduced by 20% or more since 1990 (UNEP, 2003) through a restructuring of their industry and a technological migration towards western emissions standards. The political reunification of Germany in 1990 has also had the surprising consequence that carbon emissions in a reunified Germany have been reduced by over 15% as a result of the collapse of ageing industrial infrastructure in the former East Germany.

Whatever the future of the implementation of the Kyoto Protocol, further and more stringent measures will be required in the post-Kyoto period beyond 2012. This is because in order to simply achieve *stabilization* of greenhouse gases in the atmosphere, it is necessary to remove the 3 Gt of carbon that accumulate in the atmosphere each year out of the 7 Gt that are emitted globally, i.e., a reduction of close to 50% of current values. Post-Kyoto targets require political will and technological solutions beyond the levels that are being considered in the current Kyoto implementation phase.

9.3. INTERPRETATION AND IMPLICATIONS OF ARTICLES OF THE FRAMEWORK CONVENTION

Article 2 of the FCCC poses a number of problems of interpretation, and the manner in which the objectives may be achieved. For example, the objective does not specify what levels of greenhouse-gas concentrations may be considered as "safe". This acknowledges that there is currently no scientific certainty about what a dangerous level would be. For example, a relatively modest level of climatic change may have little or no impact on certain ecosystems, while others may face extinction at that particular level of change. The question that thus arises is whether *all* ecosystems should be protected, in which case anthropogenic climate change would need to remain confined within the bounds of natural climatic variability. If only selected ecosystems were to be protected, then it would be essential to determine the thresholds of vulnerability beyond which damage may become irreversible. In many cases, vulnerability thresholds are poorly known, in part because the functioning of plants has for the most part been studied only in contemporary environments and climates. There are also ethical issues to be

addressed when determining the priorities for the protection of a particular species or ecosystem.

Adaptation of natural ecosytems to climatic change cannot be achieved without some kind of human intervention, in the form of management. There may be a degree of natural adaptation for certain species that have a reasonably large tolerance to heat and moisture stresses, potentially aided by the CO_2 fertilization effect. Sustainably managed agricultural lands, rangelands, and forests can play a key role in reducing current emissions of carbon dioxide, methane, and nitrous oxide by acting as carbon sinks. Emissions can be reduced, or carbon sequestered, through improved management of agricultural soils, restoration of degraded agricultural lands, establishment of plantations, agroforestry, forest regeneration, and the slowing down or even the reversal of deforestation. For all ecological systems, the reduction of pollution and land-use stresses would normally increase the resilience of certain plants to change.

The possible causes and predicted effects of global climate change have precipitated an intense interest in the conservation of species and their habitats. One approach to ecosystem conservation is the setting up of *refugia, migration corridors,* and possibly also *assisted migration.* Refugia are buffer-zones that can play the role of allowing ecosystems to adapt or migrate to change. National parks with restricted access, and biosphere reserves are one form of refugia. Improvements in integrated fire, pest, and disease management techniques can also enhance the resilience of species. Ecosystems in many parts of the world have been so fragmented and the population density is so high that some of these options may be impossible to implement. In addition, some biospheric reserves may be too small to become viable refugia. Zimmermann and Kienast (1999), for example, have shown that in the Swiss National Park (an area of 200 km^2 located in the south-eastern part of Switzerland), less than half the migrating species could be hosted because of the altitudinal limits of the mountains found within the park's boundaries. Furthermore, the establishment of refugia in many parts of the world could result in increasing conflicts between economic development and environmental concerns.

Global food security, as seen in Chapter 1, is highly sensitive to climate variability and change, and the manner in which this aspect is alluded to in Article 2 of the FCCC is also open to interpretation. The IPCC (1996) Report states clearly that *global* agricultural levels will be able to keep pace with population increases and with climatic change, but that there will be wide *regional* discrepancies, with the poorer nations becoming even more dependent than currently on the major producing countries for basic foodstuffs. The economic development of many nations of the south would

suffer from this increased dependency on the countries of the north, because much of the hard currency required for achieving a certain standard of well-being would be in fact used for purchasing food.

Environmental change presents a number of challenges for policy making, because of the long time scales of climate and other elements of the global environment, the long time lags between emissions and the response of the climate system to particular levels of greenhouse gases in the atmosphere, the numerous uncertainties involved, the very heterogeneous nature of climate-related impacts and the potential for irreversible damages or costs. The international cooperation that is essential for collectively addressing the truly global nature of climatic change is often minimal as a result of conflicting interests between nations or groups of nations.

Many of today's anthropogenically-induced environmental problems clearly originate in developed countries, either directly (e.g., greenhouse-gas emissions which are leading to global warming) or indirectly (e.g., by delocalizing polluting industries from the rich countries towards the developing world). The basic principle of the FCCC is that the industrialized countries should take the lead in implementing appropriate measures to reduce the amplitude of climatic change and its adverse impacts, while acknowledging the common but differentiated responsibilities and respective capabilities of all Parties to protect the climate system. Economic growth, social development and environmental protection are interdependent and mutually reinforcing components of sustainable development. Any policy decision aimed at averting the adverse impacts of change need to take into account the legitimate priority needs of developing countries for the achievement of sustainable development and the eradication of poverty.

The FCCC promotes action in spite of uncertainty on the basis of a recent development in international law and diplomacy referred to as the *"precautionary principle"* Under traditional international law, an activity has generally not been restricted or prohibited unless a direct causal link between that activity and a particular damage can be shown. But in the case of many environmental issues, such as stratospheric ozone depletion, no action could be taken if definite proof of a cause-to-effect relationship needed to be demonstrated. The international community has gradually come to accept the precautionary principle under which activities that threaten serious or irreversible damage can be restricted or even prohibited before there is absolute scientific certainty about their effects. A very successful precedent is that of the 1987 Montreal Protocol, by which all nations agreed to prohibit or significantly curtail their production of CFCs, that were suspected of playing a major role in stratospheric ozone depletion. Subsequently, the role of CFCs in the "ozone hole" problem was unequivocably demonstrated; the

signing of a treaty in the absence of definite proof was in part a tribute to the application of the precautionary principle, but was also the result of the availability of substitute products for CFCs, so that the solution to ozone depletion became an opportunity for many industrial sectors.

Application of the precautionary principle to climatic change would be just as warranted as it was in the context of the "ozone hole" problem. However, unlike the CFCs that were replaced with relative ease, CO_2 and other greenhouse gas abatement strategies pose an entirely different set of problems. Because of the dependency of the global economy almost exclusively on fossil fuels, any measures aimed at reducing greenhouse gas emissions hits at the heart of the economies of most nations. In time, addressing the issues of substantial energy savings will become inevitable, although currently, any serious attempts at achieving these objectives are complicated by the fact that economic and social development is currently governed by the availability and affordability of energy services. Reductions of greenhouse gases and environmental pollutants through cutbacks in energy production could lead to intractable development and economic problems that could overshadow the improvements in environmental quality.

The most promising options in the industrial sector are more efficient motors, control systems, co-generation, energy cascading, and materials recycling. Changes in vehicle design, propulsion systems and fuels could reduce emissions by 40% in 2025 relative to a high emissions scenario (IPCC, 1996). Projected growth in energy demand in commercial and residential structures could be cut by one-half by 2025 with more efficient heating, cooling, lighting, and appliances. Technology-based approaches for reducing greenhouse gas emissions from energy supply include gas turbines, coal and biomass gasification, production of transportation fuels from biomass, approaches to handling intermittent generation of electricity, wind energy utilization, electricity generation with photovoltaics and solar thermal electric technologies, fuel cells for power generation, and hydrogen as a major new energy carrier, produced first from natural gas and later from biomass, coal, and electrolysis. Renewable energy sources could provide a substantial portion of foreseeable energy needs of the world over the next century; potentially most promising is biofuels for electricity generation and transportation fuel.

If no policy intervention were to be implemented in the near future, the IPCC (2001) notes that there would be a substantial increase in greenhouse gas emissions in the industrial, energy and transportation sectors. An extensive array of technologies and policy measures capable of mitigating greenhouse gas emissions exists today, but there is a high degree of controversy related to the economics of implementation of appropriate

technologies and measures. These are linked to social, institutional, financial, market and legislative barriers to their application and implementation in many countries.

The choice of abatement paths thus involves balancing the economic risks of stringent emission controls now against the risks of delay. Mitigation measures undertaken in a way that capitalize on other environmental benefits could be cost-effective and enhance sustainable development. Whatever the solutions ultimately chosen, the availability of low carbon technologies is a prerequisite for, but not a guarantee of, the ability to reduce greenhouse gas emissions at reasonable cost.

9.4. THE ROLE OF SCIENCE

The pursuit of knowledge, which for almost one thousand years was considered to be a value unto itself, now finds itself under stringent political scrutiny, and there is an increasing pressure on science to be geared towards short-term economic rewards, In such a context, long-term research on the environment and climate is often seen in many countries, concerned about budget restrictions, as a secondary priority compared to domains that can contribute directly and rapidly to the economy. The early 21st century thus finds itself in a paradoxical situation, where the instrument and knowledge base required to address complex long-term environmental issues exists, but where political support is absent. Over time, such a paradox can only be detrimental to *both* the environment *and* the economy.

Scientists have a key role to play above and beyond simply providing up-to-date research results. They need not only to convince politicians of the urgency to act in terms of environmental protection and sustainable economic development, but they also need to convince society as a whole through accessible results and clearly-defined recommendations. As in many aspects of policy-making, it is through raising the awareness of the general public (i.e., the voters in a democratic system) to various issues that politicians may be moved to consider the issues at hand and attempt to define appropriate response strategies. This may be a more challenging task in certain developing countries, where access to information is often still very difficult, and where the management of environmental resources and climate is less of a priority than health, education, infrastructure and attempting to raise the general standards of living.

It is necessary to plan in terms of decades to centuries when addressing the numerous issues related to climatic change. Many of the impacts of these changes may not become apparent for several generations, which implies

that scientific persuasion needs to be efficient and coherent in order to convince political and economic actors to consider options aimed at reducing the amplitude and rapidity of climatic change. Many of the policies and decisions related to pollution abatement, climatic change, deforestation or desertification are in fact likely to provide opportunities and challenges for both the private and public sectors, if economic thinking accepts returns on investment on the long term rather than on the very short term. A carefully selected set of national and international responses aimed at mitigation, adaptation and improvement of knowledge can reduce the risks posed by climatic change to ecosystems, food security, water resources, human health and other natural and socio-economic systems.

International cooperation in a framework of bilateral, regional or international agreements could significantly reduce the global costs severe environmental stress. If carried out with care, these responses would help to meet the challenge of climatic change and enhance the prospects for sustainable economic development for the peoples and nations of the only "life-support system" that is currently available to humankind: Planet Earth.

Bibliography

Aagard, K., and Carmack, E. C. , 1989: The role of sea ice and other fresh water in the Arctic circulation. J. Geophys. Res., 94, 14,485-14,498.

Abegg, B., and R. Froesch, 1994: Climate change and winter tourism: impact on transport companies in the Swiss Canton of Graubünden. In: Beniston, M. (ed.), Mountain environments in changing climates. Routledge Publishing Company, London and New York, pp. 328-340

Abegg, B., Koenig, U., Burki, R., and Elsasser, H., 1997: Climate impact assessment in tourism. Die Erde, 128, 105-116

Alley, R. B. et al., 2003: Abrupt climate change. Science, in press.

Appenzeller, C., J. Schwander, S. Sommer, and T. F. Stocker, 1998, The North Atlantic Oscillation and its Imprint on Precipitation and Ice Accumulation in Greenland. Geophys. Res. Lett. 25, 1939-1942.

Arakawa, A., and W. H. Schubert, 1974: Interaction of a cumulus cloud ensemble with the large-scale environment, Part I. J. Atmos. Sci., 31, 674-701.

Archer, S., Schimel, D.S., and Holland, E.A., 1995: Mechanisms of shrubland expansion: land use, climate or CO_2? Climatic Change 29:91–99

Armelagos, G. J., 1991: The origins of agriculture: population growth during a period of declining health. Popul. Environm., 13, 9-22

Arnell, N., 1999: The effect of climate change on hydrological regimes in Europe. Global Environmental Change, 9, 5-23

Baltensperger U., Gäggeler H. W., Jost D. T., Lugauer M., Schwikowsko M., Weingartner E., and Seibert P., 1997: Aerosol Climatology at the High-Alpine Site Jungfraujoch, Switzerland. J. Geophys. Res., Vol 102, No 16, 19707-19715

Bantle, H., 1989. Program documentation for the Swiss climate data base at the computing center of ETH-Zurich. MeteoSuisse publication, Zurich, Switzerland (in German)

Barry, R.G. and Chorley, R.J., 1992. Atmosphere, Weather & Climate, 6th edn. Routledge Publishers, London. 392pp.

Barry, R.G., 1994. Past and potential future changes in mountain environments; A review, In: Beniston, M. (ed.), Mountain

environments in changing climates. Routledge Publishing Company, London and New York, pp. 3-33

Baumgartner, M.F., and G. Apfl, 1994: Monitoring snow cover variations in the Alps using the Alpine Snow Cover Analysis System (ASCAS), Mountain Environments in Changing Climates, M. Beniston,(ed.), Routledge Publishing Company, London and New York, 108-120.

Becker, A. and Bugmann, H. (eds.), 1997. Predicting Global Change Impacts on Mountain Hydrology and Ecology: Integrated Catchment Hydrology/Altitudinal Gradient Studies. International Geosphere-Biosphere Programme (IGBP) Report 43, Stockholm

Becker, A., and Bugmann, H. (eds.), 2001: Global Change and Mountain Regions. The Mountain Research Initiative. IGBP Report 49, Stockholm

Begert, M., et al., 2003: Homogenization of climate time series and computation of the 1961-1990 norms. MeteoSuisse Publication, 67, 170 pp, Zurich, Switzerland (in German)

Beniston, M., 1997a: Variations of snow depth and duration in the Swiss Alps over the last 50 years : links to changes in large-scale forcings. Climatic Change, 36, 281-300

Beniston, M., 1997b: From Turbulence to Climate. Springer, Heidelberg and New York, 330 pp.

Beniston, M., 2000: Environmental Change in Mountains and Uplands. Arnold Publishers, London, and Oxford University Press, New York, 172pp.

Beniston, M. (ed), 2002: Climatic change. Implications for the hydrological cycle and for water management. Advances in Global Change Research, Kluwer Academic Publishers, Dordrecht and Boston, 503 pp.

Beniston, M., 2003. Climatic change in mountain regions: a review of possible impacts. Climatic Change, 59, 5-31

Beniston, M., 2004: The 2003 heat wave in Europe. A shape of things to come? Geophysical Research Letters, 31, 2022-2026.

Beniston, M. and Schmetz, J. , 1985. A three dimensional study of mesoscale model response to radiative forcing. Boundary Layer Meteorol., 31, 149-175.

Beniston, M., Rebetez, M., Giorgi, F., and Marinucci, M. R., 1994: An analysis of regional climate change in Switzerland. Theor. and Appl. Clim., 49, 135-159.

Beniston, M., and Rebetez, M., 1996: Regional behavior of minimum temperatures in Switzerland for the period 1979 – 1993. Theor. Appl. Climatol. ,53,231-243.

Beniston, M., Fox, D. G., Adhikary, S., Andressen, R., Guisan, A., Holten, J., Innes, J., Maitima, J., Price, M., and Tessier, L., 1996: The Impacts of Climate Change on Mountain Regions. Second Assessment Report of the Intergovernmental Panel on Climate Change (IPCC), Chapter 5, Cambridge University Press, pp. 191 – 213

Beniston, M., Diaz, H. F., and Bradley, R. S., 1997: Climatic change at high elevation sites; a review. Climatic Change, 36, 233-251.

Beniston, M., and Jungo, P., 2002: Shifts in the distributions of pressure, temperature and moisture in the alpine region in response to the behavior of the North Atlantic Oscillation. Theor. and Appl. Clim., 71, 29-42

Beniston, M., F. Keller, and S. Goyette, 2003: Snow pack in the Swiss Alps under changing climatic conditions: an empirical approach for climate impacts studies. Theor. Appl. Climatol., 74, 19-31

Beniston, M., Keller, F., Koffi, B., and Goyette, S., 2004: Estimates of snow accumulation and volume in the Swiss Alps under changing climatic conditions. Theoretical and Applied Climatology, 76, 125-140

Benoit, R., 1977: On the Integral of the Surface Layer Profile-Gradient Functions. J. Appl. Meteorol. 16, 859-860

Berger, A., 1978: Long-term variations of caloric insolation resulting from the Earth's orbital elements. Quat. Res., 9, pp. 139-167.

Berger, A.., 1992: Le Climat de la Terre : Un passe pour quel avenir?, De Boeck, Brussels, Belgium, 479 pp.

Bergström, S., Carlsson, B., Gardelin, M., Lindström, G., Pettersson, A. and Rummukainen, M., 2001: Climate change impacts on runoff in Sweden - assessments by global climate models, dynamical downscaling and hydrological modelling. Climate Research 16, 101-112

Betts, A. K., 1986: A new convective adjustment scheme. Part I: Observational and theoretical basis. Quart. J. R. Met. Soc., 112, 677-691.

Betts, A. K., and M. J. Miller, 1986: A new convective adjustment scheme. Part II: Single column tests using GATE wave, BOMEX, ATEX and arctic air-mass data sets. Quart. J. R. Met. Soc., 112, 693-709.

Blatter, H., 1987: On the thermal regime of an Arctic valley glacier: a study of White Glacier, Axel Heiberg Island, N.W.T., Canada. Journal of Glaciology 33, 114, 200 - 211.

Bonan, G.B., 1995: Land-atmosphere interactions for climate system models: Coupling biophysical, biogeochemical, and ecosystem dynamical processes. Rem. Sens. Env, 51, 57-73

Bond, G. C. and Lotti, R., 1995: Iceberg discharges into the North Atlantic on millennial time scales during the last glaciation. Science 267, pp. 1005-1010.

Bordes, F. 1973: On the chronology and contemporaneity of different Paleolithic cultures in France. In, Renfrew, C. (ed.) The explanation of culture change: Models in Prehistory. Duckworth, London, pp. 217-226

Bortenschlager, S., 1993: Das höchst gelegene Moor der Ostalpen "Moor am Rofenberg" 2760 m. Festschrift Zoller, Diss. Bot., 196, 329-334.

Boville, B.A. and P.R. Gent, 1998: The NCAR Climate System Model, Version One. J. Climate, 11, 1115-1130.

Bradley, R.S., 1999: Paleoclimatology: reconstructing climates of the Quaternary. Harcourt/Academic Press, San Diego, 610pp

Brankovic, C. and Palmer, T., 2000: Seasonal skill and predictability of ECMWF PROVOST ensemble, Quart. J. R. Met. Soc., 126, 2035-2069.

Briffa, K.R., 2000: Annual climate variability in the Holocene: interpreting the message of ancient trees. Quat. Sci. Rev., 19, 87-105

Broecker, W. S., Peteet, D., and Rind, D:, 1985 : Does the ocean-atmosphere system have more than one stable mode of operation ? Nature, 315, 21-26

Broecker, W.S., 1982: Ocean chemsitry during glacial time. Geochim. Cosmochim. Acta., 46, 1689-1705.

Broecker, W.S., 2000: Abrupt climate change: causal constraints provided by the palaeoclimate record. Earth Science Reviews, 51, 137-154.

Broecker, W.S., Peteet, D.M., and Rind, D., 1985: Does the ocean-atmosphere system have more than one stable mode of operation? Nature 315, 21-26.

Brown R. D., 1998: Spatial and temporal variability of Canadian monthly snow depths 1946-1995. Atmosphere-Ocean, 36, 37-54

Brubaker, L.B., 1986: Responses of tree populations to climate change. Vegetatio 67:119–130

Bryan, P.O., 1998: Climate drift in a multi century integration of the NCAR Climate System Model. J. Climate, 11, 1455-1471.

Bryden, H. L. and Imawaki, S., 2001: Ocean Circulation and Climate: Observing and Modelling the Global Ocean (eds. Siedler, G., Church, J. and Gould, J.), Academic Press, New York, pp. 455-474.

Bugmann, H., and A. Fischlin, 1994: Comparing the behaviour of mountainous forest succession models in a changing climate,. In: Mountain Environments in Changing Climates, M. Beniston, (ed.), Routledge Publishing Company, London and New York, 204-219

Bugmann, H., and Pfister, C., 2000: Impacts of interannual climate variability on past and future forest composition. Regional Environmental Change, 3/4, 112-125

Burrows, C.J, 1990: Processes of Vegetation Change, Unwin Hyman Publishing, London, 551

Businger, J. A., 1973: Turbulent transfer in the atmospheric surface layer. In Haugen, A. (ed.), 1973: Workshop on Micrometeorology. AMS Publications, Boston, USA,, pp. 67-100

BUWAL, 2000 : Data on: www.unece.org/trade/timber/storm/swi/degats.pdf

Carraro, G., Klötzli, F., Walther, G.-R., Gianoni, P., and Mossi, R., 1999: Observed changes in vegetation in relation to climate warming. VdF Publications, ETH-Zürich, Switzerland, 110 pp.

Castles, S. and Miller, M. J., 1993: The Age of Migration: International Population Movements in the Modern World. New York: The Guildford Press.

Cavalli-Sforza, L. L., Menozzi, P., and Piazza, A., 1994: The history and geography of human genes. Princeton University Press, Princeton, USA

Cayan, D. R., 1996: Interannual climate variability and snow-pack in the Western United States. Journal of Climate, 9, 928-948

Cayan, D.R., S.A. Kammerdierner, M.D. Dettinger, J.M. Caprio, and D.H. Peterson, 2001: Changes in the onset of spring in the western United States. Bull. Amer. Meteorol. Soc., 82, 399-415.

Charlson, R.J., Lovelock, J.E., Andreae, M.O. and Warren, S.G., 1987: Oceanic phytoplankton, atmsopheric sulphur, cloud albedo and climate. Nature, 326, 655-661.

Charlson, R.J., Schwartz, S.E., Hales, J.M., Cess, R.D., Coakley, J.A., Hansen, J.E. and Hofmann, D.J., 1992: Climate forcing by anthropogenic aerosols. Science, 255, 422-430.

Chen, S. S., R. A. Houze Jr., and B. E. Mapes, 1996: Multiscale variability of deep convection in relation to large-scale circulation in TOGA-COARE.. J. Armos. Sci., 53, 1380-1409.

Chinn, T. 1996. New Zealand glacier responses to climate change of the past century. New Zealand Journal of Geology and Geophysics 39, 415-428

Christensen, O. B., Christensen, J. H., Machenhauer, B., and Botzet, M., 1998: Very high-resolution regional climate simulations over Scandinavia – Present climate. J. Climate, 11, 3204-3229

Christensen, J. H., Carter, T. R., and Giorgi, F., 2002: PRUDENCE employs new methods to assess European climate change, EOS (American Geophysical Union Newsletter), 83, 13

Christensen, J.H., and Christensen, O.B., 2003: Severe summer-time flooding in Europe, Nature, 421, 805-806

Ciais, P., P. Tans, J.W.C. White, M. Trolier, R.J. Francey, J.A. Berry, D.R. Randall, P.J. Sellers, J.G. Collatz and D.S. Schimel, 1995: Partitioning of ocean and land uptake of CO_2 as inferred by $\delta^{13}C$ measurements from the NOAA climate monitoring and diagnostics laboratory global air sampling network, J. Geophys. Res., 100, 5051–5070

Clark, M. P., Serreze, M. C, and Robinson, D. A., 1999: Atmosphere controls on Eurasian snow extent. International Journal of Climatology, 19, 27-40

CLIVAR, 2003: www.clivar.org/recent/highlight.htm

Clot, B., 2003: Trends in airborne pollen: an overview of 21 years data in Neuchâtel (Switzerland). Aerobiologia, 19, 27-234

Clottes, J., (ed) 2001: La Grotte Chauvet, l'Art des Origines. Editions du Seuil, Paris

Cohen, M., 1977: The food crisis in prehistory. Yale Univ. Press, New Haven

Commoner, B., 1991: Rapid Population Growth and Environmental Stress. International Journal of Health Services 21 (2): 199-227.

Cook, E.R., B.M. Buckley and R.D. D'Arrigo, 2000: Warm-Season Temperatures since 1600 B.C. Reconstructed from Tasmanian Tree Rings and Their Relationship to Large-Scale Sea Surface Temperature Anomalies. Clim. Dyn., 16, 79-91

Cook, E.R., R.D. D'Arrigo and K.R. Briffa, 1998: A reconstruction of the North Atlantic Oscillation using tree-ring chronologies from North America and Europe. The Holocene, 8, 9-17

Cordell, L.S., 1984: Prehistory of the Southwest. Academic Press, New York

Coughlan, J. C., and S. W. Running, 1997: Regional ecosystem simulation A general model for simulating snow accumulation and melt in mountainous terrain. Lanscape Ecology, 12, 119-136.

Craig, M. H., Snow, R. W., and LeSueur, D., 1999: A climate-based distribution model of malaria transmission in Africa. Parasitology Today, 15, 105-111

Crowley, T.J., 2000: Causes of climate change over the past 1000 years. Science, 289: 270-277.

Crowley, T. J. and North, G.R. 1991: Paleoclimatology, Oxford University Press, New York

Crowley, T.J. and Lowery, T., 2000: How warm was the Medieval warm period? Ambio, 29, 51-54

Cullen, H., R. D'Arrigo, E. Cook and M.E. Mann, 2001: Multiproxy-based reconstructions of the North Atlantic Oscillation over the past three centuries. Paleoceanography, 16, 27-39

Cumming, S.G. and Burton, P.J., 1996: Phenology-mediated effects of climatic change on some simulated British Columbia forests. Climatic Change, 34(2), 213-222

D'Arrigo, R.D., E.R. Cook, M.J. Salinger, J. Palmer, P.J. Krusic, B.M. Buckley and R. Villalba, 1998: Tree-ring records from New Zealand: long-term context for recent warming trend. Clim. Dyn., 14, 191-199

Dai A., Trenberth, K. E. and Karl, T. R., 1999: Effects of clouds, soil moisture, precipitation and water vapor on diurnal temperature range. J. Climate, 12, 2451-2473.

Davis, K., and M. S. Bernstam. eds. 1993: Resources, Environment, and Population: Present Knowledge and Future Options, Population and Development Review: a Supplement to Volume 16. The Population Council, New York: Oxford University Press

Davis, M. B., 1989: Lags in vegetation response to greenhouse warming. Climatic Change, 15, 75-82

Davis, M.B., 1986: Climatic instability, time lags, and community disequilibrium, Community Ecology, J. Diamond, and TJ. Case, (eds.), Harper and Row, New York, 269-284.

Deardorff, J.W., 1978: Efficient prediction of ground surface temperature and moisture, with inclusion of a layer of vegetation. J. Geophys. Res., 83, 1889-1903.

Dehn, M., Bürger, G., Buma, J., and Gasparetto, P., 2000. Impacts of climate change on slope stability using expanded downscaling. Engineering Geology, 55. 193-204

Delage, Y., Lei W., and Bélanger, J.M., 1999: Aggregation of Parameters for the Land Surface Model CLASS. Atmosphere-Ocean, 37, 125-137

Deque, M., 2003: Uncertainties in the temperature and precipitation response of PRUDENCE runs over Europe. Abstract from the European Science Foundation and PRUDENCE 3rd Annual Conference on "Regional Climate Change in Europe", Wengen, Switzerland, September 29-October 3, 2003

Derome, J., Brunet, G., Plante, A., Gagnon, N., Boer, G. J., Zwiers, F., Lambert, S., Sheng, J., and Ritchie, H., 2001: Seasonal prediction based on two dynamical models, Atmos.-Ocean, 39, 56-68.

Dettinger, M. D. and Cayan, D. R.: 1995, 'Large-scale Atmospheric Forcing of Recent Trends towardEarly Snowmelt Runoff in California', J. Climate 8, 606-623.

Diaz, H. F. and Bradley, R. S., 1997. Temperature variations during the last century at high elevation sites. Climatic Change, 36, 253 - 279

Diaz, H. F., and Markgraf, V., 1993: El Niño: historical and paleoclimatic aspects of the Southern Oscillation : Cambridge University Press, Cambridge, UK, 476 pp.

Dickinson, R.E., 1995: Land processes in climate models. Rem. Sens. Env. 51,27-38

Doblas-Reyes, J., Deque M., and Piedelievre, J.-P., 2000: Multi-model spread and probabilistic seasonal forecasts in PROVOST, Quart. J. R. Met. Soc., 126, 2069 - 2089.

Dukes, J. S., and Mooney, H. A., 1999: Does global change increase the success of biological invaders? Trends in Ecology and Evolution, 14, 135-139

Ekhart, E., 1948: De la structure de l'atmosphère dans la montagne. La Météorologie, 3, 3-26

Elias, S., 1997: The Ice-Age history of Southwest National Parks. Smithsonian Institution Press, Washington, D.C., 216 pp.

Emanuel, K. A., and Ivkovi-Rothman, M., 1999: Development and evaluation of a convection scheme for use in climate models. J. Atmos. Sci., 56, 1766-1782.

Emberlin J, Detandt M, Gehrig R, Jäger S, Nolard N, Rantio-Lehtimaki, 2002: Responses in the start of Betula (birch) pollen seasons to recent changes in spring temperatures across Europe. Int. J. Biometeorol., 46, 159-70.

Engelman, R., and LeRoy, P., 1993: Sustaining Water Population and the Future of Renewable Water Supplies

Epstein, P. R., Diaz, H. F., and Elias, S., 1998:. Biological and physical signs of climate change. Focus on mosquito-borne diseases. Bull Am Meteorol Soc, 78,410-417

Falloon, P., Smith, P., Coleman, K. and Marshall, S. 1998: Estimating the size of the inert organic matter pool from total soil organic carbon content for use in the Rothamsted Carbon Model. Soil Biology and Biochemistry, 30, 1207-1211.

FAO, 2000: The State of Food and Agriculture. FAO Agriculture Series, Rome, 356 pp.

Fitzharris, B. B., Allison, I., Braithwaite, R.J., Brown, J., Foehn, P., Haeberli, W., Higuchi, K., Kotlyakov, V.M., Prowse, T.D., Rinaldi, C.A., Wadhams, P., Woo, M.K., Youyu Xie, 1996: The Cryosphere: Changes and their impacts. In: Second Assessment Report of the Intergovernmental Panel on Climate Change (IPCC), Chapter 5, Cambridge University Press, pp. 241-265

Fliri, F., 1975. Das Klima der Alpen im Raume von Tirol, Universitäts Verlag Wagner, Innsbruck, München

Flohn, H., 1968. Contributions to a meteorology of the Tibetan Highlands. Atmospheric Physics Paper 130, Dept.of Atmospheric Sciences, Colorado State University, Fort Collins. 120 pp.

Fornos, W., 1992: Desperate Departures: The Flight of Environmental Refugees. Washington, D.C.,The Population Institute.

Fosberg, M.A., 1990 : Global change – a challenge to modeling. In : Process modeling of forest growth responses to environmental stress Dixon, R.K., R.S. Meldahl, G.A. Ruark, and W.G. Warren (eds.). Timber Press, Inc., Portland, OR, USA, pp. 3-8.

Fouquart, Y., 1987: Radiative transfer in climate modeling. NATO Advanced Study Institute on Physically-Based Modeling and Simulation of Climate and Climatic Changes. Erice, Sicily, 11-23 May 1986.

Frei, A. and Robinson, D. A., 1999: Northern Hemisphere snow extent: Regional variability. International Journal of Climatology, 19, 1535-1560

Frei, C., and Schaer, C., 2000 : Detection probability of trends in rare events: Theory and application to heavy precipitation in the Alpine region. Journal of Climate, 2001,14, 1568-1584

Frei, C., Schär, C., Lüthi, D., and Davies, H.C., 1998. Heavy precipitation processes in a warmer climate. Geophysical Research Letters, 25, 1431-1434

Frei T. and Leuschner, R.M., 2000: A change from grass pollen induced allergy to tree pollen induced allergy: 30 years of pollen observation in Switzerland. Aerobiologia, 16,407-416.

Friis-Christensen, E. and Lassen, K., 1991: Length of the solar cycle, an indication of solar activity closely associated with climate. Science, 254, 698-700

Fritts, H.C., 1976: Tree Rings and Climate. Academic Press, New York.

Fuhrer, J., 2003: Agroecosystem responses to combinations of elevated CO_2, ozone, and global climate change. Agriculture, Ecosystems and Environment, 97, 1-20.

Furbish, D.J. and Andrews, J.T., 1984: The use of hypsometry to indicate long-term stability and response of valley glaciers to changes in mass transfer. Journal of Glaciology, 30, 105, 199 - 211.

Galloway, R.W., 1988: The potential impact of climate changes on Australian ski fields, Greenhouse Planning for Climate Change, G.I. Pearman, (ed.), CSIRO, Aspendale, Australia, 428-437

Ganachaud, A. and Wunsch, C., 2000: Improved estimates of global ocean circulation, heat transport and mixing from hydrographic data. Nature 408, 453-457.

Garr, C.E., and Fitzharris, B.B., 1994: Sensitivity of mountain runoff and hydro-electricity to changing climate, Mountain Environments in Changing Climates, M. Beniston, (ed.), Routledge Publishing Company, London and New York, 366-381.

GCOS publications, 1992 – 2003 : World Meteorological Organization, Geneva, Switzerland (85 reports at URL: www.wmo.ch/web/gcos)

Gear, A.J., and Huntley, B., 1991: Rapid changes in the range limits of Scots Pine 4,000 years ago, Science, 251, 544-547

Gibson, K.R., 1996: The biocultural brain, seasonal migrations, and the emergence of the upper Paleolithic. In: Mellars, P., and Gibson, K.R. (eds.), Modelling the early human mind. Cambridge University Press, 33-46

Giorgi, F. and Mearns, L.O., 1991: Approaches to the simulation of regional climate change: a review. Reviews of Geophysics, 29: 191-216.

Giorgi, F., and Mearns, L. O., 1999. Regional climate modeling revisited. Journal of Geophysical Research., 104, 6335-6352

Giorgi, F., Brodeur, C.S., and Bates, G.T., 1994: Regional climate change scenarios over the United States produced with a nested regional climate model. J. Clim., 7, 375 - 399.

Giorgi, F., Hurrell, J., Marinucci, M., and Beniston, M., 1997: Height dependency of the North Atlantic Oscillation Index. Observational and model studies. J. Clim., 10, 288 – 296

Glantz, M.H., (ed.), 1988: Societal Responses to Regional Climatic Change, Westview Press, Boulder, Colorado.

Gleick, P., 1990: Environment, resources and international security and politics. In: E.H. Arnett (ed), Science and International Security: Responding to a Changing World. Washington, D.C.: American Association for the Advancement of Science, pp. 501-523

Gleick, P.H., 1987: Methods for evaluating the regional hydrologic impacts of global climatic changes, J. Hydrology, 88, 97-116.

Godde, P., Price, M.F. and Zimmermann, F.M. (eds.), 2000: Tourism and Development in Mountain Regions. CABI Publishing, Wallingford

Godfrey, J.S., R.A. Houze, K.M. Lau, R. Lukas, P.J. Webster, and R.A. Weller, 1998: TOGA-COARE: How well have we progressed towards understanding air-sea coupling in the warm pool?"COARE '98: Proceedings, Conference on TOGA-COARE, 7-14 July 1998, Boulder, Colorado.

Gordon, A.L., 1986: Interocean exchange of thermocline water. J. Geophys. Res., 91, 5037-5046.

Gordon, C., C. Cooper, C.A. Senior, H.T. Banks, J.M. Gregory, T.C. Johns, J.F.B. Mitchell and R.A. Wood, 2000: The simulation of SST, sea ice extents and ocean heat transports in a version of the Hadley Centre coupled model without flux adjustments. Clim. Dynamics, 16, 147-168.

Govi, M., 1990. Conférence spéciale: Mouvements de masse récents et anciens dans les Alpes italiennes. Proceedings of the Fifth Symposium on Landslides, Lausanne, 3,1509 -1514.

Goyette, S., Beniston, M., Jungo, P., Caya, D., and Laprise, R., 2001. Numerical investigation of an extreme storm with the Canadian Regional Climate Model: The case study of windstorm Vivian, Switzerland, February 27, 1990. Climate Dynamics, 18, 145-168

Goyette, S., Brasseur, O., and Beniston, M., 2003: Application of a new wind gust parameterisation ; multi-scale case studies performed with the Canadian RCM. J. Geophys. Res., 108, 4374-4389

Grabherr, G., M. Gottfried, and H. Pauli, 1994: Climate effects on mountain plants, Nature, 369, 448.

Grabherr, G., M. Gottfried, and H. Pauli, 2001: High mountain environment as indicator of global change. In: Visconti, G., Beniston, M., Iannorelli, E. D, and Barba, D. (eds.), Global Change and Protected Areas. Kluwer Academic Publishers, Dordrecht and Boston, 331-345.

Graham, R.L., Turner, M.G., and Dale, V.H., 1990: How increasing CO_2 and climate change affect forests. BioScience 40:575–587

Grenfell T.C. and Maykut, G.A., 1977: Theoptical properties of ice and snow in the Arctic Basin, J. Glaciol., 18, 445-463

Guilyardi, E. and Madec, G., 1997: Performance of the OPA/ARPEGE-T21 global ocean-atmosphere coupled model. Clim. Dynamics, 13, 149-165

Guisan, A., J. Holten, R. Spichiger, and L. Tessier, (eds.), 1995: Potential Impacts of Climate Change on Ecosystems in the Alps and Fennoscandian Mountains. Annex Report to the IPCC Working Group II Second Assessment Report, Publication Series of the Geneva Conservatory and Botanical Gardens, University of Geneva, Switzerland, 194 pp.

Gunn, J. M., and Keller, W., 1990: Biologial recovery of an acid lake after reduction in industrial emissions of sulphur. Nature, 345,431-433

Gustafsson, D, M. Stähli, and P.-E. Jansson, 2001: The surface energy balance of a snow cover: comparing measurements to two different simulation models. Theor. Appl. Climatol., 70, 81-96.

Gyalistras, D., von Storch, H., Fischlin, A., and Beniston, M., 1994: Linking GCM-Simulated Climatic Changes to Ecosystem Models: Case Studies of Statistical Downscaling in the Alps. Clim. Res., 4, 167 - 189

Haeberli, W., 1990. Glacier and permafrost signals of 20th century warming, Annals of Glaciology, 14, 99-101

Haeberli, W., 1995: Glacier fluctuations and climate change detection - operational elements of a worldwide monitoring strategy. WMO Bulletin 44, 1, 23-31.

Haeberli, W., and Beniston, M., 1998. Climate change and its impacts on glaciers and permafrost in the Alps. Ambio, 27, 258 – 265

Haeberli, W. and Funk, M., 1991: Borehole temperatures at the Colle Gnifetti core-drilling site (Monte Rosa, Swiss Alps). Journal of Glaciology 37, 125, 37-46.

Halpin, P.N., 1994: Latitudinal variation in montane ecosystem response to potential climatic change, M. Beniston, (ed.), Mountain Ecosystems in Changing Climates, Routledge Publishing Company, London and New York, 180-203.

Hansen-Bristow, K.J., Ives, J.D., and Wilson, J.P., 1988: Climatic variability and tree response within the forest-alpine tundra ecotone, Annals of the Association of American Geographers, 78, 505-519.

Hantel, M., Ehrendorfer, M., and Haslinger, A., 2000: Climate sensitivity of snow cover duration in Austria. International Journal of Climatology, 20, 615-640

Harris, M., 1991: Cannibals and kings, the origins of cultures. Vintage Books, New York

Harrison, E. F., Minnis, P., Barkstrom, B. R., Ramanathan, V., Cess, R. C., and Gibson, G. G., 1990: Seasonal variation of cloud radiative forcing derived from the Earth Radiation Budget Experiment. J. Geophys. Res., 95,18687-18703.

Harrison, S. J., 1993: Differences in the duration of snow cover on Scottish ski slopes between mild and cold winters. Scottish Geographical Magazine, 109, 37-44

Hastenrath, S and Greischar, L., 1997. Glacier recession on Kilimanjaro, East Africa, 1912-89. Journal of Glaciology 43 (145), 455-459

Hastenrath, S. and Kruss, P. D., 1992: The dramatic retreat of Mount Kenya's glaciers 1963-87: greenhouse forcing. Annals of Glaciology, 16, 127-133

Haugen, A. (ed.), 1973: Workshop on Micrometeorology. AMS Publications, Boston, USA, 392 pp.

Hay, S. I., Cox, J., Rogers, D. J., Randolph, S. E., Stern, D. I., Shanks, D. G., Myers, M. F., and Snow, R. W., 2002 : Climate change and the resurgence of malaria in the East African highlands. Nature, 415, 905-909

Hedberg, O., 1964: The phytogeographical position of the afroalpine flora, Recent Advances in Botany, 914-919.

Heino R., R. Brazdil, E. Forland, H. Tuomenvirta, H. Alexandersson, M. Beniston, C. Pfister, M. Rebetez, G. Rosenhag, S. Rösner, J. Wibig, 1999 : Progress in the study of climatic extremes in northern and Central Europe. Climatic Change, 42, 151-181.

Henderson-Sellers, A., and McGuffie, K., 1987: A Climate Modeling Primer. J. Wiley, 217 pp.

Hodge, S.M., Trabant, D.C., Krimmel, R.M., Heinrichs, T.A., March, R.S., and Josberger, E.G., 1998: Climate variations and changes in mass of three glaciers in western North America. Journal of Climate 11, 2161-2179

Holten J, I. (ed.), 1990: Biological and ecological consequences of changes in climate in Norway. NINA Institute Research Report, 11, 1 – 59

Holten, J.I., and Carey, P.D., 1992: Responses of climate change on natural terrestrial ecosystems in Norway, NINA Institute Research Report, 29, 1-59

Holton, J. R., 1972: An Introduction to Dynamic Meteorology. Academic Press, New York, 319 pp.

Homer-Dixon, T., 1991: On the threshold: environmental changes as causes of acute conflict. International Security, 16(2): 76-116

Horel, J.D. and Wallace, :J. M., 1981: Planetary scale atmospheric phenomena associated with the Southern Oscillation. Mon. Weather Rev., 109, 817-829

Houghton, J., 1984: The global climate. Cambridge University Press, Cambridge (UK), 233 pp.

Hughes, M. G. and Robinson, D. A., 1996: Historical snow cover variability in the Great Plains region of the USA: 1990 through to 1993. International Journal of Climatology, 16, 1005-1018

Hughes, M. K., Kelly, P. M., Pilcher, J.R., and LaMarche, V.C., (eds), 1982: Climate from Tree Rings. Cambridge University Press, Cambridge, 223 pp.

Hughes, M.K., E.A. Vaganov, S. Shiyatov, R.Touchan and G. Funkhouser, 1999: Twentieth century summer warmth in northern Yakutia in a 600 year context. The Holocene, 9, 603-308

Huntley, B. 1991: How plants respond to climate change: migration rates, individualism and the consequences for plant communities, Annals of Botany, 67, 15-22.

Hurrell J., 1995: Decadal trends in the North Atlantic Oscillation regional temperatures and precipitation. Science, 269, 676-679.

Hurrell, J. W., and van Loon, H., 1997 : Decadal variations in climate associated with the North Atlantic Oscillation. Climatic Change, 36, 301-326

IAHS (ICSI)/UNEP/UNESCO, 1994: Glacier Mass Balance Bulletin no. 3 (W. Haeberli, M. Hoelzle and H. Boesch, eds.). World Glacier Monitoring Service, ETH Zurich.

Indermühle, A., Monnin, E., Stauffer, B., and Stocker, T. F., 2000: Atmospheric CO_2 concentration from 60 to 20 kyr BP from the Taylor Dome ice core, Antarctica. Geophys. Res. Letters, 27, 735-738.

IPCC, 1990: Climate Change. The Intergovernmental Panel on Climate Change Scientific Assessment (Houghton, J., Callander, B., and Varney, S., eds.). Cambridge University Press, Cambridge and New York.

IPCC, 1994: The Radiative Forcing of Climate. Special Report of the Intergovernmental Panel on Climate Change. Cambridge University Press, Cambridge and New York, 339 pp.

IPCC, 1996: Climate Change. The Intergovernmental Panel on Climate Change (IPCC) Second Assessment Report. Cambridge University Press, Cambridge and New York. Volumes I (Science), II (Impacts) and III (Socio-economic implications)

IPCC, 1998: The regional impacts of climate change. Cambridge University Press, Cambridge and New York, 517 pp.

IPCC, 2001: Climate Change. The Inetergovernmental Panel on Climate Change (IPCC) Third Assessment Report. Cambridge University Press, Cambridge and New York

Jacobson, J., 1988: Environmental Refugees: A Yardstick of Habitability. Worldwatch Paper No. 86, Washington DC

Jaeger, J., 1983, Climate and Energy Systems: A Review of their Interactions. J. Wiley Publishers, New York.

Jochem, E., Sathaye, J., and Bouille, D. (eds.), 2000: Society, Behaviour, and Climate Change Mitigation. Advance in Global Change Research, Volume 8, Dordrecht, The Netherlands and Boston, USA. 237 pp.

Johns, T.C, et al., 2003. Anthropogenic climate change for 1860 to 2100 simulated with the HadCM3 model under updated emission scenarios. Climate Dynamics, 20, 583-612

Johnson, E. A., 1992: Fire and vegetation dynamics. Studies from the North American boreal forest. Cambridge University Press, Cambridge.

Jolly, C. L. May 1993. Four Theories of Population Change and the Environment. Population and Environment 16 (1)

Jones, D., and Cordell, L.S., 1985: The Anasazi world. Graphic Arts Center Publishing Company, Portland, USA

Jones, P.D. and Moberg, A., 2003: Hemispheric and large-scale surface air temperature variations: an extensive revision and an update to 2001. Journal of Climate, 16, 206-223

Jones, P.D., Jónsson, T. and Wheeler, D., 1997: Extension to the North Atlantic Oscillation using early instrumental pressure observations from Gibraltar and South-West Iceland. Int. J. Climatol. 17, 1433-1450.

Jones, P.D., K.R. Briffa, T.P., Barnett and S.F.B. Tett, 1998: High-resolution palaeoclimatic records for the last millennium: interpretation, integration and comparison with General Circulation Model control run temperatures. The Holocene, 8,455-471

Jones, P.D., New, M., Parker, D.E., Martin, S. and Rigor, I.G., 1999 : Surface air temperature and its changes over the past 150 years. Reviews of Geophysics, 37, 173-199

Jungo, P., and Beniston, M., 2001: Changes in the anomalies of extreme temperatures in the 20th Century at Swiss climatological stations located at different latitudes and altitudes. Theor. and Appl. Clim., 69, 1-12

Kapos, V., Rhind, J., Edwards, M., Ravilious, C., and Price, C., 2000: Developing a map of the world's mountain forests. In: Price, M.F., and Butt, N. (eds.), Forests in a sustainable mountain environment. CAB International, Wallingford.

Karl, T. R., Jones, P. D., Knight, R. W., Kukla, G., Plummer, N., Razuvayev, V., Gallo, K. P., Lindseay, J., Charlson, R. J., and Peterson, T. C., 1993: Asymmetric trends of daily maximum and minimum temperature. Bull. American Meteorol. Soc., 74, 1007-1023

Katz, R. W., and Brown, B. G., 1992: Extreme events in a changing climate: Variability is more important than averages. Climatic Change, 21, 289-302

Kay, B.H. et al., 1989: Rearing temperature influences flavivirus vector competence of mosquitoes. Med. Vet. Entomol., 3, 415-422.

Keeling, C.D., Chin, J.F.S., and Whorf, T.P., 1996: Increased activity of northern vegetation inferred from atmospheric CO_2 measurements. Nature, 382,146-149.

Keeling, C.D., and Whorf, T.P., 2000: Atmospheric CO2 records from sites in the SIO air sampling network. In: Trends: A compendium of data on global change. Carbon Dioxide Information Analysis Center, Oak Ridge National Laboratory, Oak Ridge, Tennessee, USA.

Keller, F., and Goyette, S., 2003: Snow melt under the different temperature increase scenarios in the Swiss Alps. In: de Jong, C., Collins, D., and Ranzi, R. (Eds.), Climate and Hydrology in Mountain Areas. J. Wiley Publishing Co., UK., accepted.

Keller, F., Goyette, S., and Beniston, M., 2004: Sensitivity analysis of snow cover to climate change scenarios and their impact on plant habitats in alpine terrain. Climatic Change, under review.

Keller, F., and Körner, C., 2003. The role of photoperiodism in alpine plant development. Arctic, Antarctic and Alpine Research, in press

Keller, F., Kienast, F., and Beniston, M., 2000: Evidence of the response of vegetation to environmental change at high elevation sites in the Swiss Alps. Regional Env. Change, 2, 70-77

Keller, T., 1999 : Variabilité climatique interannuelle quantifiée à partir de la densité et des isotopes stables de la cellulose du bois. PhD Thesis, University of Aix-Marseille (France), 198 pp.

Kienast, F., Wildi, O., Brzeziecki, B., Zimmermann, N., and Lemm, R., 1998: Klimaänderung und mögliche langfristige Auswirkungen auf die Vegetation der Schweiz. VdF Hochschulverlag, Zurich, 71 pp.

King, G.A. and Neilson, R.P., 1992: The transient response of vegetation to climate change : a potential source of CO_2 to the atmosphere. Water, Air and Soil Pollution, 64, 365-383.

Kirchofer, W., (ed.), 2001. Climate Atlas of Switzerland. MeteoSuisse (Swiss Weather Service) publication, Zürich, Switzerland (in German and French).

Kitayama, K., 1996: Climate of the summit region of Mount Kinabalu (Borneo) in 1992, an El Niño year. Mountain Research and Development, 16(1), 65-75

Klein, S. A., and Hartmann, D. L., 1993: The seasonal cycle of low stratiform clouds. J. Climate, 6, 1587-1606.

Klötzli, F., 1991. Longevity and stress, Modern Ecology: Basic and Applied Aspects, G. Esser, and D. Overdiek, (eds.), Elsevier, Amsterdam, 97-110

Klötzli, F., 1994. Vegetation als Spielball naturgegebener Bauherren, Phytocoenologia, 24, 667-675

Knutti, R., and Stocker, T. F., 2002: Limited predictability of the future thermohaline circulation close to an instability threshold. J. Climate, 15, 179-186.

Koenig, U., and Abegg, B., 1997: Impacts of climate change on winter tourism in the Swiss Alps. Journal of Sustainable Tourism, 5, 46-57

Körner, C. and Larcher, W., 1988: Plant life in cold climates. In: Long, S.F. and Woodward, F.I. (eds.), Plants and temperature. The Company of Biol Ltd, Cambridge, pp. 25-57

Körner, C., 1994: Impact of atmospheric changes on high mountain vegetation. In: Beniston, M. (ed.), Mountain environments in changing climates. Routledge Publishing Company, London and New York, pp. 155-166

Körner, C., 1998: Worldwide positions of alpine treelines and their causes. In: Beniston, M., and Innes, J. L. (eds.), The Impacts of Climate Variability on Forests. Lecture Notes in Earth Sciences, 74, Springer-Verlag, Heidelberg and New York, pp. 221-229

Körner, C., 1999: Alpine Plant Life. Springer-Verlag, Heidelberg and New York, 338 pp.

Krenke, A.N., G.M. Nikolaeva, and A.B. Shmakin, 1991: The effects of natural and anthropogenic changes in heat and water budgets in the central Caucasus, USSR, Mountain Res. Devel., 11, 173-182.

Krippendorf, J., 1984: The capital of tourism in danger, The Transformation of Swiss Mountain Regions, E.A. Brugger, et al., (eds.), Haupt Publishers, Bern, 427-450

Kuhn, M., 1981: Climate and glaciers. IAHS Publication 131, 3 - 20.

Kuhn, M., 1989: Response of the equilibrium line altitude to climate fluctuations: theory and observations. In: Glacier Fluctuations and Climatic Change, Kluwer, pp. 407-417.

Kuhn, M., 1990: Energieaustausch Atmosphäre - Schnee und Eis. In: Schnee, Eis und Wasser der Alpen in einer wärmeren Atmosphäre. Mitteilungen der Versuchsanstalt für Wasserbau, Hydrologie und Glaziologie der ETH Zurich 108, 21 - 32.

Kuhn, M., 1993: Possible future contribution to sea-level change from small glacier. In: Warrick, R.A., Barrow, E.M., and Wigley, T.M.L., (Eds.), Climate and sea-level change: Observations, projections and implications. Cambridge University Press, Cambrisge, UK, pp. 134-143

Lambert, S.J. and Boer, G.J., 2001: CMIP1 evaluation and intercomparison of coupled climate models. Clim. Dyn., 17, 83-106.

Lamothe, M., and Périard, D., 1988: Implications of climate change for downhill skiing in Quebec, Climate Change Digest, Atmospheric Environment Service, Downsview, 88-103

Laprise R., Caya, D., Giguère, M., Bergeron, G., Côte, H., Blanchet, J.-P., Boer, G.J. and McFarlane, N.A., 1998: Climate and climate change in

western Canada as simulated by the Canadian regional climate model. Atmosphere-Ocean, 36, 119–167.

Leavesley, G.H., 1994: Modeling the effects of climate change on water resources - A review, Assessing the Impacts of Climate Change on Natural Resource Systems, K.D. Frederick, and N. Rosenberg, (eds.), Kluwer Academic Publishers, Dordrecht, 179-208.

Lee III, R. B., Barkstrom, B. R. and R. D. Cess, 1987: Characteristics of the Earth Radiation Budget Experiment Solar Monitors. Appl. Optics, 26, 3090-3096.

Legates, D. R., and Willmott, C. J., 1990: Mean seasonal and spatial variability in gauge-corrected global precipitation. Int. J. Climatol., 10, 111-127

Letréguilly, A. and Reynaud, L., 1990: Space and time distribution of glacier mass balance in the northern hemisphere. Arctic and Alpine Research 22, 1, 43-50.

Leuschner R.M., Christen H., Jordan P. and Vonthein R.: 2000, 30 years of studies of grass pollen in Basel (Switzerland). Aerobiologia 16, 381-391.

Lindsay, S. W., and Martens, W. J. M., 1998: Malaria in the African highlands, past, present and future. WHO Bulletin, 76, 33-45

Lindzen, R.S., 1981: Turbulence and stress due to gravity wave breakdown. J. Geophys. Res., 87, 3061-3080.

Lloyd, A.H., and L.J. Graumlich, 1995: Dendroclimatic, ecological, and geomorphological evidence for long-term climatic change in the Sierra Nevada, USA, Tree Rings, Environment, and Humanity, J.S. Dean, D.M. Meko, and T.W. Swetnam, (eds.), University of Arizona, Tucson, Arizona

Loevinsohn, M., 1994: Climatic warming and increased malaria incidence in Rwanda. The Lancet, 343, 714-718

Lonergan, S, and Parnwell, M., 1999: Environmental degradation and population displacement. Environment and Security

Lonergan, S.C. and Brooks, D., 1994. Watershed: The Role of Freshwater in the Israeli-Palestinian Conflict. Ottawa: IDRC Press

Lorenz, E. N., 1963: Deterministic non-periodic flow. J. Atmos. Sci., 20, 130-141.

Lorenz, E. N., 1968: Climate determinism. Meteorol. Monogr., 8, AMS Publications, Boston

Lorenz, E. N., 1969: The predictability of a flow which possesses many scales of motion. Tellus, 21, 289 - 307.

Lorenz, E. N., 1982: Atmospheric predictability experiments with a large numerical model. Tellus, 34, 505 - 513.

Machenauer, B., 1977: On the dynamics of gravity oscillations in a shallow water model with applications to normal mode initialization. Contr. Atmos. Phys., 50, 253-271.

Maisch, M., 1992: Die Gletcher Graubündens - Rekonstruktion und Auswertung der Gletscher und deren Veränderungen seit dem Hochstand von 1850 im Gebiet der östlichen Schweizer Alpen (Bündnerland und angrenzende Regionen). Publication Series of the Department of Geography of the University of Zurich, Switzerland.

Maisch, M., 1998 : Die Gletscher der Schweizer Alpen. VdF Publishers, Zurich, 378 pp.

Manabe, S. and Stouffer, R. L, 1993: Century-scale effects of increased atmospheric CO_2 on the ocean-atmosphere system. Nature 364, 215-218.

Mann, M., and Bradley, R. S., 1999: Northern Hemisphere temperatures during the past millennium: inferences, uncertainties, and limitations. Geophys. Res. Letters, 26, 759-762

Mann, M.E., Bradley, R.S. and Hughes, M.K., 1999: Global-scale temperature patterns and climate forcing over the past six centuries. Nature, 392, 779-787.

Mann, M.E., E. Gille, R.S. Bradley, M.K. Hughes, J.T. Overpeck, F.T. Keimig and W. Gross, 2000: Global temperature patterns in past centuries: An interactive presentation. Earth Interactions, 4, 1-29

Marinucci M. R., F. Giorgi, M. Beniston, M. Wild, P. Tschuck, A. Ohmura, and A. Bernasconi, 1995: High resolution simulations of januray and july climate over the Western alpine region with a nested regional modelling system. Theor. Appl. Climatol., 51, 119-138.

Martens, P., Kovats, R. S., and Nijhof, S., 1999: Climate change and future populations at risk from malaria. Global Environmental Change, 9, 89-107

Martens, P., Niessen, L. W., Rotmans, J., Jetten, T. H., and McMichael, A. J., 1995: Potential impact of global climate change on malaria risk. Environmental Health Perspectives, 103, 458-464

Martin, E., and Durand, Y., 1998: Precipitation and snow cover variability in the French Alps. In: Beniston, M., and Innes, J. L. (Eds.), The Impacts of Climate Change on Forests, Springer-Verlag, Heidelberg/New York, pp. 81-92

Martin, E., Brun, E., and Durand, Y., 1994 : Sensitivity of the French Alps snow cover to the variation of climatic variables. Annales Geophysicae, 12, 469-477.

Martin, E., Timbal, B., and Brun, E., 1997: Downscaling of general circulation model outputs: simulation of the snow climatology of the

French Alps and sensitivity to climate change. Climate Dynamics, 13, 45-56

Martinec, J., Rango, A., and Major, E., 1983 : The Snowmelt Runoff Model (SRM) User's Manual. NASA Reference Publication 1100, Scientific and Technical Information Branch

Martinec, J., and Rango, A., 1989: Effects of climate change on snow melt runoff patterns, Remote Sensing and Large-Scale Global Processes, Proceedings of the IAHS Third Int. Assembly, Baltimore, Md, May 1989, IAHS Publ. No. 186, 31-38.McArthur, R.H., 1972: Geographical Ecology, Harper and Row, New York.

Maunder, W.J., 1986: The Uncertainty Business, Methuen and Co. Ltd, London, 420.

McArthur, R.H., 1972: Geographical Ecology, Harper and Row, New York.

McBean, G. and McCarthy, J., 1990: Narrowing the uncertainties. In: Climate Change: The IPCC Scientific Assessment, Intergovernmental Panel on Climate Change (IPCC), Houghton, J.T., Jenkins, G.J. & Ephraums, J.J. (eds.). Cambridge University Press, Cambridge, pp. 311-328.

McCorriston, J., and Hole, F., 1991: Ecology of seasonal stress and the origins of agriculture in the Near East. Amer. Anthropology, 93, 46-69

McFarlane, N.A., Boer, G.J., Blanchet, J.P., and Lazare, M, 1992: The Canadian Climate Centre Second-Generation General Circulation Model and its Equilibrium Climate. J. Clim. 5, 1013-1044

McMichael, A. J., and Haines, A., 1997: Global climate change: the potential effects on health. British Medical Journal, 315, 805-809

McMichael, A. J., Haines, A., Slooff, R. and Kovats, S., (eds) 1996: Climate Change and Human Health. WHO/WMO/UNEP. Geneva, Switzerland

McMichaels, A. J. and Kovats, R. S.: 2000, 'Climate change and climate variability. Adaptations to reduce adverse climate change impacts', Environ. Monit. Assess. 61, 49–64

McNeely, J. A., 1990: Climate change and biological diversity: policy implications, Landscape-Ecological Impact of Climatic Change, M.M. Boer, and R.S. de Groot, (eds.), IOS Press, Amsterdam.

Meier, M., 1998. Land ice on Earth: A beginning of a global synthesis. Unpublished transcript of the 1998 Walter B. Langbein Memorial Lecture, American Geophysical Union Spring Meeting, Boston, MA, 26 May 1998.

Melillo, J.M., Prentice, I.C., Farquhar, G.D., Schulze, E.-D., and Sala, O.E., 1996: Terrestrial biotic responses to environmental change and feedbacks to climate. In: Houghton, J.T., Meira Filho, L.G., Callander, B.A., Harris, N., Kattenberg, A., and Maskell, K., (eds), Climate

Change 1995. The Science of Climate Change. Cambridge University Press, Cambridge, pp 447–81

Mellars, P., 1991: Cognitive changes and the emergence of modern humans in Europe. Cambridge Archaeological Journal, 1, 63-76

MeteoSuisse, 2003: Swiss weather service report on 2003 heat wave at URL: www.meteosuisse.ch/fr/Previsions/Prevision/IndexPrevision.shtml

Meybeck, M., Green, P., and Vörösmarty, C., 2001. A New Typology for Mountains and Other Relief Classes: An Application to Global Continental Water Resources and Population Distribution. Mountain Research and Development, 21, 34-45

Michaels, A.F. and Knap, A.H., 1996: An overview of the US JGOFS Bermuda Atlantic Time-series Study and the Hydrostation S program. Deep Sea Research, 43, 157-198.

Mirza, M.Q., 1997: The runoff sensitivity of the Ganges river basin to climate change and its implications. Journal of Environmental Hydrology, 5, 1-13.

Monastersky, S., 2000: Drowned lands hold clues to first Americans. Science News, 157, 85-90

Monteith, J.L., 1973: Principles of Environmental Physics, Edward Arnold Publishers, 236 pp.

Mountain Agenda. 1998. Mountains of the World. Water Towers for the 21st Century, prepared for the United Nations Commission on Sustainable Development. Institute of Geography, University of Berne (Centre for Development and Environment and Group for Hydrology) and Swiss Agency for Development and Cooperation. Paul Haupt Publishers, Bern, Switzerland, 32 pp.

Mountain Agenda, 2001: Mountains of the World - Mountains, Energy and Transport. Price, M., Kohler, T., Wachs, T., Zimmermann, A. (eds.), Mountain Agenda, Bern, 51 pp.

Munich Re, 1999 : Annual review of natural catastrophes. Topics Journal, Munich.

Munich Re, 2002 : Topics, An annual review of natural catastrophes. Munich Reinsurance Company Publications, Munich, 49 pp.

Myers, N., 1993: Environmental refugees in a globally warmed world. Bioscience, 43, 752-761

Myers, N., and Tickell, C., 2001 : Cutting evolution down to our size. The Financial Times weekend supplement, October 27-28, 2001

Myneni, R. B., Keeling, C. D., Tucker, C. J., Asrar, G., 1999: Increased plant growth in the northern high latitudes from 1981 to 1991. Nature, 386, 698-702

Nakićenović, N., J. Alcamo, G. Davis, B. de Vries, J. Fenhann, S. Gaffin, K. Gregory, A. Grübler, T.Y. Jung, T. Kram, E.L. La Rovere, L. Michaelis, S. Mori, T. Morita, W. Pepper, H. Pitcher, L. Price, K. Raihi, A. Roehrl, H-H. Rogner, A. Sankovski, M. Schlesinger, P. Shukla, S. Smith, R. Swart, S. van Rooijen, N. Victor, Z. Dadi, 2000: IPCC Special Report on Emissions Scenarios, Cambridge University Press, Cambridge, United Kingdom and New York, NY, USA, 599 pp.

Neilson, R. P., 1986: High-resolution climatic analysis and southwest biogeography. Science 232:27–34

Nemes-Ribes, E., Sokoloff, D., Ribes, J.C., and Kremliovsky, M., 1994: The Maunder minimum and the solar dynamo, im Nemes-Ribes (ed), The solar engine and its influence on terrestrial atmosphere and climate, NATO ASI Series, vol. I 25, p 71.

Nicolis, G., and Prigogine, I., 1989: Exploring Complexity. Freeman Co., New York

Noble, I., and Gitay, H. : Climate change in desert regions. In : IPCC, 1998, The Regional Impacts of Climate Change, Watson, R. T., Zinyowera, M., and Moss, R. (eds.), Cambridge University Press, pp. 191–217

Noilhan, J., and Planton, S., 1989: A simple parameterization of land surface processes for meteorological models. Mon. Wea. Rev. 117: 536-549

Oerlemans, J., 1993: Modelling of glacier mass balance. In: Ice in the Climate System (Peltier, W.R., ed.). NATO ASI Series I, 12, Springer, 101-116.

Oke, T. R., 1987: Boundary Layer Climates, second edition. Routledge, London, 435 pp.

Oliger, J., and Sundström, A., 1978: Theoretical and practical aspects of some initial boundary value problems in fluid dynamics. J. Appl. Math., 35, 419-446

Osborne, T.J., 2002: The winter North Atlantic Oscillation: roles of internal variability and greenhouse gas forcing. CLIVAR Exchanges, 25, 54-58.

Osborne, T. J., Briffa, K. R., Tett, S. F. B., Jones, P. D., and Trigo, R. M., 1999: Evaluation of the North Atlantic Oscillation as simulated by a coupled climate model. Climate Dynamics, 15, 685-702

Overpeck, J.T., Rind, D., and Goldberg, R., 1990: Climate-induced changes in forest disturbance and vegetation. Nature, 343, 51–53

Ozenda, P., 1985. La Végétation de la Chaine Alpine dans l'Espace Montagnard Européen, Masson, Paris, 344.

Ozenda, P., and J.-L. Borel, 1991: Les Conséquences Ecologiques Possibles des Changements Climatiques dans l'Arc Alpin. Rapport Futuralp No.

1, International Centre for Alpine Environment (ICALP), Le Bourget-du-lac, France.Pauli, H., Gottfried, M., and Grabherr, G., 1998: Effects of climate change on mountain ecosystems. Upward shifting of alpine plants. World Resources Review, 8, 382-390

Paeth, H., A. Hense, R. Glowienka-Hense, R. Voss, and U. Cubasch, 1999: The North Atlantic Oscillation as an indicator for greenhouse-gas induced regional climate change. Climate Dynamics, 15, 953-960

Palmer, T.N., G.J. Shutts, and R. Swinbank, 1986: Alleviation of a systematic westerly bias in general circulation and numerical weather prediction models through an orographic gravity wave drag parameterization. Quart. J. Roy. Meteor. Soc., 112, 1001-1031

Paltridge, G. W. and C. M. R. Platt, 1976: Radiative Processes in Meteorology and Climatology. Elsevier.

Parnwell, M. J. G., 1993: Population Movements and the Third World. Routledge Publishing Company, London.

Parry, M. L., (ed), 2000 : Assessment of potential effects and adaptations for climatic change in Europe. The ACACIA Report, EU Publications, Brussels, 420 pp.

Parry, M., C. Rosenzweig, A. Iglesias, G. Fischer, and M. Livermore 1999: Climate change and world food security: A new assessment. Global Environ. Change, 9, S51-S67

Pavolov, P., Svendsen, J. I., and Indrelid, S., 2001: Human presence in the European Arctic nearly 40,000 years ago. Nature, 413, 64-67

Pebley, A.R., 1998: Demography and the Environment. Demography, 35, 377-389

Perry, A. H., 2000: Impacts of climate change on tourism. In: Parry, M. L. (ed), Assessment of Potential Effects and Adaptations for Climate Change in Europe; the ACACIA Report. Jackson Environment Institute, Norwich, and EU Publications, Brussels, pp.217-226

Perry, A. H., and Smith, K., 1996: Recreation and tourism. In: Department of the Environment, Climate Change Report, London, UK.

Peters, R.L., and Darling, J.D.S., 1985: The greenhouse effect and nature reserves: global warming would diminish biological diversity by causing extinctions among reserve species, Bioscience, 35, 707-717

Petit, J.R., Jouzel, J., Raynaud, D., Barkov, N.I., Barnola, J.-M., Basile, L, Bender, M., Chappellaz, J., Davis, M., Delaygue, G., Delmotte, M., Kotlyakov, V.M., Legrand, M., Lipenkov, V.Y., Lorius, C., Pepin, L., Ritz, C., Saltzman, E., and Stievenard, M. 1999: Climate and atmospheric history of the past 420,000 years from the Vostok ice core, Antarctica. Nature, 399, 429-436.

Pfister, C., R. Brázdil, R. Glaser, M. Barriendos Vallvé, D. Camuffo, M. Deutsch, P. Dobrovoln, S. Enzi, E. Guidoboni, O. Kotyza, S. Militzer, L. Rácz, and F.S. Rodrigo, 1999: Documentary Evidence on Climate in Sixteenth-Century Europe. Climatic Change, 43, 55-110

Philander, S.G.H., 1990: El Niño, La Niña, and the Southern Oscillation. Academic Press, San Diego, 289 pp.

Pielke, R. A., 1984: Mesoscale Meteorological Modeling. Academic Press, New York, 612 pp.

Pope, D.V, Gallani, M., Rowntree, R., and Stratton, A., 2000: The impact of new physical parameterizations in the Hadley Centre climate model HadAM3. Climate Dynamics, 16, 123-146

Poveda, G., Rojas, W., Quinones, M. L., Velez, I. D., Mantilla, R. I., Ruiz, D., Zuluaga, J. S., and Rua, G. I.: 2001: Coupling between annual and ENSO timescales in the malaria-climate association in Colombia, Environ. Health Perspect., 109, 489–493

Prentice, I.C., 1986: Vegetation response to past climate variation. Vegetatio, 67, 131–141

Prentice, I.C., 1992: Climate and long-term vegetation dynamics. In: Glenn-Lewin, D.C., Peet, R.A., and Veblen, T.T., eds: Plant Succession: Theory and Prediction. Chapman and Hall, London, pp 293– 339

Prentice, I.C., P.J. Bartlein, and T. Webb III, 1991: Vegetation and climate change in Eastern North America since the last glacial maximum, Ecology, 72, 2038-2052

Price M., Kohler, T., and Wachs, T. (eds.), 2000: Mountains of the world: Mountain Forests and Sustainable Development. Paul Haupt Publishers, Bern. 42 pp.

Price, M.F., 1990: Temperate mountain forests: common-pool resources with changing, multiple outputs for changing communities, Natural Resources Journal, 30, 685-707.

Prock, S., and Körner, Ch., 1996: A cross-continental comparison of phenology, leaf dynamics and dry matter allocation in arctic and temperate zone herbaceous plants form contrasting altitudes. Ecological Bulletins, 45, 93-103.

Quezel, P., and M. Barbero, 1990 : Les forêts méditerranéennes: problèmes posés par leur signification historique, écologique et leur conservation, Acta Botanica Malacitana, 15, 145-178

Quinn, W., V. T. Neal, and S. E. A. Mayolo, 1987: El Niño occurrences over the past four and a half centuries. Journal of Geophysical Research, 92, , 14449-14461

Rahmstorf, S., 2003: Thermohaline circulation: The current climate. Nature, 421, 699

Rameau, J.C., D. Mansion, G. Dumé, A. Lecointe, J. Timbal, P. Dupont, and R. Keller, 1993: Flore Forestière Française, Guide Ecologique Illustré, Lavoisier TEC and DOC Diffusion, Paris, 2419.

Rango, A., 1992 : Worldwide testing of the Snowmelt Runoff Model with applications for predicting the effects of climatic change. Nordic Hydrology, 23, 155-172

Ranzi, R., and Grossi, G., 1999: Ten years of monitoring areal snow pack in the Southern Alps using NOAA-AVHRR imagery, ground measurement and hydrological data. Hydrological Processes, 133, 2079-2095

Riedo, M., Gyalistras, D., and Fuhrer, J., 2000: Net primary production and carbon stocks in differently managed grasslands: site-specific sensitivity to an increase in atmospheric CO_2 and to climate change. Ecological Modelling, 134, 207-227

Riedo, M., Gyalistras, D., and Fuhrer, J., 2001: Pasture responses to elevated temperature and doubled CO_2 concentration: Assessing the spatial pattern across an alpine landscape. Climate Research, 17, 19-31

Robertson, A., Overpeck, J., Rind, D., Mosley-Thompson, E., Zielinski, G., Lean, J., Koch, D., Penner, J., Tegen, I. and Healy, R., 2001: Hypothesized climate forcing time series for the last 500 years. J. Geophys. Res., 106, 14,783-14,803

Robin, G. de Q., 1983: The climatic record in polar ice sheets, Cambridge University Press, Cambridge, 212 pp.

Rodgers, J. C., 1997: North Atlantic storm track variability and its association to the North Atlantic Oscillation and climate variability of Northern Europe. J. Climate, 10, 1635-1647

Roesch, A., Wild, M., Gilgen, H., and Ohmura, A., 2001: A new snow cover fraction parameterization for the ECHAM4 GCM. Clim. Dyn., 17, 933-946

Rotach, M., Wild, M., Tschuck, P., Beniston, M., and Marinucci, M. R., 1996: A double CO_2 experiment over the Alpine region with a nested GCM-LAM modeling approach. Theor. and Appl. Clim., 57, 209-227

Ruddiman, W.F. and Kutzbach, J.E., 1991: Plateau uplift and climatic change. Scientific American, 264, 42-50.

Salinger, M.J. and M.S. McGlone, 1989: New Zealand Climate – The past two million years. The New Zealand Climate report 1990, Royal Society of New Zealand, Wellington, 13-17.

Salinger, M.J., J.M. Williams, and W.M. Williams, 1989: CO_2 and Climate Change: Impacts on Agriculture, New Zealand Meteorological Service, Wellington.

Saltzmann, B., (Ed.), 1983: Theory of Climate. Advances in Geophysics, Vol. 25. Academic Press, New York, 505 pp.

Sato, N., P. J. Sellers, D. A. Randall, E. K. Schneider, J. Shukla, J. L. Kinter III, Y.-T. Hou and E. Albertazzi, 1989: Effects of implementing the Simple Biosphere Model in a general circulation model. J. Atmos. Sci., 46, 2757-2782.

Schimel, D.S., 1995: Terrestrial biogeochemical cycles: Global estimates with remote sensing. Rem. Sens. Env., 51, 49-56

Schmetz J. and M. Beniston, 1986 : Relative effects of solar and infrared radiative forcing in a mesoscale model. Boundary Layer Meteorol., 34, 137-155

Schmitz, W.J., 1995: On the interbasin-scale thermohaline circulation, Rev. Geophys., 33, 151-173.

Schneider, U., 1992: Die verteilung des troposphärischen Ozons in Bayrischen Nordalpenraum. PhD Dissertation, University of Mainz

Schreier, H. and P.B. Shah, 1996: Water dynamics and population pressure in the Nepal Himalayas. Geojournal, 40, 45-51

Schubert, C., 1992: The glaciers of the Sierra Nevada de Mérida (Venezuela): a photographic comparison of recent deglaciation. Erdkunde, 46, 58-64

Schweingruber, F. H., 1993: Jahrringe und Umwelt, Dendroökologie, WSL Publications, Birmensdorf, Switzerland, 474 pp.

Schweingruber, F.H., Bräker, O.U. and Schär, E., 1979: Dendroclimatic studies on conifers from central Europe and Great Britain. Boreas, 8, 427-452

Sear, C.B., Kelly, P.M., Jones, P.D. and Goodess, C.M., 1987: Global surface-temperature responses to major volcanic eruptions. Nature, 330, 365-367.

Sellers, P. J., W. J. Shuttleworth, J. L. Dorman, A. Dalcher, and J. M. Roberts, 1989: Calibrating the single biosphere model for Amozonian tropical forest using feild and remote sensing data. Part I: Average calibration with field data. J. Appl. Meteor., 28, 727-759

Senior, C. A., and Mitchell, J. F. B., 1993: CO_2 and climate: The impact of cloud parameterization. J. Climate, 6, 393-418

Serreze, M. C., Carse, F., Barry, R. G., and Rogers, J. C., 1997: Icelandic low cyclone activity: Climatological features, linkages with the North Atlantic Oscillation, and relationships with recent changes in the Northern Hemisphere circulation. J. Climate, 10, 453-464

Serreze, M.C., J. Maslanik, T.A. Scambos, F. Fetterer, J. Stroeve, K. Knowles, C. Fowler, S. Drobot, R. Barry, and T.M. Haran, 2003: A

record minimum Arctic sea ice extent and area in 2002. Geophysical Research Letters, 30, 1110.

Shiklomanov, I. A., (ed), 2001: World water resources at the beginning of the 21st century. UNESCO Publications, Paris

Shugart, H.H., 1984: A Theory of Forest Dynamics. The Ecological Implications of Forest Succession Models. Springer-Verlag, New York, 278 pp.

Siegenthaler, U. and Sarmiento, J.L., 1993: Atmospheric CO_2 and the ocean. Nature, 365, 119-125

Smidt, S., 1991. Messungen nasser Freilanddepositionen der Forstlichen Bundesversuchsanstalt. FBVA-Berichte, ISSN 1013-0713 50, Nasse Deposition, Austria.

Solomon, A. M., 1986: Transient response of forests to CO_2-induced climate change: simulation modeling experiments in eastern North America. Oecologia, 68, 567–579

Spieksma, F.T.M. and Nikkels, A.H., 1998: Airborne grass pollen in Leiden, The Netherlands: annual variations and trends in quantities and season starts over 26 years. Aerobiologia, 14, 347-358

Stahle, D.W., M.K. Cleaveland, M.D. Therrell, D.A. Gay, R.D. D'Arrigo, P.J. Krusic, E.R. Cook, R.J. Allan, J.E. Cole, R.B. Dunbar, M.D. Moore, M.A. Stokes, B.T. Burns, J. Villanueva-Diaz and L.G. Thompson, 1998: Experimental Dendroclimatic Reconstruction of the Southern Oscillation. Bull. Am. Met. Soc., 79, 2137-2152

Stephens, G.L., 1984: The parametrization of radiation for numerical weather prediction and climate models. Mon. Wea. Rev., 112, 826-867

Stephenson, D. B., Chauvin, F., and Royer, J-F., 1998. Simulation of the Asian summer monsoon and its dependence on model horizontal resolution. Journal of the Met. Soc. of Japan, 76, 237-265

Stephenson, D.B., Rupa Kumar, K., Doblas-Reyes, F.J., Royer, J.-F., Chauvin, F. and Pezzulli, S. 1999: Extreme daily rainfall events and their impact on ensemble forecasts of the Indian monsoon. Monthly Weather Review, 127, 1954-1966

Stocker, T. F., and Schmittner, A., 1997: Influence of CO_2 emission rates on the stability of the thermohaline circulation. Nature, 388, 862-865

Stocks, B. J., Wotton, B. M., Flannigan, M. D., Fosberg, M. A., Cahoon, D. R., and Goldammer, J. G., 2001: Boreal forest fire regimes and climate change. Advances in Global Change Research, 7. Kluwer Academic Publishers, Dordrecht and Boston, pp. 233-246

Stouffer, R. J., and K. W. Dixon, 1998: Initialization of coupled models for use in climate studies: A review. In: Research Activities in

Atmospheric and Oceanic Modelling, Report No. 27, WMO/TD-No. 865, World Meteorological Organization, Geneva, Switzerland, I.1-I.8.

Street, R.B., and Semenov, S.M., 1990: Natural terrestrial ecosystems. In: Tegart, W.J. KcG., Sheldon, G.W., and Griffiths, D.C. (Eds.), Climate Change: The First Impacts Assessment Report. Australian Government Publishing Service, Chapter 3.

Street-Perrott, F.A. and Perrott, R.A., 1990: Abrupt climate fluctuations in the tropics: the influence of Atlantic ocean circulation. Nature, 343, 607-612.

Street-Perrott, F.A., and Perrott, R.A., 1990: Lake levels and climate reconstructions. In: Hecht, A. (Ed.), Palaeo-Climate Analysis and Modeling. J. Wiley, New York, pp. 291-340

Stull, R. B., 1988: An Introduction to Boundary Layer Meteorology. Atmospheric and Oceanographic Science Library, Volume 13. Kluwer Academic Publishers, Dordrecht. 680 pp.

Swiss Re, 1998: Natural catastrophes and major losses in 1997: Exceptionally few high losses. Sigma 3/1998, Zurich, Switzerland.

Swiss Re, 2003: Natural catastrophes and reinsurance. Swiss Reinsurance Company Publications, Zurich, 47 pp.

Tabor, M., 1989: Chaos and Integrability in Nonlinear Dynamics: An Introduction. New York: Wiley.

Tangborn, W.V., Fountain, A.G. and Sikonia, W.G., 1990: Effect of area distribution with altitude on glacier mass balance - a comparison of North and South Klawatti Glaciers, Washington Stae, U.S.A. Annals of Glaciology 14, 278-282

Teitelbaum, M., and J. Winter. 1993: The Missing Links: The Population-Environment Dynamics in Historical Perspective. In Population Environment Dynamics: Ideas and Observations, eds., G. D. Ness, W. D. Drake, and S. R. Brechin, pp. 17-31. Ann Arbor, Michigan: The University of Michigan Press.

Tennekes, H., and Lumley, J. L., 1972: A First Course in Turbulence. MIT Press, Cambridge, USA, 300 pp.

Teranishi H, kenda Y, Katoh T, Kasuya M, Oura E, Taira H, 2000: Possible role of climate change in the pollen scatter of Japanese cedar Cryptomeria Japonica in Japan. Climate Research, 14, 65-70.

Tessier, L., Guibal, F., and Schweingruber, F. H., 1997: Research strategies in dendroecology and dendroclimatology in mountain environments. Climatic Change, 36, 267-285

Tessier, L., Keller, T., Guiot, J., Edouard, J.-L., and Guibal, F., 1998: Predictive models of tree-growth: preliminary results in the French

Alps. In: Beniston, M., and Innes, J. L. (eds.), The Impacts of Climate Variability on Forests, Springer-Verlag (Heidelberg and New York), pp. 109-120

Thompson, L. G., E. Mosley-Thompson, M. E. Davis, N. Lin, T. Yao, M. Dyurgerov and J. Dai, 1993: "Recent warming": ice core evidence from tropical ice cores, with emphasis on central Asia. Global and Planetary Change, 7, 145-156

Thompson, L.G., Mosley-Thompson, E. and Henderson, K.A., 2000: Ice core paleoclimate records in tropical South America since the Last Glacial Maximum. Journal of Quaternary Science, 15, 377-394

Tickell, C., 1990: Environmental Refugees: The Human Impact of Global Environmental Change. In Minger, T. (ed.), Greenhouse Glasnost: The Crisis of Global Warming. The Ecco Press, New York

Timmermann, A., M. Latif, R. Voss, and A. Grötzner, 1998: Northern hemispheric interdecadal variability: a coupled air-sea mode, J. Clim. 11, 1906-1931

Trenberth, K., E., 1991: Climate System Modeling. Cambridge University Press, Cambridge. 788 pp.

Trenberth, K. E., 1999: Conceptual framework for changes of extremes of the hydrological cycle with climate change. Climatic Change, 42, 327-339

Ulbrich, U., Fink, A.H., Klawa, M., and Pinto, J.G., 2000: Three extreme storms over Europe in December 1999, Weather, 56

UN, 1992: Earth Summit: Agenda 21. The United Nations Programme of Action from RioThe final text of agreements negotiated by governments at the United Nations Conference on Environment and Development (UNCED), 3-14 June 1992, Rio de Janeiro, Brazil. 294 pp.

UNEP, 2003: Data on Kyoto emission targets available at URL: http://maps.grida.no/kyoto/

UNCWR, 1998: The United Nations Conference on Water Resources, Paris, France

UNHCR, 1993. The State of the World's Refugees: In Search of Solutions. United Nations High Commissioner for Refugees. Geneva, Switzerland

UNHCR, 1995: The State of the World's Refugees: In Search of Solutions. United Nations High Commissioner for Refugees. Geneva, Switzerland

UNHCR, 2000: The State of the World's Refugees: In Search of Solutions. United Nations High Commissioner for Refugees. Geneva, Switzerland

van Loon, H., and Shea, D.J., 1985: The Southern Oscillation. Part IV: The precursors south of 15S to the extremes of the oscillation. Mon. Wea. Rev., 113, 2063-2074

Veblen, T.T., and Markgraf, V., 1988: Steppe expansion in Patagonia? Quatern. Res., 30, 331–338

Viner, D., 2002: A qualitative assessment of the sources of uncertainty in climate change impacts assessment studies. In: Beniston, M. (ed.), Climatic Change: Implications for the Hydrological Cycle and for Water Management. Kluwer Academic Publishers, Dordrecht and Boston, 139-149.

Vuille, M., and Bradley, R. S., 2000: Mean annual temperature trends and their vertical structure in the tropical Andes, Geophys. Res. Lett., 27, 3885-3888

Voltolini, S., Minale, P., Troise, C., Bignardi, D., Modena, P., Arobba, D. and Negrini, A.C., 2000: Trend of herbaceous pollen diffusion and allergic sensitisation in Genoa, Italy. Aerobiologia, 16, 245-249

Wade, L. K., and McVean, D. N., 1969. Mt. Wilhelm studies; The alpine and subalpine vegetation. Australian National University, Canberra, 225 pp.

Walther, G.-R., , Post, E., Convey, P., Menzel, A., Parmesan, C., Beebee, T.J.C., Fromentin, J.-M., Hoegh-Guldberg, O.and Bairlein, F. 2002: Ecological responses to recent climate change. Nature, 416, 389-395

Wanner, H., Rickli, R., Salvisberg, E., Schmutz, C., and Schuepp, M., 1997: Global climate change and variability and its influence on Alpine climate - Concepts and observations. Theor. and Appl. Climatology, 58, 221-243

Wardle, P., 1973: New Zealand timberlines. Arctic and Alpine Research, 5, 127-136

Warren, H.E., and S.K. LeDuc, 1981: Impact of climate on energy sector in economic analysis. Journal of Applied Meteorology, 20, 1431-1439.

Webb, T., 1987: The appearance and disappearance of major vegetation assemblages long-term vegetational dynamics in eastern North America. Vegetatio, 69, 177–187

Webb, T., P.J. Bartlein, S.P. Harrison, and K.H. Anderson, 1993: Vegetation, lake levels and climate in eastern North America for the last 18,000 years, Global Climates Since the Last Glacial Maximum, H.E. Wright, J.E. Kutzbach, T. Webb III, W.F. Ruddiman, F.A. Street-Perrott, and P.J. Bartlein, (eds.), University of Minnesota Press, Minneapolis, 415-467

Weber R.O., P. Talkner, and G. Stefanicki, 1994: Asymmetric diurnal temperature change in the Alpine region. Geophysical Research Letters, 21, 8, 673-676

Weber R.O., P. Talkner, I. Auer, R. Böhm, M. Gajic-Capka, K. Zaninovic, R. Bradzil, and P. Fasko, 1997: 20th century changes of temperatures in the mountain regions of Central Europe. Climatic Change, 36, 327-344

WMO - World Meteorological Organization, 1999: WMO statement on the status of the global climate in 1998. WMO Publication Nr. 896, Geneva, Switzerland, 11 pp.

Westing, A. H., 1992: Environmental refugees: a growing category of displaced persons. Environmental Conservation, 19, 201-207.

WGMS, 2000: Glacier Mass Balance, Bulletin, W. Haeberli and M. Hoelzle (eds.), World Glacier Monitoring Service, ETH-Zurich, Switzerland

Whetton, P. H., Hennessy, K. J., Pittock, A. B., Fowler, A. M., and Mitchell, C. D., 1992: Regional impact of the enhanced greenhouse effect on Victoria. CSIRO Division of Atmospheric Research Annual Report 1991-1992. Commonwealth Scientific and Industrial Research Organisation, Mordialloc, 64 pp.

Whetton., P. H., Haylock, M. R., and Galloway, R., 1996: Climate change and snow cover duration in the Australian Alps. Climatic Change, 32, 447-479

Whiteman, D., 2000: Mountain Meteorology. Oxford University Press, 355 pp.

WHO, 1990: Potential health effects of climatic change. Report of a WHO Task Group. World Health Organization, Geneva.

WHO, 1999: World Health Report 1999. World Health Organization, Geneva.

WHO, 2003: The health impacts of 2003 summer heat-waves. Briefing note for the Delegations of the fifty-third session of the WHO (World Health Organization) Regional Committee for Europe, 12 pp.

Widmann, M. and C. Schär, 1997: A principal component and long-term trend analysis of daily precipitation in Switzerland. Int. J. Climatol., 17, 1333-1356.

Wilson M. L., Mahanty, B., Wannebo, A., MacDonald, P., Gleason, A., Smith, R., and Aksoy, S., 2001: Vector-borne Disease Associated with Irrigation, Agriculture, and Environmental Change in Southeastern Turkey: Application of Satellite Image Analysis. Yale-New Haven Medical Center Report

Wilson, M. L., Mahanty, B., Wannebo, A., MacDonald, P., Gleason, A., Smith, R., and Aksoy, S., 2001: Vector-borne disease associated with

irrigation, agriculture, and environmental change in south-eastern Turkey: Application of satellite image analysis. Yale-New Haven Medical Center Report.

Wolter, K., and M.S. Timlin, 1998: Measuring the strength of ENSO - how does 1997/98 rank? Weather, 53, 315-324

Woodward, F.I., Smith, T.M., amd Emanuel, W.R., 1995: A global primary productivity and phytogeography model. Global Biogeochemical Cycles, 9, 471–490

World Bank, 1995: Towards environmentally sustainable development in Sub-Saharan Africa. The World Bank, Washington, DC, USA, 300 pp.

WTO, 2000: Compendium of Tourism Statistics, Year 2000 Edition. World Tourism Organization Publications, Madrid, 235 pp.

Wunderle, S., Droz, M., and Kleindienst, H., 2002: Spatial and temporal analysis of the snow line in the Alps based on NOAA-AVHRR data. Geographica Helvetica, 57, 171-183

Xue, Y., P. J. Sellers, J. L. Kinter III, and J. Shukla, 1991: A simplified biosphere model for global climate studies. J. Climate, 4, 345-364

Yao, M.-S., and Del Genio, A. D., 1999: Effects of cloud parameterization on the simulation of climate changes in the GISS GCM. J. Climate, 12, 761-779

Ye, H., 2000: Decadal variability of Russian winter snow accumulation and its associations with Atlantic sea-surface temperature anomalies. International Journal of Climatology, 20, 1709-1728

Zhang, Q., Soon, W., Baliunas, S.L., Lockwood, G.W., Ski, B.A., and Radick, R.R., 1994: A method of determining possible brightness variations of the Sun in the past centuries from observations of solar-type stars, Astrophys. J., 427, L111-L114, 1994

Zierl, B., 2001: A water balance model to simulate drought in forested ecosystems and its application to the entire forested area in Switzerland. J. Hydrology, 242, 115-136

Zimmermann, N., and Kienast, F., 1999: Predictive mapping of alpine grasslands in Switzerland: Species versus community approach. Journal of Vegetation Science, 10, 469-482.

Zorita, E. and von Storch, H., 1999: The analog method - a simple statistical downscaling technique: comparison with more complicated methods. J. Climate, 12, 2474-2489

Advances in Global Change Research

1. P. Martens and J. Rotmans (eds.): *Climate Change: An Integrated Perspective.* 1999 ISBN 0-7923-5996-8
2. A. Gillespie and W.C.G. Burns (eds.): *Climate Change in the South Pacific: Impacts and Responses in Australia, New Zealand, and Small Island States.* 2000 ISBN 0-7923-6077-X
3. J.L. Innes, M. Beniston and M.M. Verstraete (eds.): *Biomass Burning and Its Inter-Relationships with the Climate Systems.* 2000 ISBN 0-7923-6107-5
4. M.M. Verstraete, M. Menenti and J. Peltoniemi (eds.): *Observing Land from Space: Science, Customers and Technology.* 2000 ISBN 0-7923-6503-8
5. T. Skodvin: *Structure and Agent in the Scientific Diplomacy of Climate Change.* An Empirical Case Study of Science-Policy Interaction in the Intergovernmental Panel on Climate Change. 2000 ISBN 0-7923-6637-9
6. S. McLaren and D. Kniveton: *Linking Climate Change to Land Surface Change.* 2000 ISBN 0-7923-6638-7
7. M. Beniston and M.M. Verstraete (eds.): *Remote Sensing and Climate Modeling: Synergies and Limitations.* 2001 ISBN 0-7923-6801 -0
8. E. Jochem, J. Sathaye and D. Bouille (eds.): *Society, Behaviour, and Climate Change Mitigation.* 2000 ISBN 0-7923-6802-9
9. G. Visconti, M. Beniston, E.D. Iannorelli and D. Barba (eds.): *Global Change and Protected Areas.* 2001 ISBN 0-7923-6818-1
10. M. Beniston (ed.): *Climatic Change: Implications for the Hydrological Cycle and for Water Management.* 2002 ISBN 1-4020-0444-3
11. N.H. Ravindranath and J.A. Sathaye: *Climatic Change and Developing Countries.* 2002 ISBN 1-4020-0104-5; Pb 1-4020-0771-X
12. E.O. Odada and D.O. Olaga: *The East African Great Lakes: Limnology, Palaeolimnology and Biodiversity.* 2002 ISBN 1-4020-0772-8
13. F.S. Marzano and G. Visconti: *Remote Sensing of Atmosphere and Ocean from Space: Models, Instruments and Techniques.* 2002 ISBN 1-4020-0943-7
14. F.-K. Holtmeier: *Mountain Timberlines.* Ecology, Patchiness, and Dynamics. 2003 ISBN 1-4020-1356-6
15. H.F. Diaz (ed.): *Climate Variability and Change in High Elevation Regions: Past, Present & Future.* 2003 ISBN 1-4020-1386-8
16. H.F. Diaz and B.J. Morehouse (eds.): *Climate and Water: Transboundary Challenges in the Americas.* 2003 ISBN 1-4020-1529-1
17. A.V. Parisi, J. Sabburg and M.G. Kimlin: *Scattered and Filtered Solar UV Measurements.* 2004 ISBN 1-4020-1819-3
18. C. Granier, P. Artaxo and C.E. Reeves (eds.): *Emissions of Atmospheric Trace Compounds.* 2004 ISBN 1-4020-2166-6
19. M. Beniston: *Climatic Change and its Impacts.* An Overview Focusing on Switzerland. 2004 ISBN 1-4020-2345-6

KLUWER ACADEMIC PUBLISHERS – DORDRECHT / BOSTON / LONDON